PROCEEDINGS

of the

NORTH DAKOTA ACADEMY OF SCIENCE

VOLUME XXIV
Part I

ABSTRACTS

Official State Academy
(Founded December, 1908)

Published jointly by the University of North Dakota, North Dakota State University, Minot State College, Jamestown College and Dickinson State College.

1970

GRAND FORKS, NORTH DAKOTA

PROCEEDINGS

of the

NORTH DAKOTA ACADEMY OF SCIENCE

VOLUME XXIV
Part I

ABSTRACTS

Official State Academy
(Founded December, 1908)

OFFICERS

President	Roland G. Severson
President-Elect	Robert L. Burgess
Secretary-Treasurer	Ben G. Gustafson
Historian	George A. Abbott

Additional members of the Executive Committee:
William E. Dinusson
Myron L. Freeman
Jerome M. Knoblich
Paul D. Leiby
Franz H. Rathmann
Warren C. Whitman

Published jointly by the University of North Dakota, North Dakota State University, Minot State College, Jamestown College and Dickinson State College.

1970

GRAND FORKS, NORTH DAKOTA

EDITOR'S NOTE

Beginning with this volume of the Academy Proceedings, abstracts of papers given at the annual meeting are designated Part I, Abstracts. Those papers published later in full are designated Part II, Papers.

Abstracts in Part I of this volume are of papers presented at the sixty-second meeting of the Academy on May 1 and 2, 1970 at the University of North Dakota, Grand Forks. The abstracts are arranged alphabetically by author. An author index on pages 38 and 39 includes all authors and pages where their names appear.

Grand Forks, North Dakota — Alan M. Cvancara

EFFECTS OF CULTURE AGE AND GROWTH MEDIUM ON TOXIN PRODUCTION BY BACILLUS THURINGIENSIS, R. Ahmad, M. C. Bromel, and M. S. Quraishi. Dept. of Bacteriol. and Entomol., N. Dak. State Univ., Fargo, North Dakota.

Experiments were carried out to investigate the effects of culture age and culture medium on the toxin production of Bacillus thuringiensis, ATCC strain #10792. Particular attention was paid to effects on the development of the mosquito, Culex tarsalis. Three bacteriological media were employed for growth of the bacterium at seven different culture ages. Veal-infusion broth and trypticase soy broth were found to be more efficient for toxin production than was nutrient broth. Toxin concentration varied with age of culture with maximum lethal effects induced by 60 hour cultures. These results suggest that the morphogenesis of the mosquito is very sensitive to B. thuringiensis toxins. This work was supported by the NDSU Themis Project of the U. S. Dept. of Defense.

MORPHOLOGY AND HISTOLOGY OF THE NEUROENDOCRINE SYSTEM IN THE TOBACCO HORNWORM, R.A. Bell and P.I. Ittycheriah*. USDA, ARS, Metabolism and Radiation Research Laboratory, Fargo, ND 58102.

Morphological and histological studies of the brain neurosecretory cell complex in the tobacco hornworm were undertaken to obtain information on the neuroendocrine control of insect diapause. The brain neurosecretory cells were revealed by a variety of histological staining techniques. Excellent results were obtained with paraldehyde-fuchsin when applied to whole brains or thin sections (5-8 μ). Neurosecretory cells in vivo were observed in diapausing pupae under low magnification without the aid of special illumination. Certain medial cells in the pars intercerebralis were stained intensely in diapausing specimens; similar cells in developing individuals exhibited considerably less intense staining reactions. These observations led to the conclusion that diapause does not involve an inhibition of synthesis of neurosecretory material. Synthesis and accumulation of neurosecretory material seems to occur throughout the diapause period. The diapause condition is evidently due to an impairment of the mechanism involved in the transport or release of brain neurosecretion.

KINETICS OF THE IODINATION AND BROMINATION-DEGRADATION OF URIC ACID IN 10^{-4} MOLAR AQUEOUS SOLUTIONS AS A FUNCTION OF THE pH AND OF THE HALOGEN AND HALIDE ION CONCENTRATIONS. Dwight A. Benesh* and Franz H. Rathmann. North Dakota State University, Fargo, North Dakota 58102.

Rate studies for the iodination of uric acid were carried out by ultraviolet spectrophotometry over a pH range from 4.0 to 8 using phosphate buffers. The reaction of uric acid and iodine follows the second order rate equation $\log \frac{[Ao][Bo]}{[A]\cdot[B]} = \frac{\{[Ao]-[Bo]\}kt}{2.303}$. The concentrations of uric acid and iodine were 4×10^{-5} M. The rate constant, k, for the reaction at pH 6.75 was found to be $(2.25 \pm 0.20) \times 10^{3}$ liter moles^{-1} second^{-1}. Iodine was dissolved in a 0.30 M potassium iodide solution as the tri-iodide complex ion. The rate constant was determined at 351 mu, where only the disappearance of iodide was followed because uric acid also has a maximum absorbance at 287 mu. The rate constants at the respective pH's were: pH 4.35, 0.2; 5.0, 1.87; 5.75, 43.3; 6.75, 2250 7.65, 160,000; 7.95, 610,000; 8.05, 760,000 liter moles.

SEIBOLD SITE: COMPARISON WITH OTHER LATE QUATERNARY FOSSIL SITES IN NORTH DAKOTA, W. B. Bickley, Jr., Lee Clayton and A. M. Cvancara. Dept. of Geology, Univ. N. Dak., Grand Forks, No. Dak.

The Seiboid Site, a fossil site in Stutsman County, North Dakota, adds much information to what is known about the Quaternary biota of North Dakota. Until the discovery of the Seibold Site, mollusks and pollen represented a major part of the evidence used for climatic and environmental interpretation in this area.

The Seibold biota includes more than 150 species of mollusks, ostracods, insects, fish, amphibians, mammals and plants which allow an intergration of new interpretive tools with those from previously known sites. The similarity of the molluscan fauna of the Seibold Site and other North Dakota Quaternary sites makes the presence of these additional organisms important for paleoenvironmental reconstruction. The Seibold Site is the only site in North Dakota where the stratigraphic position of fossil fish of this age is known; beaver-gnawed wood, has been radiocarbon dated at 9750 $\pm$ 140 years B.P. This age and geologic setting indicate that the fish migrated eastward from the Missouri River through superglacial streams after the end of the last glaciation. Supported by the Dept. of Geology, UND. Departmental support made possible in part by an unrestricted grant from Humble Oil Co.

RAPID SCREENING OF URINARY STEROIDS COLLECTED FROM THE LABORATORY RAT UNDER NORMAL AND HYPERBARIC CONDITIONS. R. A. Bitter and T. W. Nielsen. Dept. of Physiology and Pharmacology, Sch. of Med., Univ. N. Dak., Grand Forks, North Dak.

Adrenal cortical hormones (cortisone, cortisol, and corticosterone) are involved in mammalian reactions to stress. The urinary excretion of these substances is presumed to be related to the duration and severity of the stress. In the rat, corticosterone is the major adrenocorticoid excreted. Twenty-four hour urine samples were collected from rats under conditions of normal (1 atm) and high pressures (20 and 30 atm). After hydrolysis, the urine samples were extracted with organic solvents and, along with suitable standards, spotted on glass plates coated with Silica gel containing a fluorescent indicator (Gelman, DSF-5). The plates were developed for 90 min in a solvent system composed of chloroform-acetone, 7:3. After drying, the steroids were resolved using short-wave UV light. The compounds were then eluted and quantitated, employing standard fluorometric procedures. The method outlined affords the opportunity to rapidly survey gross aspects of adrenocorticoid metabolism as related to hyperbaric stress, without separating each steroid. Supported by ONR (N0001468A0499)

CHARACTERIZATION OF BOVINE LIVER ISOLATES, C. H. Casavant and M. C. Bromel. Dept. of Bacteriol., N. Dak. State Univ., Fargo, North Dakota.

Bovine liver abscess bacterial isolates were characterized by gram reaction, morphology and biochemical reactions. Microbial strains isolated included: Staphylococcus, Bacteroides, Proteus, coliforms, diphtheroids, and several clostridial species. The Bacteroides strain, selected for further characterization, was studied as to oxytetracycline and sulfamethiazine sensitivity as well as animal toxigenicity. While resistant to 10 μg/ml sulfamethiazine the Bacteroides sp. was sensitive to 1.0 μg/ml oxytetracycline. These results suggest the etiology of bovine liver abscesses could possibly be antibiotic resistant rumen microorganisms.

ABSORPTION AND EXCRETION OF RADIOLABELED NAPHTHYL-N-METHYL-CARBAMATE (CARBARYL) BY THE RAT, Howard H. Casper and Jerome C. Pekas. USDA, ARS, Metabolism and Radiation Research Laboratory, Fargo, North Dakota.

Absorption of radiolabeled carbaryl from the gastrointestinal tract was characterized by measurement of the ^{14}C in the expired carbon dioxide, urine, feces, cage rinse, gastrointestinal tissue, and carcass of mature female rats dosed with 7.5 μM of carbaryl-^{14}C per kilogram of body weight. The data showed that at least 84.3 and 83.5% of the ^{14}C from oral doses of naphthyl-labeled carbaryl and carbonyl-labeled carbaryl, respectively, was absorbed in 24 hours. Ligation of the pylorus showed that at least 51.2% of the ^{14}C in an oral dose of carbonyl-labeled carbaryl was absorbed from the stomach in 24 hours. A time course study on recovery of the ^{14}C in expired carbon dioxide showed that the oral and intravenous doses of carbonyl-labeled carbaryl gave similar $^{14}CO_2$ expiration curves. The ^{14}C was detected in the carbon dioxide 10 minutes after dosing, and the highest expiration rate occurred at 30 to 40 minutes. In summary, the results show that the ^{14}C-label of the carbaryl-^{14}C is rapidly absorbed and imply that this absorption takes place in the anterior portion of the gastrointestinal tract.

OLFACTORY FACTORS IN LANDSCAPE EVOLUTION. Lee Clayton. Dept. of Geol., Univ. of N. Dak., Grand Forks, North Dakota.

Eolian erosion and deposition is commonly considered the cause of the dominant NW-SE trend of small stream valleys in much of the northern Great Plains because this is the direction of the prevailing winds. However, the influence of wind on the orientation of animal trails may also be a significant factor. Bison trails are conspicuous features on air photos of most parts of North Dakota. Their location with respect to water indicates that they were watering trails. In areas distant from rivers, lakes, bluffs, and other barriers, most of the trails are oriented NW-SE, probably because sensory information about the location of water, such as the odor of hydrophytes and phreatophytes, was carried by the winds. Runoff water is commonly funneled by bison trails into the heads of gullies, which erode along the trails. For this reason, the gullies tend to have the same orientation as the trails, parallel to the prevailing winds. Many valleys having this orientation were formed many tens of thousands of years ago, long before the presence of modern bison. However, trail-making mammals probably existed on the plains throughout most of the Quaternary Period, and their wind-oriented trails probably had a significant influence on the evolution of the present landscape.

DISTRIBUTION OF LAKE MUSSELS AS DETERMINED WITH SCUBA. A. M. Cvancara, Dept. of Geol., Univ. of N. Dak., Grand Forks, N. Dak.

During the summer of 1969 mussels were studied with SCUBA in northwest-trending Long Lake (T. 144 N., Rs. 36 and 37 W.), about 6.5 km northwest of Lake Itasca (town), northwestern Minnesota. Thirty-four belt transects, 20 m by 1.7 m and paralleling depth contours, were run at six stations around the lake. Bottom sediment and percentage of aquatic plant cover were recorded on white lucite with a grease pencil at five points along each transect. Measurements of shell length, height and width were made, in the field, on the 1,118 specimens recovered. Three mussel species, Anodonta grandis Say (n=42), Anodontoides ferussacianus (Lea) (n=53) and Lampsilis siliquoidea (Barnes) (n=1023), inhabit the lake and were found at maximum depths of 8, 2 and 9 m, respectively. Mussels occurred to 9 m on the southwest side of the lake, but to only 1 m on the northeast side where aquatic plant cover was greater. Correlation coefficients indicate a significant decrease ($P=0.05$) in height and height/length and an increase in width/height with depth for A. ferussacianus and L. siliquoidea. At 1 m depth, an F test indicates a significant difference ($P=0.05$) in length, height, width and width/height for L. siliquoidea between the northeast and southwest sides of the lake. A significant difference is apparent for height/length in A. ferussacianus. Supported by UND Faculty Research Grant 4522-8.

LIVER GLYCOGEN METABOLISM IN THE COLD ADAPTED RAT, D. R. Davis and S. J. Brumleve, Sch. of Med., Grand Forks, N. Dak.

Synthesis and degradation of liver glycogen were studied in the cold adapted, mildly fasting rats. Animals 4 to 8 weeks of age were exposed 10 days at 2° C or 30° C. Following this, the rats were fasted and injected intrathoracically each hour for four hours with labeled C^{14}-alanine. Animals were sacrificed hourly through the eighth hour. The incorporation of alanine into liver glycogen in the 30° C group increased linearly while the radioactivity of the 2° C group increased as a function of $\log_e$. This suggested that after a short lag, the cold group incorporated alanine faster than the warm group. The degradation of radioactivity occurred as a function of x^4 at 30° C and x^3 in the 2° C group. Radioactivity in the liver glycogen of the cold group decreased at a slower rate and the slope of the equation for degradation at 2° C is not as steep as that at 30° C. Thus, the increased liver glycogen synthesis and decreased liver glycogen breakdown suggested a possible reason for the higher liver glycogen levels in the cold adapted, mildly fasting rat. Supported in part by NASA and NIH.

HYDRODYNAMIC INTERPRETATIONS OF HOLOCENE SEDIMENTS ALONG THE TURTLE RIVER, NORTHEASTERN NORTH DAKOTA. D. E. Deal and D. M. Huff. Geol. Dept., Univ. N. Dak., Grand Forks, North Dakota.

Sediment distribution and bar-bedding characteristics were observed along a section of the Turtle River from a point about 4 miles north of Larimore to a point about 4 miles south of Manvel. This reach begins where the Turtle River is cutting through sand, silt, and gravel marginal to the Herman level of glacial Lake Agassiz and extends downstream across wave-eroded till and Lake Agassiz clay and silt. The particle size of the modern bar deposits decreases downstream from sandy gravel to sandy silt. The point-bar bedding of the sand-size material changes from types characteristic of bed forms of the upper flow regime (flat bedded and large-scale, high-angle, tabular crossbedding) to those characteristic of bed forms of the lower flow regime (large-scale, high-angle, tabular and small-scale, high-angle, trough crossbedding). These forms reflect conditions during the spring flood of 1969. Ice scars on trees indicate that the channel depth was fairly constant along this reach. The lowering of flow regime probably reflects a reduced flow velocity downstream as a result of ponding caused by the raised level of the flooding Red River and by a general reduction in stream gradient.

VOLATILE FATTY ACIDS IN THE RUMEN INGESTA AS AFFECTED BY METHOD AND TIME OF SAMPLING. F. D. Deitz, D. O. Erickson, C. N. Haugse, and W. E. Dinusson. Dept. of Animal Sci., North Dakota State Univ., Fargo, North Dakota.

Rations containing 5 combinations of alfalfa and oats and 2 combinations of alfalfa and corn were fed to determine the effect of method and time of sampling on volatile fatty acids (VFA) concentrations in sheep and cattle. Six lambs (3 fistulated) and 6 beef heifers (3 fistulated) were used as experimental animals. Samples were obtained from all animals, including those fistulated, via a suction strainer. Samples were prepared according to standard procedures and the VFA's were analyzed using an Aerograph 660 gas chromatograph. Highly significant differences ($P < .01$) were found among time and method of sampling for individual acids (acetic, propionic, butyric), and total concentration of these acids. The acetic to propionic ratio was highly significant ($P < .01$) among hours. With both the acetic to propionic and acetic to the proprionic plus butyric ratios significant ($P < .05$) between methods of sampling. VFA concentration and ratios were different among hours sampled and between methods of sampling.

A CHROMATOGRAPHIC METHOD FOR THE DETECTION OF ACETYLATION OF PAH IN ANIMALS. D.S. DeLorme and T.W. Nielsen. Dept. of Physiology & Pharmacology, Sch. of Med., Univ. N. Dak., Grand Forks, North Dakota.

p-Aminohippuric acid (PAH) is used in kidney function tests to determine renal plasma flow. The method is valid provided the species does not acetylate PAH. The acetylated moiety, p-N-acetyl-aminohippuric acid (PAAH) is not detected in the usual analytical procedure. Modifications were made in existing methods for the separation of such compounds. Pyrex plates were coated with cellulose powder (Camag) and dried. Standards containing PAH and/or PAAH, and urine samples from animals given intravenous PAH, were applied and the plates developed with a solvent system of n-butanol-acetic acid-water, 4:1:1. After the solvent front had moved 15 cm., the plates were removed, dried, sprayed with a solution of p-dimethylaminobenzaldehyde in acetic anhydride and dried again. The compounds were resolved with either UV light or heating. Rf values for PAH and PAAH were 0.61 and 0.74, respectively. If a urine sample developed both spots, the use of PAH was contraindicated in renal function testing. Supported in part by ONR (N0001468A0499).

PROTEIN CONTENT OF HARD RED SPRING WHEAT IN NORTH DAKOTA, Russell E. Doe* (spon: William Eastwood). Dickinson State College, Dickinson, North Dakota.

Factors affecting protein content of wheat are divided into uncontrollable and controllable. Climate and soil type are two factors affecting protein that are uncontrollable by man. Controllable factors affecting protein are: variety of wheat, irrigation, and fertilizer. Precipitation, variety, and fertilizer are the three most important. Excess growing season precipitation, especially in April and May, lower wheat protein because a significant quantity of the protein yielding nutrients are leached below the plant root systems. A moist July causes more starch and less protein to be transferred to the kernels from the leaves and stems. Higher quality wheat varieties are continually being developed. A sufficient amount and composition of fertilizer is required by most soils to produce maximum yielding high protein wheat. Domestic consumption of Hard Red Spring Wheat is decreasing, while our wheat exports are slightly increasing.

DETECTION OF A VIREMIA IN MICE WITH MURINE SARCOMA VIRAL INDUCED TUMORS. T. M. Dolan,* R. G. Fischer, and J. J. Kelleher*. Dept. of Micro., Sch. of Med., Univ. of N. Dak., Grand Forks, North Dakota.

The viremic period of murine sarcoma virus (Moloney) was studied in newborn and adult BALB/c mice. Mice were injected IM-IP with 3.2×10^4 FFU's of virus. Tumors appeared in newborn mice after 5 days and in adult mice after 7 days. Newborn mice began dying 12 days after infection but the primary tumors regressed and no deaths occurred with adult mice during a 28 day observation period. Plasma samples from newborn mice were tested for competent virus by direct assay in secondary NIH Swiss mouse embryo tissue culture. Defective virus was determined by coinfecting cultures with Rauscher leukemia virus. MSV appeared in the plasma after 4 days reaching a plateau of 2.0×10^4 FFU's in 9 days. Muscle tissue taken from the site of injection yielded virus 1 day earlier and 1 log higher than plasma samples. In contrast, isolations of MSV from adult mice were made only from day 7 to 9 and never exceeded 10^2 FFU's per ml of plasma. Defective virus always preceded competent virus, regardless of the age of the mice used.

LONG-TERM DEVELOPMENTAL PATTERNS OF DISPERSED EMBRYONIC HOUSEFLY CELLS: DIFFERENTIATION, P. E. Eide and M. J. Dockter*. USDA, ARS Metabolism and Radiation Research Laboratory, Fargo, ND 58102.

The differentiation and developmental patterns of dispersed embryonic house fly tissue was observed with time-lapse cinematography from the first set-up through several months. These *in vitro* developmental patterns showed many similarities to the normal *in vivo* patterns. When we used 4- or 6-hr-old embryonic material (age of egg after laying was kept at about 72°F), we saw the cells go through an attaching process. Cell aggregates occurred as the result of cell migration from cell wall stickiness or random contact between dispersed cells before seeding. A number of cell aggregates were the result of cell division rather than other processes. After 15-30 days in culture (depending on the medium used and the age of the embryo), the highly complex tissue started to give off a great number of round cells. When these cells were subcultured, they immediately started to attach, divide, and differentiate. They finally migrated to form new differential cell aggregates. For about the first 15 days, the subcultures showed much cell activity. Many divisions took place, and many morphological changes occurred. The cultures became highly differentiated, with a high degree of complexity.

CRITICAL PATH SCHEDULING, V. Emerson* (spon: Dr. D. P. Naismith). Department of Mechanical Engineering, College of Engineering, University of North Dakota, Grand Forks, North Dakota.

Critical path scheduling is a technique used by management through the optimum usage of time and available resources. The language of CPM (critical path method)-- duration, forward and backward passes, early and late start times, early and late finish times, float, and critical path-- is developed from the time sequence of activities. Basic representation of a CPM network is accomplished pictorially using events (circles), activities (solid arrows), and restraints (dashed arrows).

VOLATILE FATTY ACIDS IN THE RUMEN INGESTA AS AFFECTED BY SPECIES AND RATIONS. D. O. Erickson, F. D. Deitz, C. N. Haugse, and W. E. Dinusson. Dept. of Animal Sci., North Dakota State Univ., Fargo, North Dakota.

To determine the effects of species and ration on the volatile fatty acid (VFA) production in the rumen, 7 trials were conducted using 6 beef heifers and 6 lambs. Alfalfa in combinations with oats or corn were fed near ad-libitum in pelleted form. The differences in acetate, propionate and butyrate were significant ($P<.01$) among rations. Ratios of acetate to propionate and acetate to propionate plus butyrate were also significantly ($P<.01$) different among rations with the lowest ratios on oats and corn and the highest ratios on alfalfa. The rumen ingesta pH and total VFA production varied significantly ($P<.01$) among rations with no apparent relationship to ration fiber levels. Rumen ingesta from beef heifers was significantly higher ($P<.01$) in the individual VFA and VFA ratios, and total VFA's than from sheep with the exception of butyrate and pH. Rumen ingesta concentrations and ratios of VFA's were affected by rations and species of ruminant.

BIOTIN PRODUCTION AND UTILIZATION IN CERTAIN NATURAL ENVIRONMENTS. G. M. Fillipi and J. W. Vennes. Dept. of Microbiol. Univ. of N. Dak., Grand Forks.

Biotin levels in lakes, rivers and an overloaded sewage lagoon were determined by microbiologic assay. Biotin concentrations in most lakes and rivers ranged from 2 to 29 ng/l. Biotin in the lagoon ranged from 60 to 10,800 ng/l during the summer. Several organisms isolated from the lagoon were inoculated into Millipore-filtered lagoon waste and into chemically defined medium (modified Wright-Skeggs) to determine biotin production and/or utilization. From 24 isolates, one, identified as *Aerobacter aerogenes*, produced the most biotin when grown in Wright-Skeggs medium for 212 hours (2,200 ng/l). A millipore-filtered lagoon sample containing 6,600 ng/l biotin inoculated with a culture of *Chlorella vulgaris* contained 500 ng/l biotin after 93 hours incubation. Thus at least one bacterial species is able to produce large amounts of biotin in a sewage lagoon and at least one algal species is responsible for removal of the accumulated vitamin. Biotin thus may be a useful indicator of some ecologic changes in streams receiving waste effluents.

LOW-TEMPERATURE ASHING OF LIGNITE USING AN OXYGEN PLASMA, P. G. Freeman and W. W. Fowkes. Grand Forks Coal Research Laboratory, USDI, Bureau of Mines, Box 8213, University Station, Grand Forks, N. Dak.

Many processes utilizing lignite or other fossil fuels are concerned with the chemical and mineralogical composition of the ash. In an effort to better understand the original condition of the inorganic components in the fuel, a low-temperature oxidation unit has been used to ash lignite. In this way temperature sensitive structures are preserved. Carbonaceous material is oxidized with "active" oxygen generated in a microwave discharge under reduced pressure. Addition of a small quantity of nitrogen catalyzes formation of active oxygen at temperatures below 60° C, as determined by a thermometer inserted in a well in the reactive chamber. The low-temperature ash has been analyzed by X-ray diffraction and found to differ considerably from a corresponding high-temperature ash in that sodium occurs mainly as carbonate-sulfate in the latter and as nitrate in the former.

DISPOSAL OF SUGAR REFINING LAGOON EFFLUENTS ON FARGO SILTY CLAY SOIL, B. R. Funke and F. W. Schroer. Dept. of Bacteriol. and Dept. of Soils, N. Dak. State Univ., Fargo, North Dakota.

Infiltration rates: Very slow, no significant short term clogging effects due to effluents noted. Effects of cropping: No significant difference noted between growth of alfalfa or soybeans treated with effluent or distilled water. Sudan grass did slightly better with effluent. Barley did much better with effluent. Transpiration rates: Alfalfa (three croppings) cumulatively transpired most water, Sudan grass (two croppings) slightly less. Soybeans effective in transpiration but only one crop. Barley relatively poor. Salt accumulations: Some increases noted but concentrations below level of present concern after one season application. Soil fertility: Carbon-nitrogen ratio did not exceed 13:1 after treatment with effluent, no significant difference from treatment with water. No significant differences noted in nitrate levels. Phosphorous levels increased slightly. Soil pH treated with effluent increased from 6.5 to 7.5. No change when treated with distilled water.

DESCRIPTION OF AUTHIGENIC ANALCITE IN THE GOLDEN VALLEY FORMATION (?), SOUTHWESTERN NORTH DAKOTA, Marvin J. Furman and Frank R. Karner. Dept. of Geology, U. N. D., Grand Forks, N. D.

Authigenic analcite ($NaAlSi_3O_8 \cdot nH_2O$) constitutes up to about 60 percent of a massive, arkosic sandstone exposed on major buttes in the North Dakota Badlands. Analcite occurs as spherulites in the interstices of the arkose and as a cement in a massive bed near the top of the unit. Three types of spherulites are recognized: (1) those with no internal structure; (2) those with a radial structure; and (3) those with a massive center and peripheral radial structure. The spherulites occur individually or as coalesced masses. The average composition of the analcite, expressed as the ratio $2SiO_2:Al_2O_3 + Na_2O$, is 4.36.

Detrital minerals associated with the analcite include quartz, Na-plagioclase, K-feldspar, and illite. Sericite and minor silica are associated with analcite and may also be authigenic. The analcite is least abundant at the base of the arkose unit, and increases upward. The abundances of analcite and detrital feldspar are inversely related. Sericite frequently occurs as inclusions in the analcite.

Analcite composition, distribution with respect to the feldspars, presence of sericite, and the absence of vitroclastic textures,suggest that analcite formed by post-depositional dissociation of feldspar.

PREPARATION AND SOME CHEMICAL PROPERTIES OF POLYWATER, G. Graf and R. E. Nett.* Dept. of Biochem., N. Dak. State Univ., Fargo, North Dakota.

The conditions of polywater formation in glass and quartz capillaries were investigated and a density gradient method was developed to measure the specific gravity of polywater droplets. The transfer of microliter quantities of polywater into containers suitable for microchemical reactions was accomplished by centrifugation. In polywater, the rate of trypsin catalyzed hydrolysis of the chromogenic substrate N^{α}-benzoyl-DL-arginine p-nitroanilide was less than ten percent of the rate of hydrolysis observed in normal water.

STATISTICAL EVALUATION OF THE AUDIO-TUTORIAL BIOLOGY PROGRAM AT THE UNIVERSITY OF NORTH DAKOTA, Cary Grobe and Marjorie Behringer Depts.of Education and Biology, Univ. of N.Dak. Grand Forks, N.D.

The purpose of this study was to determine if the audio-tutorial (A-T) or the conventional method of biology instruction promotes higher achievement among learners who possess differing academic aptitudes. Seventy-nine students who had enrolled in the 101 Biology course at the University of North Dakota were randomly selected and assigned to one of the two instructional methods. Forty-one students were given a biology course taught in a conventional manner and 38 students received an identical course taught in the A-T manner. Students of the two groups were assigned to one of three aptitude levels based on the American College Test composite percentile rank. At the initiation of the study both groups were given a standardized pretest, designed and validated to measure achievement in biology. An alternate form of the pretest was administered three months later to the same students. Comparisons between the two instructional methods and within the subgroups were made on four variables employing a 3-2 way analysis of variance. The results indicated that there were no significant differences between the two instructional methods and no significant interactions among the aptitude subgroups at the .05 level.

THE EFFECT OF SELECTED HERBICIDES ON CEREAL APHIDS UNDER GREENHOUSE CONDITIONS, S. D. Hintz*, and J. T. Schulz. North Dakota State University, Fargo, North Dakota.

Reproductive capacities of the English grain aphid, Macrosiphum avenae (Fab.), greenbug Schizaphis graminum (Rond.) and oat bird cherry aphid, Rhopalosiphum padi L. were determined on barley (Hordeum vulgare L., var. Larker) in the two to three leaf stage of development, dipped in herbicide solutions of Banvel D, barban and MCPA. These were 0.22, 0.44 and 0.16 per cent solutions respectively. Fecundity of English grain aphids reared on plants treated with Banvel D, barban and MCPA was 19.7, 6.6 and 2.3 per cent greater respectively than those reared on untreated barley; greenbug fecundity increased 17.8, 21.7 and 33.7 per cent respectively. Reproductive capacities of the oat bird-cherry aphid increased 37.8 per cent when treated with Banvel D., 33.6 per cent with barban and 29.1 per cent with MCPA as compared to those reared on untreated barley. These data would suggest that these herbicides give a stimulatory effect on aphid reproduction either through the alteration of the host or aphid physiology.

INTERACTION OF HEMOGLOBIN WITH H_2O AND D_2O VAPORS AND $H \rightleftarrows D$ EXCHANGE WITH AND WITHOUT RADIATION. W. S. Hnojewyj. Coll. of Chem. and Phys., NDSU, Fargo, N. Dak.

Adsorption isotherms of H_2O on Hemoglobin at 27, 37 and 47° also of D_2O vapors on deuterited Hemoglobin at 27 & 37° measured up to 26mm A number of slopes in isotherms, due to different active sites, were established. 13.25 mg/100 of sorption as maxima of the total H_2O mono layer at 27° estimated. Illumination (visible light) of Hemoglobin in presence of O_2 + H_2O showed slight increase of weight after desorption indicating couplin of O_2, marcably lowering adsorptivity, which however partly restored at repeated H_2O sorptions. γ-ray preradiation caused not regenerable lowering of adsorptivity in the upper coverage, suggested due to damage of porphirin groups. ΔH of adsorption calculated: up to 33 at start, rapidly decreasing to 13-15kcal/mole and approaching ΔH of condensation, with adsorption increased. Readsorption of D_2O followed by complete desorption caused $H \rightleftarrows D$ exchange, which seems reversible and is not influenced by oxygenation or γ-radiation, undertaken. (Supported in parts by NIH Grant H2972 and NDSU).

THE INFLUENCE OF ADRENALECTOMY ON EMBRYONIC MORTALITY IN THERMALLY STRESSED EWES. R. H. Hoffman*, J. E. Tilton, T. J. Archbold*, I. E. Berg*, and M. L. Buchanan. Dept. of Animal Science, NDSU, Fargo, N. Dak.

Previous workers have hypothesized that a pituitary-adrenal-ovarian interaction has an effect on embryonic mortality in females subjected to stress. This project was initiated to study the results of adrenalectomy and minimal replacement therapy on mating behavior and embryonic mortality in mature ewes. Group 1 ewes were adrenalectomized and maintained post-operatively with 20 mg. hydrocortisone and 5 mg. deoxycorticosterone daily. Group 2 served as controls. All ewes were mated and immediately placed in a 31.6° C. temperature control room for 5 days. They were then removed, slaughtered, and reproductive organs were collected. Adrenalectomy did not reduce mating activity or conception rate. The adrenalectomized ewes had a 10% increase in viable embryos. There was no statistically significant difference between the two groups regarding adrenal weight, C.L. weight or ovarian weight. The results obtained indicate a possible relationship between the adrenal gland, stress, and embryonic mortality.

NUCLEAR CONDITION IN GERMINATING TELIOSPORES OF USTILAGO HORDEI L. L. Jensen* and R. L. Kiesling, Dept. of Plant Pathology, NDSU, Fargo, N. D.

Germination of U. hordei teliospores terminates in the production of a promycelium and four haploid sporidia which are the result of meiosis, but the precise location of the meiotic division is in question. Germinating teliospores were stained with coriphosphine O in phosphate buffered saline and examined with a fluorescent microscope. Examination of these stained teliospores did not confirm previous published accounts. Stained spores were variable in both their morphology of germination and nuclear condition of the sporidia and promycelium. Fusion between promycelial cells occurred with or without the production of sporidia. Also, many sporidia and promycelial cells lacked nuclei or were binucleate. This resulted from nuclear division occurring at the junction of the sporidium and promycelium. After sporidia had formed on and were removed from the promycelium, it was found to have a single mating type in many cases and both mating types in a few instances. Cytological and infection studies indicated that meiosis occurs in the promycelium. The presence of more than one true promycelium emanating from a single teliospore was not found. After the teliospore had germinated, the residual spore was found to be of only one mating type and was unable to infect a susceptible barley variety (Odessa C.I.934).

PREPARATION AND CHEMISTRY OF ARSONIUM IMINES. A.Wm. Johnson and S.G.Dwyer. Chemistry Department., Univ. of North Dakota, Grand Forks.

N-benzoyliminotriphenylarsenane(I), and other members of this stable but hitherto unknown series of arsonium imines, has been prepared by reaction of the arsine with N-bromobenzamide and subsequent deprotonation. The long wavelength carbonyl absorption of I indicates a significant contribution of the enolate structure and accounts for some of its stability and lack of reactivity. The imine could not be alkylated, even with triethyloxonium tetrafluoroborate. Thermolysis of I resulted in intramolecular deoxygenation to afford triphenylarsine oxide and benzonitrile.

Several other methods known to be successful for the preparation of phosphine imines were unsuccessful when applied to the preparation of arsine imines. N-tosylaminotri(p-tolyl)-arsonium hydroxide could be dehydrated to the imine but attempts to dehydrate N-(p-nitrophenyl)aminotriphenylarsonium-hydroxide were unsuccessful.

CARBONYL-STABILIZED ARSONIUM YLIDES. A.Wm. Johnson and Hans J.Schubert. Chemistry Dept., Univ. of North Dakota, Grand Forks.

Triphenylarsoniumphenacylide(I), an exemplary stable arsonio-carbanion (ylide) has been prepared by two routes: (1) alkylation of triphenylarsine then removal of the alpha proton, and (2) acylation of triphenylarsoniummethylide. This stable ylide could be isolated and crystallized, then subjected to a study of its physical and chemical properties. The ylide was stable in the atmosphere but would undergo hydrolysis in aqueous solution and was subject to thermolysis, affording a cyclopropane. The nucleophilicity of the ylide(I) was demonstrated by its undergoing O-alkylation, C-acylation and C-acylation. The ylide afforded olefins upon reaction with aldehydes but effected a conjugate addition with α,β-unsaturated carbonyl compounds, affording cyclopropanes. The ylide thereby exhibited characteristics common to both sulfonium and phosphonium ylides.

ACKNOWLEDGEMENT is made to the Petroleum Research Fund of the American Chemical Society for the support of this work.

BRANCHED-CHAIN α KETO ACID METABOLISM: COENZYME REQUIREMENTS OF α-KETOISOCAPROIC-α-KETO β-METHYLVALERIC ACID DEHYDROGENASE. W.A. Johnson and J.L. Connelly, Dept. of Biochem., Sch. of Med., Univ. of N. Dak., Grand Forks, North Dakota 58201

The purification and partial characterization of α-ketoisocaproic-α-keto-β-methylvaleric acid dehydrogenase (KMVD) has been reported by Bowden, Danner, and Connelly (J. Biol. Chem., 243, 1198 (1968)). This enzyme is presumed to be a multienzyme complex of similar enzymatic nature and cofactor requirements as the pyruvate dehydrogenase complex (PD). Since PD requires the cofactors thiamine pyrophosphate (TPP), lipoic acid, coenzyme A, NAD, and FAD, this work has attempted to show that these same cofactors participate in the catalytic functions of KMVD. Bound TPP has been dissociated from enzymes at alkaline pH. KMVD, when precipitated by $(NH_4)_2SO_4$ at pH 8.5 and separated from the supernatant, loses 50-75% of its catalytic activity. Addition of purified TPP restores 80-100% of the lost activity. This finding was verified by reconstitution experiments following removal of TPP with Sephadex G-25 gel at pH 8.5. Enzymatic oxidation of substrate utilizes the electron acceptor NAD or artificial oxidants such as $Fe(CN)_6^{-3}$. Preliminary experiments indicate that NADP will not substitute for NAD. Experiments are in progress to ascertain the requirements for coenzyme A, lipoic acid and flavin. (NSF-GB 12934, NDEA 69-02592)

COMPOSITION, DISTRIBUTION AND ORIENTATION OF XENOLITHS IN THE TUNK LAKE GRANITE, MAINE, Frank R. Karner and Roland A. Connors. Dept. Geology, U.N.D., Grand Forks, N. D.

Two major types of xenoliths are present in different parts of the concentrically zoned granite body. Fine-to medium-grained, dark-colored xenoliths occur in an outer marginal zone up to about 2 km in width. These partially or completely recrystallized mafic rock fragments consist of about one-half biotite, hornblende and aegirine augite, and about one-half quartz, alkali feldspar and plagioclase. Within about 1 km of the outer contact of the granite, oriented, tabular, xenoliths typically 2-10 cm long, strike parallel to the contact and dip inward 25-40°. Variations in xenolith orientation and abundance define arcuate areas parallel to the outer contact.

In the central zones of the granite body, medium-to fine-grained equidimensional xenoliths? are typically up to 3 cm in diameter and consist of about one-fourth biotite and hornblende and three-fourths plagioclase, quartz and alkali feldspar.

Gradations of xenoliths with ferromagnesian mineral clusters of normal granite are common but gradations between types are rare. Possible factors affecting xenolith variation include extent of chemical reaction with magma and rates of gravity settling, deposition on constructional floors, and convective magmatic flow. Supported by UND. Faculty Research Grant 4522-95.

THE VEGETATION OF THE MISSOURI RIVER FLOODPLAIN FORESTS, W. R. Keammerer and W. Carter Johnson, Dept. of Botany, NDSU, Fargo, North Dakota.

The floodplain forests described in this study are the only extensive remaining stands of bottomland hardwoods on the Missouri River in the Dakotas. The study area is bordered on the south by the Oahe Reservoir south of Bismarck and on the north by the Garrison Dam near Riverdale. The river is constantly engaged in erosion and deposition. Thus, forests become established that differ in composition mainly due to the age of the parent materials on which they develop. Early successional stages are composed primarily of Populus deltoides, Salix interior, Salix lutea, Cornus stolonifera, and Rosa woodsii. Fraxinus pennsylvanica and Acer negundo become established after the cottonwood canopy has closed and later successional stages contain Ulmus americana, Fraxinus pennsylvanica, Acer negundo, Rhus radicans, and Celastrus scandens. Phytosociological indices are determined for the trees by the quarter method, shrubs by belt transects, and herbs by circular quadrats. Environmental parameters are also being studied.

TEMPERATURE SENSITIVE GENES GOVERNING RESISTANCE TO RACE 6, USTILAGO HORDEI IN SEVERAL SPRING BARLEYS. R. L. Kiesling, Dept. of Pl. Path. NDSU, Fargo, N. Dak.

Spring barley varieties, Jet, Chevron, Odessa and Pannier and the F_2 populations of their crosses were inoculated with race 6, U. hordei. One half of each inoculated sample was planted in a constant temperature greenhouse at either 17°C or 22°C. Pannier was not infected at either temperature. Jet, Chevron and Odessa developed 62, 38 and 20 percent higher infections respectively at 22°C than at 17°C. The increased infection of the F_2 populations of Odessa X Jet ranged from 33 to 59 percent at 22°C. Increased infection in the F_2 populations of Chevron X Jet ranged from .44 to 26 percent at 22°C. No significant increase in infection at 22°C was found in F_2 populations of the crosses Odessa, Chevron or Jet X Pannier. These data show that the efficacy of the genes governing resistance to race 6, U. hordei in spring barley varieties Jet and Chevron are reduced by growth at 22°C. The temperature sensitivity of these genes was not expressed in crosses with Pannier whose reaction to race 6, U. hordei is temperature insensitive.

CLASSICAL SOURCES OF ORBITAL PRECESSION.
Kingsley A. Bowles* and Paul Ross* (Spon: W. S. Hnojewyj) Dept. of Physics., NDSU, Fargo, N. Dak.

Recent investigations by Dicke have cast doubt upon the adequacy of general relativity to completely explain the precession of the perhelion of Mercury. Our investigations show that the part of the precession unexplained by relativity can be accounted for by a potential energy function of the form

$$V = -\frac{k}{r} + \frac{c}{r^n}$$

The first term is the usual classical gravitational interaction and the second represents a small correction to it. n may be any number, not necessarily an integer. It is shown that the rate of precession is proportional to n(n-1)c if the orbits are nearly circular.

DIETARY GLUCOSE AND AMINO ACID TRANSPORT VIA THE INTESTINAL LYMPHATICS, E.E. Largis and F.A. Jacobs, Dept. of Biochem., Sch. of Med., Univ. N. Dak., Grand Forks, North Dakota 58201

Adult rats were prepared surgically by cannulating the mesenteric lymph duct and thereby collecting lymph coming only from the small intestine. By using ^{14}C-glucose, it was demonstrated that mesenteric lymph glucose can originate from peripheral blood and/or directly from the intestinal lumen via the mucosal cells. L-alanine and L-valine brought about an increase of both blood and lymph glucose when fed by stomach tube (4.4 mmoles/kg body wt. for rats fasted 20 hours). D-alanine at this level increased blood and lymph glucose only slightly. The ketogenic amino acid, leucine, exhibited a depressing effect on lymph and blood glucose levels that paralleled each other. Lymph glucose fluctuations generally paralleled those found in peripheral blood, but the lymph fluctuations appeared to be sharper. Phlorizin, a compound known to block glucose transport in kidney and intestine, was studied relative to the absorption of dietary glucose, revealed by analyses of lymph, blood, and urine. It was found in these *in vivo* studies that the phlorizin concentration (300 mg/kg, intraperitoneally) which blocked kidney glucose reabsorption had little or no effect on intestinal transport of glucose into mesenteric lymph.
(Supported in part by a Faculty Research grant, U.N.D.)

METABOLISM OF PLANT METABOLITES OF s-TRIAZINE HERBICIDES IN THE RAT, J. D. Larson, J. E. Bakke and V. J. Feil. USDA, ARS, Metabolism and Radiation Research Laboratory, Fargo, N. Dak.

Rats excreted 66.7% of a single oral dose (13 mg/kg) of 2-methoxy-4-ethylamino-6-sec-butylamino-s-triazine (I) in the urine as 15 metabolites. Four of these accounted for 91% of the radioactivity excreted: 2-methoxy-4,6-diamino- (16.2%); 2-methoxy-4-amino-6(4-hydroxy-sec-butylamino)- (34.2%); 2-hydroxy-4,6-diamino- (19.8%); and 2-hydroxy-4-amino-6(4-hydroxy-sec-butylamino)-s-triazines (20.8%). When the 2-hydroxy analogue of I (I-OH) was administered at the same level, three urinary metabolites were found: I-OH (10.8%); 2-hydroxy-4-amino-6-ethylamino (9%) and 2-hydroxy-4-ethylamino-6(4-hydroxy-sec-butyl-amino)-s-triazine (78.9%). Dosing with 2-hydroxy-4-amino-6-sec-butylamino- and 2-hydroxy-4-amino-6-ethylamino-s-triazine at the same level, only the parent compounds were excreted in the urine. Atrazine was metabolized to 20 urinary compounds, while hydroxy-atrazine gave only four as yet unidentified metabolites. The largest urinary metabolite from each compound has the same elution characteristics from the amino-acid analyzer as ammiline (30% from atrazine and 50% from hydroxy-atrazine).

ANTIBIOTIC RESISTANCE OF DAIRY CATTLE WASTE LAGOON ISOLATES, Y. N. Lee and M. E. Bromel. Dept. of Bacteriol., N. Dak. State Univ., Fargo, North Dakota.

Antibiotic sensitivities of 10 bacterial isolates from a dairy cattle waste lagoon were determined. Biochemical characterizations were performed on the following bacterial genera: Bacillus, Streptococcus, Clostridia, Proteus, Escherichia, Shigella, Klebsiella, Salmonella. Antibiotic disc assay on all isolates and antibiotic tube dilution assay on two isolates were performed. Results indicated growth stimulation of Bacillus and Streptococcus by both low and high concentrations (5 µg and 30 µg) of chlotetracycline. Sensitivity to both concentrations (5 µg and 30 µg) of oxytetracycline and chlorotetracycline was exhibited by Clostridia. All other genera were resistant to both concentrations of sulfamethiazine, sulfaethoxypyridazine, oxytetracycline and chlorotetracycline. These results suggest that the high level of antibiotics in animal rations may be causing the development of antibiotic resistance in potentially pathogenic bacteria.

THE DISTRIBUTION AND PERSISTENCE OF H^3-LABELLED MALE ACCESSORY SECRETION IN MATED FEMALE HOUSE FLIES, **R. A. Leopold and A. C. Terranova, USDA, Met. and Rad. Res. Lab., Fargo, N. Dak.**

Autoradiography and liquid scintillation spectrometry were used to examine the fate of a male accessory secretion which induces a loss of receptivity in once mated females. Tritium was incorporated into the secretion by injecting 1 µl of arginine-H^3 (18.0 c/mmole) into 3 day postemergence males that had mated 3 times in succession within an 8 hr period. Autoradiographs of reproductive tracts of females mated to labelled males showed that the secretion accumulated in the copulatory pouches during mating. Rapid absorption of the secretion occurs in the copulatory pouches. About 75% of the labelled material contained within these structures immediately after mating is lost within 4 hr. The heads, thoraxes, and abdomens of the mated females all displayed uptake of the labelled secretion, but the radioactivity was found to be the most persistent in the head and thorax. Approximately 80% of the radioactivity present in the abdomen at the completion of mating was absent 72 hr later. Apparently some of the radioactivity lost by the abdomen is the result of a transfer to the head and thorax after mating is completed. Maximum uptake by the head and thorax did not occur until several hours after that by the abdomen.

THE INFLUENCE OF POLLUTANTS ON DISSOLVED OXYGEN AND BENTHOS IN THE RED RIVER AT FARGO, NORTH DAKOTA, D. R. Lerfald and D. R. Scoby, Division of Natural Sciences, NDSU, Fargo, N. Dak.

Two stations were sampled for benthos in the Red River during the summer and fall of 1969. Dissolved oxygen (DO) tests conducted simultaneously by the Fargo Sewage Dept. were verified and appropriated in this research. The stations were selected to represent the upstream "freshwater" (the control) near the Fargo Water Works and the experimental variable downstream about 1000 feet beyond the Fargo sewage effluent.

No chemical analysis was made but the pollutants were assumed to be sewage effluents, agricultural runoff, and sugar beet effluent. Random dredging and DO samples were taken and it was apparent numerically that the variable had a relatively low DO content, high number of oligochaets, and low number of chironomids. A test statistic, Chi-square, proved a significant difference at the 0.5% level for the oligochaets only. Taxonomy of all organisms revealed very few different species per station with a high number of single species at both.

AN ANKLE EXERCISER FOLLOWING NATURAL FOOT MOTION, D. V. Mathsen* (spon: D. P. Naismith). Dept. of Mech. Engr., Col. of Engr., Univ. of N. Dak., Grand Forks, North Dakota.

The proper exercising of the leg muscles, acting through the ankle, is not accomplished by devices presently used for that purpose. The movement of the device constructed approaches the articulation of the foot about the ankle joint.

A study of the anatomy of the foot and ankle showed that the entire foot moves on one axis about the ankle during flexion and extension. The metatarsals and toes also move on a rotating axis which pivots in the cuneiform bones during inversion and eversion of the foot while the heel remains fixed.

The exerciser developed allows for three movements. First, full extension and flexion of the foot about an axis in line with the ankle are permitted. Secondly, inversion and eversion of the forefoot are allowed about an axis parallel to that formed within the cuneiform bones. Third, a combination of the two previously stated movements permits the foot to articulate in any desired manner.

QUICK OPENING CLOSURE FOR USE ON A LIFE SUPPORT SYSTEM, J. R. Morales* (spon: W. G. Barney). Dept. of Mech. Engr., Col. of Engr., Univ. of N. Dak., Grand Forks, North Dakota.

A basic requirement in the development of laboratory equipment for the study of animals in a high pressure environment is the ability to quickly and safely open and close the pressure chamber with full-size end openings permitting the insertion and withdrawal of equipment and animals. A restraint is imposed on the design in that the closure must be fabricated in the Mech. Engr. shop at UND. The present work proposes a quick opening closure with parts made of commercially available weld neck flanges and weld caps. The flanges are machined so that they can be locked together by means of an external ring manipulated to provide a seal against the internal pressure. A two dimensional photoelastic study was made of the threads of the meshing screws to determine the character of the stresses generated on the mating flanges and on the external ring. A four bar link mechanism provides a way for removing the door after it has been unlocked. The same mechanism will place the door in the proper position to be locked. In improving the design an experimental model should be constructed and tested under the working conditions specified in the design.

NEW SEDIMENTOLOGICAL AND PALEONTOLOGICAL EVIDENCE FOR HISTORY OF LAKE AGASSIZ: SNAKE CURVE SECTION, RED LAKE COUNTY, MINNESOTA. Stephen R. Moran, Lee Clayton, and A. M. Cvancara. N. Dak. Geological Survey and Dept. of Geol., UND, Grand Forks, N. Dak.

The Snake Curve Section is a 70-foot cutbank at the Campbell scarp in SW¼ NW¼ SW¼ sec. 18, T. 151 N., R. 44 W. It is shown diagrammatically below.

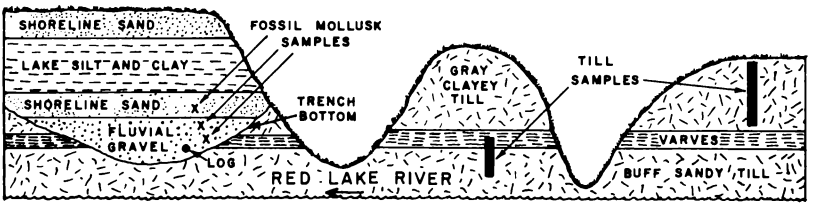

After the uppermost till was deposited, Lake Agassiz dropped well below the Campbell level, and a predecessor of the Red Lake River cut a trench down into the lower till about 12,000 B.P.; the fossil mollusks (20 species) suggest a woodland-flanked river. The lake then gradually rose above the Campbell level, filled the trench, and then dropped and deposited the upper sand as its southern outlet was eroded to the Campbell level for the first time.

TRANSMISSION OF CLAVICEPS PURPUREA CONIDIA BY THE CABBAGE LOOPER MOTH, TRICHOPLUSIA NI (HUBNER). Raul Moreno, V.D. Pederson and J. T. Schulz. Dept. of Plant Pathology and Entomology, NDSU, Fargo, N.D.

Several male sterile barley florets were artificially inoculated with a conidial suspension of Claviceps purpurea (Fr.) Tul. After symptoms of ergot appeared, 25 plants, each bearing at least one infected head, were placed inside a screened cage, and 26 one-day-old individuals of the cabbage looper moth Trichoplusia ni (Hubner) were allowed to associate with them. After 48 hr in the dark, the moths were transferred to a similar cage containing 25 healthy male sterile plants. These procedures were repeated every 48 hours until a total of 78 moths were transferred to the cage containing healthy male sterile plants. After 11 days, 28 percent of the heads of male sterile plants contained one or more infected florets. Moths were observed to feed vigorously on exudate from infected florets. After feeding, moths were examined microscopically. Conidia of the fungus were found associated with the proboscis both externally and internally. In addition, large numbers of conidia were found in the intestinal tract of the vector.

EFFECT OF CAROTID SINUS REMOVAL ON WATER AND ELECTROLYTE EXCRETION IN DOGS. J.C. Passmore. Dept. of Physiology and Pharmacology, University of North Dakota.

The action of the carotid sinus as a blood pressure buffering mechanism is well known. In the present research three sets of dogs were prepared to determine if the carotid sinus plays a role in water and electrolyte balance: a) adult control dogs; b) adult dogs from which the carotid sinuses were removed several weeks previously and c) adult dogs from which the above structures were removed at 6 to 8 weeks of age.

Under sodium pentobarbital the following were determined: blood pressure in the femoral artery, plasma volume with T1824, plasma Na and K, osmotic pressure, hematocrit, urine volume, Na and K. After control samples, animals were infused with 7% body weight of 0.9% saline or 0.45% saline or 0.76% b.w. of 17% saline. The above parameters were followed at intervals. Forty min. after infusion of 0.45% saline, urine output was double in control dogs compared to group b dogs ($P>.05$). Group b dogs showed a higher hematocrit ($P>.05$). Infusion of 0.76% b.w. of 17% saline caused diuresis in all animals but was greater in group b animals than controls ($P>.05$). Plasma volume was reduced more and hematocrit was greater than in controls ($P>.05$). Group c animals were similar to group b animals.

METABOLISM OF p-CHLOROPHENYL N-METHYLCARBAMATE IN THE CHICKEN, G. D. Paulson, M. V. Zehr and C. E. Portnoy. USDA, ARS, Metabolism and Radiation Research Laboratory, Fargo, N. Dak.

One group of mature Leghorn hens was given a single oral dose (10 mg/kg of body weight) of p-chlorophenyl-^{14}C (U) N-methylcarbamate (ring label); a second group was given a single dose of p-chlorophenyl N-methylcarbamate ^{14}C (carbonyl label). Feces, urine and respiratory gases were collected 6, 12, 24, 36 and 48 hours after dosing and analyzed for carbon-14. When the carbonyl-labeled compound was given, 68-83% of the carbon-14 was expired during the 48-hour collection period; whereas no expiratory carbon-14 was detected when the ring-labeled compound was given. Total carbon-14 excreted in the urine accounted for 94-97% of the activity given as the ring-labeled compound and 13% of the activity given as the carbonyl-labeled compound. The feces were a minor route of excretion of carbon-14 given as both the carbon-labeled and ring-labeled compound. Only trace amounts of carbon-14 were detected in the tissues of the chickens when sacrificed 48 hours after the dose was given.

THE GROWTH RESPONSE OF NITROGEN FIXING BLUE GREEN ALGAL SPECIES TO SEVERAL HERBICIDES. J. A. Peary*, D. L. Willson* and L. C. Darlington. Dept. of Biology, CWSC, Ellensburg, Wash.

The herbicides, 2,4-D, Dalapon and Tordon, in concentrations ranging from 100-20,000 ppm (parts per million) were all toxic to the three nitrogen fixing blue green algal species (Nostoc muscorum, Cylindrospermum licheniforme, Anabaena variabilis). Addition of the higher concentrations of the herbicides to the unialgal cultures resulted in a yellowing of the cultures usually within several hours after application. At the lower concentrations C. licheniforme displayed the greatest intolerance to 2,4-D and Tordon. The growth of the three species was about equally inhibited in the lower concentrations of Dalapon, but at the higher concentrations N. muscorum was more tolerant requiring a concentration of 20,000 ppm for complete inhibition. Tordon and 2,4-D yielded complete inhibition at 5,000 ppm. Previous studies have indicated that the ability of certain blue green algae to fix nitrogen is related to their growth. This study provides further evidence of the need to examine not only the effects of herbicides on higher plants but on the soil microflora as well.

SIMPLIFIED PROCEDURES FOR PREPARATION OF 2x2 SLIDES. Vernyl D. Pederson, Dept. of Plant Pathology, NDSU, Fargo, N.D.

Presentation of data visually at scientific meetings usually involves the preparation of 2x2 photographic slides. For maximum legibility of the projected image a typewriter such as the IBM Selectric with orator code 059 type style should be used to prepare tables or figures suitable for reduction to 2x2 slide format. Data may be prepared for graphical presentation by typing directly on non-reproducible, blue cross-section-lined tracing paper. The typewriter is used to mark reference points and to title coordinates, curves or bars. Lines and/or bars are applied by India ink or adhesive tape. The tables or figures are photographed with Kodalith type 3 - 35 mm film, then developed and reversed by special chemical processes to yield high quality positive slides suitable for projection.

TRANSPORT OF SULFATE BY THE SMALL INTESTINE IN-VITRO, Jerome C. Pekas. USDA, ARS, Metabolism and Radiation Research Laboratory, Fargo, North Dakota.

The transport of inorganic radiolabeled sulfate across rat small intestine was investigated with everted and noneverted intestinal sacs incubated (37° C; 95% O_2 - 5% CO_2) in Krebs-Ringer bicarbonate media containing 1.19 mM sulfate ($MgSO_4$) and 1 mg/ml glucose to which $Na_2{}^{35}SO_4$ was added (2 X 10^5 dpm/ml). After 2-hr incubation of everted sacs with identical mucosal and serosal fluids, the $^{35}SO_4^=$ concentration of the serosal fluid from cranial sacs decreased, whereas that from caudal sacs increased. The $^{35}SO_4^=$ was concentrated in the serosal fluid of caudal sacs by net mucosal-to-serosal transport. Inclusion of ouabain inhibitor (10^{-5}M) in serosal and mucosal fluids did not change the general behavior of the $^{35}SO_4^=$ movements. The rate of unidirectional mucosal-to-serosal sulfate transport, measured by excluding $Na_2{}^{35}SO_4$ from the serosal fluid (total $SO_4^=$ concentration of mucosal and serosal fluids was identical; 1.19 mM) and expressed as the average (n = 3) percent $^{35}SO_4$ recovered in the serosal fluid, was 0.7, 2.0, and 8.4% for equal-sized sacs from the cranial, mid, and caudal intestine, respectively. Evidence of slight net serosal-to-mucosal transport (secretion) by everted sacs of cranial intestine could not be verified with noneverted sacs.

MORPHOLOGICAL CHANGES IN THE BRAIN AND CORPORA CARDIACA-ALLATA COMPLEX DURING METAMORPHOSIS OF THE TOBACCO HORNWORM. Dale Picard* and R.A. Bell. USDA,ARS, Metabolism and Radiation Research Laboratory, Fargo, ND 58102.

The brain neuroendocrine system in tobacco hornworms consist of large neurosecretory cells located in the brain whose elongated axons terminate in the corpora cardiaca and corpora allata. The corpora cardiaca are paired structures located posterior to the brain and are attached laterally to the foregut. The paired corpora allata are connected with and lie directly behind the corpora cardiaca. Our purposes were to observe and document the gross structural changes occurring in the brain and associated corpora cardiaca-allata complex during metamorphosis. During larval feeding, the brain is bi-lobed, opaque, and resembles the shape of a peanut; the corpora cardiaca are flat, transparent, and appear largely as a plexus of nerve fibers; the corpora allata are opaque, cylindrical and joined to the corpora cardiaca by 2 or more nerves. At 3-4 days after larval feeding and before pupal cuticle is formed, the optic lobes characteristic of the adult brain appear. With the advent of pupation and formation of adult cuticle, extensive changes occur in the structure of the brain and corpora cardiaca-allata complex. These changes are described and illustrated by photographs.

SYNTHESIS AND PROPERTIES OF ISOXAZOLES: THE 3(2',4'-DICHLOROPHENYL)-5-METHYL-ISOXAZOLE-4-CARBOXYLIC ACID AND SOME OF ITS ESTER AND AMIDE DERIVATIVES. Franz H. Rathmann and James M. Sannes*. North Dakota State University, Fargo, North Dakota 58102.

The 2,4-dichlorobenzaldehyde was converted to its oxime, m.pt. 149°C. Chlorination by Cl_2 yielded the corresponding α-chloroxime, or hydroxamic acid chloride, $C_7H_4ONCl_3$, m.pt. 36°C. Condensation of this chloroxime with sodio-acetoacetic ester yielded the 3(2', 4'-dichlorophenyl)-5-methyl-isoxazole-4-carboxylic acid ethyl ester, m.pt. 150°. Hydrolysis of the ester by alcoholic NaOH gave the free acid. The free acid is then converted by means of thionyl chloride to the acid chloride, and the latter reacted with various alcohols, ammonia, amines, anilines, and hydrazines to form the respective esters, amides, anilides, and hydrazides.

N.M.R. and mass-spectroscopic data were determined. Cf also Rathmann, et.al., Proceedings XXI, pp. 208-209 (1967).

BRAIN GABA LEVELS IN MICE PRETREATED WITH CAFFEINE OR PENTOBARBITAL AND EXPOSED TO 60 ATM HE-O_2. T. Ritter* and B. De Boer. Dept of Physiol. & Pharm., Sch. of Med., UND, Grand Forks, North Dakota.

Gamma aminobutyric acid (GABA), a normal product of brain metabolism, has been shown to increase with hypoxia and with exposure to environments of helium-oxygen (He-O_2) at ambient or high pressures with oxygen partial pressure (PO_2) maintained at 0.2-0.4 atmospheres (atm). Brain levels of GABA decrease with exposure to oxygen at high press (OHP) or convulsant agents.

This investigation was to determine the effects of caffeine, a mild stimulant, and pentobarbital a depressant drug, on brain GABA levels of mice subsequently exposed to He-O_2 at 1 or 60 atm with PO_2 at 0.2-0.4 atm. Control and injected mice were exposed to He-O_2 1 atm or were placed in a Bethlehem Hyperbaric chamber and compressed (1.0 atm/min) to 60 atm, maintained for 12 hrs. and decompressed (0.2 atm/min). The animals were sacrificed and brain GABA levels assayed. At 1 atm pentobarbital mice showed higher GABA levels (267 ug/g brain) than caffeine (239 ug) or controls (231). At 60 atm GABA levels were higher for pentobarbital (272 ug/g) and control (259 ug) but remained low for the caffeine group (226 ug). It appears that high GABA levels protect against high pressure stress. Supported by ONR N0001l-68-A0499.

PHENOLIC MEDIATION OF PLANT MICROSOMAL CELLULOSE BIOSYNTHESIS AND UREA HERBICIDE N-DEMETHYLATION, D. G. Rusness* and D.S. Frear
Crops Research Division, ARS, USDA, Metab. and Rad. Res. Lab., Fargo, North Dakota 58102

Microsomes isolated from etiolated cotton seedling hypocotyl extracts N-demethylate substituted 3-(phenyl)-1,1-dimethylurea herbicides (Phytochem., 8:2157, 1969). Based on the acetolysis assay method (Biochem. Z., 342:308, 1965), these microsomes also incorporate glucose from UDPG into H_2O soluble and insoluble β-1,4-glucan(s) and into H_2O insol. non-cellulosic linkages (assumed to be β-1,3). Passage of the microsomes through Sephadex G-25 separates a low mol. wt. fraction which is sensitive to the Folin-Ciocalteau phenol reagent. Addition of the concentrated fraction back to the microsomes suggests noncompetive inhibition of herbicide N-demethylation. The H_2O sol. β-1,4-glucan synthesis is inhibited 80-90% in the presence of this fraction. The ratio of H_2O insol. β-1,3:β-1,4 glucosyl linkages in the presence of the fraction is 19:1, and is 2:1 in its absence. Data suggest that the concentration of this microsomal bound fraction increases with the time in which the harvested tissue is exposed to the atmosphere. The possibility of an allosteric response to tissue injury is proposed.

IMPLEMENTATION OF AUDIO-TUTORIAL BIOLOGY AT NORTH DAKOTA STATE UNIVERSITY. D. R. Scoby and C. M. Pedersen*. Dept. of Botany, NDSU, Fargo, North Dakota.

Having accepted the philosophy and experimental results of S. Postlethweit and P. Sparks, it was possible to establish an A-T biology program at NDSU in six weeks.

In the fall of 1969, 750 students were enrolled in the biology program designed as follows:

1) General Assembly Sessions (GAS)-Two hours per week used for administrative purposes, tests, films, and applicable lectures dealing with environmental, social, and moral problems.

2) Small Assembly Sessions (SAS)-One hour per week, conducted by a graduate student, allowing personal contact and an opportunity to discuss biological problems facing man.

3) Independent Study Session (ISS)-Open 68 hours per week and handled by 15 undergraduate lab assistants.

Of 682 students evaluating the program, 82.6% felt the A-T course should be continued, while 17.4% answered in the negative. Results as to grade received and average time spent in lab revealed the following correlation: A-2.78 hours, B-2.2 hours, C-1.77 hours, D-1.2 hours, and F-0.39 hours. Data indicated a greater percentage of A's and B's and a lesser percentage of F's as compared to previous years.

THE EFFECTS OF PRESSURE ON LIVER PROTEINS. G.C. Sharma, Dept. of Physiol. and Pharm., Sch. of Med., UND, Grand Forks, N. Dak.

Previous investigations in our laboratory have shown that mice maintained at high pressures (HP) for 24 hrs. or longer lost weight although supplied with food and water. It has also been shown that liver weights of animals maintained at 60 atmospheres (atm) for 12 hours were less than for controls at 1 atm.

We have observed that mice subjected to 60 atm for 24 hrs. lose approximately 10% of their body weight. The loss occurs primarily during the first 6 hrs. after being placed in the hyperbaric chamber. Pretreatment with caffeine appears to enhance the weight loss. This loss occurs irrespective of availability of water during the experimental period. The dry-wet weight ratios of livers were the same for HP and ambient animals suggesting that weight loss was due to changes in solid tissue. Previous reports have indicated that microsomal content of livers of mice at 60 atm was less than at 1 atm; if animals were pretreated with pentobarbital before HP exposure, the liver microsomal levels were significantly lower. Pretreatment with pentobarbital reduced mortality ratios in mice subjected to 60 atm. Supported by ONR N00014-68-A0499.

CHANGES IN WHOLE BLOOD STORED AT VARIOUS TEMPERATURES AND IN VARIOUS GASEOUS ENVIRONMENTS. S.J. Sherry and C.A. Zogg. (spon: R.H. Wilson). Dept. of Physiology and Pharmacology, Sch. of Med., Univ. of N.Dak., Grand Forks, N.Dak.

Stored human erythrocytes undergo progressive deterioration lesions which render the blood unfit for transfusion purposes. The object of this study was to determine if gaseous metabolic inhibitors could supplement or replace low temperatures in delaying these lesions. The blood samples were stored in an acid-citrate-dextrose media, gassed with N_2 or CO_2 and stored at either 4° or 21° C for 21 days. After 0, 6, 11, 15, 18, 20 and 21 days of storage, aliquots were assayed to determine the plasma levels of K+ and Na+ ions, glucose, and lactic acid. The whole blood pH and osmotic fragility of the erythrocytes were also determined. The two types of gases used did not greatly delay the progression of the storage lesions. Storage with CO_2 showed some delay in erythrocyte deterioration at both temperatures studied. This was exemplified by reduced glucose utilization and lactic acid production as compared to the blood stored with air or N_2. The exchange of K+ and Na+ ions between the cells and plasma was greater for samples stored with CO_2 than with the other gases. ONR

COMPARISON OF MALE GENITALIA OF FOUR SPECIES OF ANTS OF GENUS FORMICA L., J. Singleton* (spon: P.B. Kannowski). Dept. of Biol., Univ. N. Dak., Grand Forks, North Dakota.

Male genitalia of Formica obscuripes, F. ulkei, F. subnuda, and F. pergandei were described, figured and measured. Mean, range, coefficient of variability, standard deviation and coefficient of difference were calculated for comparison of twenty-one different genitalia measurements. Formica subnuda and F. pergandei showed least variation in size, while F. obscuripes varied most with F. ulkei being intermediate. The components of the genitalia of these four species are similar. The length of the tactile hairs on the stipes and pygostyles, the curvature of the vosellae and the terminal ends of the sagittae showed differences that may be use to separate species. These species occupy similar habitats and overlap in their mating flights. The males are indistinquishable by casual observation as well as difficult to identify with existing taxonomic keys, hence a study of the genitalic valves is useful in identifying species. Certain genital variations are consistent within each species and can be valuable taxonomically in association with other morphological characters.

EFFECT OF DEPTH OF SUBMERGENCE ON GERMINATION OF ECHINOCHLOA CRUSGALLI (L.) BEAUV., F. E. Smeins*. Dept. of Biol., Univ. of N. Dak., Grand Forks, North Dakota.

Echinochloa crusgalli is an introduced European annual grass that grows in cultivated fields, waste areas and on margins of disturbed, ephemeral, non-saline wetlands. The objective of this study is to determine influence of depth of submergence on germination and growth. Three replicates of 100 seeds were germinated under six treatments: moist germination towels in the dark, petri dishes with moist germination paper in the light, saturated soil (light), soil submerged 10 cm (light), submerged 15 cm (light) and submerged 20 cm (light). Germination values were 85, 84, 61, 45, 25, and 5% for the six treatments, respectively. At 20 cm no seedlings survived. Cold treatment and light are not necessary for germination. Restriction from deep waters is primarily related to germination requirements. The mechanism for lack of germination has not been delimited but the gaseous environment, probably oxygen tension, may be the controlling factor.

IMMUNOCHEMICAL PROPERTIES OF WALKER 256 CARCINOMA HISTONES. H. W. Spencer and R. H. Wilson. Dept. of Physiology and Pharmacology, Sch. of Med., Univ. N. Dak., Grand Forks, North Dakota.

It had been reported that calf thymus histones are antigenic, nonantigenic, or weakly antigenic. Experiments were carried out to test for complement fixing antibody production against histones of Walker 256 carcinoma. Histones were separated from tumors by ethanol-HCl leeching. The resulting nucleohistones were grossly separated by Sephadex gel filtration and the resultant fractions separated by gradient elution on cellulose column. The histones were conjugated to bovine serum albumin. The histones were dissolved in normal saline and emulsified in complete Freund's adjuvant. The antigens were injected subcutaneously into the toepads of male New Zealand rabbits. Intraperitoneal booster doses were given at 3 and 4 weeks. Sera were obtained by cardiac puncture and frozen. Microtiter complement fixation test was utilized showing that the histones were weakly antigenic. Supported in part by American Cancer Society, North Dakota Division, Inc.

HYDROXYLATION OF 2,4-DICHLOROPHENOXYACETIC ACID IN PLANTS, R. C. Steen* and J. R. Fleeker. Dept. of Biochem., N. Dak. State Univ. Fargo, North Dakota.

Studies on the mechanism of 2,4-D inactivation by hydroxylation were conducted with a number of economically important weeds of North Dakota. The amounts of 2-chloro-4-hydroxy-, 2,3-dichloro-4-hydroxy-, and 2,5-dichloro-4-hydroxyphenoxyacetic acids produced in these plants from the herbicide are reported. The results are discussed with regard to the hydroxylation-induced migration reactions of aryl groups.

TEMPERATURE CHANGES IN THE RAT DURING EXPOSURE TO HE-O_2 BETWEEN 1-40 ATM. L.C. Stetzner and B. De Boer, Dept. of Physiol. and Pharm., Sch. of Med., UND, Grand Forks, North Dakota.

Helium (He) at ambient temperature and pressure is known to affect the thermal balance of homiotherms. This disturbance has been reported to have a metabolic equivalent of 86° F (He-O_2) as compared to 75-76° F (air). Our experiment was designed to determine temperature responses in rats maintained in He-O_2 at constant temperature (86°F) at pressures from 1-40 atm. Thermister probes were attached and the animal was restrained in a plexiglass cage and placed in a Bethlehem Hyperbaric chamber. Temperatures were recorded by a tele-thermometer (Yellow Springs Instrument Co.) during compression at 0.33 atm/min to 40 atm, 4-hour exposure at this pressure, and decompression at 0.08 atm/min (total time 14 hrs.). Control animals were exposed to He-O_2 or air at ambient pressure. Increased pressure of the He-O_2 environment was accompanied by decreases in body temperature. At 40 atm the mean temperature decreases were: surface 5.1°F, subcutaneous 6.3°F and rectal 5.5°F. These differences, based on 10 experimental and 10 control animals provide direction for further studies on the regulation of body temperature while under pressure. Supported by ONR N00014-68-A-0499.

EFFECTS OF CAFFEINE UPON PHYSIOLOGICAL FUNCTIONS OF MICE MAINTAINED AT HIGH PRESSURE. D. A. Stites*, J. Reinhardt* and B. De Boer. Dept. of Physiol. and Pharm., Sch. of Med., UND, Grand Forks, North Dakota.

Earlier investigations have shown that subjecting mice to 60 atmospheres (atm) for varying time periods was accompanied by weight loss and changes in liver and brain constituents. Mice pretreated with caffeine (100 mg/kg) showed greater weight loss than high pressure controls. When maintained at 60 atm for 12 hours approximately 35% of the caffeine animals died before decompression was completed. Maintaining mice at 60 atm for 6 hours was also accompanied by increased mortality. Liver studies showed a greater decrease in microsomal protein N for mice pretreated with caffeine than for high pressure controls. Supported by ONR N00014-68-A0499.

STRATIGRAPHIC SIGNIFICANCE OF FOSSIL RHINOCEROS REMAINS IN SLOPE COUNTY, NORTH DAKOTA, W. J. Stone. Dept. of Geol., Univ. N. Dak., Grand Forks, No. Dak.

The recent recovery of a complete rhinoceros mandible from strata tentatively mapped as Miocene Arikaree Formation is of considerable stratigraphic interest. The fossil was collected from a green channel sandstone 20 feet below the top of White Butte in Slope County, North Dakota (SW¼NE¼SE¼ sec. 25, T. 134 N., R. 101 W.). The specimen resembles the genus Subhyracodon, a characteristic middle Oligocene form collected lower in the section elsewhere in the state, but the much larger overall size and circular shape of the ramus suggests Diceratherium, a late Oligocene to Miocene genus.

The occurrence of a late Oligocene to Miocene rhinoceros in the Arikaree (?) strata is significant in that 1) it implies a transitional age for these deposits and 2) it supports the possibility that the green sandstones capping buttes in southwestern North Dakota may merely be channel facies of the upper Brule Formation (late Oligocene). Further collection from these strata is neccessary to clarify their age.

GEOGRAPHIC, GENETIC AND SPECIES VARIATIONS OF DIPTERAN ACCESSORY GLAND PROTEINS. **A.C. Terranova and R.A. Leopold, USDA, Met. and Rad. Res. Lab., Fargo, N. Dak.**

The factor responsible for preventing remating in the female house fly originates in the accessory secretion of the male. It has been identified as a proteinaceous material resembling the protamines. Since mating refusal appears to be common to many species of Diptera, it was desirable to determine if the proteins contained in the accessory secretion of various related strains and species were similar. Disc gel electrophoresis of a physiologically active acid extract of the isolated ducts was performed on 8 geographic and 16 genetically different strains of Musca domestica. The acrylamide gels were electrophoresed in a system designed for the separation of basic proteins. The resultant protein patterns showed no major qualitative or quantitative differences. Electrophoresis of the accessory glands of related Diptera showed some qualitative and quantitative differences, but also a great deal of similarity. Bioassay of the extracts from the different species resulted in mating refusal between species as well as within species. From the results it is tentatively concluded that a similar mechanism is responsible for second mating inhibition.

THE EFFECT OF AGE AND DOSE ON THE VIREMIC RESPONSE IN CHICKS INFECTED WITH AVIAN RETICULOENDOTHELIOSIS VIRUS (STRAIN T).
K. D. Thompson* and R. G. Fischer. Dept. of Microbiology, Univ. of N. Dak., Grand Forks, N. Dak.

A quantitative study of the effect of age and dose on the viremic response was determined in RE virus infected chicks. In the study of the age effect two groups of chicks were used, 8 hours old and 7 days old. Each chick in both groups received 75 LD_{50} of RE virus. Blood was collected from each group of chicks at various times throughout the viremia and assayed for RE virus. The results showed an increase in the virus titer corresponding with an increase in time post-infection. A peak titer of 4.6 LD_{50} of virus appeared on days 9 and 10 post-infection with little or no difference in the virus titers due to a difference in age. In the study of the dose effect on the viremic response, four groups of chicks were injected with different doses of RE virus; 7.5, 25, 50, and 75 LD_{50} per chick. Blood was collected from each group of chicks and assayed for virus daily beginning on day 8 post-infection. The results indicated peak virus titers of 4.6 LD_{50} of virus on days 10 and 11 post-infection. However, there was a slower initial response and a slightly lower peak titer in the groups receiving the lower doses.

THE AGE AND GROWTH OF THE YELLOW PERCH PERCA FLAVESCENS (MITCHILL) IN THE LITTLE MISSOURI ARM OF LAKE SAKAKAWEA, NORTH DAKOTA, 1968,
C. H. Wahtola Jr.*, B. L. Evenhuis* and J. B. Owen. Dept. of Biol., Univ. N. Dak., Grand Forks, North Dakota.

The age, rate of growth and biological characteristics of yellow perch, Perca flavescens (Mitchill), in the Little Missouri arm of Lake Sakakawea were investigated during the summer of 1968. A total of 1,968 yellow perch were captured with gill nets and seines. Scale samples were projected and read from 372 perch, and data from these were used for age assessment and growth calculations. Four age classes were distinguished. The sex ratio in the catch from gill nets was 2.91 females per male and 1.64 females per male with seines. The overall sex ratio was 2.38 females per male. The population was found to be in poor condition as indicated by the low n value for the length weight regression (2.4266) and a coefficient of condition of 1.03. It was postulated that stress and competition with goldeye (Hiodon alosoides) along with a food deficiency for the older fish may be the reason for the stunted population.

THE PRESETTLEMENT VEGETATION OF RICHLAND COUNTY, NORTH DAKOTA, Linda K. Walsh and Robert L. Burgess. Dept. of Botany, NDSU, Fargo, North Dakota.

The original land survey notes taken in 1871 were the basis for a study of the presettlement vegetation of Richland County, N. D. Pre-1900 geological, topographic, and plat maps were helpful in reconstructing the exact location of natural features in the county. The surveyors' notebooks yielded quantitative and qualitative information regarding timber, savanna, shrubland, tall grass prairie and marsh found in the county. The presettlement vegetation of Richland County was predominately tall grass prairie with smaller areas of forest, savanna, and marsh. A floral list comprising thirty species was compiled, and notes on environment were tabulated. A detailed map of the vegetation of the county prior to settlement is presented.

A COMPARISON OF THE EFFECT OF LENGTH OF EXPOSURE TO HIGH PRESSURE HELIUM-OXYGEN ON BRAIN GAMMA-AMINOBUTYRIC ACID LEVELS IN MALE AND FEMALE MICE. Dou-Mei Wang, Roderick L. Reinke, and Russell H. Wilson. Dept. of Physiology and Pharmacology, Sch. of Med., Univ. N. Dak., Grand Forks, North Dakota.

The effect of helium (He) on brain gamma-aminobutyric acid (GABA) levels was studied in 124 male and 128 female mice. These mice were exposed to He-oxygen (O_2) mixtures at either 1 or 60 atmospheres (atm) for variable periods of time with physiologic O_2. The mice were compressed to 60 atm for 1 min, 12 hrs, or 24 hrs. After decompression, the brains were removed and GABA levels determined. Significant increases in GABA were found in all mice exposed to He-O_2 at 1 atm, in males at 60 atm for 1 min, and in both sexes at 60 atm for 24 hrs. There was no significant difference in GABA levels between sexes when all groups were considered. Both pressure and the He atm contributed to the increase in GABA. Supported in part by ONR (N00014-68-A-0499).

EFFECT OF HELIUM AT AMBIENT AND 60 ATMOSPHERES ON THE ACTIVITY OF GLUCOSE-6-PHOSPHATASE IN THE MOUSE LIVER. Tsun-Wen Wang, Roderick Reinke, Robert Olson, and Russell H. Wilson. Dept. of Physiology, Sch. of Med., Univ. of N. Dak., Grand Forks, North Dakota.

Nitrogen (N_2) at 7 atm is an anesthetic. Helium (He) was substituted for N_2 in the breathing mixture. This study was to determine the effects of He on the hepatic mammalian glucose -6-phosphatase activity. Ninety-five male and 81 female mice were exposed to He-oxygen (O_2) mixtures varying from 1 to 60 atm for variable periods of time with a physiologic P_{O_2}. For each sex group, there was an ambient air control group of mice. All N_2 was removed from the chamber with He-O_2 and compressed to 60 atm with He for 1 min, 12 hrs and 24 hrs. Decompression was at a rate of 0.15 atm per min. The livers were removed and placed in 0.25 M of sucrose at 0° C. Glucose-6-phosphatase activity as P_1 was then determined. Analysis of the data showed a significant increase in the microsomal glucose-6-phosphatase activity in all mice. Glucocorticoid and/or catecholamine increases could have caused the increased enzyme activity. Supported in part by ONR N0001468A0499.

THE EFFECT OF MELATONIN ON CORTICOSTERONE LEVELS IN THE RAT, R. E. Wiederanders, John Young* and Robert Hapip*. Harmon Park Res. Lab., Williston, N. Dak.

We have proposed a mechanism whereby the pineal gland might affect the adrenal output (Proc. N. Dak. Acad. Sci., 21, 171, 1967) and have gathered some evidence for it by injecting melatonin into the median eminence and under the skin of the white rat. We found a decrease in plasma corticosterone in the injected animals that is significant to the 2% level of confidence.

NORTH DAKOTA FLEAS. III. ADDITIONAL RECORDS FROM MAMMALS. Carlene E. Woods and Omer R. Larson. Dept. of Biol., Minot State College, Minot, N. D. and Dept. of Biol., Univ. N. Dak., Grand Forks, N. D.

During the course of an ecological study of Echinococcus multilocularis by one of us (C.E.W.), extensive numbers of small mammals were collected. Between 1 June 1969 and 30 November 1969, 954 of these mammals were examined for fleas. A total of 410 fleas were removed, and subsequently processed and mounted on slides. Among these fleas there appear to be five species previously unreported from North Dakota. These, represented by 16 specimens, are: Rhadinopsylla (Rectofrontia) fraterna, Malaraeus euphorbi, Megabothris lucifer, Ctenophthalmus pseudagyrtes, and Corrodopsylla curvata curvata. These additions now bring to 32 species the known flea fauna of the state.

EFFECT OF A THIOCARBAMATE HERBICIDE (DIALLATE) ON EPICUTICULAR LIPIDS OF PISUM SATIVUM. Gary L. Zander, Gerald G. Still* and David G. Davis* Metabolism and Radiation Research Laboratory, USDA-ARS and Department of Biochemistry, NDSU, State University Station, Fargo, N. Dak.

Epicuticular lipids were reduced by 80% when peas (Pisum sativum) were treated with S-(2,3-dichloroallyl)diisopropylthiocarbamate (Diallate) in the vapor phase. These results were supported by scanning electron microscopy and carbon replica transmission electron microscopy. The distribution of the surface lipids between classes of compounds was not significantly altered, except in the case of the n-alcohols, which were reduced by 20%. It is speculated that Diallate interferes with the biosynthesis of a precursor to the elongation-decarboxylation pathway of surface lipid synthesis.

THE SUBARACHNOID SPACE INTERPRETED AS A SPECIAL PORTION OF THE CONNECTIVE TISSUE SPACE. R. G. Frederickson* and F. R. Haller* (spon: F. N. Low). Dept. of Anatomy, Sch. of Med., Univ. N. Dak., Grand Forks, North Dakota.

The subarachnoid space of vertebrates contains cerebrospinal fluid which surrounds the brain and spinal cord. This space is customarily interpreted as an epithelial-lined cavity supported by connective tissue (Ham, A. W., Histology, p. 517, 6th ed., 1969). However, the leptomeningeal cells lining this cavity do not form a typical squamous epithelium. In fine structure they do not possess boundary (basement) membranes. They also lack the junctional complexes that are common to all epithelia. Gaps between cells allow communication between the subarachnoid space and the extracellular space of the meninges, which contains various types of connective tissue fibrils. Blood cells and free macrophages are found in areas of open communication. In fact, leptomeningeal cells themselves possess characteristics similar to fibroblasts. These cells are highly attenuated like fibroblasts and contain similar dispositions of ergastoplasm, Golgi complex, lipid droplets and cytoplasmic vacuoles. In view of these morphologic features the subarachnoid space is interpreted to be a cleared-out, fluid-filled compartment of the connective tissue space.

AUTHOR INDEX

AUTHOR INDEX

PROCEEDINGS

of the

NORTH DAKOTA ACADEMY OF SCIENCE

VOLUME XXIV

Part II

(PAPERS)

Official State Academy

(Founded December, 1908)

OFFICERS

President	Roland G. Severson
President-Elect	Robert L. Burgess
Secretary-Treasurer	Ben G. Gustafson
Historian	George A. Abbott

Additional members of the Executive Committee:

William E. Dinusson
Myron L. Freeman
Jerome M. Knoblich
Paul D. Leiby
Franz H. Rathmann
Warren C. Whitman

Published jointly by the University of North Dakota, North Dakota State University, Minot State College, Jamestown College and Dickinson State College.

1971

GRAND FORKS, NORTH DAKOTA

PROCEEDINGS

of the

NORTH DAKOTA ACADEMY OF SCIENCE

VOLUME XXIV

Part II

(PAPERS)

Official State Academy

(Founded December, 1908)

Published jointly by the University of North Dakota, North Dakota State University, Minot State College, Jamestown College and Dickinson State College.

1971

GRAND FORKS, NORTH DAKOTA

PRINTED BY THE UNIVERSITY OF NORTH DAKOTA PRESS

EDITOR'S NOTE

On May 1 and 2, 1970, the 62nd annual meeting of the North Dakota Academy of Science was held at the University of North Dakota, Grand Forks, North Dakota, Presentations at that meeting were published in April, 1970 as Proceedings of the North Dakota Academy of Science, volume XXIV, Part I, Abstracts. This second part of the volume includes those complete papers which were submitted in manuscript form at the time of the meeting.

Grand Forks, North Dakota — Alan M. Cvancara

TABLE OF CONTENTS

TABLE OF CONTENTS

NUCLEAR CONDITION IN GERMINATING TELIOSPORES OF *USTILAGO HORDEI* (PERS.)[1]

L. L. Jensen[2] *and R. L. Kiesling*

Plant Pathology Department

North Dakota State University, Fargo, North Dakota 58102

INTRODUCTION

Ustilago hordei (Pers.) Lagerh., the casual organism of barley covered smut, invades only during the seedling stage and produces smut sori in the barley inflorescence and upper leaves. Selfing studies, using sporidia from single teliospores, are being conducted to determine the number of genes in *U. hordei* conditioning virulence on the barley variety Pannier (C. I. 1330). These studies, in many instances, produced unexplainable results. The 3-celled promycelium should have both a plus (+) and minus (−) mating type present and, therefore, be capable of infecting a susceptible barley variety (2). Although this was found to be true, promycelia with only a single mating type, *i.e.*, either (+) or (−), were found (Jensen, unpublished data). This study was undertaken to ascertain if any nuclear condition in the germinating teliospore was responsible for the results obtained and to determine where meiosis takes place.

The germinating teliospore of *U. hordei* produces a promycelium with three cells. However, four-celled promycelia have been reported (4). The spore acts as the fourth cell when the promycelium is three-celled. Each cell of the promycelium produces a haploid sporidium by budding when the teliospore is germinated on an enriched nutrient media. Under natural conditions and on minimal media, the sporidial stage is omitted, and fusion between promycelial cells occurs (2). After fusion of compatible promycelial cells or sporidia, an infection hyphae is produced and infection occurs in the presence of a susceptible host.

Fischer and Holton (2) described the migration of a diploid nucleus into the promycelium during teliospore germination. The nucleus undergoes a mitotic division with one diploid nucleus migrating toward the spore and the other migrating toward the tip of the promycelium. A cross wall is formed between the diploid nuclei. The two nuclei undergo a meiotic division to form a three-celled promycelium and a one-celled spore, each cell being haploid and uninucleate. Each cell then produces a haploid sporidium.

Paravicini (10), according to Fischer and Holton, reported that the first division takes place in the spore with one nucleus migrating into the promycelium and the other remaining in the spore. The

[1]Journal No. 242 North Dakota Agricultural Experimental Station.
[2]Currently 1st Lt., U.S. Air Force.

nucleus remaining in the spore then can give rise to another promycelium.

METHODS AND MATERIALS

Cytological study.—Teliospores of race 10, *U. hordei* were germinated on 2% potato dextrose agar (PDA) or on 22 x 55 mm glass cover slips placed in a humidity chamber. Spores placed on PDA required 12 hours to germinate; those placed on cover slips required 24 hours. After germination, the cover slips were removed from the humidity chamber and allowed to air dry to affix the germinated spores to the cover slip. The teliospores germinated on PDA were affixed to cover slips coated with Haupt's (5) adhesive by cutting small blocks of agar on which the spores had germinated and inverting the block onto a cover slip. After the agar block had remained on the cover slip for approximately five minutes, it was carefully removed and the cover slip allowed to air dry.

The germinated teliospores were stained using a modification of Keble and Jay's (5) fluorescent staining procedure (Kiesling, unpublished data). The procedure was as follows:

1. Kill and fix for 30 minutes in Carnoy's fixative (5).
2. Wash 2 minutes in Keeble's buffer (Keeble's buffer consists of 0.1M phosphate buffered saline (0.85% NaCl), pH 7.1, containing 0.2% phenol.)
3. Wash 5 minutes in Keeble's buffer.
4. Stain for 5 minutes. (The stain consists of one part 1/200 solution of coriphosphine O in 0.1M acetate buffer, pH 4.4; and 9 parts Keeble's buffer.)
5. De-stain for 5 minutes in Keeble's buffer.
6. De-stain for 2 minutes in Keeble's buffer.
7. Remove cover slip; drain or blot dry.
8. When cover slip is dry (not too dry for best results) mount with mineral oil on glass microslide.

If the cover slip preparation dried too much, colors faded; however, the colors could be restored by rewashing in Keeble's buffer.

After staining, the germinated teliospores were examined with a Leitz fluorescent microscope to determine the nuclear condition of the promycelium and sporidia.

Infection study.—Spores of race 10, *U.hordei*, were germinated on PDA until the four sporidia were formed (12 hours). Then, by using a micromanipulator (Brinkman Model 3050.46) the four sporidia were separated from the promycelium and teliospore. The promycelium was then separated from the teliospore. The six components, *i.e.*, four sporidia, promycelium, and teliospore, were moved to separate areas on the PDA, and the colonies were allowed to develop from them. The individual colonies were transferred to V-8 juice agar (11).

Mating type for each component was determined using the method described by Bauch (1) and modified by Lade and Jensen (8). Mating type in *U. hordei* is controlled by a single factor pair. Thus two sporidia have a (+) mating type and two a (−). For infection to take place, a (+) and (−) sporidium must unite to form a compatible dikaryon.

Individual mono-sporidial lines plus lines derived from the promycelium and teliospore were mated according to the results of the Bauch test. Nonmated monosporidial lines and incompatible mating checks were used to verify the results of the Bauch test (Table I). All fungal lines were inoculated onto the susceptible barley variety, Odessa (C.I.934) using the method described by Lade and Kiesling (9). The inoculated seeds were then planted, three seeds per pot in autoclaved soil in six-inch pots. The plants were grown to maturity under 16 hour day lengths at 22±2 C. At maturity the presence of smutted heads was used to indicate that two lines were compatible and the percent smutted heads was recorded.

TABLE I
COMPATIBLE AND NONCOMPATIBLE CROSSES OF THE COMPONENTS OF A SINGLE TELIOSPORE

Component	Mating type	Noncompatible crosses	Compatible crosses	
1. Sporidium	(−)	1x2	1x3	3x5
2. Sporidium	(−)	3x4	1x4	4x5
3. Sporidium	(+)	1x5	2x3	5x6
4. Sporidium	(+)	2x5	2x4	
5. Promycelium	(−)	3x6	1x6	
6. Spore	(+)	4x6	2x6	

RESULTS AND DISCUSSION

Stained teliospores showed considerable variability in both their morphology of germination and the nuclear condition of the promycelium and sporidia. Spores germinated on PDA produced three-celled promycelia. However, four-celled promycelia were not uncommon, occurring approximately 2% of the time. A similar situation was reported by Huttig (4). Typical sporidia were formed from each promycelial cell. Each sporidium was produced near a septation except for the terminal sporidium which emanated from the tip of the promycelium. Only one true promycelium was observed emanating from a single teliospore. Although when the promycelium was removed from the spore, a large sporidium was initially produced. This large sporidium underwent a nuclear division typical of other sporidia. When teliospores were germinated on minimal media sporidia were notably absent. Most promycelium produced conjugation tubes between the promycelial cells (Figure 1D). Some promycelia were observed producing both conjugation tubes and sporidia.

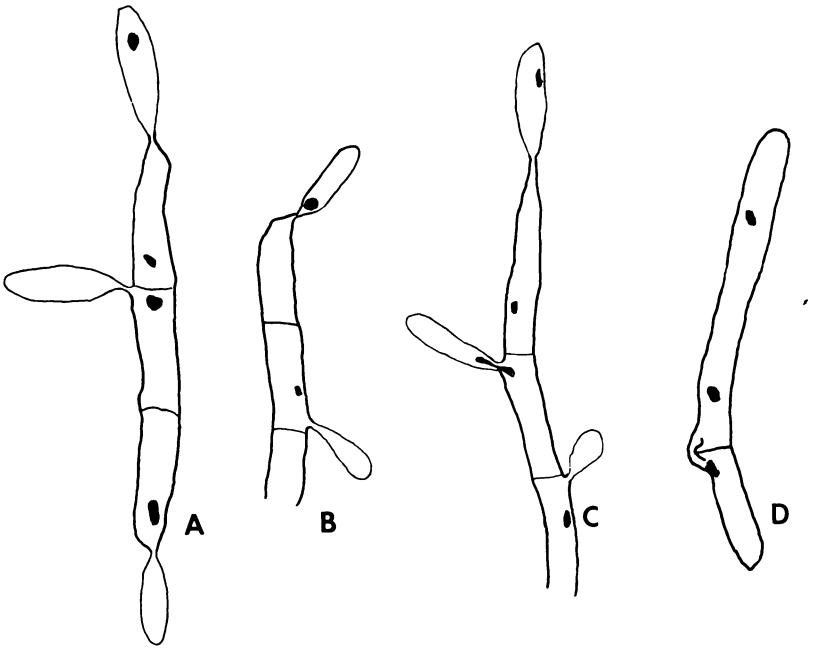

FIGURE 1—Variations in the nuclear condition of promycelia from germinated teliospores of *U. hordei* (X1000). A) Failure of mitosis between promycelial cell and sporidium resulting in an anucleate sporidium. B) Failure of mitosis between promycelial cell and sporidium resulting in an anucleate promycelial cell. C) Normal mitosis between promycelial cell and sporidia. D) Conjugation tube between promycelial cells.

The nuclear condition of the promycelium and sporidia was variable. Two divisions were observed occurring in the promycelium. A single nucleus, assumed to be diploid, migrated to the center of the promyclium. This nucleus underwent a division and each of the two daughter nuclei migrated in opposite directions, one towards the terminal end of the promycelium, the other towards the spore. A second division occurred in each of the daughter nuclei. The tetrad of daughter nuclei produced by the two divisions were the only nuclear divisions observed to occur in the promycelium. Further divisions involved the production of sporidia by budding and

were assumed to be mitotic. When conjugation tubes were produced, no further divisions occurred. It was observed during sporidial production and the subsequent nuclear division usually associated with it, that the nucleus often failed to divide. This nucleus would then migrate to the baseof the sporidium where it might divide. This would result in a sporidium with two nuclei, no nucleus, or a single nucleus. The corresponding promycelial cell would then be anucleate (Figure 1B). The same situation could occur in a promycelial cell which would leave an anucleate sporidium (Figure 1A). This situation was observed in all promycelial cells and not confined to any particular cell.

Inoculation of a susceptible barley variety (Odessa) with lines derived from the teliospore components confirmed that the promycelium was of only one mating type. All nonmated monosporidial lines and mated incompatible lines (Table I) gave no infection whereas all compatible crosses tested gave a consistently high infection (35% or greater).

Typical promycelium of *U. hordei* are reported to contain both a (+) and (−) mating type and are capable of infection (2). Although this was generally the case, the promycelium was shown to be atypical in many instances. Mating type tests and infection studies demonstrated that some promycelia were of only one mating type and unable to infect the susceptible barley variety, Odessa. Cytological evidence suggests that the cause of the single mating type condition was due to a failure of mitosis when the nucleus was at the junction of the promycelium and the sporidia.

Previous reports of the germination process do not show any abnormalities in the process (2). However, considerable morphological variability was found to be the case. This type of variability was reported to occur in *U. maydis* by Kernkamp and Petty (7).

Holton (3) reported that the first division in the promycelium was mitotic and the second meiotic. According to his observations, the two terminal cells of the promycelium should be of opposite mating type since the second division is the only segregating division. This was not found to be the case. Although two divisions were observed, segregation for mating type was found to occur in the first division. Sporidia of the same mating type were isolated from the two terminal promycelial cells 67% of the time. Sporidia of opposite mating type were isolated 33% of the time and were presumed to be the result of crossing over during the first division. Reports by Paravicini (11) that the first division occurred in the teliospore were not confirmed. If the first division were mitotic and occurred in the teliospore the spore should contain nuclei of both mating types. In no case was a teliospore found that contained both mating types. The above data indicate that meiosis takes place in the promycelium and that the two divisions observed represent the two divisions of meiosis.

LITERATURE CITED

1. Bauch, R. 1922. Kopulationsbedringungen und sekundäre geschlechlsmerkmale bei *Ustilago violaceae*. Biol. Centralbl. 42: 9-38.
2. Fischer, G.W., and C. S. Holton. 1957. Biology and control of the smut fungi. Ronald Press Co., New York. 622 p.
3. Holton, C.S. 1936. Origin and production of morphologic and pathogenic strains of the oat smut fungi by mutation and hybridization. J. Agr. Res. 52:311-317.
4. Huttig, W. 1931. Uber den einfluss der temperatur anf die keimung and geschlechtsvertteilung bei brandpilzen. Zeitschr. f. Bot. 24:529-557.
5. Jensen, W. A. 1962. Botanical histochemistry. W. A. Freeman and Co., San Francisco. 408 p.
6. Keeble, S. A., and R. F. Jay. 1962. Fluorescent staining for the differentiation of intracellular ribonucleic acid and deoxyribonucleic acid. Nature 193: 695-696.
7. Kernkamp, M. F., and M. A. Petty. 1941. Variation in the germination of chlamydospores of *Ustilago zeae*. Phytopathology 31: 333-340.
8. Lade, D. H., and L. L. Jensen. 1967. The use of differential media in determining the Bauch test for *Ustilago hordei* (Pers.) Lagerh. Proc. North Dakota Acad. of Sci. 21: 204.
9. Lade, D. H., and R. L. Kiesling. 1967. A method for sporidial inoculations for covered smut of barley. Proc. North Dakota Acad. of Sci. 21: 121-123.
10. Paravicini, E. 1917. Untersuchungen uber das verhalten der zellkerne bei der fortpflanzung der brandpilze. Ann. Mycol. 15: 57-96.
11. Tuite, J. 1969. Plant pathological methods. Burgess Publ. Co., Minneapolis. 239 p.

TEMPERATURE SENSITIVE GENES GOVERNING RESISTANCE TO RACE 6, *USTILAGO HORDEI* (PERS.) IN SEVERAL SPRING BARLEY VARIETIES[1]

R. L. Kiesling

Plant Pathology Department

North Dakota State University, Fargo, North Dakota 58102

INTRODUCTION

The reactions of spring barley varieties to the 13 races of *Ustilago hordei* (Pers.) Lagerh., are classified as susceptible, resistant, or intermediate depending upon the percent of plants that become infected following innoculation of a variety. Barley varieties classifed as inter-

[1]Journal No. 241, North Dakota Agricultural Experiment Station.

mediate in their reaction to *U. hordei* may develop from 5 to 26 percent smutted plants (8). The percent of infected plants developing after each inoculation is nearly constant for specific combinations of race, temperature during growth, and variety (1, 8).

Kiesling (1) reported that Jet gave an intermediate reaction to race 6, *U. hordei*. Thomas and Person (9) attributed an intermediate type reaction to a gene for virulence in *U. hordei* which the authors described as the "5-percent virulent" gene. Three genes governed resistance to race 6 in the highly resistant variety, Pannier (2). One of these genes appeared to be incompletely dominant and temperature sensitive. Pannier and Jet had genes governing resistance to race 6 which were allelic or closely linked (2).

Infection of barley plants by *U. hordei* may be total, all tillers infected, or partial, some tillers on the plant remaining healthy. The ratio of totally to partially infected plants is affected by the temperature at which the inoculated plants are grown and their genetic composition conditioning resistance (1, 3, 4).

MATERIALS AND METHODS

Seeds of the covered barley varieties, Odessa (C.I.934), Chevron (C.I.1111), Pannier (C.I.1330), and the F_2 progeny of their crosses were dehulled by hand, soaked in water for 2 hours and germinated in moist chambers for 22 hours at 20°C. Seed of the naked barley variety, Jet (C.I.967), was soaked for 2 hours, germinated for 22 hours in a moist chamber at 20°C and then depericarped with sharp, pointed tweezers to expose the coleoptile.

The germinated barley seeds of the varieties and their crosses were inoculated with a 25 percent concentration of spores of race 6, *U. hordei*, in talc. The inoculated seedlings were incubated for 24 hours at 20°C. The inoculation was repeated at the end of the first incubation period, and the seedlings were again incubated for 24 hours at the same temperature. Following incubation, each seed lot was divided in half and planted in 6 inch clay pots at a depth equal to the length of the coleoptile of each seedling. Each half of a lot was grown in a greenhouse maintained at 17 or 22°C. A 20 hour day length was used.

RESULTS

The percent infection of the barley varieties Chevron, Jet and Odessa by race 6, *U. hordei*, was higher when the inoculated plants were grown at 22°C than at 17°C (Table I). Percent infection, based on partially and totally infected plants, was increased more in the varieties Jet and Chevron than in Odessa. The totally infected plants increased 42 percent in Odessa and 22 percent in Jet. Odessa was susceptible at both temperatures, but the number of totally infected plants increased from 20 per 91 plants at 17°C to 57 per 90 plants at 17°C to 57 per 90 plants at 22°C. Jet was highly resistant at 17°C. The number of totally infected Jet plants increased from 0 per 54 plants at 17°C to 12 per 54 plants at 22°C. Chevron was only moder-

ately resistant at 17°C and susceptible at 22°C, but the number of totally infected plants was 2 per 25 at both temperatures.

In the F_2 progeny of the cross, Odessa X Jet, the totally infected plants increased from 12 per 177 plants at 17°C to 60 per 178 plants at 22°C which was an increase of 27 percent. Based on the number of partially and totally infected plants, the average increase in smutted plants for this cross was 44 percent (Table I).

The two F_2 lines of the cross, Odessa X Chevron, which were tested developed different levels of infection (Table I). Line 3-20 had a much higher rate of infection at both temperatures than did line 3-13. Even at the higher infection rate, line 3-20 developed 32 percent more smutted plants at 22°C. In these two lines the number of totally infected F_2 plants increased from 17 per 141 plants at 17°C to 53 per 140 plants at 22°C which was an average increase of 26 percent.

Four of the lines of the cross, Chevron X Jet, showed no or little increase in infection at 22°C. The two lines, 8-18 and 8-19 (Table I), which developed higher percent infections at 22°C had 10 of 12 infected plants with very late, short tillers which were infected whereas the rest of the tillers were healthy. The number of totally infected plants was low, 2 per 213 individuals at 17°C and 5 per 209 individuals at 22°C.

The crosses of Odessa, Chevron, or Jet X Pannier showed no or very little increase in infection at 22°C. There were no totally infected plants in any of the F_2 progeny of these crosses.

DISCUSSION

The reactions of Chevron, Jet and Odessa to race 6, *U. hordei* were sensitive to temperature. The increase in the number of totally infected plants in the intermediate varieties, Chevron and Jet, at 22°C reflected the degree of temperature sensitivity of the genes governing resistance to race 6, *U. hordei*. When the growth temperature was kept at 22°C, the number of totally infected plants increased more in the susceptible variety, Odessa, less in the intermediate variety, Jet, and not at all in the intermediate variety Chevron. Based on the number of partially and totally infected plants at 17°C, however, Jet was more resistant than Chevron. Odessa was the most susceptible variety at both temperatures. Chevron was rated as susceptible to race 6, *U. hordei* by Shands (7) whose rows of Chevron ranged from 32.5 to 97.5 percent infected.

Both Wells (10) and Metcalfe (6) had difficulty in establishing the dominance of the gene in Jet which governed resistance to race 6, *U. hordei*. If the F_2 populations of the cross, Odessa X Jet, were subjected to analysis for goodness of fit to single gene ratios, the data in some trials obtained in the test at 17°C would fit a 3:1 ratio whereas those obtained in the test at 22°C would fit a 1:3 ratio. At 17°C, therefore, a single, dominant gene seems to govern resistance

TABLE I

EFFECT OF TWO TEMPERATURES ON THE PERCENT INFECTION OF FOUR BARLEY VARIETIES, CHEVRON, JET, ODESSA, AND PANNIER, AND THE F_2 PROGENY OF THEIR CROSSES BY RACE 6, *USTILAGO HORDEI*

VARIETY OR CROSS	F_2 LINE NO.	INFECTION AT 17° %	INFECTION AT 22° %	INCREASE IN INFECTION %
Chevron		12	50	38
Jet		2	63	61
Odessa		57	77	20
Pannier		0	0	0
Odessa X Jet	1-33	20	56	36
	1-34	27	74	47
	1-35	14	47	33
	1-36	12	71	59
Odessa X Chevron	3-13	5	50	45
	3-20	49	81	32
Chevron X Jet	8-14	3	8	5
	8-15	8	8	0
	8-16	3	7	4
	8-17	0	3	3
	8-18	0	11	11
	8-19	0	26	26
Odessa X Pannier	5-39	0	1	1
	5-43	2	2	0
Chevron X Pannier	11-15	2	2	0
Jet X Pannier	9-3	0	0	0

whereas at 22°C the gene governing resistance appears to be recessive. Based upon the reactions of the Jet parent, however, many of the homozygous, resistant plants in the F_2 population of the cross, Odessa X Jet, tested at 22°C would be read as susceptible. In order to avoid misinterpretation of F_2 phenotypic responses, testing of the progeny of this cross should be carried out at 17°C since this temperature allows full expression of the gene governing resistance in Jet. Based on the data obtained at the lower temperature, the gene in Jet is dominant.

Although Shands (7) used Chevron as a susceptible parent, the data presented in this paper indicate that Chevron has a resistance gene(s) which conditions a low resistance which is expressed at low temperatures. The increase in the percent of smutted plants when inoculated F_2 progeny of the cross, Odessa X Chevron, were grown at 22°C was close to the percent increase obtained at 22°C in testing the parent Chevron. The percent smutted plants varied too much,

however, between lines 3-13 and 3-20 (Table I) to attempt to indicate the number of genes involved.

The cross, Chevron X Jet, did not show a high degree of increased susceptibility at 22°C to race 6, *U. hordei*, in four of the six lines tested. The increased number of infected, late tillers in lines 8-18 and 8-19 showed that the fungus colonized portions of the crown tissues of F_2 plants of this cross. Although the effects of temperature on the percent infected plants was diminished in this cross, its effects were not entirely prevented as is shown by the low percent increases in lines 8-14 through 8-17 (Table I).

Pannier is reported to have three independent genes governing resistance to race 6, *U. hordei* (3). No increased infection rate at 22°C was demonstrated for the crosses of Chevron or Jet X Pannier. The data for the cross Jet X Pannier indicated that the gene for resistance in Jet and one of those in Pannier were either allelic or closely linked. Only a slight increase in the infection rate at the higher temperature was shown for the cross, Odessa X Pannier. This increase was no greater than the population of susceptible plants that would be expected in this cross (3). The effect of Pannier on temperature sensitivity cannot be explained at this time.

Although the infection rate of the susceptible variety, Odessa, was 57 percent at 17°C, it still was well above the susceptible range set up by Tapke (8). No selections of Odessa (C.I.934) which are resistant to race 6, *U. hordei*, have been reported. In a genetic study of races 6 and 10, *U. hordei*, Lade (5) recovered lines of the fungus which were avirulent on Odessa, which is susceptible to all known races of *U. hordei*. Perhaps the difference in response of Odessa to race 6, *U. hordei* at 17°C and 22°C is indicative of minor gene resistance to race 6.

SUMMARY

The genes conditioning resistance to race 6, *U. hordei*, in Chevron and Jet are temperature labile. Significantly higher infection rates were obtained at 22°C than at 17°C in both parent and F_2 cross progeny populations. The data indicate that the gene governing resistance to race 6, *U. hordei*, in Jet is dominant and that tests for its expression should be carried out at 17°C. No conclusions were developed as to the number of genes governing resistance to race 6, *U. hordei*, in Chevron. When Chevron and Jet were crossed, a decrease in the sensitivity of the resistance of the F_2 progeny at higher temperatures was noted. No satisfactory explanation for this decrease was determined. None of the F_2 populations of crosses between Chevron, Jet, or Odessa X Pannier exhibited a differential response to race 6, *U. hordei*, inoculations when grown at 17°C or 22°C.

REFERENCES

1. Kiesling, R. L. 1962. Effect of temperature and point of inoculalation on the symptomology of barley covered smut. (Abstr.) Phytopathology 52: 16-17.

2. ————. 1962. The effect of pericarp on covered smut infection of naked barley varieties. (Abstr.) Phytopathology 52:738.
3. ————. 1969. The inheritance of resistance to *Ustilago hordei* in spring barley. Proceedings of the Second International Barley Genetics Symposium. In Press.
4. ———— and G. A. Peterson. 1966. Interpretation of partially-smutted plants in studies of the inheritance of covered smut resistance. (Abstr.) Phytopathology 56:884.
5. Lade, Dennis H. 1968. Inheritance of pathogenicity of *Ustilago hordei*. Ph.D. Thesis. North Dakota State University.
6. Metcalfe, D. R. 1962. Inheritance of resistance to loose smut, covered smut and false loose smut in the barley variety, Jet. Can. J. Pl. Sci. 42: 176-189.
7. Shands, R. G. 1956. Inheritance of covered smut resistance in two barley crosses. Agron. J. 48: 81-86.
8. Tapke, V. F. 1937. Physiologic races of *Ustilago hordei*.. J. Agr. Res. 55: 683-692.
9. Thomas, P. L., and Clayton Person. 1965. Genetic control of low virulance in *Ustilago*. Can. J. Genet. and Cytol. 7: 583-588.
10. Wells, S. A. 1958. Inheritance of reaction to *Ustilago hordei* in cultivated barley. Can. J. Pl. Sci. 38: 45-60.

TRANSMISSION OF *CLAVICEPS PURPUREA* (FR.) CONIDA BY THE CABBAGE LOOPER MOTH *TRICHOPLUSIA NI* (HUBNER)[1]

Raul Moreno,[2] V. D. Pedrson[2] and J. T. Schulz[3]

Departments of Plant Pathology and Entomology

North Dakota State University, Fargo, North Dakota 58102

INTRODUCTION

Ergot, caused by the fungus *Claviceps purpurea* (Fr.) Tul., is a well known disease which occurs frequently on cereal grains and native and cultivated grasses in North Dakota. The disease could be a limiting factor for production of hybrid barley seed in North Dakota due to the extreme susceptibility of the plant. Florets which remain open for longer than normal periods of time and delayed pollination combine to predispose hybrid barley to infection. There are no known strains resistant to the disease.

Three principal means of dissemination of the casual fungus have been acknowledged: a) wind or insect-borne ascospores, b) insect-born conidia, and c) local dissemination of conidia by splashing

[1]Journal No. 245 North Dakota Agricultural Experiment Station.
[2]Department of Plant Pathology.
[3]Department of Entomology.

rain. Ascospores probably account for primary infections, whereas insect-borne conidia probably account for most secondary spread.

Numerous observations of insects associated with ergot—infected grasses have been made in the field (1, 3) but experimental proof of disseminator relationships is lacking. Recently, observations in North Dakota (2) indicated that moths are closely associated with the presence of the disease in hybrid barley under field conditions. The present paper will provide experimental evidence of dissemination of conidia of *C. purpurea* by moths.

MATERIALS AND METHODS

Several male sterile barley florets were inoculated with a conidial suspension of *C. purpurea*. After the first symptoms appeared, 25 equal-sized plants were selected and placed inside a wire screen cage together with 26 one-day-old individuals of the cabbage looper moth *Trichoplusia ni* (Hubner). Simultaneously, 25 healthy plants were placed inside each of 2 similar cages. Each of these plants bore at least 2 heads in the early flowering stage. After 48 hours, the 26 moths were transferred from the cage containing infected plants to one of the cages containing healthy plants. The plants in the third cage served as controls.

Following removal of all moths from the cage containing the original infected plants, another population of 26 moths was liberated inside this cage and were allowed to remain for 48 hours. This process was repeated so that 78 moths were finally transferred to the cage containing healthy plants. All three cages were maintained in an environment of 80-90% relative humidity and 21-25 C during the experimental period. Alternating 12-hour light and dark periods were provided continuously. Darkness was achieved by covering the cages with black plastic. At the beginning of each 12-hour dark period, the heads were sprayed with a fine mist of water to maintain high humidity and simulate conditions of dew in the field.

RESULTS AND DISCUSSION

Symptoms of ergot on healthy heads were first observed 7 days after the first transfer of moths from the cage containing infected heads. After 11 days, 28% of the heads of male sterile barley exposed to the moths contained one or more infected florets. All of the heads on plants maintained moth free remained healthy (Table I).

During dark periods the activity of the moths increased and their feeding habits could readily be observed. As they flew and encountered the heads of male sterile barley they momentarily probed the florets with their proboscises. Upon encountering ergot exudate in infected florets, however, they would feed for several seconds before moving to other florets (Figure 1A). There was no indication that moths were attracted to ergot exudate; however, contact with actual exudate appeared to provide a powerful feeding stimulus.

After feeding, moths were examined microscopically. Conidia were found associated with the proboscis both externally and internally (Figure 1B). In addition, large numbers of conidia were found in the intestinal tract of the disseminator.

TABLE I
NUMBER OF HEADS OF ERGOT-INFECTED MALE STERILE BARLEY*

Healthy Plant Treatment	Number Healthy Heads	Number Heads Infected Days Following Exposure							Total Infected Heads
		6	7	8	9	10	11	12	
Exposed to moths	50	0	4	2	2	2	4	0	14
Unexposed to moths	50	0	0	0	0	0	0	0	0

*Following association with moths previously exposed for 48 hours to the sphacelial stage of ergot in infected male sterile barley florets.

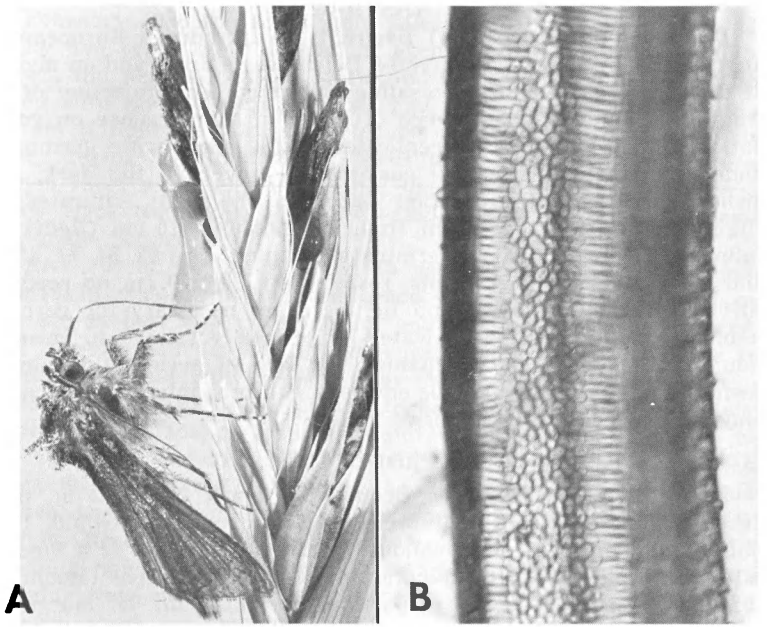

FIGURE 1A—Cabbage looper moth *Trichoplusia ni* (Hubner) feeding on exudate from ergot-infected male sterile barley floret (2X). B. Conidia of *Claviceps purpurea* within the food channel of the maxilla following a 30 second feeding period (100X).

LITERATURE CITED

1. Atanasoff, D. 1920. Ergot of grains and grasses. U.S. Dept. Agr. Bur. Plant Ind. Mimeo Publ. 172 p.
2. Mongolkiti, S., V.D. Pederson, and J. T. Schulz. 1969. Insects associated with ergot-infected male sterile barley. Proc. N. Dak. Acad. Sci. 23:25-30.
3. Parris, G., and B. Moore. 1961. Tentative insect vectors of *Claviceps paspali* of Dallas grass in Mississippi. Plant Disease Reptr. 45:503-533.

EFFECT OF DEPTH OF SUBMERGENCE ON GERMINATION OF *ECHINOCHLOA CRUSGALLI* (L.) BEAUV.

Fred E. Smeins[1]

Department of Biology

University of North Dakota, Grand Forks, North Dakota 58201

ABSTRACT

Echinochloa crusgalli (L.) Beauv. is an introduced European annual grass that grows in cultivated fields, waste areas and on margins of disturbed, ephemeral, non-saline wetlands. The objective of this study is to determine influence of depth of submergence on germination and growth. Three replicates of 100 seeds were germinated under six treatments: moist germination towels in the dark, petri dishes with moist germination paper in the light, saturated soil (light), soil submerged 10 cm (light), submerged 15 cm (light) and submerged 20 cm (light). Germination values were 85, 84, 61, 45, 25, and 5% for the six treatments, respectively. At 20 cm no seedlings survived. Cold treatment and light are not necessary for germination. Restriction from deep waters is primarily related to germination requirements. The mechanism for lack of germination has not been delimited but the gaseous environment, probably oxygen tension, may be the controlling factor.

INTRODUCTION

Echinochloa crusgalli (L.) Beauv. (barnyard grass) is an introduced European species widespread in North America (Gould, 1968). This annual grass occurs on moist disturbed sites and is a weed in cultivated fields of North Dakota and surrounding areas (Buchholtz, 1954; Frankton, 1963). It is particularly abundant on margins of ephemeral, non-saline, cultivated wetlands (Dix and Smeins 1967; Smeins 1967) where its seeds may provide food for waterfowl (Met-

[1]Present address: Department of Range Science, Texas A&M University, College Station, Texas 77843.

calf, 1931). Commonly associated species are the amphibious pioneers, *Alisma triviale* Pursh, *Beckmannia syzigachne* (Steud.) Fern., *Eleocharis acicularis* (L.) R. S., *E. engelmannii* Steud. var. *monticola* (Fern.) Svenson, *Gratiola neglecta* Torr., *Polygonum lapathifolium* L. and *Veronica peregrina* L. var. *xalapensis* (HBK.) St. John & Warren (Smeins, 1967).

Echinochloa crusgalli is generally absent from sites that have greater than 30 cm of standing water for more than 4 weeks. Since it only occurs in shallow water or after drawdown of water levels, the effect of water depth in limiting its distribution and abundance is evident. The objective of this study was to determine the influence of depth of submergence on seed germination and early growth of *E. crusgalli.*

METHODS

Seeds were collected on 5 September 1966 near Mayville, North Dakota. The site was a shallow depression within a regularly cultivated field on clay loam soil with a surface (0-15 cm) salinity of 1.2 mmho/cm. *Echinochloa* was dominant and *Eleocharis engelmannii* was the major associate. The seeds were placed in paper envelopes, transported to the laboratory and stored at room temperature. On 19 February 1968 the seeds were selected for experimentation. Initially 100 seeds were placed in each of three moist germination towels and kept in constant dark, and 100 each in three petri dishes fitted with moistened fiter paper and kept in constant light to ascertain if light was necessary for germination. Distilled water was added regularly. None of the seeds were pretreated. High germination rates were obtained within one week (Table I) and further trials were conducted with untreated seeds kept under a normal day-night sequence.

Five cm of soil were added to each of 12 small glass aquaria (26x15x15 cm). One hundred seeds were evenly distributed over the soil surface in each aquarium and covered with a thin layer of soil to hold them in place. These units were used to evaluate seed germination and growth under four moisture conditions. Water was added to the aquaria as follows: three were maintained with water to the soil surface, no standing water, three with 10 cm, three with 15 cm and three with 20 cm of standing water. All experimental work was conducted under greenhouse conditions during February, March and April of 1968. Water temperatures varied from 60 to 70° F. Records for germination were kept daily for 30 days and seedling heights were measured at the end of the 30 day period. Heights were measured from the soil surface to the distal portion of each plant.

RESULTS

Treatment of *Echinochloa crusgalli* seeds is not necessary to obtain high germination rates and dormancy does not appear to be present. Seeds stored dry at room temperatures for approximately

18 months did not lose viability and germinated readily in germination towels or petri dishes in the presence or absence of light. Maximum germination was obtained with germination towels and petri dishes whereas increased depth of submergence resulted in decreased germination rates (Table I). At 20 cm water depth few seeds germinated. Germination began after two days in germination towels, petri dishes and saturated soil, but not until the fourth day at 10 and 15 cm depth and 7 days at 20 cm.

After 30 days water levels in the three submerged treatments were lowered to the soil surface. Within 1 or 2 days seeds began to germinate and by the end of two weeks the percentage germination was nearly as high as the original saturated soil (Table I). Thus, a 30 day period of flooding does not affect viability of the seeds.

Height of plants at 30 days showed response to depth of submergence (Table I). Increased water depth decreased height of seedlings from a range of 12-20 cm in saturated soils to a range of 7-10 cm, 3-10 cm and 0-3 cm in 10, 15 and 20 cm of water, respectively. Of course, later initiation of germination in the flooded aquaria may account for some difference in height. Viability of seedlings appeared less favorable at greater depths and after removal of standing water seedlings that initiated growth under water did not continue to grow and were soon passed by seedlings which germinated after drawdown. By 30 days after drawdown seedlings from late germinations had attained the same heights as plants initially grown on saturated soil.

DISCUSSION

Germination and growth of *E. crusgalli* seeds is intimately related to water depth and duration. Water of greater than 20 cm depth almost completely eliminates germination and little, if any, growth occurs at this depth. The influence of the water is almost certainly indirect through its impact on other environmental factors. Since light and temperature are probably not involved, gas exchange, particularly oxygen tension, seems a strong candidate. Field observations tend to support this contention because germination occurs in both clear and extremely turbid waters when the water approaches a favorable depth (< 10 cm). Jones (1933) found *E. crusgalli* seeds not to germinate or grow in California rice fields or greenhouse experiments when water depths were greater than 20 cm and suggested low oxygen tension as the major controlling factor. He showed that dense algal growth which shaded seedlings completely retarded their development. The present results suggest that light may affect seedling growth but not germination of *E. crusgalli.*

Conditions for establishment of *E. crusgalli* can now be more clearly elaborated. Field measurements indicate the plant requires disturbed, usually cultivated, moist, non-saline substrates (Smeins, 1967). In the presence of these conditions it appears that depth of

TABLE I

INFLUENCE OF DEPTH OF SUBMERGENCE ON SEED GERMINATION AND SEEDLING GROWTH OF *ECHINOCHLOA CRUSGALLI* (L.) BEAUV.*

Treatment	Percent Germination (30 days)	Mean Percent Germination (30 days)	Mean and Range of Seedling Heights (cm) (30 days)	Mean Percent Germination 30 days after Removal of standing water
Germination Towel 1	90		Not measured	
Germination Towel 2	85		Not measured	
Germination Towel 3	81	85	Not measured	
Petri dish 1	88		Not measured	
Petri dish 2	80		Not measured	
Petri dish 3	84	84	Not measured	
Saturated soil 1	70			
Saturated soil 2	63		15	
Saturated soil 3	51	61	12-20	
10.0 cm water 1	45			
10.0 cm water 2	41		8	
10.0 cm water 3	49	45	7-10	60
15.0 cm water 1	29			
15.0 cm water 2	24		6	
15.0 cm water 3	21	25	3-10	54
20.0 cm water 1	8			
20.0 cm water 2	4		0.6	
20.0 cm water 3	4	5	<1	56

*N is equal to 100 in all trials.

water regulates the presence and abundance of the species through its influence on germination and seedling growth. The plant acts ecologically as a pioneer species and has several associates (see Introduction) that have similar but not identical requirements for establishment. Thus, superimposed on the factors of the physical environment which influence establishment is the competitive relationship between these similar pioneer species. Which species becomes dominant or most abundant in any one place is the result of all factor interactions and a small difference of a few centimeters of water may provide the competitive advantage for one species at the expense of another.

LITERATURE CITED

Buchholtz, K. P. (ed.). 1954. Weeds of the North Central States. Univ. Ill. Agr. Exp. Sta. Regional Publ. No. 36, 239 p.

Dix, R. L. and F. E. Smeins. 1967. The prairie, meadow and marsh vegitation of Nelson County, North Dakota. Can. Jour. Bot. 45:21-58.

Frankton, D. 1963. Weeds of Canada. Can. Dep. Agr. Publ. 948. 196 p.

Gould, F. W. 1968. Grass systematics. McGraw-Hill Book Co., New York. 382 p.

Jones, J. W. 1933. Effect of depth of submergence on the control of barnyard grass and the yield of rice growth in pots. Jour. Amer. Soc. Agron. 25:578-583.

Metcalf, F. 1931. Wild-duck foods of North Dakota lakes. USDA Tech. Bull. No. 221. 72 p.

Smeins, F. E. 1967. The wetland vegetation of the Red River Valley and Drift Prairie Regions of Minnesota, North Dakota and Manitoba. Unpublished Ph.D. Thesis, Dep. of Plant Ecology, Univ. of Saskatchewan, Saskatoon.

MALE GENITALIA COMPARED IN FOUR SPECIES OF THE ANT GENUS *FORMICA* L.

Jeurel Singleton

Department of Biology

University of North Dakota, Grand Forks, North Dakota 58201

ABSTRACT

Superficial genitalic structures are noted and compared in *Formica ulkei* Emery, *F. obscuripes* Forel, *F. pergandei* Emery and *F. subnuda* Emery. Means, ranges, standard deviations and confidence limits were calculated using the measurements of twenty-one different genitalic indices. Shape and size variations occur in the genitalia of these four species. Length of the sagitta is the only measurement that can be used alone as a key character because in *F. pergandei*

it showed no overlap in its range with the other species studied. The other measurements can not be used alone as key characters to separate species because of extensive overlap. Superficial genital structures, shape and size variations, and measurements of the genitalic valves can be used collectively to separate species.

INTRODUCTION

Genital morphology can be a valuable aid in identifying male ants at the specific level. Clausen (1938) noted differences in species of *Camponotus, Formica, Lasius* and *Polyergus.* Forbes (1952) compared several species of *Camponotus* and found *C. pennsylvanicus* closer to *C. herculeanus* than to other species of the genus. Forbes and Brassel (1962) used terminal segments and genitalic valves of *Polyergus* males to separate subspecies. Wheeler (1968) concluded that subspecies of *Polyergus rufescens* Latreille could not be separated by the characters of the male genitalia. She noted individual variations in sagittal length and number of teeth on the halves of the sagitta. Krafchick (1959) made a comparative generic study of the male genitalia of North American ants. He constructed a key to subfamilies and genera of the Formicidae based on the genitalia. Wheeler (1913) used male genitalia to separate subgenera and groups in the genus *Formica.*

METHODS

Males of *Formica ulkei* Emery, *F. obscuripes* Forel, and *F. pergandei* Emery, were collected during the summers of 1967, 1968, and 1969 at the University of North Dakota Oakville Prairie Biological Station, Grand Forks County, North Dakota. *Formica subnuda* Emery males were obtained near East Devils Lake, Ramsey County, North Dakota in the summers of 1968 and 1969. All males were collected during their mating flights.

Usually, the ants were fixed in 85 per cent ethyl alcohol; the genitalia were extracted, cleared, and mounted on slides with Canada balsam. Some were killed in trichloro, trifluoroethane or in methyl chloride and later transferred to 85 per cent alcohol. Eosin E was used to stain some specimens; others were left unstained.

Twenty-one measurements were taken (Figures 1-5). These are comparable to those of Clausen (1938) and Forbes (1952) but with the additions indicated in Figures 2-4. Measurements were made with an ocular micrometer mounted on an AO Spencer Microstar compound microscope and magnified 100 times. Drawings were made with the aid of a camera lucida. Calculations were done on the IBM 360-30 computer at the University of North Dakota Computer Center. The terminology of Clausen (1938) was used to describe the valves.

OBSERVATIONS

All valves are paired. Right and left sides of the genitalia were not distinguished in this study. The relative positions of the valves and valve components are shown in Figure 6.

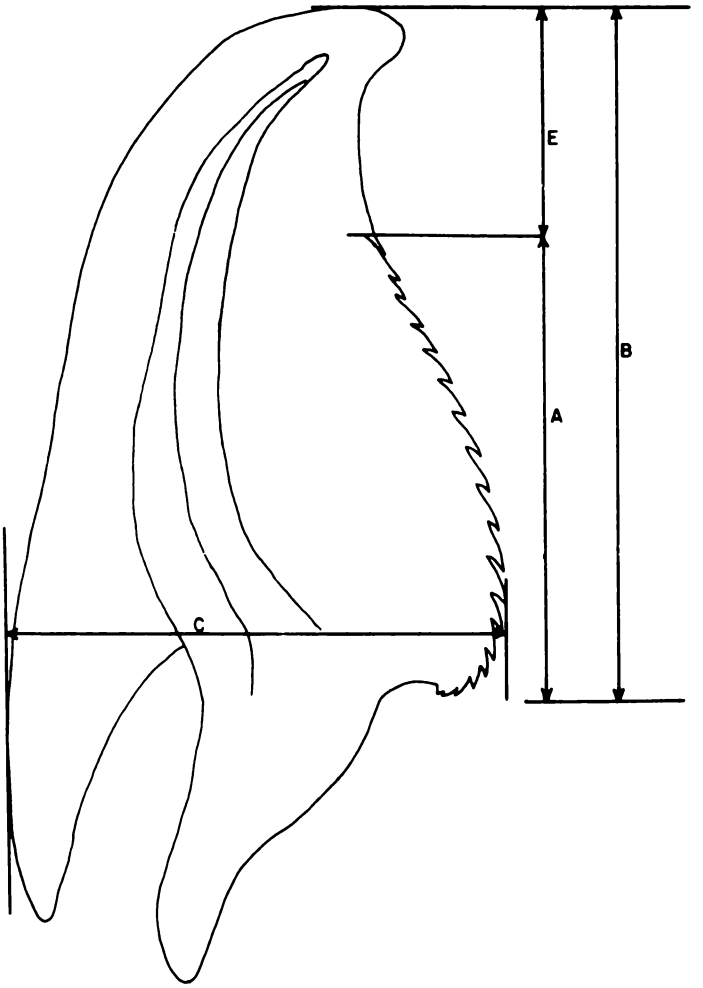

FIGURE 1—Sagitta measurements (see List of abbreviations for explanation of letters).

The roughly circular basal ring, lamina annularis or cardo, anchors the genitalia to the tenth tergum and ninth sternum. This structure is seen as the dotted line underlying the subgenital plate in Figure 6. A narrow, heavily sclerotized band forms the ventral cardo surface whereas a broad band forms the dorsal surface.

The large, bulbous, basel squamulae connect at the dorsal margins

but do not touch at the ventral surface and extend terminally to form the tapered stipes. Numerous points of muscle attachment are present in the bulbous squamulae. The squamulae form the lateral outermost valves, with the volsella-lacinia complex forming the median valve and the sagitta or penis valve being the innermost.

Lying on the inner surface of the eighth sternum is the shield-shaped subgenital plate or ninth sternum with a rudder-like projection extending towards the gaster. Some variations in the plate marginal outlines seen in the four species are shown in Figure 7. Short sensory hairs and long tactile hairs protrude posteriorly from the ventral surface of the plate. Sensory pores are also present on

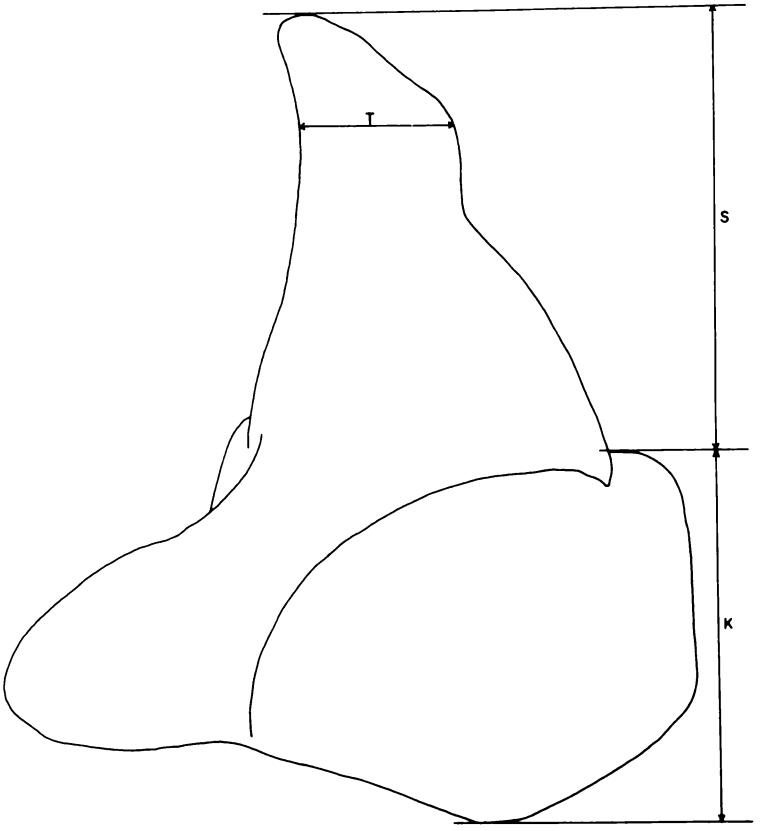

FIGURE 2—Volsella-lacinia measurements (G, W, and F were not taken by Clausen, 1938 nor Forbes, 1952). Letters are explained in List of abbreviations.

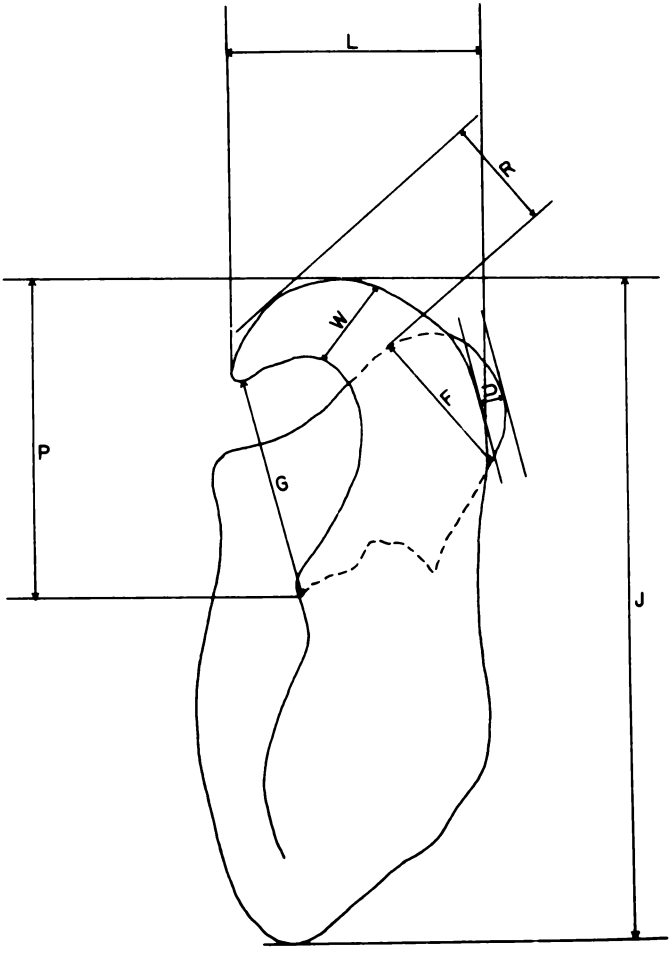

FIGURE 3—Stipes-Squamula measurements (T was not taken by Clausen, 1938 nor Forbes, 1952).

this plate. Figure 8 shows some of the hairs and pores and their arrangement on this plate.

Two roughly club-shaped pygostyles project posteriorly from the dorsal margin of the subgenital plate. Short sensory hairs and pores dot the membranous portion of this plate. Long sensory hairs and sensilla basiconica cover the pygostyles (Figure 9).

The posterior margins of the sagittae are strongly sclerotized. These margins are also pitted with sensory pores. Usually the sagitta mid and dorso-caudal regions have patches of sensory pores but no hairs. Sclerotized ridges or bands are present on the mesal portions of the sagittae in all four species (Figure 10).

The dorsal margins of the stipes bear sensory hairs of various lengths, whereas the ventral margins, the membranous parts of the stipes, have few sensory pores and usually no hairs. Sensilla basi-

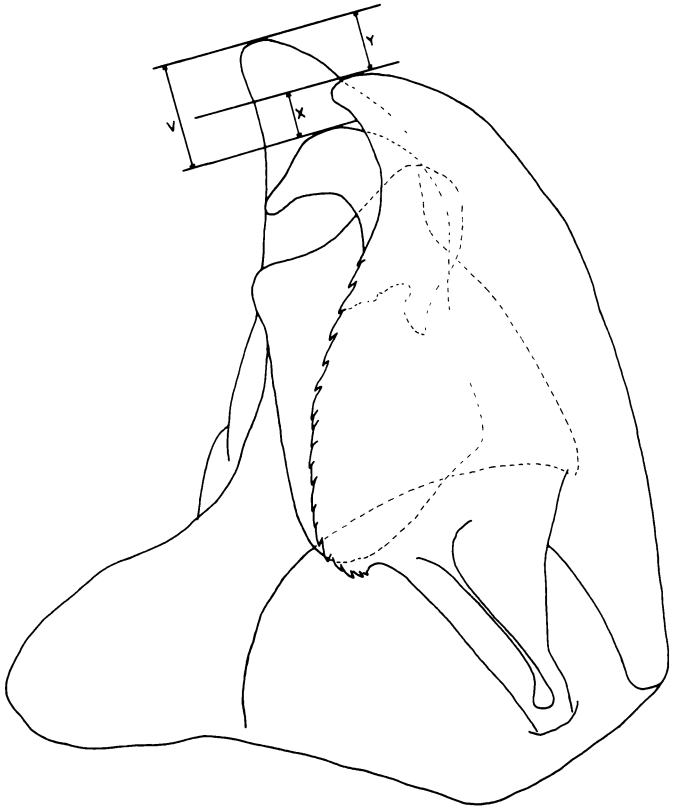

FIGURE 4—Measurements of relative positions of distal terminations of all valves (V was not taken by Clausen, 1938 nor Forbes, 1952).

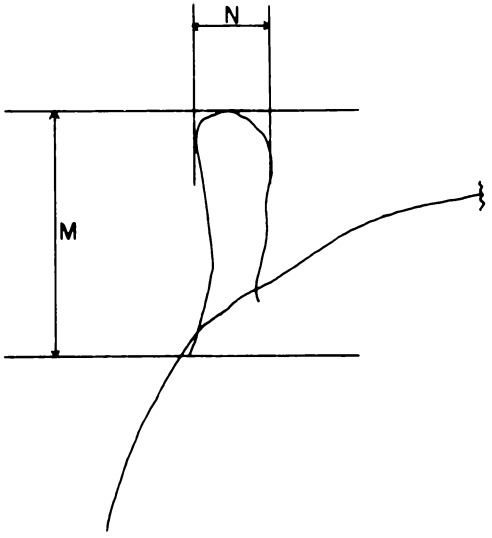

FIGURE 5—Pygostyle measurements (see List of abbreviations for letter explanations).

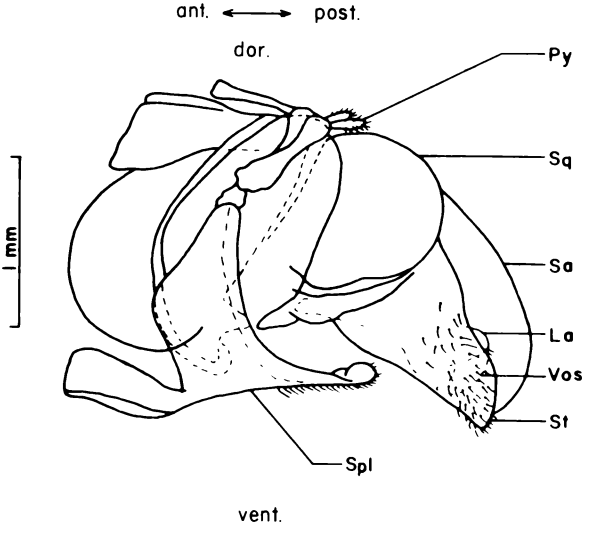

FIGURE 6—Lateral view of the relative positions of the valves (re-drawn after Clausen, 1938) (see List of abbreviations for letter explanations).

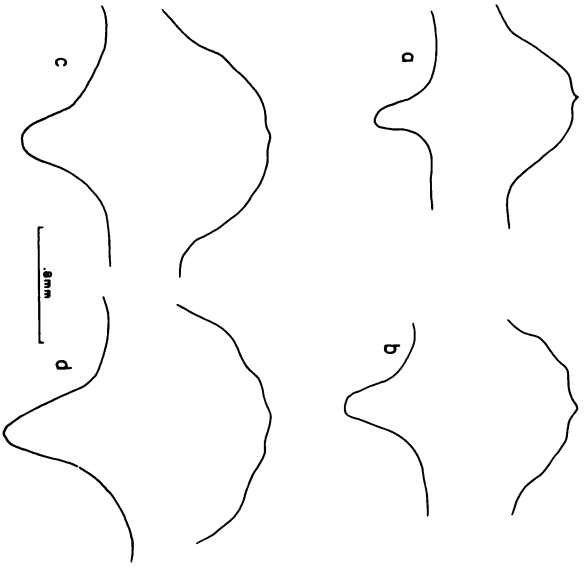

FIGURE 7—Marginal outlines of subgenital plates (a = *F. obscuripes*, b = *F. ulkei*, c = *F. submuda*, and d = *F. pergandei*).

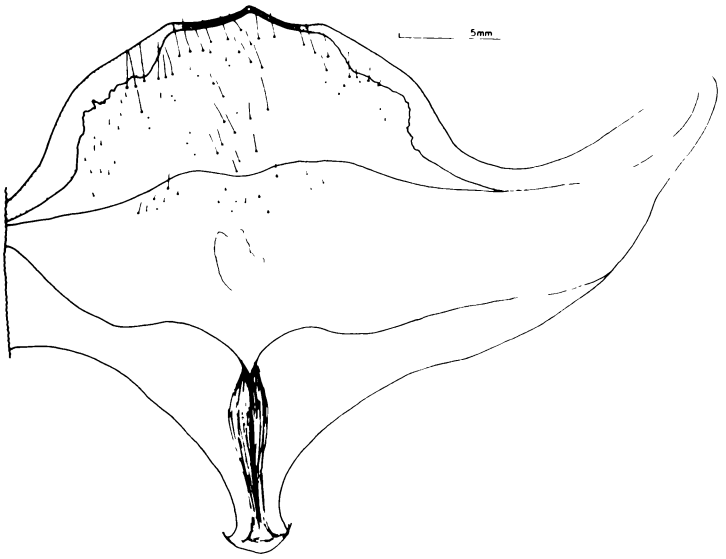

FIGURE 8—Structural details of a subgenital plate *(F. ulkei)*.

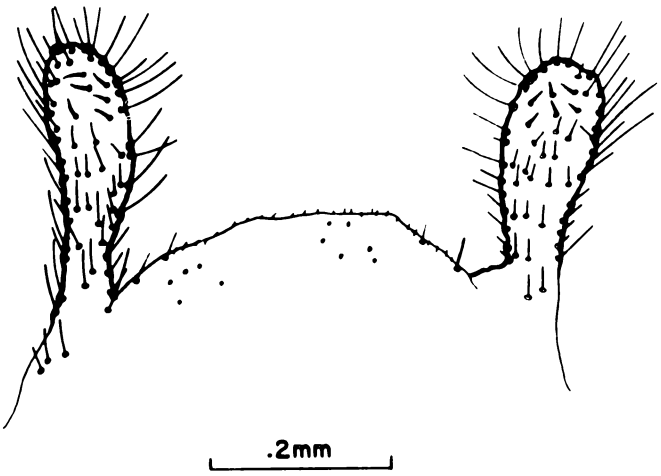

FIGURE 9—Structural details of the pygostyles (*F. obscuripes*).

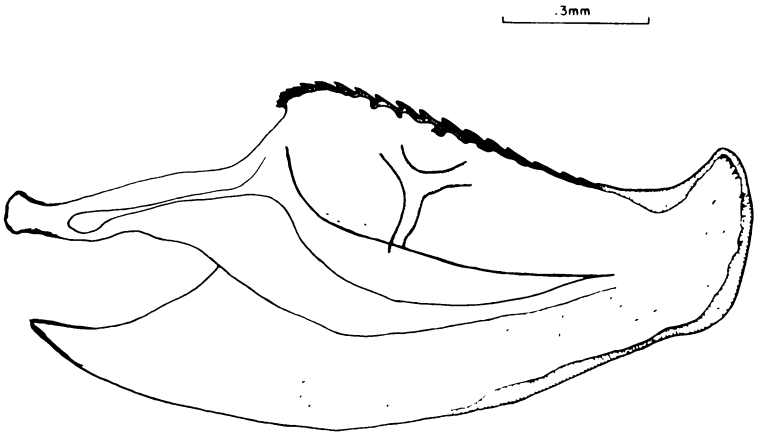

FIGURE 10—Lateral view of a sagitta showing superficial structures (*F. subnuda*).

conica are found on the dorsal surfaces of the volsella and lacinia in a confined area. Sometimes these sensilla extend over the terminal margin of the lacinia. The hook-like volsella with its tapering and pointed tip forms a basal junction with the knob-like lacinia; this plate has small sensory "warts" covering the surface which is convex towards the sagitta. The relative positions of these superficial structures are shown in Figure 11.

RESULTS AND DISCUSSION

A comparison of the genitalic measurements for the four species is given in Tables I and II. The occurrence of superficial genitalic structures and valvular shape variations in these four species is shown in Table III.

Schug (1966) noted much size variation in the male copulatory organs among the same species in his study of the genus *Formica*.

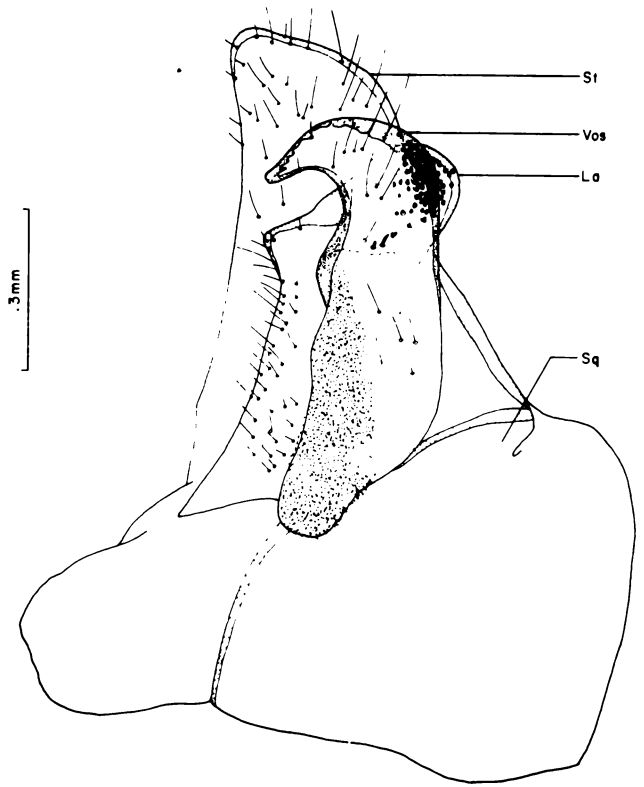

FIGURE 11—Inside lateral view of the median and outer valves (*F. obscuripes*) (see List of abbreviations for explanations of letters).

TABLE I

COMPARISONS OF GENITALIC VALVE MEASUREMENTS OF FOUR SPECIES OF THE GENUS *FORMICA* L.

Character		*ulkei*	*subnuda*	*pergandei*	*obscuripes*
Sagitta					
A	Rg	500-715	500-787	514-973	473-715
No.=50	Mn	631.5	590.6	685.9	598.1
	Sd	44.46	62.43	84.15	71.19
B	Rg	944-1001	930-1073	116-1287	787-1001
No.=50	Mn	981.5	1023.9	1139.1	927.9
	Sd	125.74	73.60	93.40	122.80
C	Rg	572-743	582-787	615-858	572-672
No.=50	Mn	654	671.9	722.9	628
	Sd	33.71	46.85	64.66	24.14
E	Rg	258-473	273-586	314-715	144-544
No.=50	Mn	307.5	382.2	434.5	287.3
		108.91	140.40	158.93	118.32
Z	Rg	14-25	13-19	14-22	12-25
No.=50	Mn	17.6	16.1	16.8	19.2
	Sd	3.04	2.68	2.96	4.14
Median Valve					
J	Rg	815-944	701-916	916-1059	643-858
No.=60	Mn	860	836.8	987.2	784.1
	Sd	24.11	51.24	16.62	46.22
P	Rg	329-372	286-500	300-472	229-286
No.=60	Mn	348.9	317.8	334.3	250.3
	Sd	10.30	38.23	13.27	23.89
G	Rg	186-286	143-372	215-286	141-215
No.=60	Mn	238.4	215.1	239.8	178.6
	Sd	36.48	27.21	17.52	18.23
W	Rg	86-127	72-157	115-172	72-129
No.=60	Mn	111.2	123.6	144.9	90.5
	Sd	8.73	25.53	13.64	11.04
L	Rg	273-344	273-358	358-458	244-344
No.=60	Mn	323.6	330.5	396.66	299.4
	Sd	22.19	26.75	22.74	19.81
U	Rg	-14-58	-29-43	14-72	14-58
No.=60	Mn	36.0	19.2	40.8	40.3
	Sd	14.95	13.21	11.86	11.41
R	Rg	72-186	143-244	172-258	115-200
No.=60	Mn	150.1	181.4	221.6	152.8
	Sd	20.09	25.97	19.81	17.37

TABLE I (Cont.)

Character		*ulkei*	*subnuda*	*pergandei*	*obscuripes*
F	Rg	143-215	143-186	157-215	143-215
No.=60	Mn	200.1	164.1	200.4	186.9
	Sd	15.01	11.42	14.71	19.23
Squamulae-stipes	Rg	657-787	630-844	715-901	601-801
K	Mn	737.3	720.4	794.9	713.8
No.=30	Sd	40.24	71.88	53.82	46.90
S	Rg	858-1073	787-1087	787-1073	787-959
No.=30	Mn	921.9	952.5	917.8	862.4
	Sd	86.70	71.34	56.80	24.11
T	Rg	244-273	200-386	286-358	229-286
No.=30	Mn	253.5	259.4	325.7	259.9
	Sd	10.35	45.40	24.55	14.55
V	Rg	186-258	86-273	129-200	115-200
No.=30	Mn	250.3	170.7	157.9	163.5
	Sd	101.31	42.91	20.54	22.91
X	Rg	43-175	29-229	100-172	72-186
No.=30	Mn	88.5	127.0	159.9	117.3
	Sd	29.18	45.15	131.68	30.28
Y	Rg	86-186	0-215	14-115	14-115
No.=30	Mn	142.2	83.9	51.2	44.0
	Sd	38.14	62.24	26.08	25.75
Pygostyles					
M	Rg	229-330	215-344	286-458	229-300
No.=78	Mn	280.4	262.3	358.9	281.3
	Sd	23.53	30.7	28.77	71.63
N	Rg	43-100	58-86	72-115	58-86
No.=78	Mn	79.7	67.2	95.0	78.6
	Sd	10.23	8.63	14.15	12.82

*Measurements are in microns

TABLE II

CONFIDENCE LIMITS (t-VALUES OR STUDENT-t) OF THE GENITALIC VALVE INDICES MEASUREMENTS

*Variables	1-2	1-3	1-4	2-3	2-4	3-4
Sagittae						
A	3.742	-3.999	2.796	-6.365	-0.550	5.578
B	-2.223	4.870	18.231	-5.818	19.512	20.561
C	-2.171	-6.614	4.386	-4.471	5.828	9.622
E	-3.226	-5.060	1.111	-1.894	4.095	5.822
Z	2.521	1.254	-2.264	-1.228	-4.432	-3.332
Median Valve						
J	-6.248	3.425	-3.432	-4.055	17.804	16.814
P	6.049	4.322	45.120	-2.820	12.804	23.618
G	3.932	-0.278	11.261	-5.877	8.556	18.605
W	-3.506	-16.501	11.243	-5.729	9.111	24.367
L	-1.529	-17.653	6.244	-14.465	7.177	24.760
U	6.448	-1.938	-1.756	-9.358	-9.261	0.234
R	-9.062	-19.467	-0.786	-7.709	8.855	20.054
F	14.679	-0.085	5.427	6.463	-6.463	5.547
Squamulae-Stipes						
K	1.105	-4.618	2.045	-4.470	0.412	6.118
S	2.018	-0.729	-1.051	-2.385	-7.901	-16.941
T	-0.678	-14.599	-1.930	-6.925	-0.060	12.423
V	3.748	4.810	4.498	1.785	1.129	-0.974
X	-3.853	-2.851	-3.679	-1.274	0.964	1.701
Y	4.298	10.605	11.493	2.612	3.195	1.063
Pygostyles						
M	4.109	-17.349	-0.100	-19.082	-2.139	8.255
N	8.227	-7.685	0.569	-14.740	-6.520	7.516

*Variables = species of ants compared. 1 = *F. ulkei*. 2 = *F. subnuda*, 3 = *F. pergandei*, 4 = *F. obscuripes*.

TABLE III

OCCURENCE OF SUPERFICIAL GENITALIC STRUCTURES AND VALVE SHAPE IN FOUR SPECIES OF THE ANT GENUS *FORMICA*

		ulkei	*obscuripes*	*pergandei*	*subnuda*
Sagitta	sclerotized ridges	prominent	slightly prominent	very prominent	very prominent
	caudal tips	tapered to point	truncate then tapered to point	rounded	truncate or tapered to pin point
	lateral location of sensory pores	sub-mesal; dorso caudual	sub-mesal; dorso caudual	throughout	throughout
	sensory hairs	none	few, mixed length	none	none
Median Valve	extension of sensilla basiconica over terminal margin of valve	over	not over	over	not over
	spiniform projections	none - few	many	many	many
	spiniform arrangements	clusters of three's	rows	rows or clusters	rows or clusters
	length of spiniforms	long - short	long-medium, mixed	long-short or mixed	long-short, mixed and some curved
	volsella tip shape	tapered to sharp point	tapered to upturned point	widening then tapered to rounded point, caudal margin concaved	widening then tapered to claw-like tip

TABLE III (continued)

		ulkei	*obscuripes*	*pergandei*	*subnuda*
Outer Valve	terminal tips	tapered to point	truncate then pointed	truncate or tapered to point	truncate or tapered to rounded point
	membranous portion				
	sensory pores	scattered	dense	scattered	scattered
	sensory hairs	none	medium long	short	short
Pygostyles	shape	clubbed	distinctly clubbed	clubbed	rod-like
	hairs	long, slender	long, bristle like	long, slender	long, slender
	membranous portion				
	sensory hairs	few	many and short	many in bunches forming hexagonal patterns	many
	sensory pores	few and small	large and scattered	concentrated at median terminal margin; small and medium	2 clusters near pygostyles; large

He concluded that because of the abundance of overlap existing in the size measurements of several species in this genus sexual isolation might not exist among the species. Differences in mating flight period for species of *Formica* living in the same habitat could be a means of sexual isolation (Kannowski, 1963). In the species studied, it is possible that size and shape variations are not distinct enough to prevent interspecific copulations.

Minor posterior marginal outline variations occur on the subgenital plates of different individuals in the same species as well as in different species. Wheeler (1968) found no subspecific constant key character in these plates in any nest series of *Polyergus rufescens*.

The genitalia are important in sense reception as indicated by the abundance of tactile hairs, sensory hairs, sensory pores, and sensilla basiconica. The position of sensilla basiconica on opposing surfaces of the volsella-lacinia and the shape of the median valve suggest a clasping function for this valve. There are no records of the relative positions of these valves during copulation in *Formica*. A clasping function may be further enhanced by the presence of spiniform projections at the junction of the volsella and lacinia. There has been no previous reference to these structures in formicine ants.

The strong ridges and folds on the sagitta could be the attachment points for muscles that extend and retract this organ readily during copulation. Since the actual connection time during copulation varies from four seconds to more than two minutes in *Formica* (Kannowski, 1963), it would seem likely that these organs must be introduced into the female tract and withdrawn quickly.

Measurements of all except the length of the sagittae could not be used as key characters to separate the four species because of overlap. Overlapping was not analyzed in this study.

Variations in the shape of the pygostyles, shape of the volsella and lacinia complex, shape of the posterior margins of the subgenital plates, arrangements of the spiniform projections, and the length of the whole ant (Wheeler and Wheeler, 1963) can be useful in separating species, in conjunction with other morphological characters such as the number and dimensions of antennal segments, position of the petiole, segmentation of maxillary palpus, etc., (Smith, 1943).

SUMMARY

This study describes, figures, and compares the external genitalic valves and subgenital plates of *Formica obscuripes*, *F. ulkei*, *F. subnuda*, and *F. pergandei*. Measurements of different indices of the genitalia do not reveal key characters that can be used alone to identify species. These measurements may be used with other morphological characters of the genitalia and body of the male ant to identify species. The genitalic components of these four species are similar, but variations in shape and size are evident. Location and

arrangement of superficial genital structures can be an aid to identify species. Genitalia function in sense reception is evident by the presence of tactile and sensory hairs, sensory pores and sensilla basiconica. Median valve shape variations and inner valve size variations suggest use of these organs as possible units to separate taxonomic groups and species.

ACKNOWLEDGMENTS

I wish to thank the following people: Dr. Paul B. Kannowski, University of North Dakota, under whose direction this study was made; Miss Carlene Woods, Minot State College, for making the drawings, and Miss Amy Wu and Mr. Charles Wahtola, both of the University of North Dakota, for assistance with data analysis. A portion of this research was facilitated by National Science Foundation grant GB-6514 to Dr. P. B. Kannowski.

LIST OF ABBREVIATIONS

A = length of serrated edge of sagitta from first to last distinct tooth
ant = anterior (towards the gaster of ant from the genitalia)
B = total length of sagitta
C = width of widest point sagitta at right angles to B
dor = dorsal
E = distance from posterior margin of sagitta to first distinct tooth
F = width of lacinia
G = inside curved distance of volsella from tip to end of ventral sclerotization
J = total length of middle valve
K = total length of squamula
L = length from dorsal margin of volsella to tip of volsella
La = cuspis volsellaris (Snodgrass, 1935) volsella or middle valve (Tuxen, 1956)
N = total length of pygostyles
Mn = mean
N = width of pygostyles
No. = number of parts measured
P = distance from the caudal margin of volsella to the junction of lacinia
post. = posterior
Py = pygostyles
R = distance between dorsal margin of lacinia to curve of volsella
Rg = range
S = total length of stipes
Sa = sagitta (= lamina aedeagalis or penis valve) (Snodgrass, 1935) inner valve (Tuxen, 1956)
Sd = standard deviation
Spl = subgenital plate
Sq = squamula (= lamina parameralis or basi paramere) (Snodgrass, 1935) outer valve or gonostylus (Tuxen, 1956)

St=stipes (=paramere) (Snodgrass, 1935) gonocoxites or gonoforceps (Tuxen, 1956)
T=width of terminal part of stipes
U=distance that lacinia extends beyond volsella
V=distance between tip of volsella and tip of stipes
vent.=ventral
Vos=volsella (=digitus volsellaris) (Snodgrass, 1935) middle valve or gonostylus (Tuxen, 1956)
W=width of curved section of volsella
X=distance between tip of volsella and tip of sagitta
Y=distance between tip of sagitta and tip of stipes
Z=number of distinct teeth on ventral margin of sagitta

REFERENCES

Clausen, R. 1938. Untersuchungen über den Männlichen Copulationsapparat der Ameisen, speziel der Formicinae. Mit. Schweiz. Ent. Ges. 17:233-346.

Forbes, J. 1952. The genitalia and terminal segments of the male carpenter ant, *Camponotus pennsylavanicus* DeGreer (Formicidae, Hymenoptera) J. New York Entomol. Soc. 60:157-170.

Forbes, J. and R. W. Brassel. 1962. The male genitalia and terminal segments of some members of the genus *Polyergus* (Formicidae, Hymenoptera) J. New York Entomol. Soc. 70:79-87.

Kannowski, P. B. 1963. The flight activities of formicine ants. Symp. Genet, et Biol. Ital. 12:74-102.

Krafchick, B. 1959. A comparative study of the male genitalia of North American ants (Formicidae) with emphasis on generic differences. Dissertation, Univ. of Maryland, 78p. (Univ. Microfilms, Inc., Ann Arbor, Mich.

Schug, A. 1966. Untersuchungen über Grossenvariabilitat des Männlichen Kopulationsapparates bei verschiedenig (*Formica*-Artem) Zool. Anz. 177(5/6):390-399.

Smith, M. R. 1943. A generic and subgeneric synopsis of male ants of the United States. Amer. Midl. Nat. 30(2):273-321.

Snodgrass, R. E. 1935. Principles of insect morophology. McGraw-Hill Book Company, Inc. New York. 667p.

Tuxen, S. L. (ed.) 1956. Taxonomist's glossary of genitalia in insects (1st ed.). Ejnar Munksgaard, Copenhagen. 326p.

Wheeler, G. C. and Jeanette Wheeler, 1963. The Ants of North Dakota. Univ. of North Dakota Press, Grand Forks, 326p.

Wheeler, J. 1968. Male genitalia and the taxonomy of *Polyergus*. Proceed. of Entomol. Soc. Wash. 70(2):156-164.

Wheeler, W. M. 1913. A revision of the ants of the genus *Formica* L. Bull. Mus. Comp. Zool. Harvard. 53(10):379-565.

NORTH DAKOTA FLEAS. III. ADDITIONAL RECORDS FROM MAMMALS

Carlene E. Woods[1] *and Omer R. Larson*

Department of Biology

University of North Dakota, Grand Forks, North Dakota 58201

INTRODUCTION

In our continuing survey of the North Dakota flea fauna, we have collected five species which previously have not been reported in the state. These additions, which bring to 32 the reported species in North Dakota, are discussed in regard to their North American distributions and host relationships.

METHODS

Between 1 June 1969 and 30 November 1969, many small animals were collected during an ecological study of *Echinococcus multilocularis* Leuckart. The senior author examined 954 of these animals for fleas in the laboratory.

A total of 410 fleas were recovered and placed in 70 percent ethanol; later they were bleached in 10 percent potassium hydroxide, washed in distilled water, dehydrated in 95 and 100 percent ethanol, cleared in oil of wintergreen and mounted in Canada balsam.

Representative slides of all fleas collected in this study were deposited in the University of North Dakota Parasitology Collection with accession numbers.

RESULTS AND DISCUSSION

Family Hystrichopsyllidae

Rhadinopsylla (Rectofrontia) fraterna (Baker)

No. 611 from *Peromyscus maniculatus,* Ward Co., 12 June 1969, 1 female.

No. 690 from *P. maniculatus,* Ward Co., 18 November 1969, 2 males.

Although a widespread flea, having been reported from Massachusetts to Oregon and California, and from New Mexico to Canada, *R. fraterna* is generally collected in small numbers. Somewhat larger collections have come from nests of wood rats in Utah and Montana (Tipton, 1950; Senger, 1966).

R. fraterna shows little host specificity as it has been found on a variety of animals including pika, wood rat, vole, shrew, ground squirrel, chipmunk, weasel, ferret, prairie dog, jackrabbit, and burrowing owl. We believe that our specimens constitute one of the few reports of this flea from *Peromyscus maniculatus.*

Ctenophthalmus pseudagyrtes Baker

No. 612 from *Peromyscus maniculatus,* Ward Co., 12 June, 1969, 1 male.

---

[1]Present address: Science Division, Minot State College, Minot, North Dakota 58701.

No. 670 from *Microtus pennsylvanicus*, Ward Co., 7 September 1969, 1 male, 1 female.

An exceedingly widespread and non-specific flea, *C. pseudagyrtes* has been reported from virtually every type of mammal except bats and man. Fuller (1943) even recorded a single specimen from a muskrat in New York. In their classification of host specificity, Benton and Cerwonka (1960) placed *C. pseudagyrtes* in class five. Such fleas are defined as "species which show no apparent host preference, occurring on a wide variety of unrelated hosts in approximately equal numbers."

The geographic range of *C. pseudagyrtes* in the eastern half of North America appears to be as extensive as its host distribution. Specimens have been reported along the Atlantic coast from New Brunswick and Nova Scotia to Florida. Westward the flea exists across the Canadian provinces to Alberta, and through the midwest to Kansas and Nebraska. Reports from the western portion of the United States are rare. Montana records include one from *Microtus ochrogaster* (Senger, 1966), and another from *Microtus* sp. (Hubbard, 1947). In addition, one flea was taken from *Rattus n. norvegicus* in Utah (Stark, 1959).

The apparent scarcity of *C. pseudagyrtes* in North Dakota may be attributed to the westward location of the state, and to the uneven distribution of this flea on small mammals. Despite the parasite's reported lack of host specificity, the work of Jameson (1950) in New York and Ontario suggests that shrews may be frequent hosts. At the present time, the flea fauna of North Dakota shrews is virtually unknown.

Corrodopsylla curvata curvata (Rothschild)

No. 631 from *Sorex cinereus*, Grand Forks Co., 9 July 1969, 1 female.
No. 660 from *S. arcticus*, Grand Forks Co., 20 August, 1969, 2 males.

C. c. curvata is a very typical flea of shrews. Benton and Cerwonka (1960) placed it in class three—"species which are able to exist as parasites of two or more species and within that group of hosts show little or no host preference."

Another subspecies, *C. c. obtusata*, exists in North America but is found only west of the Cascades. In the United States *C. c. curvata* has been reported from Montana and Utah eastward through the Midwest to the New England states. In Canada the range of this flea extends from east-central British Columbia to New Brunswick and Nova Scotia.

Family Ceratophyllidae

Malaraeus euphorbi (Rothschild)

No. 689 from *Peromyscus maniculatus*, Ward Co., 18 November 1969, 1 male, 1 female.

The records of *M. euphorbi* suggest that its geographic distribution is limited to western North America. States and provinces in

which the flea has been found include New Mexico, Utah, Montana, Saskatchewan, Alberta, and British Columbia. As in the case of *Rhadinopsylla fraterna,* the largest collections of *M. euphorbi* have come from the nests of wood rats (*Neotoma* spp.). In addition, this flea has been found on *Peromyscus maniculatus, Microtus ochrogaster,* and *Mustela frenata.*

Megabothris lucifer (Rothschild)

No. 646 from *Microtus pennsylvanicus,* McHenry Co., 16 July 1969, 1 male.

No. 668 from *Clethrionomys gapperi,* McHenry Co., 5 September 1969, 1 male.

No. 669 from *M. pennsylvanicus,* McHenry Co., 5 September 1969, 1 female.

Males of this species exhibit variable setation on their movable process. Holland (1949) described three types in which the middle seta varied in shape and development. Our specimens tend to be similar to his "type b."

Although *M. lucifer* has been taken from weasels and ground squirrels, it appears to prefer microtines. The majority of records for this rare species are from the Canadian provinces of British Columbia, Alberta, and Saskatchewan. Presumably, the only previous United States record is from Montana (Prince, 1943).

ACKNOWLEDGMENTS

We wish to express our appreciation to the following people: Dr. William L. Jellison, Hamilton, Montana confirmed our identifications of *Malaraeus euphorbi* and *Megabothris lucifer;* Dr. Robert W. Seabloom, University of North Dakota identified the juvenile *Sorex arcticus;* and Miss Jeurel Singleton, University of North Dakota, trapped the shrews and collected their fleas.

REFERENCES

Benton, A. H. and R. H. Cerwonka. 1960. Host relationships of some eastern Siphonaptera. Am. Midl. Nat. 63:383-391.

Fuller, H. S. 1943. Studies on Siphonaptera of eastern North America. Bull. Brooklyn Ent. Soc. 38:18-32.

Holland, G. P. 1949. The Siphonaptera of Canada. Canada Dept. Agr. Tech. Bull. 70, 306 p.

Hubbard, C. A. 1947. Fleas of Western North America. Iowa State Coll. Press, Ames. 533 p.

Jameson, E. W., Jr. 1950. The external parasites of the short-tailed shrew, *Blarina brevicauda* (Say). J. Mammal. 31: 138-149.

Prince, F. M. 1943. Species of fleas on rats collected in states west of the 102D meridian and their relation to the dissemination of plague. Pub. Health Rep. 58: 700-708.

Senger, C. M. 1966. Notes of fleas (Siphonaptera) from Montana. J. Kansas Ent. Soc. 39: 105-109.

Stark, H. E. 1959. The Siphonaptera of Utah. U. S. Pub. Health Serv., Commun. Dis. Center, Atlanta, Georgia. 239 p.

Tipton, V. J. 1950. New distributional records for Utah Siphonaptera. Grt. Basin Nat. 10: 1-4.

THE AGE AND GROWTH OF THE YELLOW PERCH *PERCA FLAVESCENS* (MITCHILL) IN THE LITTLE MISSOURI ARM OF LAKE SAKAKAWEA, NORTH DAKOTA, 1968

C. H. Wahtola, B. L. Evenhuis and J. B. Owen

Department of Biology

University of North Dakota, Grand Forks, North Dakota 58201

INTRODUCTION

The ubiquitous yellow perch, *Perca flavescens* (Mitchill), is one of the most common forage fish in Lake Sakakawea although the reservoir, with its fluctuating water levels and large size (326,000 surface acres), might be considered non-typical yellow perch habitat. This species, which is common to natural waters and small impoundments of the eastern and midwestern United States and southern Canada, is often stunted (Eschmeyer, 1937). Since the biology of the yellow perch population in Lake Sakakawea has not been previously investigated, this study was initiated to determine age composition, rate of growth, length-weight relationships, and condition factors.

METHODS

Yellow perch were taken at eight stations equally distributed along the entire length of the Little Missouri Arm of Lake Sakakawea between April and September 1968 (Figure 1). Three types of gill nets were utilized, *i.e.*, 36×50, 36×25 and 125×6 feet. The first two were deep nets constructed of vertical sections 6 feet wide of ½, ¾, 1, 1¼, 1½ and 1¾ inch, bar mesh, nylon gill netting, respectively. The third was a standard experimental gill net constructed of 25 foot sections 6 feet in depth of ¾ through 1¾ inch mesh. Of a total of 1,968 fish, 834 were taken in gill nets, and an additional 1,134 young of the year were captured with a 50 foot bag seine.

All fish were measured to the nearest millimeter total length, weighed to the nearest gram and their sex determined by internal observation. Scale samples were taken from 834 fish from immediately behind the left pectoral fin and a sample of scales for age determination was drawn. Length-weight relationship and coefficient of condition (K-TL) was computed for the 372 fish.

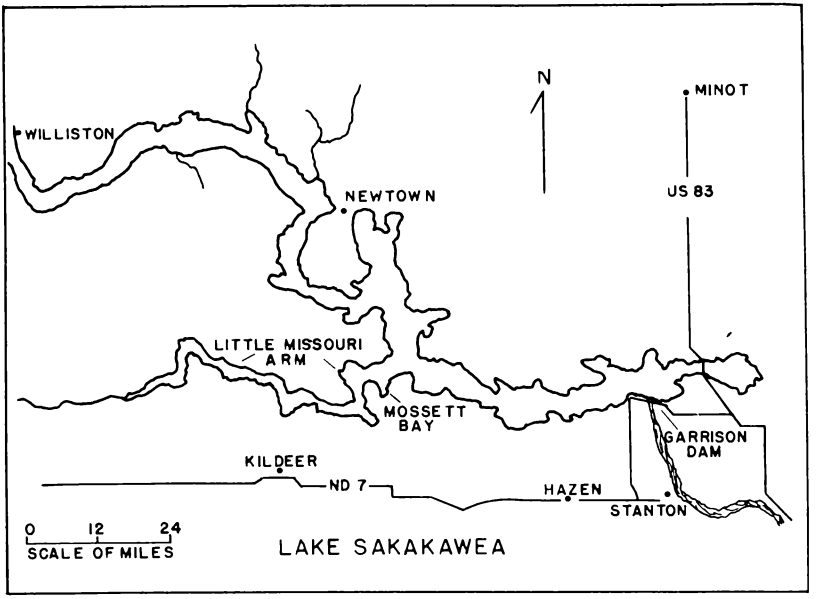

FIGURE 1—Lake Sakakawea (Garrison Reservoir) showing the location of the Little Missouri Arm.

The length-weight regression was computed by the method of least squares for a general parabola $W=cL^n$, expressed in logarithmic form. Scale impressions made on cellulose slides and projected with a Bausch and Lomb microprojector, were read twice for confirmation of age determination. The method of least squares was used to fit the straight line regression of scale radius to total length. The Y-intercept, or the point at which scales were first laid down was 3.1 mm. A direct proportion nomograph was used for age analysis.

RESULTS

Yellow perch in the Little Missouri Arm of Lake Sakakawea were found to have a maximum life span of four years. Average calculated lengths of male and female perch indicated that growth was most rapid in the first year of life, and was somewhat reduced in the second and third years (Table I).

The length-frequency polygon clearly showed peaks for age classes O and I, an apparent absence of age class II and one broad peak for age classes III and IV (Figure 2). The absence of a peak for Age class II in the length-frequency polygon may be due to a reproductive failure in 1966.

The line of best fit for the length-weight regression was described

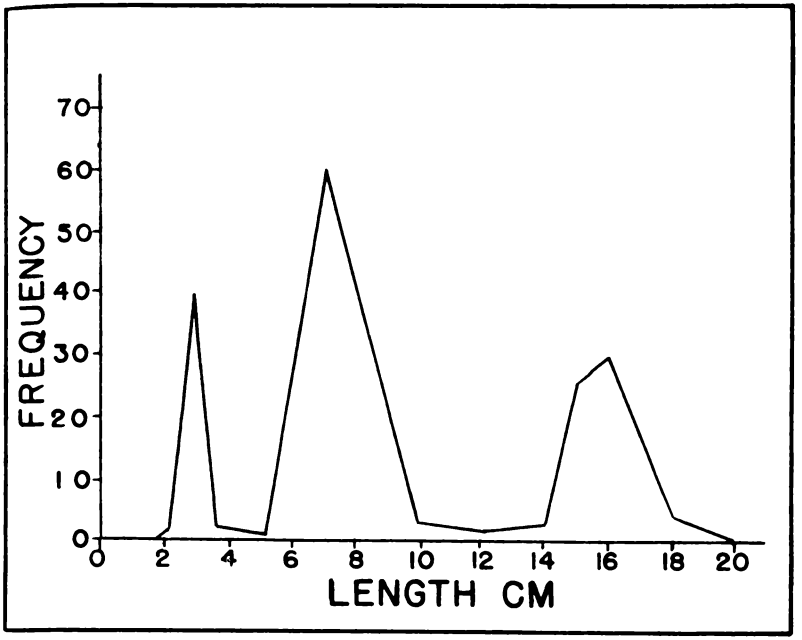

FIGURE 2—Length-frequency polygon of age class O (2-4 cm), age class I (5-10 cm) and age classes III and IV (14-20 cm) of yellow perch from the Little Missouri Arm, Lake Sakakawea, 1968.

TABLE I
CALCULATED LENGTH (MM) AT EACH ANNULUS FOR 372 YELLOW PERCH TAKEN FROM THE LITTLE MISSOURI ARM, LAKE SAKAKAWEA, 1968

Year Class	Age Group	No. of Fish	Length at Capture (mm)	Annulus I	II	III	IV
1968	O	87	27				
1967	I	115	79	71			
1966	II	15	131	74	112		
1965	III	105	158	83	126	152	
1964	IV	50	188	85	129	161	181
Average calculated length				81	126	155	181
Average annual increment				81	45	29	26

by the equation Log W = -3.7632 + 2.4266 Log L (Figure 3). It was found that the curve fitted the empirical data well, except for the larger fish.

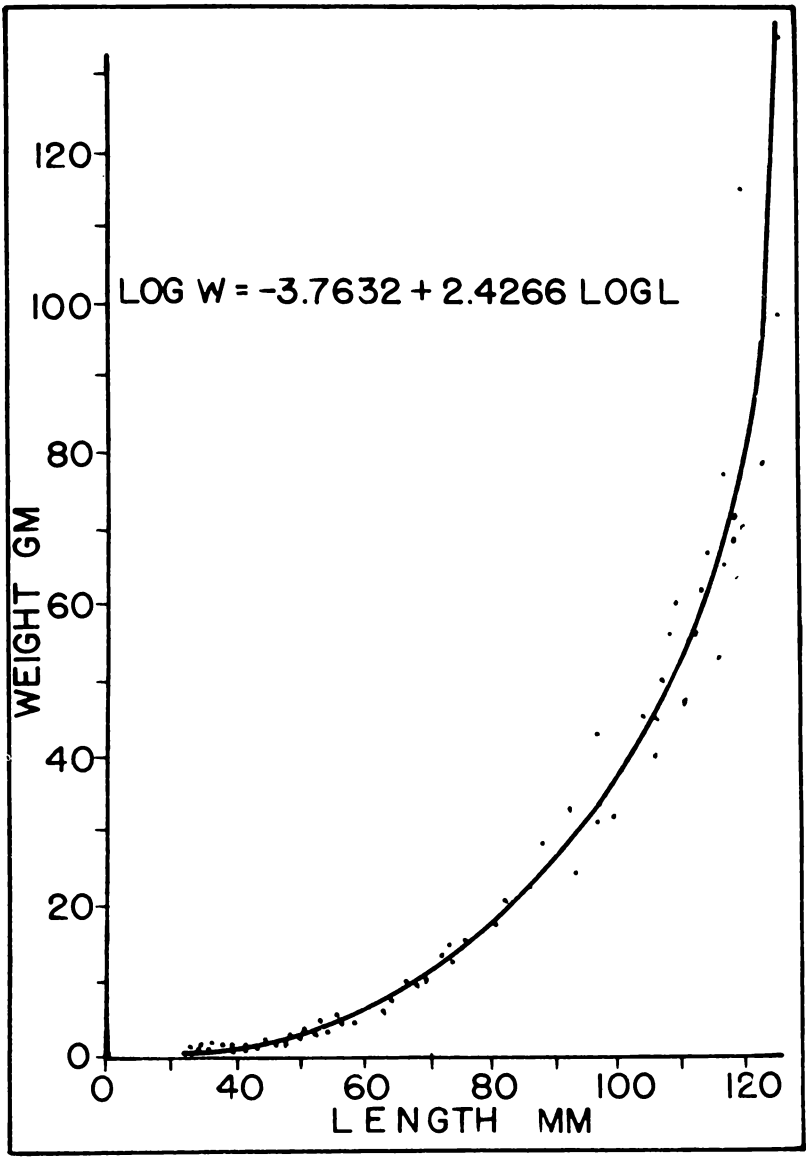

FIGURE 3—Relationship between length and weight of yellow perch from the Little Missouri Arm, Lake Sakakawea, 1968.

The coefficient of condition, K-TL, of the yellow perch population had a rather low overall average. Age class III had the poorest condition, whereas age class II had the best (Table II).

TABLE II
COEFFICIENT OF CONDITION, K-TOTAL LENGTH, FOR 372 YELLOW PERCH TAKEN FROM THE LITTLE MISSOURI ARM, LAKE SAKAKAWEA, 1968

Age	I	II	III	IV	I-IV
K-TL	1.10	1.18	0.96	0.99	1.03

The overall sex ratio for 1,968 fish was found to be 2.38 females per male. Fish captured by gill net (834) had a ratio of 3.91 females per male, while those captured by seine (1134) had a ratio of 1.64 females per male.

The mesh selectivity was the most striking aspect of the study. Of the 834 taken in gill nets 802 (94%) were caught in the ¾ inch mesh.

DISCUSSION

It seems most likely that yellow perch in effect do not live longer than four years in the reservoir, as only year classes 1964 through 1968 were captured and results of annual test nettings by the North Dakota Game and Fish Department reveal only occasional yellow perch over four years of age (Hill, 1966). Yellow perch in other waters commonly exceed seven years of age (Carlander, 1950). However, growth in length of perch in the reservoir during their first four years of life was comparable with that reported for yellow perch populations elsewhere (Schneberger, 1935; Harkness, 1922; and Hile and Jobes, 1940).

Not only are the perch in the reservoir small due to their relatively brief life span, but their condition factor or plumpness in relation to their length is also poor. Carlander (1950) reported the average K-TL or condition factor for yellow perch in the United States to be 1.3. The mean K-TL for yellow perch in the Little Missouri Arm was 1.03 or well below the average and generally declined as the fish become older.

It is recognized that the n value or the slope of the length-weight regression for an average population should be approximately 3.0, and that deviations for this value reflect the condition of the population. The n value of 2.4266 for yellow perch in the Little Missouri Arm also suggests poor condition.

Alm (1946) postulated that the reason for the occurrence of stunted populations is primarily an inadequate food supply in the environment. If a population becomes too numerous in proportion to the available food, a deficiency occurs, and there will be a deterioration of the growth rate (*i.e.*, a stunted population). There may also be competition for food between yellow perch and goldeye

(*Hiodon alosoides*). Goldeye are the most abundant fish in Lake Sakakawea and it has been shown that perch (Pearse and Achtenberg, 1920) and goldeye (Heib, 1968) feed on similar organisms. The older perch, which need small fishes to feed on to maintain good growth to the larger sizes, may be unable to feed on fry for a sufficient period of time. The largest perch of age group IV are too small to feed on fry except during brief periods after which the normally growing fry may become either too large or too rare to remain available to the perch as food. Thus it may be that the inability to procure sufficient food may eliminate older yellow perch from the population.

ACKNOWLEDGMENTS

We wish to express our sincere appreciation to Dr. James Reilly, who critically reviewed the manuscript. This study was supported by the North Dakota Game and Fish Department and the U. S. Bureau of Commercial Fisheries under the provisions of P.L. 88-309.

REFERENCES

Alm, G. 1946. Reasons for the occurrence of stunted fish populations with special regard to the perch. Report Swed. St. Inst. Fresh Water Research 25: 1-46.

Carlander, K. D. 1950. Handbook of freshwater fisheries biology. Wm. C. Brown Co., Dubuque, Iowa. 429 p.

Eschmeyer, R. W. 1937. Some characteristics of a population of stunted perch. Papers Mich. Acad. Sci. Arts and Letters, 22: 612-628.

Harkness, W. J. K. 1922. The rate of growth of the yellow perch *(Perca flavescens)* in Lake Erie. Ont. Fish. Res. Lab., 6: 89-95.

Heib, R. N. 1968. Observations in the life history of the goldeye, *Hiodon alosoides* (Rafinesque), in Moccasin Bay on the Little Missouri Arm, Garrison Reservoir, North Dakota. Unpublished Masters thesis, University of North Dakota. 45 pp.

Hile, R. and F. W. Jobes. 1940. Age, growth and production of yellow perch, *Perca flavescens* (Mitchill) of Saginaw Bay. Trans. Amer. Fish. Soc. 80: 102-122.

Hill, W. J. 1966. Test netting survey of Garrison Reservoir. N. Dak. State Game and Fish Dept., Dingell-Johnson Project F-2-R-14. (Mimeographed.)

Pearse, A. S. and H. Achtenberg. 1920. Habits of the yellow perch in Wisconsin lakes. U. S. Bureau Fish. Bull. 36: 293-366.

Schneberger, E. 1935. Growth of the yellow perch, (*Perca flavescens* Mitchill) in Nebish, Silver, and Weber Lakes, Vilas County. Wisconsin Trans. Wis. Acad. Sci. Arts and Letters. 29: 103-130.

COMPOSITION, DISTRIBUTION, AND ORIENTATION OF XENOLITHS IN THE TUNK LAKE GRANITE, MAINE

Frank R. Karner and Roland A. Connors

Department of Geology

University of North Dakota, Grand Forks, North Dakota 58201

INTRODUCTION

Distribution, orientation and recrystallization of inclusions of older rocks (xenoliths) in igneous bodies may provide evidence of magmatic conditions and processes which often cannot be inferred from study of the igneous rocks themselves. These processes include bulk or differential transport of constituents of magma by gravitational settling or flotation and by convection or other types of currents, deposition of constituents on the floors of magma chambers, and chemical reaction and mechanical deformation both during and after crystallization. Several aspects of the distribution of xenoliths in the Tunk Lake granite are described here and the implications for magmatic processes are given.

GEOLOGIC SETTING

The post-tectonic Tunk Lake granite pluton (1) is intruded into Middle Devonian granites, the Bays-of-Maine igneous complex (2) and older metamorphic rocks in southeastern Maine. Its area of outcrop is 180 km^2 and nearly circular (Figure 1). Marginal aegirine augite and magnetite granites grade to hornblende and biotite granites and biotite quartz monzonite in the core (Figure 1).

The pluton is a single intrusion zoned by differentiation of a magma of composition similar to the calculated average of the body. Crystallization began along the margin where a sample of the original magma was frozen against the enclosing rocks forming a chill zone, zone I. The mineralogy of the marginal rocks indicates that they crystallized at relatively high temperature compared to those of the core which contain minerals that apparently formed at lower temperatures in the presence of abundant water. During crystallization, aqueous fluids streamed inward, removed silica from the partially crystalline margin and concentrated it in the still molten core, producing the major chemical variation observable in the pluton.

DISTRIBUTION OF XENOLITH TYPES

Two major zones of xenoliths are present (Figure 1). In the outer zone subangular, platy xenoliths, typically 2-10 cm long, consist of fine to medium-grained greenish-grey rock (Figure 2). In the central zone, thoroughly recrystallized, medium-grained xenoliths 1-2 cm in diameter are recognized as more or less equi-dimensional concentrations of ferromagnesian minerals (Figure 3).

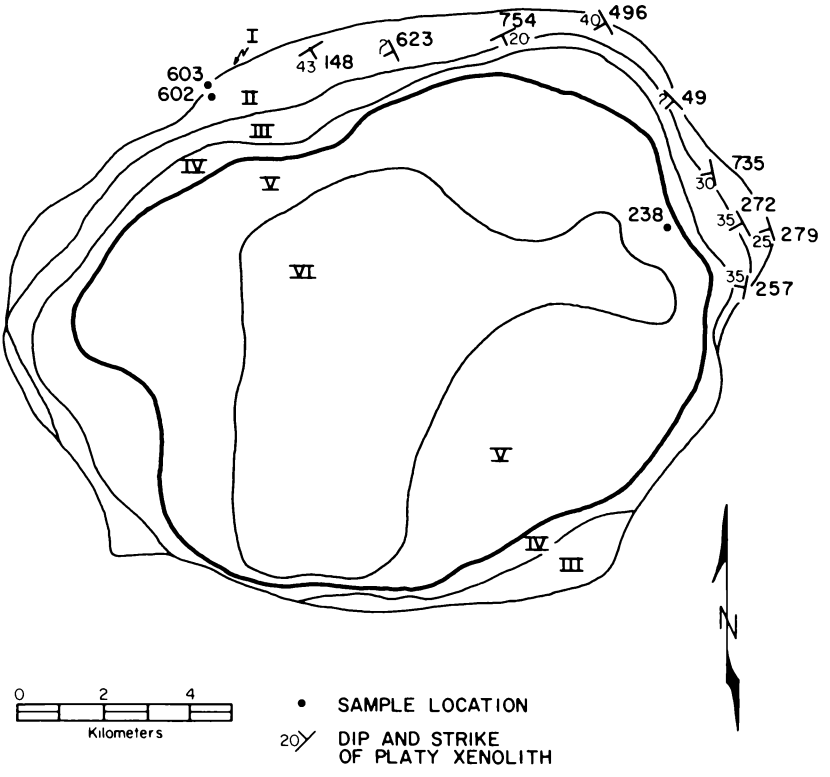

FIGURE 1—Location map of Tunk Lake pluton. Gradational petrographic zones include: II—Hornblende-aegirine augite granite, III—Hornblende granite, IV—Hornblende-biotite granite, V—Biotite granite, and VI—Biotite quartz monzonite. A thin zone (I) of magnetite-aegirine augite granite is found at some locations at the pluton's outer margin. The heavier line between zones IV and V is also an approximate boundary between the zones of major xenolith types. Samples not located by dots are shown by dip and strike symbols.

In the outer zone, close to the contact, some xenoliths are relatively unaltered, medium-grained augite-hornblende gabbro or diorite (Table I). Others have margins, one to a few millimeters wide, consisting predominantly of aegirine augite as mosaics of small grains grading outward to larger crystals (Figure 4). Typical xenoliths are fine-grained aggregates of about one-third aegirine augite and two-thirds albite-rich microperthite often surrounding cores of less

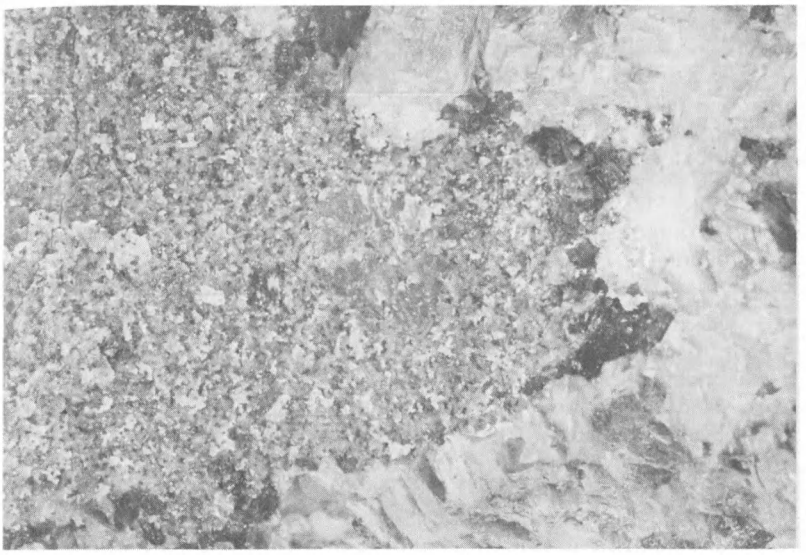

FIGURE 2—Xenolith from margin. Fine-grained, recrystallized, mafic xenolith consisting of about one-third aegirine augite and two-thirds perthite in coarse-grained aegirine augite-hornblende granite. **33X. Location 272.**

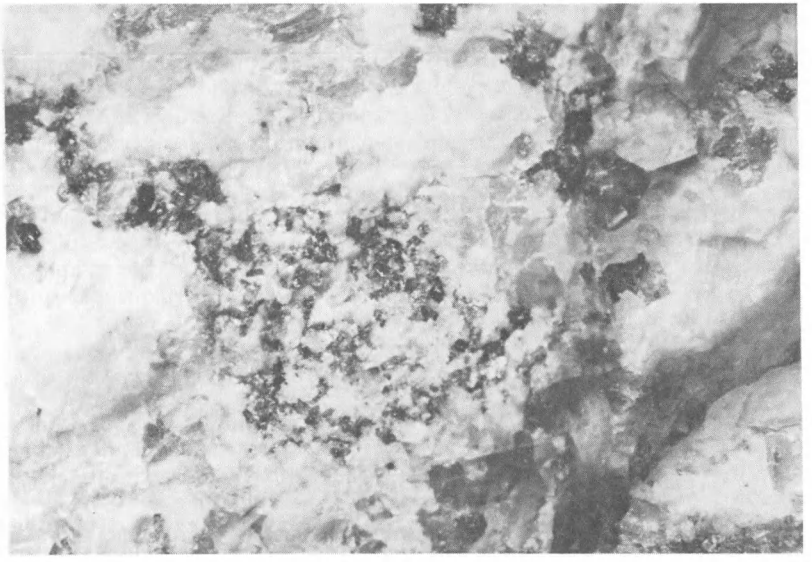

FIGURE 3—Xenolith from inner zone. Medium-grained, equidimensional recrystallized xenolith in biotite granite. 5.1X. Location 238.

TABLE I
MINERAL COMPOSITION OF XENOLITHS*

	A**	B	C	D	E	F	G	H
Plagioclase	5	6	5	5	<1	7	7	5
Perthite					7	<1	<1	<1
Quartz					<1	<1	<1	2
Augite	2	2	1	1				
Aegirine augite					3	3		
Hornblende	2		1					1
Biotite	1	2	3	4			3	2

*Approximate major mineral compositions, given in parts per ten, have been determined using standard, semi-quantitative optical and x-ray techniques (3).

**A. Medium-grained relatively unaltered gabbro-diorite of outer zone (Loc. 603,279).
B. Medium-grained large xenolith of outer zone (Loc. 602).
C. Medium-grained core of xenolith of outer zone (Loc. 602).
D. Typical fine-grained xenolith core of outer zone (Loc. 602,257).
E. Typical fine-grained outer margin of xenolith of outer zone (Loc. 272, 257).
F. Narrow transition zone between types D and E (Loc. 272, 275).
G. Typical medium-grained xenolith of inner zone (Loc. 238).
H. Typical medium-grained xenolith of inner zone (Loc. 238).

completely recrystallized gabbro-diorite consisting of plagioclase, and biotite (Table I, Figure 4). Coarser recrystallized xenoliths can be identified and these seem to be gradational in texture and composition with the normal ferromagnesian mineral clusters of the enclosing granite.

In the central zone only extensively recrystallized xenoliths are common, making up about 0.1 percent of the rock. They are typically aggregates of plagioclase, biotite, hornblende and quartz (Table I, Figure 5). As in the outer xenolith zone, they are gradational with the normal ferromagnesian clusters of the surrounding rock.

ORIENTATION AND DISTRIBUTION OF XENOLITHS IN THE MARGINAL ZONE

Slab-like xenoliths strike parallel to the contact of the granite and the country rock in the northwestern, northeastern and eastern margins of the pluton (Figure 1). They dip inward at angles of 20-45°.

A detailed study (3) of xenolith distribution was made along a 75 m strip of well-exposed rock extending westward from the eastern outer contact (Location 279) of the pluton (Figure 6). A total of 360

xenoliths were observed in 426 m^2 exposed area, giving an average frequency of 1.2/m^2 (Figure 6). Xenolith abundance varies cyclically along the length of the strip (Fig. 6), averaging about 0.3 percent of the rock. Approximately 70 percent of all xenoliths are elongate and less than 10 cm in length (3). A strong preferred orientation of strikes of elongate xenoliths shifts from N. 10° W. at the contact to N. 40° W. (Figure 6).

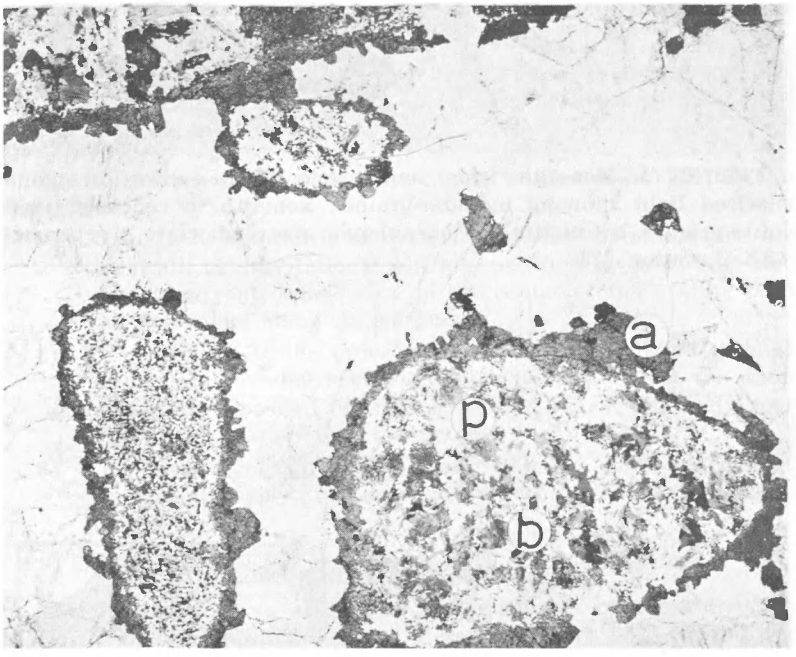

FIGURE 4—Rimmed xenoliths from margin. Thin section in plane polarized light showing aegirine augite surrounding medium-grained gabbro-diorite (upper left) or fine-grained, recrystallized gabbro-diorite (lower left) and intermediate xenoliths (lower right, middle) in coarse-grained aegirine augite granite. a=aegirine augite, b=biotite, p=plagioclase. 4.4X. Location 602.

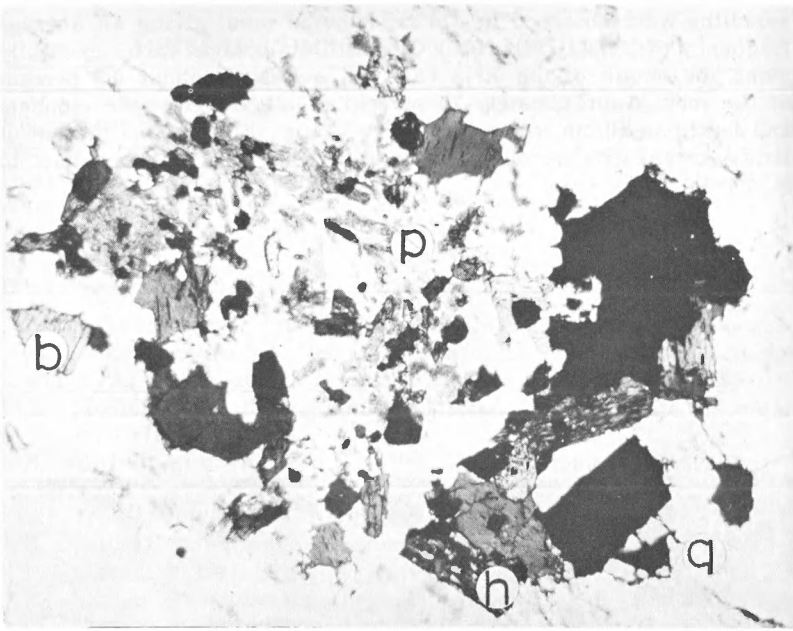

FIGURE 5—Xenolith from inner zone. Thin section in plane polarized light showing medium-grained xenolith in coarse-grained biotite granite. b = biotite, h = hornblende, p = plagioclase, q = quartz. 17.3X. Location 238.

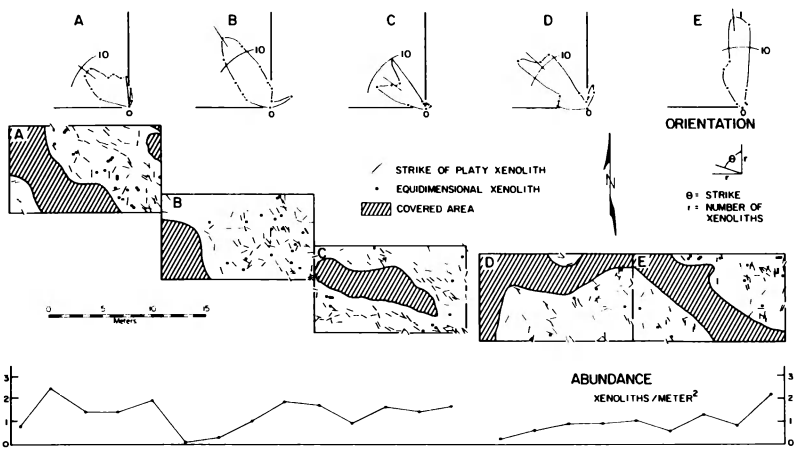

FIGURE 6—Xenolith distribution. Mapped distribution of xenoliths in two segments of a strip extending westward from contact. Location 279. The covered area between C and D is 50 meters wide.

CONCLUSIONS

Xenolith composition, distribution and orientation in the Tunk Lake pluton may be summarized as follows:

1) The outer zone of the pluton contains about 0.3 percent of platy mafic xenoliths typically less than 10 cm in length.
2) The typical outer xenoliths consist of gabbro-diorite recrystallized from original medium-grained plagioclase-augite mineral assemblages to fine-grained perthite-aegirine augite assemblages.
3) The inner zone of the pluton contains about 0.1 percent of equidimensional, extensively recrystallized xenoliths one to several centimeters in diameter.
4) The typical inner xenoliths are medium-grained aggregates of plagioclase, biotite, hornblende and quartz.
5) In both zones there are gradations between the xenoliths and the ferromagnesian mineral clusters of the enclosing granite.
6) In the outer zone xenoliths typically strike parallel to the granite margin and dip 20°-45° inward.
7) In a single area of the outer zone studied in detail, xenolith abundance varies cyclically in a strip oriented perpendicular to the granite margin.

The following working hypotheses are suggested for future investigation:

1) Xenolith orientation and cyclical variation of abundance are the result of gravitational settling modified by magmatic convection currents which rose in the center of the granite body and descended along its margins.
2) The xenoliths of the inner zone may have circulated through the magma chamber several times whereas those of the outer zone were deposited on a constructional floor relatively soon after incorporation into the magma.
3) The ferromagnesian minerals and possibly some feldspar of the granite may be extensively recrystallized xenolithic material.

ACKNOWLEDGMENTS

The authors wish to acknowledge the support of the University of North Dakota through Faculty Research Grant 4522-95 and the Summer Research Professorship Program.

REFERENCES

(1) Karner, F. R., 1968, Compositional variation in the Tunk Lake granite pluton, southeastern Maine: Geol. Soc. America Bull., v. 79, p. 193-222.

(2) Chapman, C. A., 1962, Bays of Main igneous complex: Geol. Soc. America Bull., v. 73, p. 883-887.

(3) Karner, F. R., 1968, X-ray analyses of cement-rock cores, In Anderson, S. B., and Haraldson, H. C. Cement-rock possibilities in Paleozoic rocks of eastern North Dakota: N. Dak. Geol. Surv. Rept. of Inv. 48, p. 41-55.

(4) Connors, R. A. Master's Thesis, Univ. of N. Dak., in preparation.

DESCRIPTION OF AUTHIGENIC ANALCITE IN THE EOCENE GOLDEN VALLEY FORMATION? SOUTHWESTERN NORTH DAKOTA

Marvin J. Furman and Frank R. Karner

Department of Geology

University of North Dakota, Grand Forks, North Dakota 58201

ABSTRACT

Authigenic analcite ($NaAlSi_2O_6 \cdot H_2O$) constitutes up to about 60 percent of a massive, arkosic sandstone exposed on several major buttes in southwestern North Dakota. Analcite occurs as spherulites in the interstices of the arkose and as a cement in a thin analcimolite bed near the top of the arkose unit. Three types of spherulites are recognized: (1) those with a radial structure; (2) those with a massive center and a peripheral radial structure; (3) those with no internal structure. The spherulites occur individually or as coalesced masses. The average composition of the analcite, expressed as the ratio $2SiO_2:Al_2O_3+Na_2O$, is 4.26.

Detrital minerals associated with the analcite include quartz, Na-plagioclase, K-feldspar, and illite. Sericite is associated with analcite and may also be authigenic. The analcite is least abundant at the base of the arkose unit, and increases upward. The abundances of analcite and detrital feldspar are inversely related. Sericite frequently occurs as inclusions in the analcite.

Analcite composition, distribution with respect to the feldspars, presence of sericite, and the absence of vitroclastic textures, suggests that analcite formed by post-depositional dissociation of feldspar.

INTRODUCTION

Tertiary rocks in southwestern North Dakota have been reported to contain authigenic analcite (1). The major occurrences of analcite found in this study are in rocks capping eleven major buttes in Dunn, Golden Valley, Slope and Stark Counties. The rocks are of questionable age, but have been tentatively assigned to the Golden Valley Formation of Eocene age (2). The Tertiary sequence is extensively interlayered with pyroclastic materials. Bentonite beds are

frequently present directly above and below the analcite-bearing rocks.

The primary method of investigation used in this study was x-ray diffraction using previously described methods (3). Identifications of minerals and semi-quantitative analyses of the minerals comprising the analcite-bearing rocks were made. The results of the semi-quantitative analyses are expressed as the ratio of the measured intensity of the mineral component of the sample to the 100 percent intensity of a pure standard, corrected for absorption.

ANALCITE-BEARING ROCKS

Analcite-bearing-arkose.—Arkose is the major cap rock on the buttes and has a maximum thickness of approximately 70 feet. It has been classified on the basis of the relative amounts of metamorphic rock fragments, feldspar, and clay. In compairson to the composition of typical arkoses, however, it is deficient in feldspars. The analcite is not visible in hand specimen. The modal composition of the arkose is given in Figure 1.

Analcimolite.—Small exposures of analcimolite are present at the tops of some of the buttes. The analcimolite, a rock type in which analcite is consistently the principal mineral component, occurs at the top of the arkose section. The rock is well-indurated and purple to maroon. The maximum thickness of the analcimolite is approximately 4 feet. The modal composition is given in Figure 2.

DESCRIPTION OF ANALCITE

Analcite occurs in the interstices of the arkose as individual spherulites and as aggregates of spherulites. Three types of spherulites are recognized on the basis of internal structure: 1) spherulites with well-defined radial structure (Figure 3); 2) concentrically structured spherulites with a massive center and peripheral radial structure (Figure 4) and 3) spherulites without internal structure or a poorly-defined internal structure (Figure 5). Spherulites in the aggregates are distorted to polyhedral shapes (Figure 5).

Analcite in the analcimolite occurs as a matrix and appears massive. However, a red stain outlines what might be individual grains (Figure 6).

Analcite composition, expressed as the ratio $2SiO_2:Na_2O+Al_2O_3$, has been determined by Saha's method (4). Table I gives the composition of analcite in the arkose and analcimolite from samples representing the stratigraphic and lateral extent of these rocks.

DETRITAL MINERALS

Detrital quartz and feldspar grains in the analcite-bearing arkose are corroded. There is an inverse relationship between analcite and detrital feldspar abundances (Figure 7 and 8). The trend of the analcite-plagioclase relationship is better defined than the analcite-potassium feldspar relationship. The analcite in the arkose is most

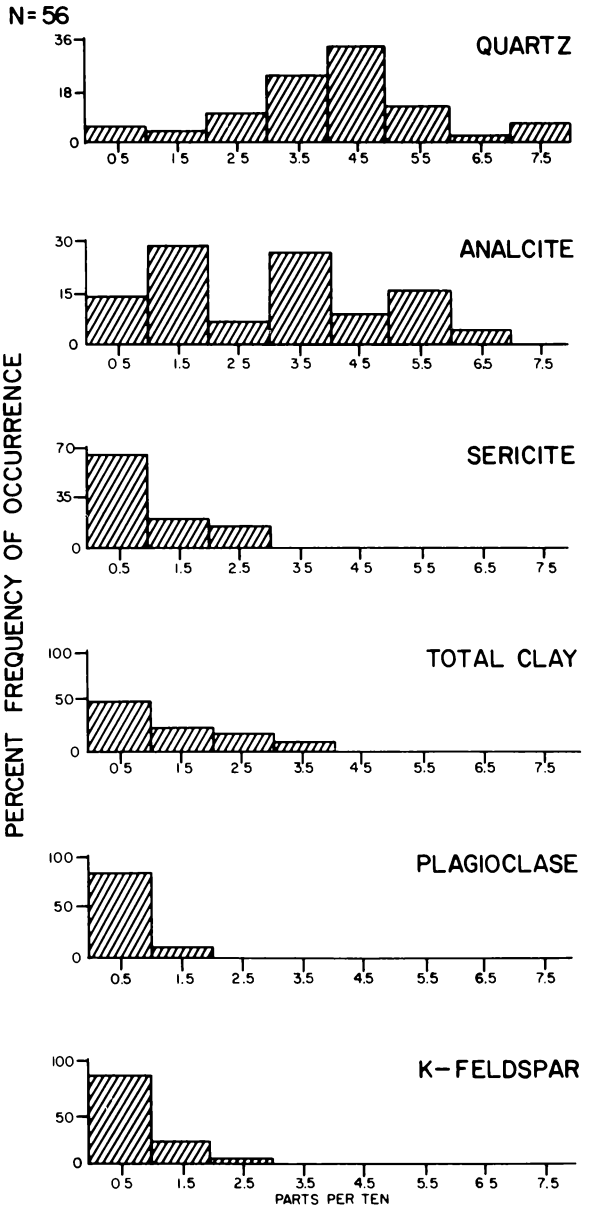

FIGURE 1—Modal composition of analcite-bearing arkose.

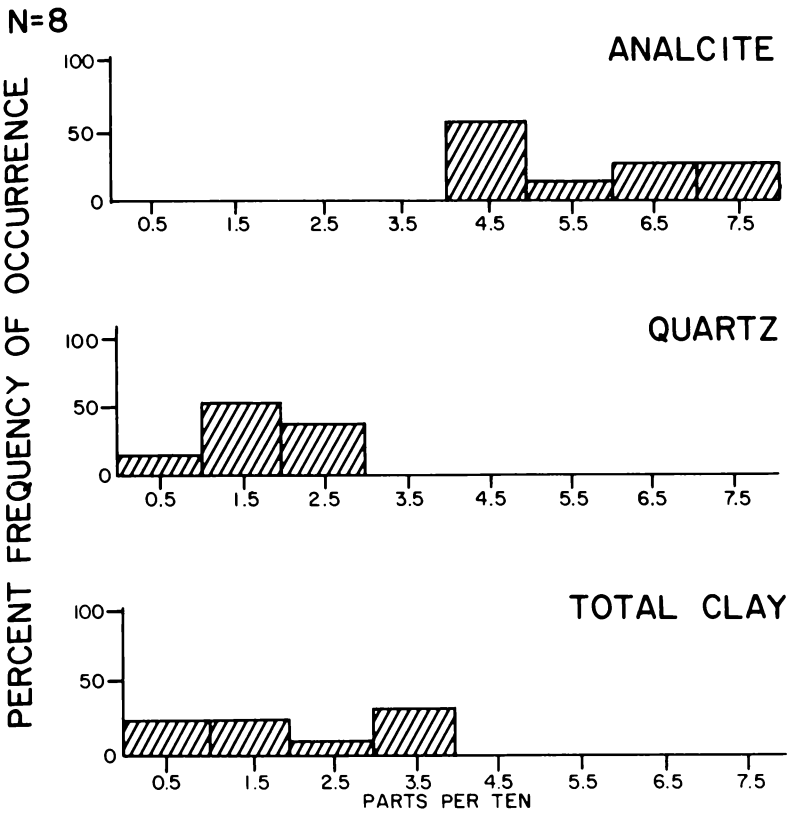

FIGURE 2—Modal composition of analcimolite.

TABLE I
COMPOSITION OF ANALCITE

Specimen	$2SiO_2:Na_2O+Al_2O_3$
Arkose, Flat Top Butte (4670)*	4.28
Analcimolite, Bullion Butte (4775)	4.28
Arkose, Bullion Butte (4684)	4.35
Arkose, Sentinel Butte (4686)	4.28
Arkose, Sentinel Butte (4678)	4.52
Arkose, Slide Butte (4727)	4.42
Analcimolite, Slide Butte (6994)	4.00
Analcimolite, Chalky Buttes (6995)	4.13
Analcimolite, Chalky Buttes (6996)	3.91

*University of North Dakota Geology Department sample number.

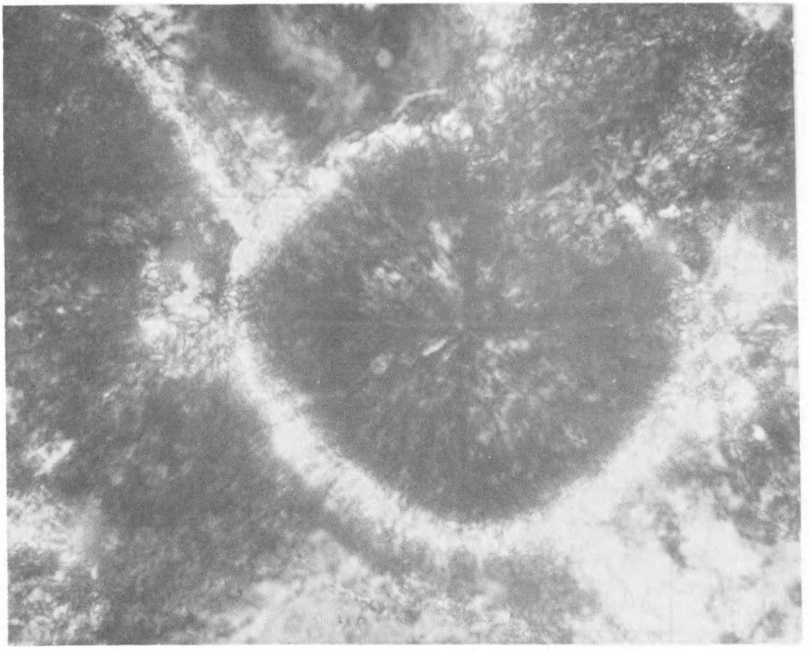

FIGURE 3—Spherulite showing radial structure characterized by maltese cross. 600X; crossed nicols.

abundant at the top of the section and decreases downward. Correspondingly, the feldspars are most abundant at the base of the section and decrease upwards (Figure 9) (5).

OCCURRENCE OF SERICITE

Sericite occurs in the arkose as randomly oriented inclusions in the analcite spherulites, as interstitial matrix coexisting with a finer-grained illitic matrix, and replacing detrital feldspars and quartz. Multiple origins are recognized for illite in sedimentary rocks (6). The possible significance of the sericite-analcite association in the arkose, is that sericite is produced with analcite in mineral synthesis reactions between albite and water (7).

CONCLUSIONS

There is a recognized genetic association between analcite and volcanic glass in sediments (8). The close proximity of pyroclastic materials to analcite-bearing rocks warrants consideration of volcanic glass as a possible precursor to the analcite. A survey of the occurrences of analcite believed to have originated from pyroclastic materials shows that the vitroclastic texture is commonly preserved. This texture is not present in the arkose or analcimolite, suggesting that the analcite has not been derived from volcanic glass. Analcite not originating from volcanic glass generally has a relatively low Si:Al ratio (9). The Si:Al ratio of the Golden Valley analcite is low, 2.0-2.3, further suggesting that volcanic glass may not be the parent material.

The analcite-feldspar distribution suggests that the analcite has been derived from the detrital feldspars. There is no textural evidence of replacement of feldspar by analcite. The corroded condition of the feldspars suggests that they have dissociated in the interstitial water. It is proposed that the interstitial solution became saturated with respect to analcite, and analcite precipitated. The mineral which

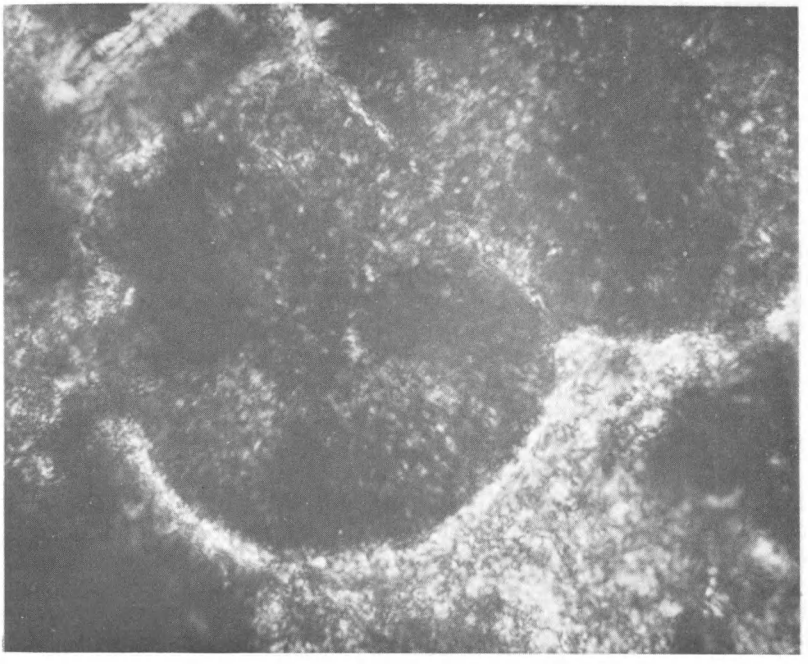

FIGURE 4—Spherulite with a massive center and a peripheral radial structure. 600X; crossed nicols.

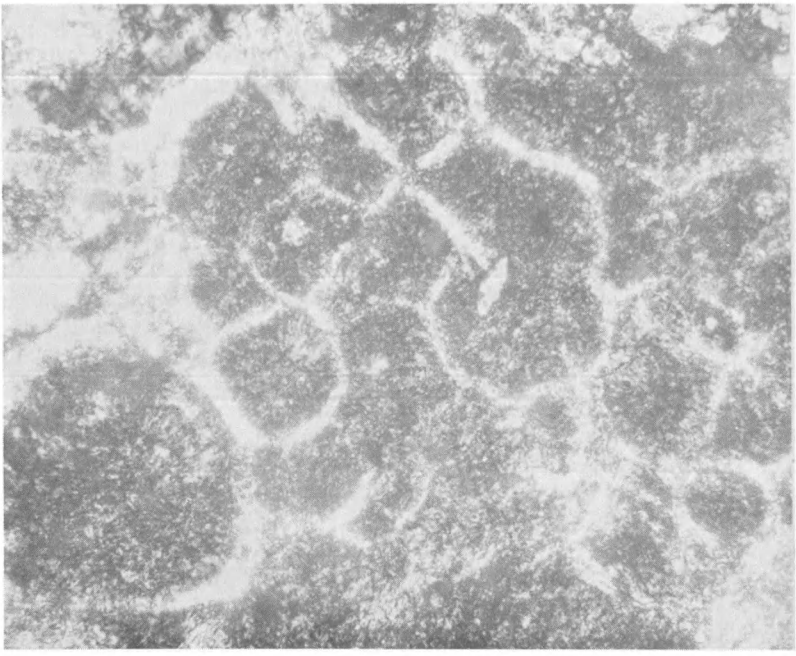

FIGURE 5—Distorted spherulites in aggregate. A number of spherulites show no internal structure. 300X; crossed nicols.

precipitates depends on the relative activities of Na^+, H^+, and H_4SiO_4 in the interstitial solution (10). The vertical distribution of the analcite and feldspars is attributed to the removal of interstitial water, the reaction media, with increasing depth of burial. Thus, the dissolution of the feldspars was impeded, halting the reaction sequence.

It is suggested that individual spherulites coalesced to form the aggregates. The growth of the spherulites in close proximity resulted in their mutual interference and distortion of shape.

Analcite in the analcimolite has a different occurrence than analcite in the arkose, and it is therefore suggested that the origins are different. Occurrence of the analcite as matrix is similar to the occurrence of typical sedimentary cements, for example, calcite and silica. The analcimolite rests on the analcite-bearing arkose. There is no indication of massive depletion of analcite from arkose directly underlying the anacimolite. Suggested origins for analcimolite-like rocks are by direct precipitation from surface waters (11), and by crystallization of sodium-aluminum silicate gels (12).

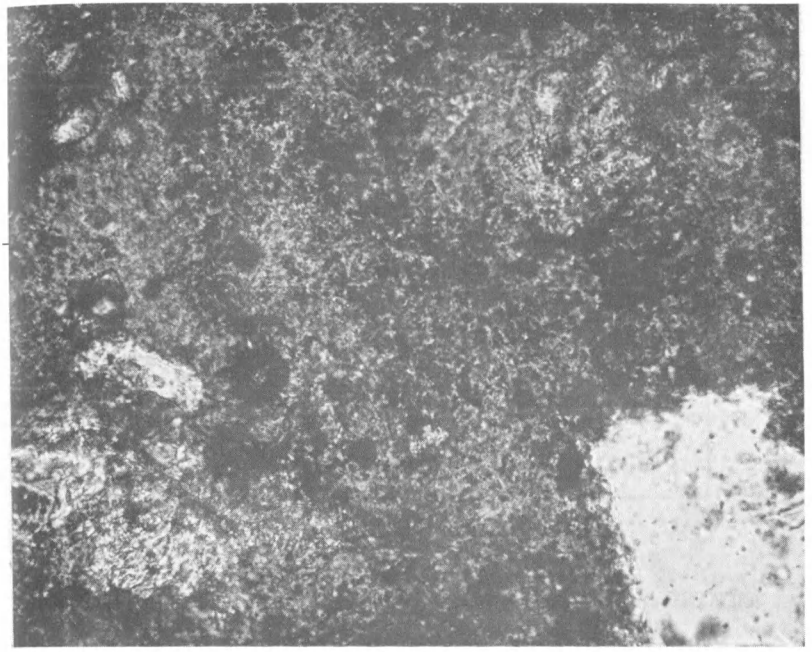

FIGURE 6—Analcimolite texture. 300X; crossed nicols.

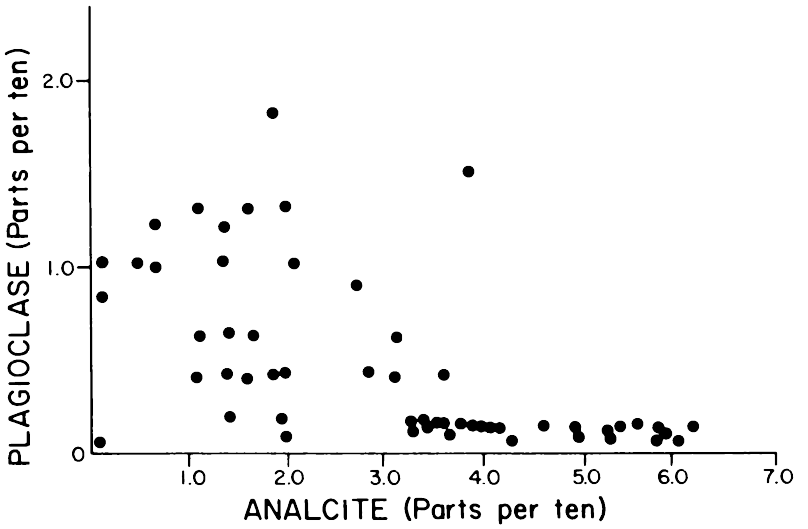

FIGURE 7—Variation of analcite-plagioclase in arkose.

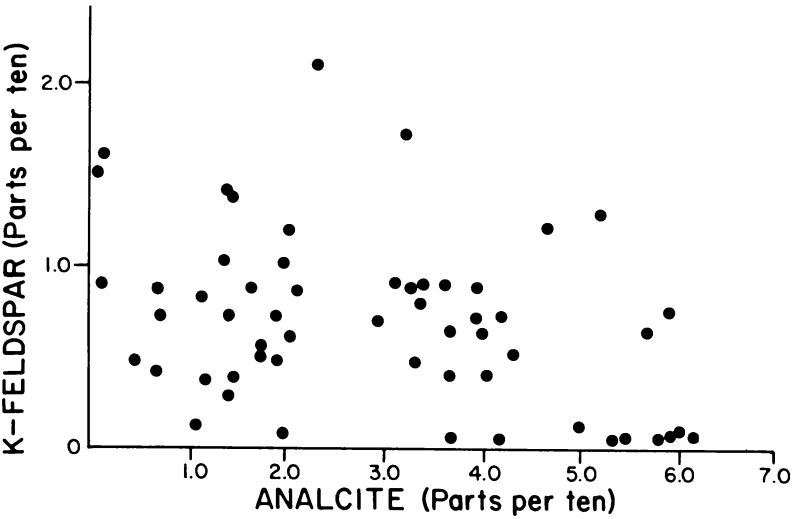

FIGURE 8—Variation of analcite-K-feldspar in arkose.

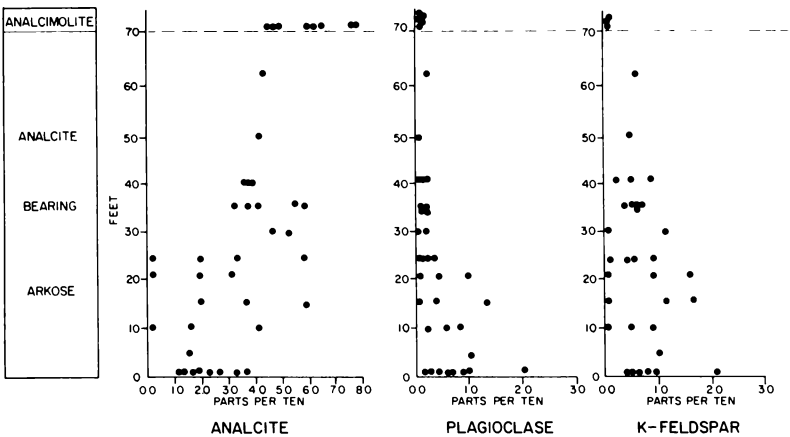

FIGURE 9—Vertical distribution of analcite, plagioclase, and K-feldspar in analcite-bearing rocks.

REFERENCES AND NOTES

1. E. R. Beroni, H. L. Bauer, U. S. Dept. of Interior, TEI-123, 93 (1952).
2. N. M. Denson, U. S. Geol. Surv. Prof. Paper, 650-B, B63 (1969).
3. F. R. Karner, *in* N. D. Geol. Surv. Rept. of Invst., 48, 41 (1968).
4. P. Saha, Am. Min., 44, 300 (1959); 46, 859 (1961).
5. Data taken from unpublished M. S. thesis: Authigenic Analcite in the Golden Valley Formation? Southwestern North Dakota, by M. J. Furman.
6. A. L. Reesman, W. D. Keller, J. Sed. Pet., 37, 592 (1967).
7. G. W. Morey, W. F. Chen, Am. Min., 40, 996 (1955).
8. D. S. Coombs, Royal Soc. New Zealand Trans., 82, 65 (1954); K. S. Deffeys, J. Sed. Pet, 29, 602 (1959).
9. D. S. Coombs, J. T. Whetten, Geol. Soc. Am. Bull., 78, 269 (1967).
10. P. C. Hess, Am. J. Sci., 264, 289 (1966).
11. F. B. Van Houten, J. Geol., 68, 666 (1960); Am. J. Sci., 260, 561 (1962).
12. H. P. Eugster, B. F. Jones, Science, 161, 160 (1968).
13. Field work for this study was supported by the N. D. Geol. Surv.; the authors are indebted to W. J. Stone for the use of his samples.
14. This paper is part of a M.S. thesis submitted to the University of North Dakota.

NEW SEDIMENTOLOGICAL AND PALEONTOLOGICAL EVIDENCE FOR HISTORY OF LAKE AGASSIZ: SNAKE CURVE SECTION, RED LAKE COUNTY, MINNESOTA

Stephen R. Moran

North Dakota Geological Survey

and

Lee Clayton and Alan M. Cvancara

University of North Dakota, Grand Forks, North Dakota 58201

ABSTRACT

The Snake Curve Section is a 70-foot cutbank 4 miles west of Red Lake Falls on the right bank of the Red Lake River where it crosses the Campbell Scarp of Lake Agassiz. The section consists of

15 feet of buff, sandy till overlain by up to 6 feet of less consolidated pebbly loam derived from the till. Overlying this is a 5-foot bed of varved clay and silt that is, in turn, overlain by at least 20 feet of gray clayey till. A buried valley, filled with 15 feet of fluvial sand and gravel, is eroded into these units. Overlying this sand and gravel is a conformable sequence of 10 feet of shoreline sand, interbedded with silt and clay, 15 feet of interlaminated silt and clay, and 15 feet of shoreline sand. Fossil mollusks collected from the fluvial sand and gravel and the overlying shoreline sand indicate a woodland-flanked stream.

Following two glacial advances, the first from the northeast and the second from the northwest, the Snake Curve site was covered by the waters of Lake Agassiz. The level of the lake lowered and a rived flowed westward across the site. The radiocarbon age of a log from this buried stream valley, 9,890 ± 150 BP (I-4853), indicates that this low-water period was responsible for the major unconformity which is recognized throughout the southern part of the basin, in Lake Agassiz sediments. The lake again rose, depositing the transgressional sequence of shoreline sand overlain by laminated silt and clay. Because wave agitation in Lake Agassiz extended to a depth greater than 15 feet, it is not possible for the quiet-water silt and clay to have been deposited while the lake stood at the Campbell Scarp, whose toe is 15 feet above the top of this sediment at the Snake Curve site. The lake level, therefore, rose above the Campbell level during this transgression. At a later date, the lake fell to the Campbell Scarp, where it stood for several hundred years before it began to fall for the last time.

INTRODUCTION

Some of the best exposures of Quaternary deposits in northwestern Minnesota occur in cutbanks of the Clearwater and Red Lake Rivers near Red Lake Falls. These cutbanks expose a sequence of two glacial tills separated by lacustrine silt and clay. The exposures at the Snake Curve Section, 4 miles west of Red Lake Falls in SW¼NW¼SW¼ sec. 18, T. 151 N., R. 44 W. (Figure 1), contain also a buried valley filled with stream sediment that stratigraphically overlies the upper glacial till and is overlain by lake sediment (Figure 2).

The Snake Curve Section is located where the Red Lake crosses the Campbell Scarp. This scarp was cut by Lake Agassiz when its southern outlet was at the level of the Precambrian granite at Browns Valley, Minnesota. The presence of the buried stream valley, along with the overlying deep-water lake sediment, indicates that Lake Agassiz drained and refilled to a level above the Campbell level during the deposition of the sediments that are exposed in the Snake Curve Section. A well preserved molluscan fauna from the stream sediment and the conformably overlying shoreline sediment indicates

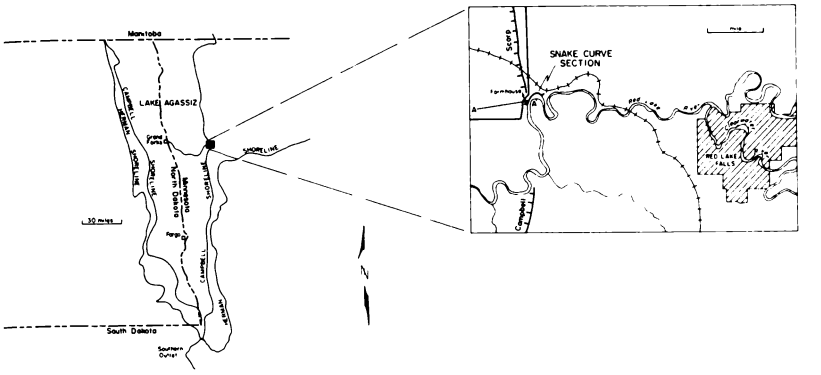

FIGURE 1—Location of Snake Curve Section.

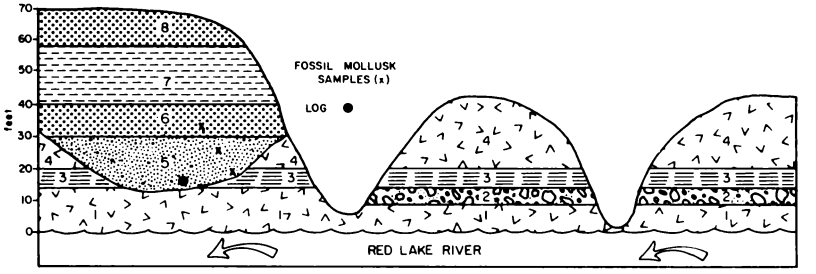

FIGURE 2—Diagram of the Snake Curve Section.

the presence of a woodland-flanked river during this period of low water in the Lake Agassiz basin.

OBSERVATIONS

Outcrop description.—Two glacial tills separated by lacustrine sediment are exposed at the base of the Snake Curve bluffs. A valley fill containing fluvial sand and gravel is cut into these units and the entire sequence is overlain by a second sequence of lacustrine sediment. As much as 50 feet of section is obscured by mass wasting,

and vegetation occurs along much of the exposure; additional unobserved units may also be present (Figure 2).

Unit 1 consists of 5 to 15 feet of reddish brown, consolidated, silty, sandy, slightly pebbly loam (till) having massive to large columnar structure. This till contains pebbles composed largely of granitic rock, limestone, and dolostone. The base of unit 1 is not exposed and the thickness of the unit is unknown.

The sharp but comformable upper contact of unit 1 is marked either by the first occurrence of lenticular, brown silt beds a few millimeters thick or by an abrupt change to unit 2, a brown, pebbly to slightly pebbly loam that is less pebbly and considerably less compact than the underlying till. Unit 2 possesses obscure bedding unlike the more massive till of unit 1. Unit 2, which is locally absent, is 1 to 5 feet thick. It becomes finer grained upward, changing progressively from 21-43-36 (% sand - % silt - % clay) near the base to 12-33-55 near the top. Where unit 2 is absent, the silt beds in the upper part of the lower till become thicked and more numerous through an interval of 1 to 3 feet.

Unit 3, lacustrine silt and clay, is 2 to 5 feet thick, and conformably overlies unit 1 or 2 throughout the entire section. Near its base, unit 3 contains beds of thinly laminated, brown silt up to 6 inches thick, interbedded with beds of brown, pebbly loam up to 3 inches thick. The bedding becomes progressively thinner upward where individual beds are only a few millimeters to a few centimeters thick. In the upper half of unit 3, dark gray to black clay beds a few millimeters thick, rather than brown silt beds, are interbedded with the brown pebbly loam. In the upper part of the unit, beds of gray pebbly clay replace the beds of brown pebbly loam.

Locally, unit 3 is considerably contorted. Structures in unit 3 include flow rolls, overthrust faults, load casts, and piercement structures. Some of these structures are believed to have resulted when pebbly loam mudflows and turbidity currents flowed over weak, saturated, unconsolidated lacustrine silt and clay. In some instances, these flows incorporated the underlying beds, folding or faulting them. In other cases, the load of the pebbly loam beds was greater than the bearing strength of the clay and silt, and the pebbly loam beds foundered, producing piercement structures. Some of the structures may have been formed when unit 3 was overridden by the glacier that deposited the overlying till, unit 4. Many of the structures formed as the result of mass movement following the erosion of the present Red Lake River valley. Numerous landslide blocks appear to have moved on failure surfaces in unit 3.

Unit 4, dark gray, very slightly pebbly to slightly pebbly clay (till), everywhere conformably overlies unit 3. Unit 4 has a maximum thickness of 20 feet. Where unit 4 is thinner, the overlying material is laminated lacustrine clay rather than lacustrine sand

which occurs above the thicker sections. The clay may be part of unit 3 that has been carried up into the till along failure surfaces of post-depositional slump blocks. Along much of the exposure the upper contact of unit 4 is not exposed. In the outcrops examined, the till has a coarse, angular, blocky structure that is characterized by slickensides along the block faces. This structure resulted from the slumping deformation of the outcrops that followed the erosion of the present valley.

A valley has been eroded through the entire sequence above unit 1 at the south end of the exposure. The lowest point in the valley fill is several feet below the top of unit 1. Unit 5, which consists of 10 to 15 feet of flat-bedded gravel, sandy gravel, and dune cross-bedded, gravelly sand, occurs in the buried valley. Numerous gastropods, bivalves, and a 4-inch log (spruce?) were collected from unit 5.

Approximately 10 feet of flat-bedded shoreline sand, with ripple cross-bedding, unit 6, overlies unit 5. Some silt and clay is interbedded with the sand. An extensive fauna of small gastropods and bivalves was collected near the base of this unit.

Unit 7 consists of approximately 15 feet of thinly laminated lacustrine silt overlying the shoreline sand of unit 6. The contact between the two units is conformable. No fossils were observed in unit 7.

Unit 8 consists of 15 feet of thin bedded, fine-grained, well-sorted shoreline sand overlying the lacustrine silt of unit 7. This sand is flat-bedded with ripple cross-bedding. The contact between the two units is conformable.

Properties of the tills.—The Snake Curve Section affords an excellent opportunity to study the characteristics of the sediments deposited by the last two glaciers to cover the area. Using information obtained from this exposure, it will be possible to recognize and trace these two tills into other areas where they are not so clearly exposed. The two tills are clearly different in the Red Lake Falls area. They are separated by lacustrine sediments of units 2 and 3 and their composition is so different that even casual observation indicates that they are separate tills. The two tills differ because of the large amount of locally derived lake sediments in the upper till, unit 4. The lake sediment was undoubtedly deposited in a lake which was similar in distribution to Lake Agassiz. The upper till probably becomes more like the lower till as they are traced laterally out of the Red River Valley because of the absence of lacustrine sediment to alter the characteristics of the upper till. For this reason, we have studied the composition of the two tills in order to characterize them by properties that are less likely to change laterally than color and pebble lithology. It is hoped that correlations beyond the Red River Valley will be possible, using these characteristics.

Three samples from unit 1, the lower till, and fourteen samples from the upper till, unit 4 (Figure 2), have been analyzed for texture

and carbonate content. Examination of these data (Figure 3) reveals marked differences between the two tills.

Molluscan fauna.—Mollusks were collected from four sediment samples from units 5 and 6 (Figure 2). The samples are listed by accession numbers (Department of Geology, University of North Dakota) in descending stratigraphic order.

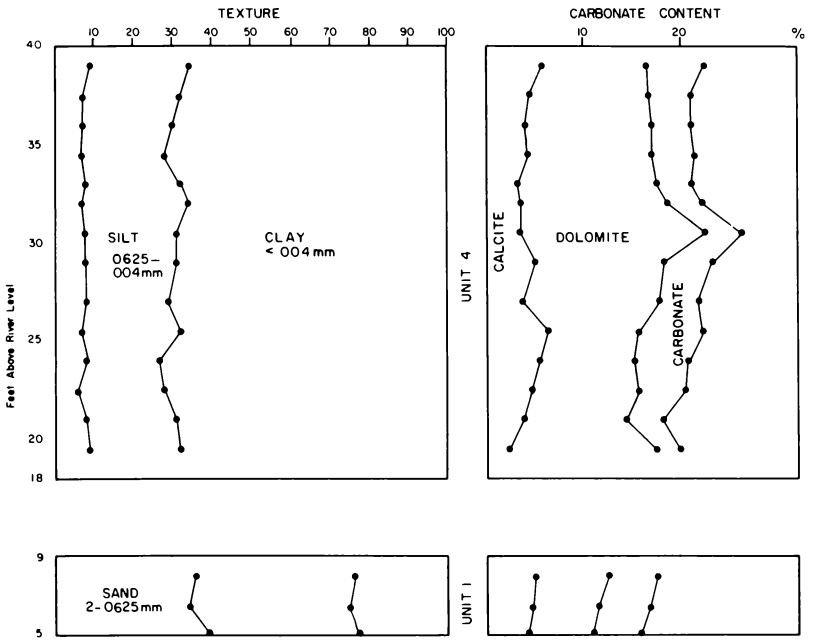

FIGURE 3—Texture of the till matrix and gasometrically determined carbonate content of the < 200-mesh fraction of units 1 and 4.

A407. Includes an 8-13 cm-thick interval of sand between beds of silt and clay in unit 6. The base of the interval is 4.78 m above the bottom of the buried valley. The sample size was 2.7 liters.

A408. Includes a 72-cm interval of sand and gravel in unit 5. The base is 4.11 m above the bottom of the buried valley. The sample size was 1.87 liters.

A409. Includes a 15-cm interval of sand and gravel in unit 5. The base is 0.85 m above the bottom of the buried valley. The sample size was 2.01 liters.

A410. Composite grab sample of sand and gravel in unit 5. The sample was somewhat larger than samples A408 and A409.

The samples were wet sieved, using sieves having standard Wentworth subdivisions. The grain diameter mode for samples A407, A408, and A409 was medium sand, and the intermediate diameter of the largest particle in each sample was 12.8 mm, 22.8 mm, and 29.5 mm, respectively. Mollusks were picked from the material retained on the 16 mesh sieve (Tyler) (very coarse sand and coarser).

Specimens were counted from samples A407 to A409 and these values were adjusted for a sediment sample size of 2.00 liters so that direct comparisons could be made between samples (Table I). Numbers of valves of bivalves were divided by two to determine the number of individuals for each sample.

At least 20 molluscan species were collected from unit 5 (samples A408 to A410): 5 bivalves, 11 aquatic gastropods and 4 terrestrial gastropods. Three species of pisidiids appear to be present. This fauna represents one of the largest taken at a single locality from glacial Lake Agassiz sediments in the southern part of the basin (see Tuthill, 1963; Tuthill, Laird and Kresl, 1965; and Zoltai, 1969 for comparison). It is unusual in containing terrestrial gastropods, which are lacking from most late Wisconsinan collections from the mid-continent region. Shells of pisidiids and branchiate gastropods are more aboundant in sample A408 and pulmonate gastropod shells are more abundant in sample A409.

Sample A407 from sand between beds of silt and clay in unit 6 (Figure 2), has yielded a molluscan fauna essentially the same as that of the underlying sand and gravel of unit 5. The proportion of shells of branchiate and pulmonate gastropods and pisidiids is similar to that of sample A408. The numbers of shells of pisidiid bivalves and branchiate gastropods increase upward, and the numbers of shells of pulmonate gastropods decrease upward. The total number of individuals is greatest in unit 6 (sample A407), largely because of a greater number of shells of *Pisidium* sp. (Table I).

INTERPRETATIONS

Till source.—The ice which deposited the lower till probably advanced from the northeast. The pebbles appear to consist largely of limestone, dolostone, and granitic rock; shale pebbles are rare.

The pebbles contained in the upper till consist largely of soft clay pebbles derived from lacustrine sediment and a few carbonate and shale pebbles. The pebble lithology, as well as the texture, strongly suggest that the upper till has been derived largely from pre-existing lacustrine sediment. The presence of the shale pebbles suggests that the glacier flowed from the northwest across Cretaceous shale. Such an interpretation is consistent with other evidence in North Dakota and Manitoba that indicates that the last ice advance to cover this region did, in fact, advance from the northwest (Elson, 1955).

Till correlations.—The correlations of the till units exposed in the Snake Curve Section with the till units in other areas is uncer-

TABLE I

MOLLUSKS FROM UNITS 5 AND 6 OF THE SNAKE CURVE SECTION, RED LAKE COUNTY, MINNESOTA

Mollusk name	Number of individuals per 2.00-liter sample at three stratigraphic levels				Habitat**					
	*A410	A409	A408	A407	1	2	3	4	5	6
BIVALVES										
Anodontoides ferussacianus (Lea)	.....	.....	.....	0.4				X	X	
Lasmigona complanata (Barnes)	X	.....	.....	.....				X	X	X
Lamsilis siliquoidea (Barnes)	X	0.5	.....	0.7				X	X	X
L. ventricosa (Barnes)	X	.....	.....	.....				X	X	X
Pisidium sp.	X	28.5	30.5	101.0			X	X	X	X
Sphaerium sp.	X	8.5	36.4	24.0			X	X	X	X
AQUATIC GASTROPODS										
Valvata tricarinata (Say)	X	2.0	2.1	1.5				X	X	
V. lewisi Currier	.....	.....	1.1	.....				X		
Probythinella lacustris (Baker)	X	5.0	41.7	25.9				X	X	X
Amnicola limosa (Say)	X	8.0	50.3	74.0				X	X	X
Stagnicola palustris (Miller)?	X	.....	.....	.....			X	X	X	
Fossaria obrussa (Say)	X	1.0	?2.1	?0.7			X			
Ferrissia rivularis (Say)	X	13.0	7.5	8.9					X	X
Gyraulus parvus (Say)	X	37.0	9.6	18.5				X	X	
Helisoma anceps (Menke)	X	2.0	14.9	5.9				X	X	X
Planorbula armigera (Say)	X	.....	.....	.....			X			
Physa gyrina (Say)	X	2.0	2.1	5.2			X	X	X	
TERRESTRIAL GASTROPODS										
Catinella avara (Say)?	X	.....	1.1	2.2	X	X				
Oxyloma retusa (Lea)?	X	.....	.....	.....		X				
Discus cronkhitei (Newcomb)	X	?1.0	?1.1	1.5	X					
Zonitoides arboreus (Say)	X	?1.0	.....	.....	X					
Total of individuals		109.5	200.5	270.4						

*Accession number of the Department of Geology, University of North Dakota; A410 represents a composite grab sample and only species presence is indicated. Accessions A409 to A407, in ascending stratigraphic order, refer to samples on which specimen counts were made and adjusted to a common sample size of 2.00 liters. Figure 2 shows the location of samples.

**General habitat for each species: (1) Woodlands and other shaded areas, (2) areas near water, (3) intermittent ponds or streams, (4) permanent ponds or lakes, (5) streams and (6) rivers. Note: Question marks after numerals indicate the uncertain occurrence of a species.

tain. Ross and Karner (1967) reported two tills separated by 51 feet of lacustrine clay at Grand Forks, North Dakota. Although these two tills differ considerably in texture from the till units in the Snake Curve Section, the upper till is significantly finer in texture (27-28-45) than the lower (49-13-38). The uppermost two tills encountered in borings west of the Pembina Escarpment in Ramsey County, North Dakota, also exhibit the same textural relationship; the upper till has a significantly finer texture than the lower (J. P. Bluemle, North Dakota Geological Survey, personal communication).

Whether the tills in these three areas are correlative is unknown. The considerable distance between the areas and consequent changes in composition make correlation difficult, but the similar textural relationships between the tills in each area is suggestive of their equivalence. Additional mineralogical studies will help clarify the relationships.

Environmental analysis (units 5 and 6).—In the samples from unit 5, (A408 to A410), the aquatic molluscan fauna as a whole is typically neither lacustrine nor fluvial. However, species characteristic of stagnant, intermittent water bodies (that is, *Planorbula armigera, Fossaria obrussa* and *Stagnicola palustris*) are rare. The limpet, *Ferrissia rivularis*, is characteristically a stream or river species (Basch, 1963, p. 430). Shells of the unionid bivalves are relatively large and thick, as is generally true for river forms. One species, *Lasmigona complanata*, typically occurs in streams or rivers, although it does occur in ponds and lakes (Parmalee, 1967, p. 52). The small number of species of unionids (four) is suggestive of a stream or smaller river. *Lampsilis ventricosa* seems somewhat anomalous in the assemblage because it generally occurs in the larger rivers, such as the Red and Red Lake Rivers (Cvancara, 1966). Two of the terrestrial gastropods, *Discus cronkhitei* and *Zonitoides arboreus*, normally require the shade and cover of woodlands. Therefore, the molluscan fauna suggests primarily a stream or smaller river flanked, at least partially, by woodlands. Small ponds adjacent to the stream could have contributed the relatively rare forms that are typical of small, stagnant water bodies.

The fossil assemblage found in unit 6 (sample A407) is also suggestive of a woodland-flanked stream or small river. The occurrence of sample A407 in shoreline sand between beds of silt and clay suggests that the stream or small river emptied into a lake with fluctuating water level.

Sequence of events.—The following sequence of events is suggested by the data obtained from the Snake Curve Section in combination with the previously known information regarding the Lake Agassiz basin (Elson, 1967).

We do not know when the glacier that deposited the buff, sandy till of unit 1 first entered the area of Red Lake Falls from the northeast. We assume that this advance occurred during the Late Wis-

consinan because the contacts of unit 1 with units 2 and 3 and the contact of unit 3 with unit 4 appear to be conformable. On this basis, unit 1 appears to be separated from unit 4 by only a short time. A lake was formed between the ice front and the highland to the south as the glacier which deposited unit 1 receded from the Red River Valley. Masses of saturated debris sporadically flowed from the ice across the floor of the lake to form unit 2 and the base of unit 3. As the distance between the ice front and the Snake Curve site became greater, the debris flows become fewer and thinner, and quiet, deep-water sedimentation produced the upper part of unit 3.

The glacier which deposited the till of unit 4 advanced into the Red Lake Falls region from the northwest, presumably toward the end of Late Wisconsinan time. The relationship of this glacier to the Holt-Edinburg moraine is unknown. If the till of unit 4 proves to be related to the Holt-Edinburg moraine, the lacustrine sediment of unit 3 was deposited in Lake Agassiz and the underlying till of unit 1 is of Late Wisconsinan age. On the other hand, if unit 4 is traced beyond the Holt-Edinburg moraine, unit 3 may represent a pre-Agassiz lake of the Red River Valley, and the age of unit 1 remains in doubt.

The ice that deposited unit 4 began its retreat approximately 12,500 years B. P. (Elson, 1967). As the ice margin melted northward in the Red River Valley, Lake Agassiz was immediately formed between the glacier and the highland to the south. The level of Lake Agassiz at this time, which was determined by the lowest southern outlet through Browns Valley, is marked by the Herman strandline (Figure 1). The flow of water through the southern outlet eroded the glacial sediment that filled the valley. At the same time the earth's crust was buoyantly rebounding as the weight of the northward-receding glacier was removed. The combined effect of the lowering of the outlet of the lake and the rising of the land caused the shoreline of Lake Agassiz to fall and recede toward the center of the basin. The glacier then retreated far enough northward to expose a lower outlet in Ontario. The level of Lake Agassiz dropped as it drained eastward into the Lake Superior basin. We do not know how far the level of the lake dropped but it was far enough so that the shoreline, which up until that time had been east of Red Lake Falls, shifted westward until it was west of the Snake Curve site.

A river, ancestral to the modern Red Lake River, flowed westward across the exposed lake floor on which a forest was growing. The channel of this river was cut about 25 feet below the lake plain, the top of unit 4, which at the Snake Curve site is at an elevation of 960 feet (Figures 2, 4). Based on the radiocarbon age of wood from the deposits of this stream, 9890 ± 150 B. P. (I-4853), this low level stand of Lake Agassiz occurred about 10,000 years B. P., not 12,000 B. P. as indicated by Moran and others (1970).

The glacier advanced a short distance again, blocking the eastern

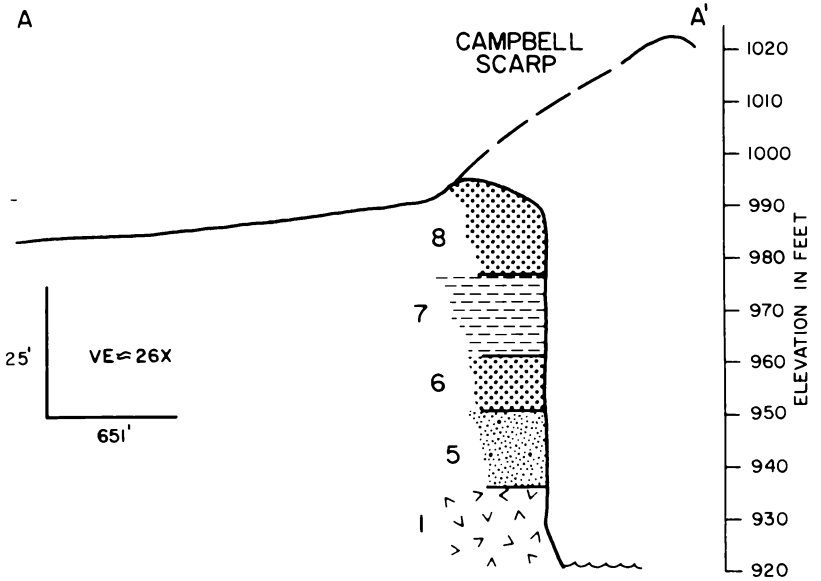

FIGURE 4—East-west cross section showing the relation of the Snake Curve Section to the Campbell Scarp. Location of the section is shown on Figure 1.

outlet of Lake Agassiz and causing the water to rise back to the level of the southern outlet. As the water rose, the shoreline shifted eastward to some point east of the Snake Curve site. The transgressive sequence of shoreline sand (unit 6) passing gradationally upward into interlaminated silt and clay (unit 7) was deposited during this rise in level of the lake. The present elevation of the floor of the lake (the top of unit 7) at the time the shoreline stood at its highest level is about 975 feet at the Snake Curve site. The lake then lowered to the Campbell level causing the shoreline to shift westward to the Snake Curve site. At this time unit 8 was deposited. For several hundred years Lake Agassiz stood at the Campbell level cutting the prominant scarp, the toe of which is at 990 feet at the Snake Curve site. The eastern outlet was opened for the final time permitting Lake Agassiz to drain from this area about 9,000 B. P. Since that time the Red Lake River has cut its present trench.

Discussion—The sequence of events just described differs from that presented by Elson (1967, Figure 6). Elson indicated that Lake Agassiz never rose above the Campbell Scarp after the well-documented drainage at 10,000 B. P. Evidence at the Snake Curve Section

indicates that the water *did* rise above the Campbell Scarp after unit 5 was deposited, about 9,900 B. P.

Three possible expanations can be given for the sequence of events that allowed the water level to rise above the Campbell Scarp. (1) The lake refilled to a level above the Campbell level because the southern outlet, which had been previously cut down to the Precambrian granite (Campbell level), had subsequently been partly refilled by fluvial deposition during the low-water period. Erosion of this fluvial valley fill in the outlet caused the level of the lake to drop back to the Campbell level. However, if this sequence occurred, the erosion of the valley fill in the outlet may have been too rapid to permit the amount of sedimentation that occurred at the Snake Curve site. (2) The lake refilled to the southern outlet, which had not yet been cut down to the Campbell level. Subsequent erosion of the remaining fill in the outlet caused the lake to drop to the Campbell level for the first time. Elson (1967, Figure 6), however, indicated that Lake Agassiz first stood at the Campbell level well before this time. Because the early history of Lake Agassiz is not as well documented as more recent events, additional information is needed to resolve this apparent conflict. (3) Removal of water from the Lake Agassiz basin when the eastern outlet was opened, initiating the lower lake level at 10,000, caused the crust to buoyantly rebound. When the eastern outlet was reblocked and the lake refilled, the weight of water caused the crust to again subside. Because the mass unbalance resulting from the presence of Lake Agassiz was not uniformly distributed, both the rebound and the subsequent subsidence was not uniform throughout the basin. As a result the southern outlet and the Snake Curve site would have undergone different amounts of vertical movement. The southern outlet may have been higher relative to the Snake Curve site when the lake refilled than it had been before the lake drained. Further study involving the rate and amount of isostatic adjustment as well as the rate of draining and refilling of the lake is needed to evaluate this possibility

REFERENCES

Basch, P. F., 1963. A review of the Recent freshwater limpet snails of North America (Mollusca: Pulmonata): Bull. Mus. Comp. Zool., v. 129, no. 8, p. 399-461.

Cvancara, A. M., 1966. Mussels of the Red River Valley in North Dakota and Minnesota and their use in deciphering drainage history, p. 187-196, *in* W. J. Mayer-Oakes, ed., Life, land and water, Proceedings of the 1966 conference on environmental studies of the Glacial Lake Agassiz region: Winnipeg, Univ. Manitoba, 414 p.

Elson, J. A., 1955. Surficial geology of the Tiger Hills region. Manitoba: New Haven, Conn., Yale Univ., Ph.D. Dissert. (unpub.), 316 p., illus.

————, 1967. Geology of glacial Lake Agassiz, p. 37-95, *in* W. J. Mayer-Oakes, ed., Life, land and water, Proceedings of the 1966 conference on environmental studies of the Glacial Lake Agassiz region: Winnipeg, Univ. Manitoba, 414 p.

Moran, S. R., Lee Clayton, and A. M. Cvancara, 1970. New sedimentological and paleontological evidence for history of Lake Agassiz: Snake Curve Section, Red Lake County, Minnesota: N. Dak. Acad. Sci. Proc., v. 24, pt. 1, p. 22.

Parmalee, P. W., 1967. The fresh-water mussels of Illinois: Ill. State Mus. Pop. Sci. Ser., v. 8, 108 p.

Ross. J. D., and F. R. Karner, 1967, Petrography of core and well samples from Lake Agassiz and associated sediments, Grand Forks, North Dakota: N. Dak. Acad. Sci. Proc., v. 21, p. 147-161.

Tuthill, S. J., 1963. Molluscan fossils from upper Glacial Lake Agassiz sediments in Red Lake County, Minnesota: N. Dak. Sci. Proc., v. 17, p. 96-101.

————, W. M. Laird, and R. J. Kresl, 1965. Fossiliferous marl beneath lower Campbell (Glacial Lake Agassiz) beach sediments: N. Dak. Sci. Proc., v. 18, p. 135-140.

Zoltai, S. C., 1969. Sampling fossil mollusks from Glacial Lake Agassiz sediments: Jour. Paleontology, v. 43, no. 2, p. 534-537.

SEIBOLD SITE: COMPARISON WITH OTHER LATE QUATERNARY FOSSIL SITES IN NORTH DAKOTA

W. B. Bickley, Jr., Lee Clayton and Alan M. Cvancara

Department of Geology

University of North Dakota, Grand Forks, North Dakota 58201

Third Place Winner

A. Roger Denison Student Research Competition

ABSTRACT

The Seibold Site, a fossil site in Stutsman County, North Dakota, adds much information to our knowledge of the Quaternary biota of North Dakota. Until the discovery of the Seibold Site, mollusks and pollen represented a major part of the evidence used for climatic and environmental interpretation in this area.

The Seibold biota includes more than 160 species of mollusks, ostracods, insects, fish, amphibians, mammals and plants, which allow an integration of new interpretive tools with those from previously known sites. The similarity of the molluscan fauna of the Seibold Site with that of other North Dakota Quaternary sites makes the presence of these additional organisms important for paleoenvironmental reconstruction. The Seibold Site is the only site in North Dakota where the stratigraphic position of fossil fish has been radio-

carbon dated at 9750 ± 140 years B.P. The age and geologic setting indicate that the fish migrated eastward from the Missouri River through superglacial streams after the end of the last glaciation.

INTRODUCTION

Until 1969 the late Quaternary fossil record in North Dakota was represented by only a few species of a presumably extremely varied and abundant fauna and flora. Previously the only taxa that had been studied in detail were mollusks and plants. Conclusions drawn from those groups, though valid and important, were limited by lack of biotal diversity. The discovery of the Seibold Site with its very diverse fossil biota adds much to our knowledge of the late Quaternary paleoecology of North Dakota.

DISCUSSION

Previous studies.—A majority of the late Quaternary fossil research in North Dakota has been confined to a series of superglacial deposits in the Missouri Coteau in central North Dakota.

Clayton (1961) reported on several molluscan faunas collected from ice-contact deposits in Logan and McIntosh Counties. This study was the first involving late Quaternary mollusks in North Dakota.

Thompson (1962) reported mollusks, ostracods, moss and wood from samples taken near a dugout in McIntosh County. His conclusions were based mainly on sedimentology and mollusks.

Most of the molluscan research in North Dakota has been done by Tuthill (1961, 1962, 1963, 1967, 1969). He studied forty late Wisconsinan fossil sites from superglacial and ice-walled stream and lake deposits and found that the faunas were dominated by gill-breathing gastropods. This contrasted with the present fauna of the Coteau which is dominated by lung-breathing gastropods. Tuthill explained this change in population structure as a response to the climatic change known to have taken place in North Dakota about 10,000 B.P. (Tuthill, 1963).

Tuthill (1963, 1967) classified the forty sites into stream and lake habitats based on faunal assemblages and associations, their ecology and sedimentology. Finally, he suggested (Tuthill and others, 1964; Tuthill, 1969) from the mollusk types present at his sites, that the environment and the plants and animals associated with it must have been similar to that of the forest-lake region of northern Minnesota today.

McAndrews and others (1967) have done the only extensive Quaternary pollen study in North Dakota; unfortunately, their material was not radiocarbon dated. Woodworth Pond, where a core was taken, is 14.5 km north-northwest of the Seibold Site. Pollen analysis of the sediment in the core indicates a major climate change, represented by a shift from forest to grass pollen, at about 9,000 to 10,000 B.P. The same analysis also indicates a dry period about 4,000 to 8,000 B.P. Dating of these changes is based on correlations with

similar shifts in pollen profiles from Minnesota, South Dakota and Manitoba.

The Prophet Mountain Site, briefly studied by Sherrod (1963), is very similar to the Seibold Site. Before the discovery of the Seibold Site, this was the only site in North Dakota where late Quaternary fish had been found.

Seibold Site.—The Seibold Site involves a late Quaternary lake deposit in the SW¼NW¼ sec. 21, T. 141 N., R. 67 W. on the Vernon Seibold farm in northwest Stutsman County, North Dakota (Figure 1). Like most of the other late Quaternary sites, it is on the Missouri Coteau. However, unlike the other sites, except three (Prophet Mountain Site, Woodworth Pond and Thompson's Site), the Seibold Site is in a slough within a morainic depression; the other sites are on hillsides.

The stratigraphy at the Seibold Site (Figure 1), from oldest to youngest is, (1) nearly unfossiliferous, gray, pebbly silt, (2) poorly fossiliferous, gray, laminated silt, (3) very fossiliferous, gray, brown and green, organic mud, (4) fossiliferous, gray, calcareous clay, (5) fossiliferous, gray to brown, sandy mud, (6) nearly unfossiliferous, buff, muddy sand, and (7) fossiliferous, gray to brown, sandy mud. Units 5 and 7, constituting a sandy mud facies, merge together at the northern part of the exposure.

The fossil biota from the Seibold Site constitutes at least 160 species. Table I is a partial list of the plants and animals already identified. Changes within the sediments at the Seibold Site are similar to those observed at other sites. Gastropods at the Seibold Site underwent the same population structure shift (gill-breathing to lung-breathing) observed by Tuthill in his studies. Pollen data (C. T. Shay, University of Manitoba, unpublished data) from the lower part of the Seibold sequence (mainly unit 3) also closely approximates that of McAndrews and others (1967). The climate change indicated by shift from forest to open woodland vegetation occurred during the deposition of unit 3. Beaver-gnawed wood found where the change occurs has been dated at 9750 ± 140 B.P. Indications of the warm period, roughly 8,000 to 4,500 B.P., have also been found. This environmental interpretation is based mainly on mollusks and not on pollen. The dating of this warm period is after R. A. Bryson (Department of Meterology, University of Wisconsin, personal communication, 1969). The similarities of the molluscan fauna and pollen profiles at the Seibold Site to those at other Coteau sites make the additional plants and animals present at the Seibold Site extremely important for a more complete paleoenvironmental reconstruction.

Reconstruction.—The plants and animals listed in Table I allow, with the help of the stratigraphy, the reconstruction of the following paleoenvironmental sequence.

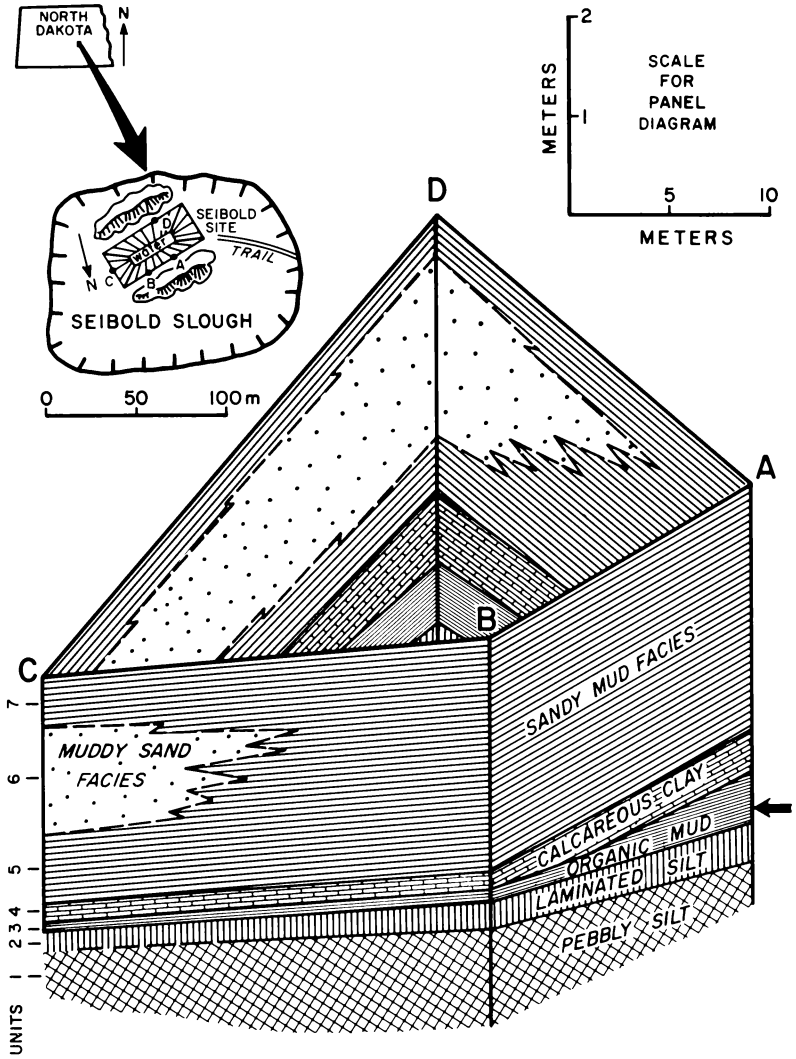

FIGURE 1—Stratigraphic panel diagram of the sequence at the Seibold Site which is within the Seibold Slough (hachured area). Letters refer to measured sections; datum for the section is the floor of the slough. Heavy arrow indicates the position of beaver-gnawed wood that has been radiocarbon dated at 9750 ± 140 B.P.

TABLE I

PARTIAL LIST OF SEIBOLD BIOTA AND STRATIGRAPHIC POSITION OF THE TAXA

Taxa	*Stratigraphic Unit*
Animals	
Beaver	3
Muskrat	3
Leopard frog	3
Fish	2,3,4,5
Yellow Perch	3
Brook Stickleback	3
Killfish	3
Brassy Minnow	3
Minnow	3
Ostracods (18 species)	1,2,3,4,5,6,7
Insects (80 genera)	2,3,4,5,6,7
Mollusks (11 species)	1,2,3,4,5,6,7
Amphipods	3
Plants (only unit 3 studied in detail for plants)	
Stonewort	2,3,4,5,7
White birch	3
White spruce	3
Willow	3
Poplar	3
Alder	3
Larch	3
Juniper	3
Buffaloberry	3
Grass	3
Sage	3
Wild onion	3
Prairie-clover	3
Pondweed	3
Water milfoil	3
Arrowhead	3
Cattail	3
Sedge	3

Units 1 and 2 indicate the presence of a glacial lake undoubtedly having a high rate of sedimentation. Fossils are scarce in these units. If a high sedimentation rate did exist it may have served to mask the actual number of fossils present. Fish (perch) first appear in unit 2. The Seibold Site is the only site in North Dakota where the stratigraphic position of fossil fish of late Quaternary age is known. The age and geologic setting indicate that the fish must have migrated eastward from the Missouri River through superglacial streams after the end of the last glaciation. The lake was probably surrounded by

forest at this time because spruce needles (probably white spruce) were found in unit 2. Evidence interpreted from ostracods present indicates that this was an oligotrophic lake (L. D. Delorme, Inland Waters Branch, Canada Department of Energy, Mines and Resources, Calgary, Alberta, written communication to A. Cvancara, 2/18/70).

Unit 3 marks the second phase in the history of the lake. A distinct lithologic change at the top of unit 2 is probably due to a change from turbid water (from the melting glacial ice) to clean water (after the cessation of melt-water flow). The fossils of this unit are very abundant, diverse and so well preserved that amphipod eyes are clearly visible. The excellent fossil preservation is probably due to the lack of oxidation. Unit 3 was continuously below the water table even during the driest parts of the Holocene. The plants and animals, including beaver, muskrat, frogs, fish, mollusks, and aquatic and terrestrial plants, are similar to those found in the forested lake country of Minnesota today. Shay's interpretation of pollen collected from unit 3 indicates that the unit was deposited as vegetation around the lake gradually changed from spruce forest to grass. During this time the lake was eutrophic (L. D. Delorme, written communication to A. Cvancara, 2/18/70).

Unit 4 marks the third phase in the history of the lake. Evidence interpreted from the fossils present (mainly mollusks) indicate that the lake was now shallow (probably about 1 meter). Lung-breathing mollusks predominated, and fish were still present but in decreasing numbers. The vegetation around the lake was now mainly grass. The lake had changed to a slough.

Unit 5 represents a period in the history of the lake similar to that of unit 7. A decrease in the number of mollusks present in samples taken from this unit seems to indicate that the water may have been slightly shallower than when unit 4 was deposited. Fish were still present in the slough but probably not common. Only two fish bones were found in samples from this unit. The vegetation around the lake at this time was probably similar to that found around sloughs in central North Dakota today.

Unit 6 represents a dry period in the history of the lake. Water probably stood in the depression only during the spring. Ostracods are the only continuously represented part of the biota. Fish died out at the beginning of this time. The vegetation around the lake was probably short grass.

Unit 7 was deposited under essentially modern conditions.

CONCLUSIONS

Fossil and stratigraphic evidence from the Seibol Site allows a much broader and more complete interpretation and reconstruction of the late Quaternary environment than was possible at previously investigated sites.

ACKNOWLEDGMENTS

We wish to thank the Vernon Seibold family for their patience; enthusiasm, and cooperation during this investigation. We also wish to thank S. H. Richards of the North Dakota Fish and Game Department for his help during the initial stages of this study. Finally, we thank C. T. Shay, Allan Ashworth, John Brophy, L. D. Delorme, R. R. Miller, T. M. Cavender, J. N. Keel, and George Lammers for the information they supplied for this study.

REFERENCES

Clayton, Lee, 1961, Late Wisconsin Mollusca from ice-contact deposits in Logan County, North Dakota: N. Dak. Acad. Sci., Proc., v. 15, p. 11-18.

McAndrews, J. H., Stewart, R. E., and Bright, R. C., 1967, Paleoecology of a prairie pothole; a preliminary report, *in* Mid-western Friends of the Pleistocene Guidebook, 18th Ann. Field Con.: N. Dak. Geol. Survey Misc. Ser. 30, p. 101-113.

Sherrod, Neil, 1963, Late Pleistocene fish from lake sediments in Sheridan County, North Dakota: N. Dak. Acad. Sci,. Proc., v. 17, p. 32-36.

Thompson, Neil, 1963, Postglacial fresh-water limestone, marl, and peat from south-central North Dakota: N. Dak. Acad. Sci., Proc., v. 16, p. 16-21.

Tuthill, S. J., 1961, A molluscan fauna and late Pleistocene climate in south-eastern North Dakota: N. Dak. Acad. Sci., Proc., v. 15, p. 19-26.

————, 1962, A checklist of North Dakota Pleistocene and Recent Mollusca: Sterkiana, no. 8, p. 12-18.

————, 1963, Mollusks from Wisconsinan (Pleistocene) ice-contact sediments of the Missouri Coteau in central North Dakota: Grand Forks, University N. Dak. (unpublished master's thesis), 102 p., 2 pls.

————, 1967, Late Pleistocene Mollusca of the Missouri Coteau district, North Dakota; a note and bibliography, in Mid-western Friends of the Pleistocene Guidebook, 18th Ann. Field Conf.: N. Dak. Geol. Survey Misc. Ser. 30, p. 73-82.

————, 1969, A comparison of the late Wisconsian molluscan fauna of the Missouri Coteau district(North Dakota) with a modern Alaskan analogue: Grand Forks, University of N. Dak. (unpublished doctor's thesis), 234 p., 9 pls.

————, Clayton Lee, and Laird, W. M., 1964, A comparison of a fossil Pleistocene molluscan fauna from North Dakota with a Recent molluscan fauna from Minnesota: American Midland Naturalist, v. 71, no. 2, p. 344-362.

PHOTOCHEMICAL TRANSFORMATIONS OF BIOLOGICALLY ACTIVE COMPOUNDS

Virgil I. Stenberg

Department of Chemistry

University of North Dakota, Grand Forks, North Dakota 58201

Invitation Paper

INTRODUCTION

Photochemistry, or the chemistry introduced by the action of light, has undergone interesting trends over the past several hundred years. In Europe reports appeared in the 1880's of reaction solutions placed on rooftops and irradiated for months at a time. The work ups of the reaction solutions were something to be marveled at, and the accuracy of the work was quite good. Photochemistry remained a phenomena of the spectroscopists during the first part of this century. In the last twenty years it has become an important synthesis tool for organic chemists. Outstanding examples of its use lie in the syntheses of chlorophyll, caryophyllene, and cubane.

In recognition of the diversity of fields represented at this meeting of the Academy, I feel it is necessary to review, in an over-all manner, the basic concepts of photochemistry before going on to the specifics of our research. Most fundamental is the realization that light is quantized, *i.e.*, it comes to us in discrete energy packages, rather than in some indescribable fluid form or whatever other concepts one may harbor. Further, the total energy of these packages can now be determined and calculated. This was an important advance because photochemical reactions must have light with sufficient energy to break chemical bonds. The majority of chemical bonds, with which the organic chemists are concerned, range in bond dissociation energies of 70-120 kcal/mol. On scanning the electromagnetic spectrum and observing the associated energies of various wavelengths, it is obvious that radiation in the near ultraviolet range, *i.e.*, *ca.* 70-140 kcal/mol, minimally satisfies the requirements. X-Rays and γ-rays much exceed the required energies. The latter two groups of irradiation, because of the excess energy they possess, might well be suspect of being indiscriminate in their chemical action.

Even ultraviolet irradiation comes under the same accusation of possibly being indiscriminate in its chemical action. However, this is not borne out in actual results. Only certain groupings on molecules are light absorbers, and a molecule must absorb light in order to react. In relatively large organic molecules, such as the alkaloids, it is possible to activate only a portion of the molecule much the same way as a surgeon is able to operate on one portion of a patient without disturbing the rest of the body. The assumption implicit here is that the resulting induced chemistry occurs on, or adjacent to, the

light-absorbing portion of the molecule. This is well demonstrated in practice, although energy transfer processes do occur within molecules in special situations.

It should not be assumed every photon which is absorbed by a molecule causes a molecular raarrangement. It may, in which case the "quantum yield" or efficiency is unity. More frequently, it is less than one. In other words, the energy of the photon is lost in other ways a portion of the time. This "lost" energy disappears down several lanes. First, it may simply be converted to thermal energy. Second, it can be emitted, usually with a slightly longer wavelength. Third, it can be transferred to a second kind of molecule in solution, which goes on and does its thing. Rare instances occur where the energy of the photon is used in creating a chemical reaction which goes nowhere, *e.g., cis-trans* isomerization of alkenes where both isomers are present initially. Photochemistry has been invaluable in the synthesis of compounds of unusual structure. This is possible because the photochemical reactions can be done at room temperature or lower and yet allow the reacting molecules to become very reactive or "hot." Examples of unusual compounds synthesized *via* photochemistry are illustrated below.

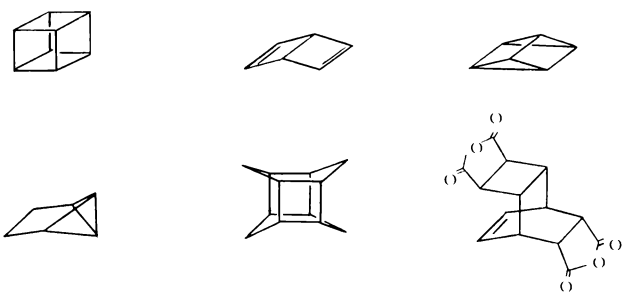

RESULTS AND DISCUSSION

Dr. W. E. Cornatzer of the University of North Dakota Biochemistry Department called our attention to reports of work (1, 2) he and others had done on ultraviolet irradiation of acidic quinine solutions. It was evident that among the products present, there was a new antimalarial agent. With the current interest in antimalarial agents for the Vietnamese renegade, *Plasmodium berghei*, we undertook the investigation of the photoproducts with the National Institute of Health as a silent partner. The first undergraduate to work on the project concluded in his senior thesis that it was not fruitful to study the reaction further, but he had isolated an oil. He is now working with the Nobel Prize winner, Dr. Willard Libby of the University of Southern California. We continued the investigation *via* the able chemist, Enrique F. Travecedo. I might well add here, the photochemistry of the alkaloid systems is intriguing not only because of

the possibility of developing new pharmacologically active compounds but also their rigid molecular structure is excellent for stereochemical analysis of photochemical reactions.

Quinine, I, (*ca.* 0.01 mol/700 ml) was irradiated through quartz with a 550-W Hanovia lamp in 2 *N* HCl solution, and the reaction

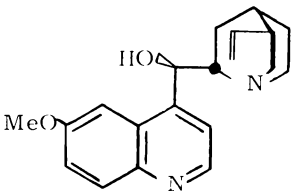

I

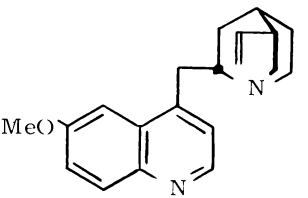

II

progress was monitored by silica gel tlc. The reaction solution developed a product which migrated faster than the parent alkaloid. The irradiation was terminated after 70 hr., at which time 40-50% of the quinine could be recovered. The solution was made alkaline, extracted, and separated *via* alumina column chromatography to provide a photoproduct in a 10% yield (% of starting material). Infrared, ultraviolet, elemental, and nmr analyses proved this compound to be 9-deoxyquinine, II. The compound was synthesized by means of the known route and compared to the photoproduct as a final proof of identity. The yield of 9-deoxyquinine increased to 32% and the reaction time was reduced to a third when the irradiation was done in a 233:77 2-propanol:2 *N* HCl solution.

Quinidine, an isomer of quinine, undergoes an analogous reaction to provide 9-deoxyquinidine. This structure has also been proven by comparison to independently synthesized 9-deoxyquinidine. Cinchonine and cinchonidine which are structurally identical to guinidine and quinine, respectively, in all aspects, except by the absence of a methoxy group on the quinoline ring, gave the corresponding 9-deoxy compounds on irradiation as well. The remaining asymmetric centers of deoxyquinine and deoxyquinidine did not isomerize during the irradiation. Optical rotations of these compounds were identical with those of the respective, independently synthesized compounds.

This reduction does not conform to any of the known photochemical oxidation-reduction reactions and is, therefore, a new photochemical reaction.

On the basis of model studies it is evident that the quinuclidine superstructure of the cinchona alkaloids restricts the orientation of the 9-OH group. If the proposed mechanism were correct, the optimum angle for elimination is 90°, provided the elimination is dependent on aromatic π-orbital overlap. To determine the influence of stereochemistry, the reduction of 4-hydroxymethylquinoline, a mole-

cule which does not have as much restriction on the movement of the CH_2OH group and probably has a predominance of the 90° dihedral angle conformer, was done for comparison. The reaction proceeded as expected, producing 4-methylquinoline; but the reaction was complicated by side reactions which resulted in lower yields of the reduction product. Thus, the quinuclidine side chain has the effect of hindering the side reactions from occurring, possibly because of steric factors. However, no conclusions can be made concerning the stereochemical implications of the OH orientation.

The postulated mechanism, published in our first paper on this subject (3), predicts that the reaction should be successful for 2-hydroxymethylquinoline also. This was tried and, indeed, the reaction proceeded. The slower rate of reaction for 2-quinoline carbinol may be attributued to steric hinderance offered by the $—CH_2OH$ group to the approaching hydrogen donor during the initial step of hydrogen abstraction. Unfortunately, 3-hydroxymethylquinoline was unavailable.

The relatively low yield of deoxyquinine during the irradiation of quinine, together with the fact that polymeric material is formed which accounts for a large portion of the remainder of products, indicated that the vinyl group participated in the reaction either by (1) internal energy transfer and/or (2) radical polymerization. To evaluate this, dihydroquinine was irradiated under comparable conditions to that of the quinine irradiation. The yield of the corresponding deoxy compound was considerably higher than for the corresponding reaction of quinine. Less polymeric material was obtained with the former reaction. Although this does not allow a clear determination of the exact mode of participation of the vinyl group, certainly this group does contribute to different reaction products, probably by polymerization.

We have been successful in sensitizing the photoreduction of cinchonine with benzophenone ($E_t = 68$ kcal/mol) using 350 nm low pressure lamps. The reaction proceeds to a higher yield with the sensitizer than without, *i.e.*, 73% *vs.* 34%. This, together with the known fact that the phosphorescence of quinoline can be sensitized by benzophenone, is strong evidence the reaction proceeds *via* the $T^1(\pi,\pi^*)$ state.

The success with the hydroxymethylquinolines led us to study the hydroxymethylpyridines. In accordance with prediction, irradiation of 2- and 4-(hydroxymethyl)pyridines in aqueous acid—2-propanol solutions provide the corresponding methylpyridines and 1,2-dipridylethanes. Only retarded formation of 3-methylpyridine with low yields resulted from the irradiation of 3-(hydroxymethyl)pyridine. Neither the methylpyridines nor the 1,2-(dipyridyl)-1,2-ethanediols serve as precursors for the dipyridylethane products. It has also been demonstrated that the 1,2-dipyridylethanes do not generate the methylpyridines in the reaction solution. Since oxygen does not have

any effect on the hydroxymethylpyridine reaction, a singlet state mechanism is implied contrary to the triplet mechanism of the alkaloids.

We were intrigued by the disappearance of the pyridine chromophore in the ultraviolet spectrum during the irradiation of the hydroxymethylpyridines. An attempt at trapping a suspected imine intermediate, *via* its acetal, led to the discovery of a second reaction of the series, the photoalkylation of pyridine. Irradiation of pyridine in HCl-methanol solutions with the 253.7 nm line of Hg through quartz under nitrogen produces 2- and 4-methylpyridines, 1-(2-pyridyl)-2-(4-pyridyl)ethane, and 1,2-di(4-pyridyl)ethane. The products were compared (ir, nmr, glpc retention time, and tlc) to authentic materials except for 1-(2-pyridyl)-2-(4-pyridyl)ethane. Its structure was inferred by ir and nmr spectra correlation with 1,2-di(2-pyridyl)ethane and 1,2-di(4-pyridyl)ethane.

Various compounds obtained in the course of this investigation have been tested for antimalarial activity. These compounds have not demonstrated enough activity to merit further testing.

ACKNOWLEDGMENTS

This investigation was supported by research grant 1-R01-AI-08138 from the National Institutes of Health, U. S. Public Health Service.

REFERENCES

1. G. C. Kyker, W. E. Cornatzer, and M. M. McEwen, *J. Biol. Chem., 162,* 353 (1946).
2. G. C. Kyker, M. M. McEwen, and W. E. Cornatzer, *Arch. Biochem., 12,* 191 (1947).
3. V. I. Stenberg, E. F. Travecedo, and W. E. Musa, *Tetrahedron Lett.,* 2031 (1969).

INTERACTION OF HEMOGLOBIN WITH H_2O AND D_2O VAPORS AND H⇆D EXCHANGE EFFECT, WITH AND WITHOUT PRERADIATION

W. S. Hnojewyj

College of Chemistry and Physics

North Dakota State University, Fargo, North Dakota 58102

ABSTRACT

Adsorption isotherms of H_2O on hemoglobin at 27, 37 and 47°, also of D_2O vapors on deuterited hemoglobin at 27 and 37°, measured up to 26 mm of equilibrium pressure. A number of slopes in isotherms due to different active sites were established. 13.2 mmoles/g of sorption as maxima of the total H_2O monolayer at 27° were estimated. Illumination (visible light) of hemoglobin in presence of $O_2 + H_2O$ showed a slight increase of weight after desorption, indicat-

ing coupling of O_2 (oxygenation) and markable lowering of adsorptivity, which, however, partly restored at repeated H_2O sorption. γ-ray preradation of hemoglobin caused not regenerable lowering of adsorptivity in the upper coverage, probably due to damage of porphirin groups. ΔH of H_2O adsorptions were calculated: up to 33 at the start, rapidly decreasing to 13-15 kcal/mole, and approaching ΔH of condensation with adsorptions increased. Readsorptions of D_2O followed by complete desorptions caused exchange of all labile hydrogens in the hemoglobin by deuterium. This seems reversible and is not influenced by oxygenation or γ-radiation.

INTRODUCTION

A series of sorption studies of various vapor-gases on completely desorbed dried natural proteins and alike synthetic polymers, have demonstrated many interesting facts concerning their physico-chemical behaviors in relation to their structures. The complete dehydrations of some enzymatic proteins like lysozyme (1) β-lactoglobulin (2), and insulin (3), were achieved during the prolonged desorptions by means of high vacuum technique in a temperature range of 27-57° at high vacuum (10^{-4} - 10^{-5}mm of pressure). However, only insulin, as a protein with the smallest molecular weight, showed a slight loss of its original weight at higher temperature (57°) due to the probable sublimation.

The dehydration of synthetic polymers, demonstrated a marked dependence on the substituents as it was observed with the poly-L-glutamic acid (4) and its derivatives. In the mentioned temperature range, the poly-L-glutamic acid and its (more lyophillic) sodium substituent were found to be completely dehydrated in a high vacuum. Each repeated sorption of H_2O to a higher coverage caused, however, some degradation affecting the original weight of the polymer (loss), significant for a sodium substituent only. This degradation decreased with a lowering of temperature.

The rough S-shape of sorption isotherms of vapors have been found to consist of many slopes, which were dependent on surface area and temperature.

It was suggested that the appearance of slopes in isotherms were caused by the functional groups in adsorber molecules (1, 2, 3).

Really, since protein and synthetic polymer molecules have many kinds of active group-sites with different affinity-adsorptivity for H_2O (or else), the saturation of such sites should follow in order of their activity. Hence, during isothermic sorption by exposing the vapor in small increments, an appearance of separate slopes may be expected. The number of formed separate slopes in an isotherm have to be related to the number of kinds of active sites. The case is not excluded where two or more different kinds of active sites may have the same adsorptivity at a particular temperature; hence, it may have been demonstrated by the same slope along the isotherm. Therefore, for distinguishing of all active sites (functional groups or their combinations), the proper temperatures for sorption (adsorption and desorption) have to be properly chosen. Now, an application of the BET method (5) in the usual way, concerning the monolayer sorp-

tions on proteins and similar compound molecules, could lead to erroneous results.

It seems that an interpretation of the amounts adsorbed along an isotherm in a so-called monolayer region should be redefined, at least for proteins and alike molecules, as: (a) *the particular monolayers*, formed on specific group-sites and characterized by their slopes, and (b) *the total monolayer*, represented by the sum of the amounts sorbed along the particular monolayer slopes up to equilibrium equal to saturation pressure. Because experimentally it was observed that the amount adsorbed along the uppermost slope goes into multilayer before a particular monolayer has been accomplished, it was suggested that an approximation by extending the uppermost slope to the saturation pressure should be done. So, the cross-point ordinate at the pressure of saturation of the isotherm could be assumed as *the total monolayer* of adsorption. It is remarkable that these approximations of total monolayers from adsorption and desorption as well as for different isotherms were found to be in good agreement with experimental tolerance in the range 25-35° for natural proteins and alike synthetic compounds mentioned above.

Furthermore it was established that the successive adsorptions of D_2O vapor followed by complete desorptions caused the exchange of labile hydrogen atoms in lyophilized solids by deuterium from D_2O up to 70-92% (1, 2, 4) and 100% in insulin. The $H \rightleftarrows D$ exchangeability seems reversible, where the temperature plays only a kinetic role (1). In investigated natural proteins was established also a relationship between the amount of total monolayer adsorption of H_2O and $H \rightleftarrows D$ exchangeability, and an equivalency of H_2O to labile H-atoms as a minimum.

In the case of stressed aromatic lyophobic nature of adsorber molecules like 4-chloro-3, 5-dimethylphenol-formaldehyde heptauer (6), however, showed only about 13% of expected adsorption, but still 100% $H \rightarrow D$ exchange. From the latter it was concluded than an adsorption of D_2O is not prerequisite for $H \rightarrow D$ exchangeability but it may occur by collisions between D_2O molecules in a surrounding with functional groups containing labile hydrogens in solids.

These data of sorptions and $H \rightarrow D$ exchangeability may reveal information on the molecular structure and probably provide information on the mechanism of reactions of unknown very complex natural and synthetic polymer compounds. Extension of similar investigations on the model polymers therefore is desirable.

In this paper some results are reported of similar investigations on the human homogeneous hemoglobin. The purpose is to recheck the previous data and conclusions reached regarding sorptivity, $H \rightleftarrows D$ exchangeability and their relation to the functional groups of the hemoglobin molecule as well as to try further investigation of preradiation effect on hemoglobin, which may be also of special interest for physiological science.

EXPERIMENTAL

General procedure and apparatus for sorptions. —The sorption procedure followed basically previously described methods (1, 2).

The samples of the human homogeneous lyophilized hemoglobin, containing mostly $Fe^{3}+$, and twice recrystallized, were obtained from the Nutr. Biological Corp., Cleveland, Ohio. The sample of hemoglobin in a light glass bucket was suspended from a hook of a fine glass rod attached similarly to the lower end of a quartz helical spring hanging in a vertical glass tube sealed to the vacuum system. The whole length of the spring was surrounded by a jacket with circulating water at a constant temperature of 40°. The calibrated quartz helical spring had a sensitivity of 2.476 mg/mm at this temperature. An extension of this spring during the sorptions was measured by a traveling microscope to ± 0.002 mm of precision. The suspended bucket with the sample of protein was adjusted in another closed glass tube which was connected by a joint to the vertical tube bearing the quartz helical spring. This adjustment supplied enough length for a vertical extension of the bucket with the sample during sorptions. Another jacket with circulating water from a thermostat surrounded the sample and permitted control of a definite temperature, which was experimentally required to an accuracy of ± 0.005°.

After pumping at 10^{-4} mm of pressure (measured by a McLeod gauge) and raising the temperature up to 47° for a period of 5 days, the sample reached a constant weight of 567.6 mg. This was subjected to a series of adsorptions of H_2O up to 23-30% and complete desorptions. Such a treatment showed an additional loss in weight of the sample; 0.070% after the first adsorption-desorption, and only 0.026% after the second adsorption-desorption. Further adsorptions-desorptions of H_2O demonstrated a constant reproduction of weight of the sample equal to 567.06 mg, which was assumed to be dry and used for determination of isotherms.

Triply distilled H_2O and D_2O (99.5%), outgased during a series of freezing and thawing while pumping to a pressure of 10^{-6} mm, were used for sorptions.

The isotherms of H_2O adsorptions at 47, 37 and 27° were determined after many repetitions of measurement runs, *i.e.*, until their reproducibilities were established. These isothermic data were plotted as the sorbed amounts versus the equilibrium pressures of H_2O vapor (Figure 1 curves 1, 2 and 3. The equilibrium pressures in the system during sorptions were measured by a Pirany gauge in the lower range and the a mercury manometer sealed into the sorption system in a higher range of pressure. Readings of manometric pressures were taken to ±0.005 mm of accuracy, and also corrected to the density of mercury at 0°.

After the determination of H_2O isotherms were accomplished, the samples were completely desorbed at 27°; at 37° they demonstrated no change in their original weight. These samples were subjected to a series of various treatments: sorption of O_2 for determination of its isotherms (not presented here), photo-oxygenation in the presence of O_2 and H_2O under visible light, γ-preradation with and without H_2O and the H→ D exchange process followed by a determination of the adsorption isotherms for D_2O at 27° and 37°. The particular experimental procedures are described below.

Some other samples of hemoglobin in a similar sorption system, however, with a quartz helical spring of higher sensitivity (1.259 mg/mm), were prepared analogically. Their dry weight was 161 mg. These samples were subjected first to control only some points of the H_2O isotherms at 27°, 37° and 47°. The data were found agreeable with those previously determined on the first samples. Afterwards, these samples were completely desorbed and not "treated", as mentioned, but were only subjected to D_2O vapor for the determination of H→D exchangeability following the same method described below. After the maximum above of H→D exchange was reached, (*i.e.*, deuteration of sampes was accomplished), it was followed by complete desorption at 47°.

Further, the adsorption isotherms of D_2O vapor on this deuterated sample at 27° and 37° were determined by two runs of measurements and the subsequent complete desorptions at each temperature. These data were plotted as the amounts sorbed versus the equilibrium pressures of D_2O vapor (Figure 4, curves 1 and 2).

H→D exchangeability procedure. — The process is based on an interaction between the protein and D_2O, where D-atoms of D_2O are replacing the labile H-atoms present in protein. As a result of an exchange of atoms the protein gained in weight. This interaction process could be schematically expressed by an equation (1)

$$\text{Prot} - H_n + mD_2O \rightarrow \text{Prot} - H_{n-m}D_m + mHDO \qquad (1)$$

Here, n - is the total number of labile hydrogens present in protein; m - is the number of D_2O molecules, that underwent an exchange. After the completion of a desorption a new partly deuteriated protein with a new constant weight is established, which may be designated as Prot $H_{n-m}D_m$.

Numerous sorptions of D_2O on the same sample would result in a maximum of exchange, depending on the conditions of the experiment. On a 100% exchangeability, the molecular weight of fully deuteriated protein (Prot-D_n) should gain the value equal to n x 1.0066, where 1.0066 = D - H (difference of atomic weights of deuterium and hydrogen).

The experimental determination of H→ D exchange was conducted in such a way so that amounts of D_2O vapor absorbed were *regulated* to avoid any contraction of the sample surface.

For an acceleration of adsorptions the temperature could be lowered, then raised up to 47° and the sample equilibrated for 4 hours. The amount of D_2O absorbed was measured. Complete desorption followed by opening a capillary to the vacuum preventing "blowing off' of the sample. At 10^{-3} mm of pressure the normal stopcock was opened to the pumps and a desorption continued at 10^{-6} mm of pressure until a definite constant weight was reached. The constant increase of weight of the protein was determined from a plot (not presented) of D_2O content data vs. desorption time. This was characterized by a dropping curvature until a complete desorption of D_2O was achieved, and afterwards remained constant during the further desorption at 10^{-6} mm of pressure and exhibited a parallel line to the time axis. The ordinate of such a line in certain units (weight per 100 of original sample) was assumed as the real gain

of weight due to H→D exchange caused by this amount of D_2O absorbed.

Such adsorptions-desorptions of D_2O were repeated on the same sample of hemoglobin until no further gain of weight was observed. This was assumed as the maximum exchangeability of solid hemoglobin under the conditions of these experiments.

The magnitude of the total successive gains of weight due to H→D exchange vs. the summated amounts of D_2O adsorbed which caused such gains of weights are shown in Figure 3 for two samples of hemoglobin. The particular value of exchange between two points (as difference of ordinates) can be found and the amount of the sorbed D_2O which caused this exchange is equal to a difference of their abscissas.

Photo-oxygenation procedure. — Following a complete desorption at 37° and 47° the sample of hemoglobin was equilibrated with H_2O vapor at 27° up to 10.12 per 100 of original weight. Further O_2 was added up to 160 mm of pressure. This increase of pressure resulted in an increase of weight from 10.12 per 100 to 11.01 per 100 of content over a 1-hour time lapse. Subsequently, the weight dropped to 10.2 per 100 and remained practically constant in dark or natural light.

A further addition of O_2 was made raising the pressure to 360 mm. A similar result occurred giving a new equilibrium weight gain of 10.70 per 100 of original weight. This was exposed to an additional source of light (100 watt), irradiating the sample for 72 hours. No loss or gain in weight of the sample was observed.

Complete desorption, lasting approximately 10 days, with temperature raised to 57° then lowered to 27° and equilibrated to a constant weight, showed a 0.1485 gain in weight per 100 of original sample weight. Samples were used further for readsorptions of H_2O.

γ-irradiation procedure. — After H_2O was completely desorbed from the sample, the system was exposed to the air during the transfer of the sample into a special glass tube closed by a combined joint-cap. This joint-cap has a stopcock and another joint. By this joint the tube with the sample was attached to the vacuum system again and completely desorbed during 24 hours at 10^{-6} mm of pressure. Then the tube containing this sample of hemoglobin under vacuum was closed, separated from the vacuum system and located vertically in the center of the chamber for γ-irradiation using special clamps. Cobalt-60 rods were used as a source for γ-irradiation (L = 250 mm, d = 3 mm), held in a radiation cylinder of 125 mm diameter.

This source located originally at the bottom of a water cooling system was moved vertically upward from the cooling system as far as the sample, and the sample was adjusted in the center of the radiation cylinder (formed by Co^{60}-rods).

The time of γ-irradiation started at the moment the sample was centered in the γ-irradiation cylinder and lasted for 3 hours.

The γ-irradiation source was again lowered to the bottom of the cooling system and the tube with the sample of hemoglobin was taken from the chamber for further investigations.

After two additional sorptions of H_2O vapor and one O_2-sorption the same samples were exposed for the second time to γ-radiation

but in the presence of air at similar conditions, for 3 hours using the same source equal to 382,564 R/hour.

RESULTS

Adsorption of H_2O vapor on solid dry hemoglobin. — The sample of obtained human hemoglobin was found to contain 1.808% of volatiles, mostly H_2O and technological impurities. The experimental conditions of the completely dry sample at 47° permitted the adsorption of up to 4 mmoles/g of H_2O. The reproducible adsorption isotherm at this temperature was evaluated and contained one distinguished slope. (Figure 1, curve)1. Complete desorption of the sample and the followed lowering of temperature to 37°, caused no change of the sample's weight. Measurements at this temperature, with in-between saturations up to 27% of H_2O, caused practically no deviations in isothermic data (Figure 1, curve 2). The shape of this isotherm as approximated, is found to consist of many slopes; however, they are not distinguished at this scale. The maximum of H_2O adsorption at this temperature reached the value of about 6 mmoles/g. A further saturation up to 20-21% of H_2O equilibrated at 27° and complete desorption at high vacuum for 2 days showed no change in the original weight of the sample. The adsorption isotherm at 27° was determined by many runs (Figure 1, curve 3). These runs were found to be practically reproducible except the first one demonstrated initially slightly lower data. It was possible to extend the measurements almost into the region of the total monolayer coverage. The S-shape isoherm consists of a number of approximated slopes, which are easily recognized. At this temperature the sample was submitted to a series of sorptions of O_2 and H_2. Such a treatment of the sample did not affect the sorptive capacity of hemoglobin for H_2O, which was established after recheck of the isotherms at 27° and 37°. Afterwards the shape of the isotherms in a region of a low equilibrium pressure at 27° and 37° was measured repeatedly and more precisely. The measurements in regions of the equilibrium pressures from 0 to 0.500-0.700 mm. are shown in Figure 2.

It was established that the H_2O isotherms contain a number of approximated slopes from the very beginning of adsorptions, the continuations of which are the isotherms shown in Figure 1. The total number of slopes at 27° was six.

Photo-oxygenation oxidation and its effect on H_2O adsorptivity.— The sample of hemoglobin at 27° was equilibrated with H_2O vapor to which was added O_2 and illuminated for 72 hours with visible light (100 watt). Then the gas-vapor phase was collected in a bulb by means of liquid nitrogen cooling. The gas-vapor phase underwent a mass-spectroscopic analysis (Table I).

The hemoglobin sample was completely desorbed at 27°-57° and 10^{-6} mm of pressure over a 10-day period. This treatment resulted in an increase of weight up to 0.1485 per 100 which is equivalent to $3O_2$ per molecule of hemoglobin.

From the above results the mass-spectroscopic analysis favors the loss in weight of the sample after complete desorption (formation of CO_2). The fact, however, is established that the weight of the

sample increased. Therefore, the adsorption of O_2 could occur on hemoglobin as a result of the photochemical effect.

TABLE I

COMPOSITION OF GAS-VAPOR PHASE EQUILIBRATED UPON THE HEMOGLOBIN SAMPLE AFTER 72 HOURS OF IRRADIATION BY VISIBLE LIGHT (100 WATT)

Component	Partial Pressure (mm)	Content %
air (N_2+O_2)	0.350	5.01
O_2	5.474	78.29
CO_2	0.046	0.66
H_2O	1.122	16.04
Total pressure	6.992	100.00
Observed pressure	7.04	

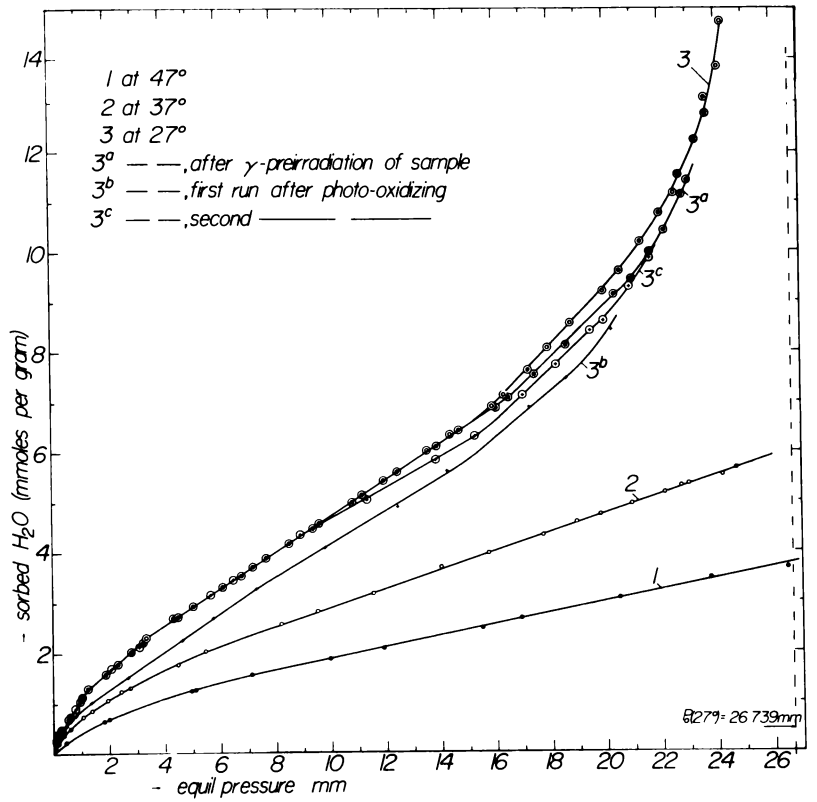

FIGURE 1—Adsorption isotherms of H_2O vapor on solid hemoglobin.

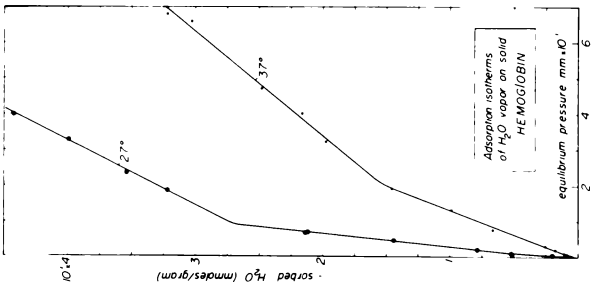

FIGURE 2—Adsorption isotherms of H_2O vapor on solid hemoglobin.

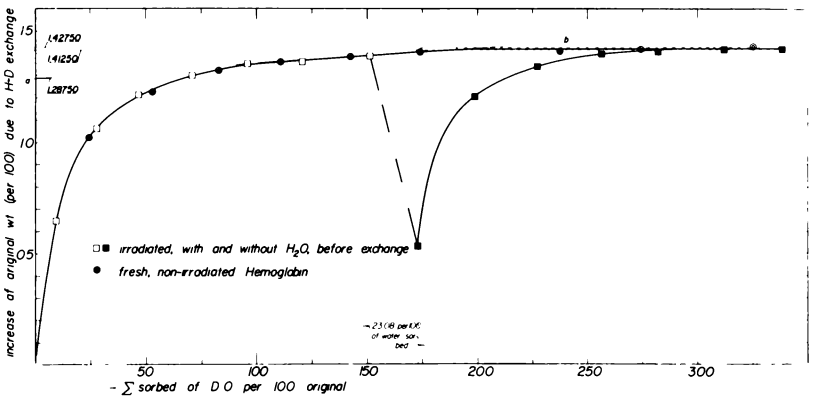

FIGURE 3—Exchange effect on dry, solid hemoglobin (oxidized form) due to the reaction Prot-H+D_2O→Prot-D+HDO, as a result of repeated sorptions.

The influence of the photo-oxygenation on the H_2O adsorptivity of the sample was investigated at 27°. As a result of repeated measurements of the adsorption isotherm, it was established that the first run isotherm was noticeably lowered (Figure 1, curve 3b). This lowering of the adsorptive capacity for H_2O is probably due to the occupation and/or blocking of some sites of the hemoglobin molecule by the presence of oxygen, as well as chemical oxidation. The adsorption-saturation of H_2O vapor to a higher content and then a complete desorption indicated a slight loss in weight of the photo-oxygenated sample and at the same time showed an increase of its H_2O adsorptivity (Figure 1, curve 3c). This isotherm seems to be reproducible, but still below the original one in the region of coverage at about 5 mmoles/g of adsorbed H_2O.

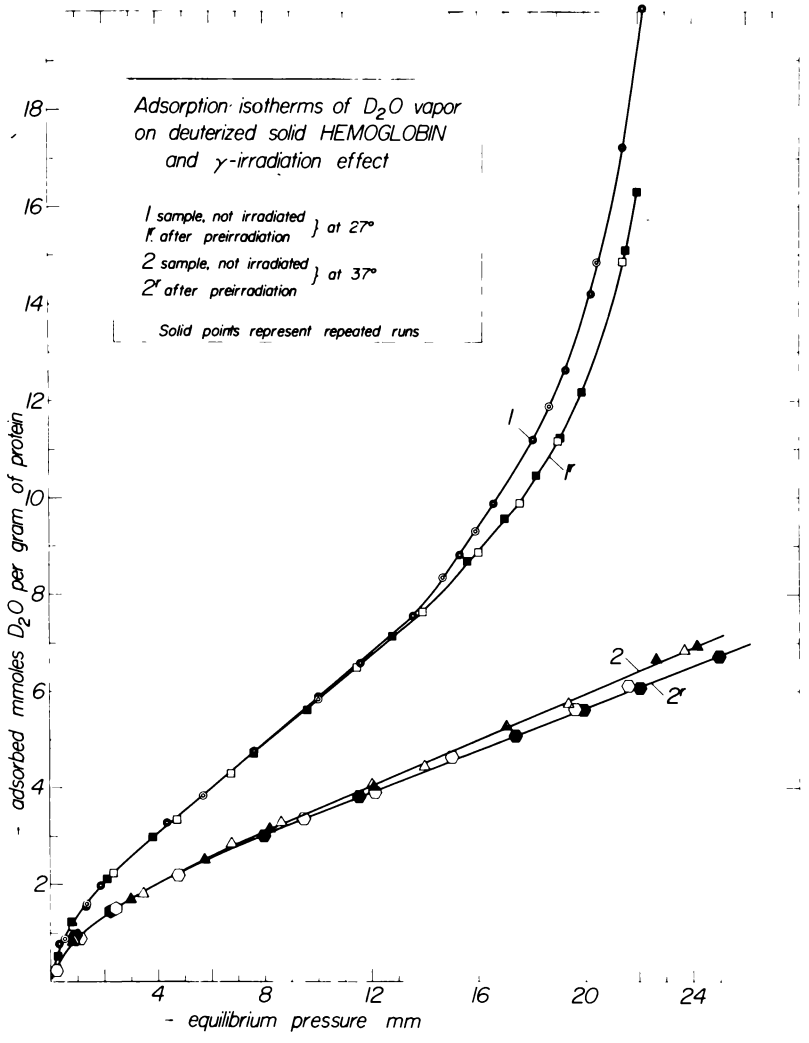

FIGURE 4—Adsorption isotherms of D_2O vapor on deuterized solid hemoglobin and γ-irradiation effect.

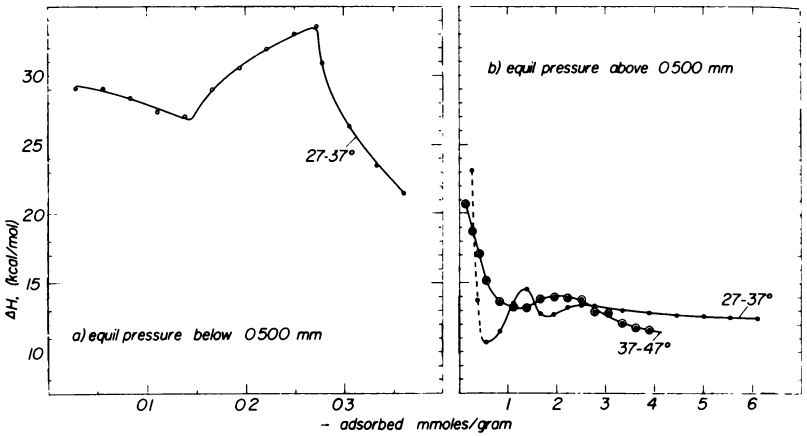

FIGURE 5—Differential heats of adsorption of H_2O vapor on solid hemoglobin.

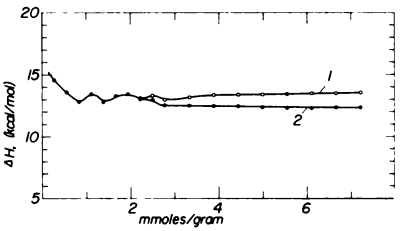

FIGURE 6—Differential heats of adsorption of D_2O vapor on deuteriated hemoglobin; 1. Sample irradiated before deuteriation, 2. sample not irradiated.

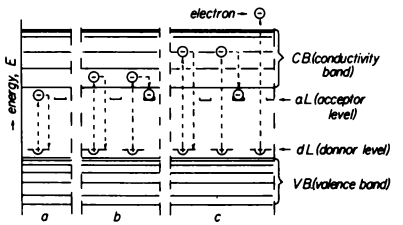

FIGURE 7—Schematic band-model of an illuminating substance.

γ-irradiation of hemoglobin and its influence on adsorptivity of H_2O. — The first γ-irradiation was accomplished on the same completely desorbed sample, which afterwards was exposed to the air while transferring it into the sorption system and then completely desorbed, for 5 days at 47° and 10^{-6} mm of pressure (see Experimental). The effect of the first γ-irradiation showed an increase of original weight equal to 0.045%. This is probably due to an adsorption of O_2 from the air by an "excited" protein.

The H_2O reproducible isotherm was determined after two runs, at 27° on the same sample (Figure 1, curve 3a).

This and the original isotherms are in agreement up to 6.8 mmoles/g of H_2O adsorbed and after that it follows a slightly lower course, but still higher than after a photo-oxygenation.

The second γ-irradiation of the same sample with adsorbed and equilibrated H_2O up to 21.2% and in the presence of O_2 (see Experimental) demonstrated an opposite effect, namely a loss of original weight equal to 0.085%. Conducting H_2O sorption the loss of weight increased additionally by 0.026% after the one run. Therefore, the total loss of original weight is 0.111%.

On this sample the H_2O isotherm determined after one run showed practically no change in adsorptive capacity for H_2O and is almost identical with the isotherm after the first γ-irradiation (Figure 1, curve 3a).

Following complete desorption at 47° and then equilibrating at 27° the sample was exposed again for O_2 adsorption in portions up to 480 mm of pressure for 4.5 days. The purpose was to determine O_2 isotherm on the irradiated sample and compare it with the O_2-isotherm obtained on the fresh (not irradiated) one. It showed that γ-irradiation of hemoglobin lowers adsorptivity for O_2 down to below 50% (O_2 adsorption data are not presented in this paper).

$H \rightleftarrows D$ exchangeability. — The sample of the above described treatments (irradiations and sorptions) and the freshly prepared one (treated only with H_2O) were used for the $H \rightleftarrows D$ exchange at 47°. The measurements demonstrate that almost identical $H \rightarrow D$ exchange was obtained on the treated and the freshly prepared samples (Figure 3).

The $H \rightarrow D$ exchange up to the difference between 60%, denoted as the first stage of exchange, occurred very rapidly and demonstrates practically a linear dependence of exchange versus the amount of adsorbed D_2O vapor. This may mean that, the most labile H-atoms involved in this stage of $H \rightarrow D$ exchange are energetically equivalent even being originated from different functional groups (sites) of hemoglobin.

Further exchange follows a marked diminishing increase of the original weight. It is characterized by a curvature and suggests a participation of energetically different kinds of H-atoms in this second stage of exchange.

The final stage of exchange progressed on the slope "ab" (Figure 3) until the maximum.

In attempting to check the reversibility of $H \rightarrow D$ exchange it was

adsorbed about 23 per 100 of H_2O on the sample which previously was treated and already deuteriated up to 97%.

The complete desorption showed a reverse exchange according to equation (2) and resulted in a loss of weight from 1.38 to 0.53 per 100, *i.e.*, equal to about 38% deuteriation.

$$\text{Prot - } D_n + mH_2O \rightarrow \text{Prot - } {}_{n-m}H_m + mHDO \quad (2)$$

The maximum H→D exchange was reached again by D_2O sorptions on this sample and is characterized by a horizontal line of the same value for both samples (Figure 3). The increase of the original weight calculated from the measurement data was found to be 1.4275-1.4125 per 100.

Molecular weight of completely dry hemoglobin (human) calculated from the recently established data of amino-acid composition (7) was found to be equal to 64,204 with $4H_2O$ bound to hemes for "the deoxygenated form" and 64,259 for "the oxygenated form". The number of labile H-atoms present in its molecule was calculated and found to be equal to 912 and 904, respectively (Table II). Hence, the theoretical expected maximum increase of original weight due to H→D exchange should be 1.4298 and 1.4160 per 100, respectively.

The molecular weight of hemoglobin is calculated as follows:

	$(\alpha+\beta)$ globin parts according to B (Table II)		= 61810.58
(1)	4 hemes ($C_{34}H_{32}N_4Fe\ O_4$) 616.138 x 4 = 2464.55		
	subtracted $8H_2O'$ (8).	144.24	= 2320.31
			about 64,131.00

(2)	Oxygenated form	In the presence of 40 bound to heme-groups MW is equal to	= 64,259
(3)	Deoxygenated form	In the presence of H_2O, which substitutes O_2 in heme-groups, MW is equal to	= 64,204

In case (3), the number of labile H-atoms in hemoglobin molecules increases to 912.

Comparing the experimental and theoretically calculated data it could be concluded that all the labile H-atoms present in solid hemoglobin are exchanged during the repeated sorptions of D_2O vapor.

Adsorption of D_2O on Deuteriated Hemoglobin. — The D_2O vapor adsorption isotherms at 27° and 37° on the deuteriated sample are found to consist of one distinguishable slope (Figure 4). The absolute amount of D_2O adsorbed as approximated is of higher order than the adsorption of H_2O based on similar sequences of experiments. It is significant that adsorptivity for D_2O on the treated (irradiated) sample was lower than in the case of the not irradiated one.

The appearance of a single slope may be due to the substitution of H-atoms by D-atoms, possessing a double mass, causing energo-structural changes of a protein molecule, with probable extended overlappings by different active sites (groups).

'Due to propionic bonds of hemes to globin.

TABLE II

ACTIVE GROUPS AND LABILE-HYDROGENS PRESENT IN HUMAN HEMOGLOBIN A IN SOLID STATE (7)

A. Smallest unit containing α and β chains

Number of Amino Acids			Active Groups (sites)									
α	β	Σ	-C(=O)-NH-	R-OH	Ar-OH	=NH	$-NH_2$	-C(=O)-OH	-C(=O)-NH_2	-C(=O)-N-	-C(=O)-	Σ
141	146	287	273	32	6	34	28	33	8	14	-	
Contributions of endgroups (H_2O)			-1	-	-	-	+1	+1	-	-	-	
Contribution of 2 hemes				-	-	-	-	-	-	-	4	
Totals			272	32	6	34	29	34	8	14	4	43
B. Actual molecule of hemoglobin = A x 2												
282	292	574	544	64	12	68	58	68	16	28	8	866
Labile H-atoms			544	64	12	68	116	68	32	0	0	904

Different heats of adsorption of H_2O and D_2O on hemoglobin (original and deuteriated). — The differential heats of H_2O are calculated by the Clausius-Clapeyron equation on the original sample from the isotherms (Figure 1-2) at 27°-37° and shown in Figure 5. The ΔH curve consists of several peaks, with a maximum of about 33 kcal/mole at the low coverage of about 0.27 mmoles/g, and a minimum of about 10.5 kcal/mole at a higher coverage of 0.5 mmoles g of adsorbed H_2O; both approach the value of heat of H_2O condensation (Figure 5, a and b). The ΔH values at 37° - 47° are fluctuating similarly (Figure 5, b).

The ΔH curves of D_2O adsorption on the deuteriated sample are based on the isotherms from Figure 4 and are shown in Figure 6. The calculated values in a relatively higher range of coverage as compared to H_2O, show the maximum of about 15 kcal/mole at a coverage of about 0.3 mmoles/g, and the minimum of about 13.2 kcal/mole with a fluctuating decrease to 1 mmole/g of coverage.

The latter value of ΔH remains constant on the treated (irradiated) sample, while it demonstrates a continuous decrease of ΔH, reaching 12 kcal/mole at a coverage of about 7 mmoles/g of D_2O absorbed, on the sample not irradiated.

DISCUSSION

Monosites or monolayer coverage of H_2O (D_2O) on solid hemoglobin. — It is concluded, that the presence of different kinds of adsorption sites in a hemoglobin molecule are basically responsible, during a sorption process, for the appearance of separate slopes in an adsorption isotherm. Their appearance depends on the kind, number and adsorptive capacity of the exposed sites, which are observed experimentally.

The method for the determination of the total monosites (monolayer) coverage-adsorption involves an extrapolation of the uppermost slope of the isotherm to the saturation pressure as the ordinate (see Introduction). It is understood, that the cross point on the ordinate defines *the total monosites coverage* as the sum of all kinds of *the particular adsorption-coverages.*

The H_2O-isotherm at 27° (Figure 1, curve 3 and Figure 2) is found to consist of approximately 6 slopes. The structural formula of the hemoglobin molecule indicated the presence of nine functional groups (sites) which may cause 9 slopes (Table II). Such a discrepancy is suggested that some active groups may possess almost equal adsorptivity affinity for H_2O and will, therefore, appear in one slope. Furthermore, certain "overlappings-interactions" may also occur that will affect the appearance of the separate slopes. This seems to be a justification for deviations between the theoretical and experimentally found number of slopes.

The experimentally approximated total monosites (monolayer) coverage for the hemoglobin from the same isotherm (Figure 1, curve 3), is found to be equal to 13.2 mmoles/g. This is equivalent to 850 molecules of H_2O per molecule of hemoglobin as compared to the structural formula, which consists of 866 group-sites (assuming H_2O per site) calculated from Table II.

This indicates, that hemoglobin, though being a larger molecule than the other investigated natural proteins is almost completely reopened on H_2O adsorption monosites coverage and consequently is more reactive.

The total monosites coverage for completely deuteriated hemoglobin determined from D_2O isotherm at 27° showed 13.7 - 14.3 mmoles/g, equivalent to 898-937 molecules of D_2O adsorbed per molecule of protein, or markedly more than in the case of H_2O. Therefore, a deuteriation of hemoglobin results in additional molecule reopening. Still, the method for the determination of *the total monosites (monolayer)* may be considered as justified.

Photo-oxygenation and γ-irradiation. — In an attempt to find an approach for interpretation of the irradiation effect on hemoglobin, the obtained data of experimental results as well as the preliminary tests can be summarized as follows.

Under visible light it was established, that (1) in the presence of only O_2 or H_2O no effect of H_2O-adsorptivity on hemoglobin occurred. (2) In the presence of both H_2O and O_2, an increase of original weight was established upon complete desorption (see Experimental). The analysis of the gas-vapor phase showed the presence of CO_2 and N_2 (air) (Table I). Since the complete dehydration was accomplished at the experimental condition, an increase of weight of the hemoglobin sample could be only due to the coupling of oxygen to the protein (hemoglobin). The amount of coupled oxygen, however, should be of a higher value than was determined, because even a very small amount of CO_2 and N_2 as decomposition products of protein could have compensated its weight.

It is unknown whether the loss of original weight of the sample could be achieved at the experimental conditions due to decomposition, on a continuation of the visible irradiation (as it is favored by mass-spectroscopic analysis (Table I), or, if an "equilibrium" (stationary state) is already reached. This, however, is not important for the purpose mentioned above. The amount of O_2 is coupled (adsorbed) to hemoglobin and could not be completely desorbed. An additional, even a very small amount, being also originally adsorbed, was used for "real oxidation," *i.e.*, the formation of CO_2 and N_2 as the products of decomposition of hemoglobin. Assuming that the formation of decomposition products is the final stage of the oxygenation of hemoglobin, "real oxidation," the residual amount of oxygen which is still coupled to protein after a desorption, must be combined physically and/or chemically. The original stage of interaction is the physically bonded oxygen, which on reaching a certain concentration results in chemical adsorption. The locations of physically and chemically adsorbed oxygen on a hemoglobin molecule are the active sites (groups) which are responsible for H_2O adsorption, but being occupied by oxygen are causing the marked lowering for H_2O - adsorptivity (Figure 1, curve 3b).

It is interesting that the main part of the oxygen is "washed off" by subsequent sorptions of H_2O vapor also demonstrating a regeneration of adsorptivity of hemoglobin in a process denoted as photo-oxygenation. The changes which occurred on heme-groups of hemo-

globin, providing an establishment of "O_2-heme" equilibrium (9, 10) can not be discussed as long as the study of O_2-adsorption is not completed. Since the above described results are of a photo-effect nature, it is suggested that the interaction between the participants of reaction is originated by the photo-chemical formation of hydrogen peroxide (H_2O_2) from the presence of H_2O and O_2. The hemoglobin itself participates in this photo-formation of H_2O_2 as a catalyst (11) (semi-conductor or even phosphorus) according to the schematically submitted reaction-steps:

(a)	Prot. $+h\upsilon \rightleftarrows$ Prot. ^+e	excitation
(b)	Prot. $^+e+\frac{1}{2}O_2 \rightleftarrows$ Prot. $^+O^-$	Photo-adsorption; coupling of oxygen
(c)	Prot. $^+O^- + OH^- \rightleftarrows$ Prot. $+ HO_2^-$	recombination and
(d)	$HO_2^- + H_2O \rightleftarrows OH^- + H_2O_2$	formation of H_2O_2

It is understood that the degree of excitation (see a above) of protein depends on the quantum value of the photons of irradiation, which could be charaterized by the number of replaced electrons as well as their energetical levels on the surface of the hemoglobin molecule.

Referring to a band-model of a crystalline form containing all kinds of energy levels according to the established nomenclature (12, 13), the excitation of hemoglobin can be represented (idealized) as the "jumping" of electrons between a valence band (-V.B.) or donor levels (-D.L.) and conductivity bond levels (-C.B.) (Figure 7). In detail, in the case of weak excitation energy (small energy photons), the electron's "jumps" may not even reach the conducting band -C.B. (Figure 7-a), while at a higher excitation energy they can reach the C.B. and fall back or be trapped on the A.L. (acceptor level), retaining the excited state also after the excitation has stopped (Figure 7-b), or even leave the C.B. demonstrating the dissociation (Figure 7-c).

An earlier study (11) of the photo-formation of H_2O_2, however, on ZnO-semi-conductors and -phosphorus indicated that reactivity (activation) of an excited state is dependent not only on the energy of an excitation but also involves a kinetic parameter conditioning the resonance between the illuminating sites of adsorbent and adsorptive.

On the basis of the above mentioned description, the experimental data on hemoglobin under visible irradiation suggests that the effect of excitation was mostly on the sites (functional groups) of hemoblobin (Figure 7-a), as a physical coupling of oxygen, which itself may not be excited but already dissolved in H_2O.

Effect of γ-irradiation: (1) On a hemoglobin sample in the absence of O_2 and H_2O a transferring ("jumping") of electrons may occur up to the conductivity band-levels and a trapping on the acceptor levels (Figure 7b-c). As a result of this, and adsorption of the electron affine oxygen on the surface takes place and an increase of weight of the sample after an exposure to air is experimentally

established (see first γ-irradiation). Since the adsorptivity for H_2O is very close to the original one it is evident that γ-irradiation practically has no effect on the sites (groups) responsible for H_2O adsorption. It is, however, most probable that the heme-groups, which exhibit octahedral complexes surrounding the Fe-atoms by different resonant ligands (8, 10) conditioning its phosphorus-properties, are affected but could not be detected by H_2O sorptions[2]. Therefore it is concluded that the increase of weight of the sample is due to the adsorption of O_2 on the heme-groups of the hemoglobin molecule only. If it adsorbed on the sites (functional groups) the adsorptivity for H_2O would be decreased and this is not the case. This also is in agreement with visible light irradiation where no effect was observed because of weak excitation (no trapping of electrons) (Figure 7).

(2) In the presence of O_2 and H_2O under γ-irradiation the course of schematic reaction (Figure 7b-c), should go almost exclusively through all the stages to the completion, *i.e.*, formation of H_2O_2, which may effect the hemoglobin molecule in causing decomposition, especially the heme-groups. The experimental data support this idea, since after the second γ-irradiation a loss of weight after complete desorption was established.

Clarification of the radiation effect, as a result of lowering adsorptivity for O_2 down to 50% of the original on the heme groups will be presented elsewhere.

CONCLUSION

An adsorption of H_2O vapor on the solid homogeneous dry hemoglobin shows high lyophility and a practically complete structural reopening of the molecule at a total monosites coverage. Its deuteriation in solid state is reached at 47° of desorption up to 100% of all labile H-atoms after many sorptions of D_2O vapor.

A photo-oxygenation of hemoglobin, observed in the presence of H_2O and O_2, suggests a photo-formation of H_2O_2, which seems to slightly affect the functionalities. A significant lowering of an adsorptive capacity for H_2O is caused by visible light irradiation due to an occupation (or blocking) by physically adsorbed oxygens on the active sites responsible for H_2O-adsorption. These, however, could be "washed off" from hemoglobin by the repeated sorptions of H_2O, that demonstarted marked regeneration of its H_2O-adsorptivity.

Deuteriated hemoglobin possesses a higher ability to adsorb D_2O vapor than the original one for an adsorption of H_2O.

The differential heats of adsorption, ΔH, are found to be higher for H_2O than for D_2O vapor especially at a lower coverage. This was also observed in the previous studies; however, since the entropies are unknown the relative strength of H_2O and D_2O bonds to hemoglobin are uncertain.

An irradiation effect as a lowering of an adsorptivity for D_2O vapor was found to be more marked on deuteriated hemoglobin. No

[2]8 carboxyl groups of propionic origin attached to the hemes of hemoglobin molecules being affected by an irradiation could cause only a 1% change (lowering) of H_2O adsorptivity at a monosites coverage.

effect was found of preirradiation for H→D exchangeability at the conditions of the experiments.

ACKNOWLEDGMENTS

The author would like to express his deep appreciation to Dr. L. H. Reyerson for his helpful advice and for providing the opportunity of starting this investigation. Appreciation is also extended to Drs. Lumry, Jensen, Boyer, Huges and Lagerquist for many helpful discussions on the subject. This work was supported in part by NIH-H2972 and NDSU grants.

REFERENCES

1. Wasyl S. Hnojewyj and Lloyd H. Reyerson, J. Phys. Chem. *65*, 1694 (1961).
2. Lloyd H. Reyerson and Wasyl S. Hnojewyj, J. of Phys. Chem. *64*, 811 (1960).
3. Wasyl S. Hnojewyj and Lloyd H. Reyerson (in preparation).
4. Wasyl S. Hnojewyj and Lloyd H. Reyerson, J. of Phys. Chem. *67*, 711 (1963).
5. Brunauer, F., Emmet, P. H. and Taylor, E. J., J. Am. Chem. Soc., *60*, 309 (1938).
6. Hnojewyj, W. S. and Peterson, R. A., Proc. N. Dak. Acad. Sci. *22*, 45 (1968).
7. Braunitzer *et al.* and Konigsberg *et al.* Adv. In. Prot. Chem. Vol. *16*, 297 (1961), Acad. Press, Inc., New York and London.
8. Granick, S., Ann. N.Y. Acad. Sci. *48*, 659 (1947).
9. Anson, M. L. and Mirsky, A. E., Physical Rev. *10*, 506-546 (1930).
10. West, E. S. and Todd, W. R., Textbook of Biochemistry, The McMillan Co., New York, 1955.
11. W. Hnojewyj, Zur photo-chemischen-Bildung und Zersetzung von Wasserstoff-peroxyd on Zinkoxyd-Katalysatsren, Ph.D. Thesis, Luedwig-Maximilian University, Munich, Germany, (1955).
12. W. Schotky Halbleiterproblem Vieweg und Sohn, Braunschweig, 1954 Referat von W. Schotky und F. Stoeckmann, "Betrachtungen ueber die Nature der Stoerstellen in Halbleitern und Phosphoren."
13. F. Stoeckmann, Naturwiss, *39*, 226 (1952).
14. Wynans, J., Jr., Advances in Protein Chem. *4*, 407 (1948).

KINETICS OF THE IODINATION AND BROMINATION-DEGRADATION OF URIC ACID IN 10^{-4} MOLAR AQUEOUS SOLUTIONS AS A FUNCTION OF THE pH AND HALOGEN AND HALIDE ION CONCENTRATIONS

Dwight A. Benesh and Franz H. Rathmann

Department of Chemistry

North Dakota State University, Fargo, North Dakota 58102

ABSTRACT

Rate studies for the iodination of uric acid were carried out by ultraviolet spectrophotometry over a pH range from 4 to 8 using phosphate buffers. The reaction of uric acid and iodine follows the second order rate equation. The rate constant, k, for the reaction at pH 6.75 was found to be 2.25 ± 0.20 x 10^3 liter moles^{-1} second^{-1}. Iodine was dissolved in a 0.30 M potassium iodide solution as the tri-iodide complex ion. The rate constant was determined at 351 mμ, where only the disappearance of iodine was followed because uric acid also has a maximum absorbance at 287 mμ. The rate constants at the respective pH's were: pH 4.35, 0.2; 5.0, 1.87; 5.75, 43.3; 6.75, 2250; 7.65, 160,000; 7.95, 610,000 and 8.05, 760,000 liter moles^{-1} seconds^{-1}. Preliminary studies using the bromine-potassium bromide-tri- (and penta-) bromide-hypobromite system indicate a shift to lower pH values, and considerably faster reaction rates.

INTRODUCTION

Boerth and Rathmann, in dealing with the halogenation-degradation of polutants in water purification, have shown that the reaction of uric acid with chlorine appears to proceed in accordance with a second order rate equation (1). Present work involves a more detailed study of the mechanism-kinetics of this reaction.

Uric acid is held in solution in the urine by the urea and disodium hydrogen phosphate present. Uric acid is a 2, 6, 8-trihydroxypurine which may be written as the two extreme tautomeric formuulae (a) and (b), as well as various intermediates. From its absorption spectrum it is concluded that the carbonyl form (b) strongly predominates in this equilibrium (2).

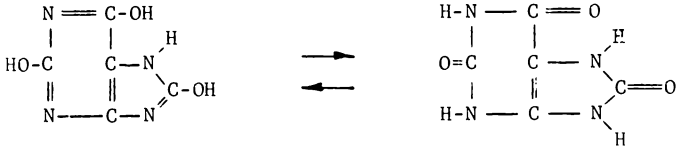

(a) (b) (1)

The concentration of chlorine in the local swimming pools is 1 to 2 ppm or 1 gram chlorine per 1000 liters of water, or 1.41×10^{-5} M. Therefore, we have conducted this study also in the 10^{-5}M range.

The uv spectrum of uric acid shifts in the direction of decreasing milli-micron units as the pH decreases, and as form b is converted to form a. Therefore, to keep this variable constant and under control, pH buffers of known pH values were prepared, using various relative volumes of 0.30 M K_2P0_4 and H_3P0^4. The phosphate buffer was used because it does not have a significant uv absorbance to interfere in this spectral range, and does not react with iodine, as do almost all organic buffers. Also it can be prepared in considerably higher concentrations than the reactants, so as to be an effective buffer.

The chemical properties of the halogens, fluorine, chlorine, bromine and iodine, are similar except that the reactivity usually decreases from fluorine to iodine. Since the reaction with chlorine, Cl_2, occurs rapidly to be followed accurately in detail by the instrumentation at our disposal, it was hoped that the relatively slower reaction of uric acid with a less reactive halogen would yield more reliable experimental data. Hence, the least active of the halogen group, namely, iodine, was chosen for studying the reaction with uric acid.

MATERIAL AND METHODS

Iodine was dissolved in potassium iodide solution in order to increase the concentration-stability of the solutions against its volatile nature, as well as to control better the concentration of the I_2 in solution.

Buffer solutions were prepared at pH values from 4 to 10. The reaction was followed at various pH values to obtain an overall picture of the chemical kinetics.

The Beckman DK-2 ratio-recording spectrophotometer with a Heath recorder was used to record the course of iodination of uric acid. Absorbance of iodine and/or uric acid was taken as the index for following the chemical reaction.

Experiments were also made using a Cary ratio-recording spectrophotometer equipped with a constant temperature bath. Most of the measurements were made using 1 cm square uv quartz cells; some were made with a 10 cm path-length quartz-window cell.

The iodine was standardized by use of standard sodium thiosulfate, standard potassium dichromate and starch-iodide solutions.

Iodine reacts with water according to:

$$I_2 + H_2O \rightleftharpoons H^+ + I^- + HIO \qquad (2)$$

The equilibrium of this equation shifts to the left in an acidic solution, where iodine is somewhat volatile. The equilibrium constant for this reaction (3a), is given by:

$$K_h = (H)\,(I)\,(HIO) = 4.6.10^{-13} \qquad (3)$$

at 25°C, taking into account also the tri-iodide equilibrium 3b.

$$I_2 + I^- \rightleftarrows I_3^-$$

In a strongly basic solution the equilibrium of (2) lies to the right,

and the hypoiodous acid dissociates according to:

$$HIO \rightarrow H^+ + IO^- \quad (4)$$

In strongly alkaline solution, especially on heating, decomposition-disproportionation takes place:

$$3\ HIO \rightleftarrows HIO_3 + 2HI \quad (5)$$

Light accelerates the hydrolysis of iodine by causing decomposition of hypoiodous acid according to:

$$2HIO \xrightarrow{h\nu} 2H^+ + 2I^- + O_2 \quad (6)$$

Oxidation of iodide by air liberates free I_2 according to:

$$4\ I^- + 4\ H^+ + O_2 = 2\ I_2 + 2\ H_2O \quad (7)$$

Iodine reacts with iodide ions formed by hydrolysis, or otherwise added, to form tri-iodide ions:

$$I_2 + I^- \rightleftarrows I_3^- \quad (8)$$

Iodine was dissolved in potassium iodide so as to maintain 99% of it in the tri-iodide complex, I_3^-. The 99% was selected so that this would be constant within experimental error, and would provide for convenient calculations. The equilibrium constant for equation (8) has a value of 570 liters/mole (4). From this we calculated

$$Keq = 570 = (I_3^-) / (I_2)\ (I^-) \quad (9)$$

what concentration of potassium iodide would be required to maintain the stable I_3^- at about 99% of the total I_2 present; i.e. 0.164 M KI.

A 0.30 M potassium iodide solution was prepared because in the experiments a constant concentration of 0.100 M potassium iodide was more easily maintained and its uv absorption is negligible. Under these conditions of 0.100 M KI, the iodine is present about 98% as triiodide and 2% as free iodine. The 0.30 M KI·I_2 solution was prepared using boiled distilled-deionized water for dissolving 0.1524 g (0.00060 moles) sublimed iodine crystals. The theoretical concentration of iodine was 6.01×10^{-4} M. One month after the preparation the stock solution was titrated again, and it was found that the concentration had decreased slightly to 5.64×10^{-4} M. The iodine was standardized with sodium thiosulfate by using 100 ml iodine stock solution, 50 ml distilled water, 1-2 g KI, 2 ml 2N H_2SO_4, and 2 ml of starch.

The uric acid was prepared by putting 14 to 24 mg into a one liter volumetric flask containing boiled, deionized distilled water. Before dilution was completed 5 ml of saturated mercuric iodide, about 6×10^{-7} moles HgI_2, was added to prevent bacterial decay. Because of the low solubility of uric acid in cold water, hot water was used to hasten the solubility of the uric acid. The solutions were then allowed to return to room temperature before final volumetric dilution was completed.

Phosphate buffers were prepared from stock 0.30 M phosphoric acid and 0.30 M potassium phosphate. The buffers were prepared by adding 10 ml of 0.30 M K_3PO_4 to 400 ml boiled, deionized, distilled water in a 600 ml beaker. The 0.30 M H_3PO_4 was titrated into this solution with a 10 ml buret as the solution was mixed with a magnetic

stirrer. The pH was determined by a Zeromatic II pH meter, accurate to within ±0.02 of a pH value.

REACTION STUDIES

Experimental preliminaries. — The experimental extinction coefficient for I_2 in KI, actually 98% as I_3^-, was determined at 351 mμ and 287 mμ with the Hitachi-Perkin-Elmer 139 spectrophotometer. The pH 7 buffer and distilled water were used as diluents for I_2 when determining the extinction coefficient. The procedure was similar to the one used when the reactions were studied. Hypodermic syringes were used to measure 1.0 ml I_2, 1.0 ml buffer, and 1.0 ml water into the 3.0 ml quartz cells. In another run, 1.0 ml water was used instead of a 1.0 ml buffer. There were no significant differences in the recorded absorbance values for I_2 in distilled water. The iodine solutions were prepared in 50 ml volumetric flasks and diluted to 50 ml with 0.30 M KI. The extinction coefficients are reported as 2.64 x 10^4 and 4.0 x 10^4 liter cm^{-1} mole $^{-1}$ at 353 mμ and 287.5 mμ, respectively, for the triiodide ion (5). Our results are 2.47 x 10^4 at 351 mμ and 3.67 x 10^4 at 287 mμ.

The concentrations of iodine (*i.e.* I_2-KI) to be used so as to give an inital absorbance value of 0.80 were calculated from the Beer's Law equation.

The uric acid solutions were prepared to a concentration of 5.9 x 10^{-4} M, corresponding to the calculated iodine concentration. In the special scans from 700 mμ to 220 mμ, uric acid has maximum absorbances at 287 mμ and 233 mμ.

The 351mμ wave length was chosen to follow the iodination of uric acid because at this wave length only the triiodide ion absorbs, whereas at 287 mμ both uric acid and I_3^- absorb. The potassium iodide absorption from 240 mμ on downwards masks the uric acid peak at 233 mμ.

Experimental procedure. — Three matched 10 mm quartz cells containing 3 ml of solution each were used in these experiments. The cells were thoroughly rinsed (5 times) with deionized distilled water. Hypodermic syringes were used to measure accurately 1 ml aliquots into the reaction cell: 1 ml uric acid, 1 ml buffer and 1 ml iodine. In the earlier experiments, first the uric acid and the buffer were added, to maintain the reaction at a particular pH. Then the cell was placed into the light-path, and the Heath recorder was started. The reaction began as soon as the iodine was injected, and was thus recorded on the Heath as a function of time with the chart speed set usually at 5 seconds per inch.

The experiments were repeated with successively decreasing concentrations of iodine while keeping uric acid constant, and also using different initial concentrations of uric acid and iodine. Buffers from pH 4 to 10 were used so as to obtain an insight into the variation of the reaction kinetics with respect to pH. These studies were carried out using both the Beckman DK-2 and the Cary 14 instruments.

In later experiments the sequence of filling the cell with the reactants was reversed, with iodine being injected first, followed by uric acid. The experiment was then conducted as cited above.

The above experiments were duplicated at 287 mμ. While the

TABLE I

SECOND ORDER RATE DATA: REACTION TEMPERATURE, 30°C.

Time (seconds)	Absorptions (O.D.)	Concentration at time, t: A* $[I_2]\cdot10^{-5}$ mole liter	ΔA^{**} $[I_2]x10^{-5}$ mole liter	B*** [Uric Acid]:10^{-5} mole liter	$\log\left(\frac{AoB}{ABo}\right)$
0	———	4.099****	———	3.980****	———
5	0.655	2.645	1.455	2.525	0.007
10	0.519	2.098	2.002	1.978	0.013
15	.0429	1.730	2.370	1.610	0.019
20	0.358	1.445	2.655	1.325	0.023

*A = Concentration of total available iodine in 10^{-5} moles per liter.
**ΔA = Decrease in A = reacted iodine
***B = Uric acid concentration in 10^{-5} moles liter at time t.
****Calculated concentration at t = 0.

products of the reaction appear to give a small residual absorption at 287 mμ, the results of this investigation were generally in agreement with those obtained at 351 mμ. It was of course necessary to make a correction for the residual absorption due to the unreacted uric acid as well as that due to unreacted iodine.

DETERMINATION OF ORDER OF REACTION

The plot: $\log \frac{AB_o}{A_oB}$ versus t yielded a straight line with a slope $= \frac{(A_oB_o)\cdot k}{2.303}$ This signifies that the iodine-uric acid reaction is of second order.

The rate constant, k, was determined from the experimental absorption data by the DK-2 and the Cary 14 at 351 mμ, applying the second order equation. The concentration of iodine present at any instant of time, t, was calculated by applying the Beer's Law equation, using our knowledge of the extinction coefficient, and reading the absorbance at t. It was assumed that one mole of iodine reacts with one mole of uric acid. Thus, the amount of iodine used was equal to the amount of uric acid reacted.

From these data the rate constant was calculated to be 2.21 x 10^3 liter-mole^{-1}-seconds^{-1} (Table I). The k values obtained from different runs with the same order of concentrations were within experimental errors. The k remained relatively constant when the iodine concentration was decreased, whereas k remained relatively constant when the iodine concentration was decreased, holding the other reactant in both cases (Table II). A plot was made relating k and the arbitrary parameter, p = ratio $\frac{\text{(uric acid)}}{\text{(iodine)}}$.

TABLE II

RATE CONSTANT VERSUS URIC ACID-IODINE RATIO

Uric Acid, ml	Iodine, ml	Ratio $p = \frac{\text{uric acid}}{\text{iodine}}$	k, in liter-mole^{-1}-second^{-1}
1.00	1.0	1.00	2.32×10^3
1.00	0.8	1.25	2.12×10^3
1.00	0.6	1.67	2.18×10^3
1.00	0.4	2.5	2.25×10^3
0.80	1.0	0.80	3.38×10^3
0.60	1.0	0.80	3.38×10^3
0.50	1.0	0.50	5.30×10^3

The average value for k was determined to be 2.25×10^3 liter-mole^{-1}-second^{-1} for $p > 1$, and increases for $p < 1$.

The rate constants determined at their respective pH's are tabulated as follows in Table III.

TABLE III

RATE CONSTANT, SECOND ORDER AS A FUNCTION OF THE pH, AT 30°C

Initial pH of Buffer used	Actual pH in Reaction	k, liter-mole^{-1} -seconds^{-1}	log k
4.0	4.35	0.20	0.07
5.0	5.00	1.87	0.27
6.0	5.75	43.3	1.64
7.0	6.75	2.25×10^3	3.35
8.0	7.55	1.60×10^5	5.20
9.0	7.95	6.10×10^5	5.79
10.0	8.05	7.60×10^5	5.88

BROMINATION

A brief preliminary study was carried out making use of bromine in potassium bromide. Besides its weak absorption in the visible region, tribromide ion absorbs very strongly at 267 mμ, overlapping the uric acid band at 287mμ, thereby introducing complications into the calculations.

Bromine was dissolved in a 3.1 M potassium bromide solution so as to maintain 98% of the bromine as the stable tribromide ion. This solution was standardized by the iodide - thiosulfate - starch method described above. The fact that the equilibrium constant, k, is equal to 16 for the equilibrium,

$$Br_2 + Br^- \rightleftarrows Br_3^-$$

indicates that the Br_3^- is much less stable than the I_3^-, for which K = 570. It is important to maintain the equilibrium so that nearly all, in our case 98%, of the bromine is in the tribromide ion form. That is why the high, 3.1 M, potassium bromide concentration is required.

Water supplies never contain anywhere near such high salt concentrations, but for lesser salt concentrations the fraction of Br_2 in the tribromide form is very sensitive to small changes in the salt concentrations (as well as to small variations in pH) (Table IV).

TABLE IV

BROMINE-TRIBROMIDE EQUILIBRIUM AS A FUNCTION OF BROMIDE ION CONCENTRATION: TOTAL $Br_2 = 4.6.10^{-3}$M

Percentage to be present as		Molarity of KBr Required
Br_3^-	Br_2	
99	1	6.18
98	2	3.1
90	10	0.55
80	20	0.25
60	40	0.093
50	50	0.06
25	75	0.02

Qualitatively the bromine-uric acid reaction is also catalyzed by OH, *i.e.* sensitive to pH, as is the iodine reaction. The high rate effect is, however, shifted to lower pH values. At pH 5 and 6 the rates are too fast for our type of instrumentation, whereas the rates for iodine are not too rapid until pH 8 is reached. Our colleague, Dr. C. W. Fleetwood, has just completed construction of a cell and a mixing device by which we hope to determine the initial-reaction rates above pH 8 for iodine and above pH 5 or 6 for bromine.

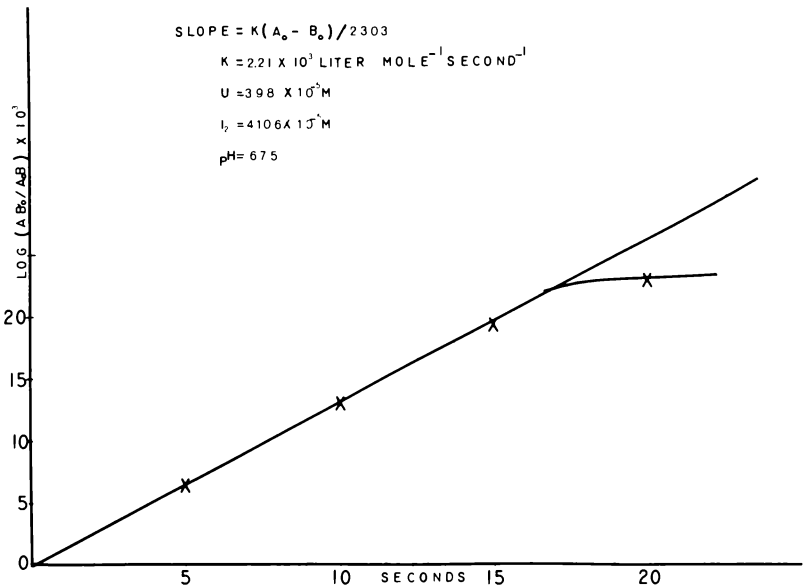

FIGURE 1—Log $\frac{AB_0}{A_0B}$ versus time, for the initial rate of the iodine-uric acid reaction.

DISCUSSION

Figure 1 shows the reaction of iodine and uric acid to be initially second order. Figure 2 shows k to be relatively constant for values of $p>1$. The values of k averaged $2.25\pm0.1 \times 10^3$ liter-mole^{-1}-second^{-1} over this region. Considering other uncertainties, such as the determination of extinction coefficient, response of the instrument, and preparation of solutions, k may be taken to be $2.25\pm0.2 \times 10^3$ liter-mole^{-1}-second^{-1} at pH 6.75, 30° C.

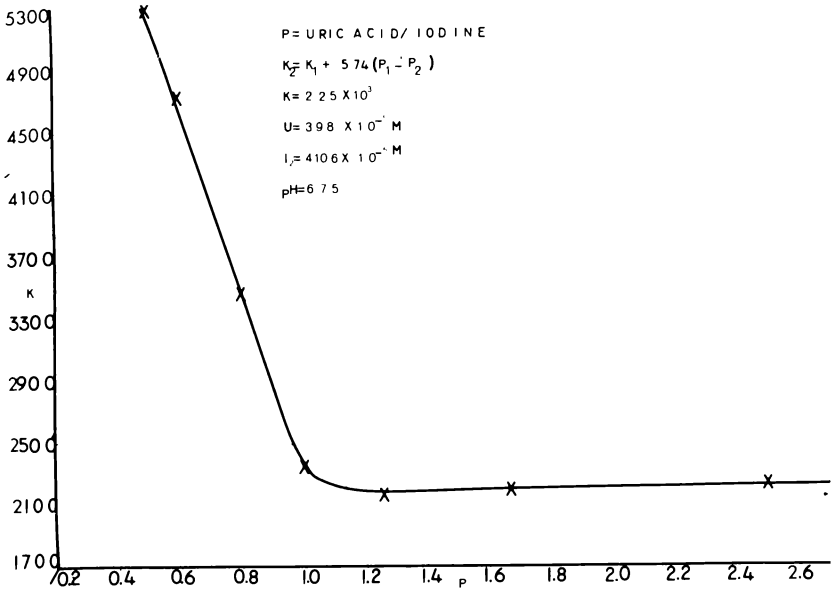

FIGURE 2—Ratio (uric acid/iodine) = $p = \frac{(B_o)}{(A_o)}$ versus the rate constant k;

The rate constant was found to increase for values of $p<1$. The variation may be represented empirically as:

$$k_2 = + 5.75 (p_1 - p_2) \times 10^3, \quad p_2<p_1<1 \qquad (10)$$

Figure 3, for a ratio p = 1 at pH 6.75, shows a marked deviation between the theoretically extrapolated, and the actual experimental, curves after about fifteen seconds. The absorption as extrapolated on the basis of a second order rate of reaction is then greater than the actual experimental absorption. This gives rise to the thought that there may be a competing substance for utilizing iodine, *i.e.*, an already reacted uric acid molecule. Figure 1 above also shows a deviation from the straight line after about 15 seconds. This once again indicates the presence of a reacting competitor which absorbs only slightly at 287 mμ and not at all at 351 mμ.

Calculations were carried out to determine the order and the rate constant for the competitor versus iodine reaction. Because of the lack of direct experimental measurements on the amount of this substance present at any instant of time, neither order nor rate constant could be assessed successfully.

Figure 4 gives the variation of the rate constant k with respect

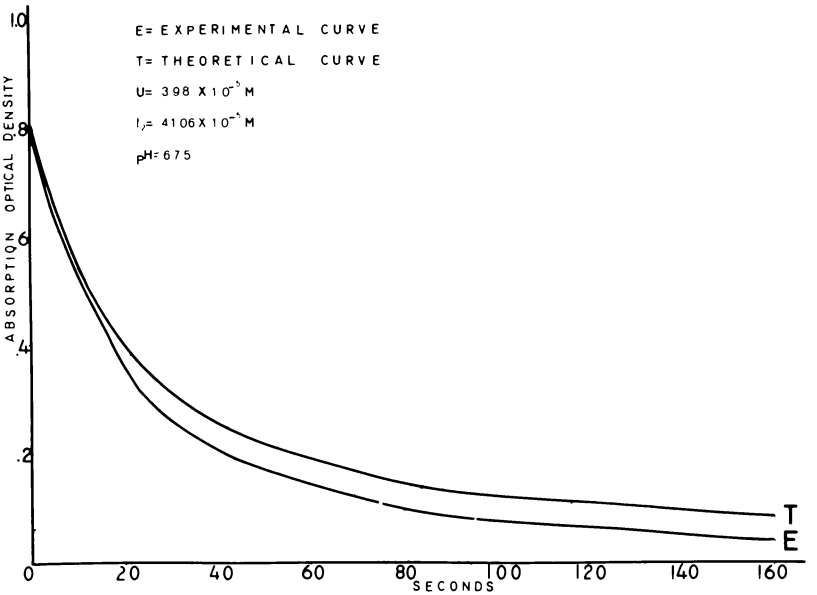

FIGURE 3—Absorbance versus time, for uric acid - iodine, p = 1, at pH 6.75.

to pH. The rate constant was plotted on a logarithmic scale and the pH on a linear scale. The graph yields a straight line, and the variation of k with respect to pH may be represented empirically by:

$$\log \frac{k_2}{k_2} = 1.875\ (pH_2 - pH_1) \qquad (11)$$

This equation shows that the reaction progresses very rapidly at higher pH values.

ACKNOWLEDGMENTS

We thank Dr. Wunnava V. Subbarao, Department of Electrical and Electronics Engineering, North Dakota State University, for some very valuable help in the mathematical interpretation of the experimental data.

The work upon which this paper is based was supported in part by funds provided by the United States Department of the Interior through the North Dakota Water Resources Research Institute as authorized under the Water Resources Act of 1964, Public Law 88-379.

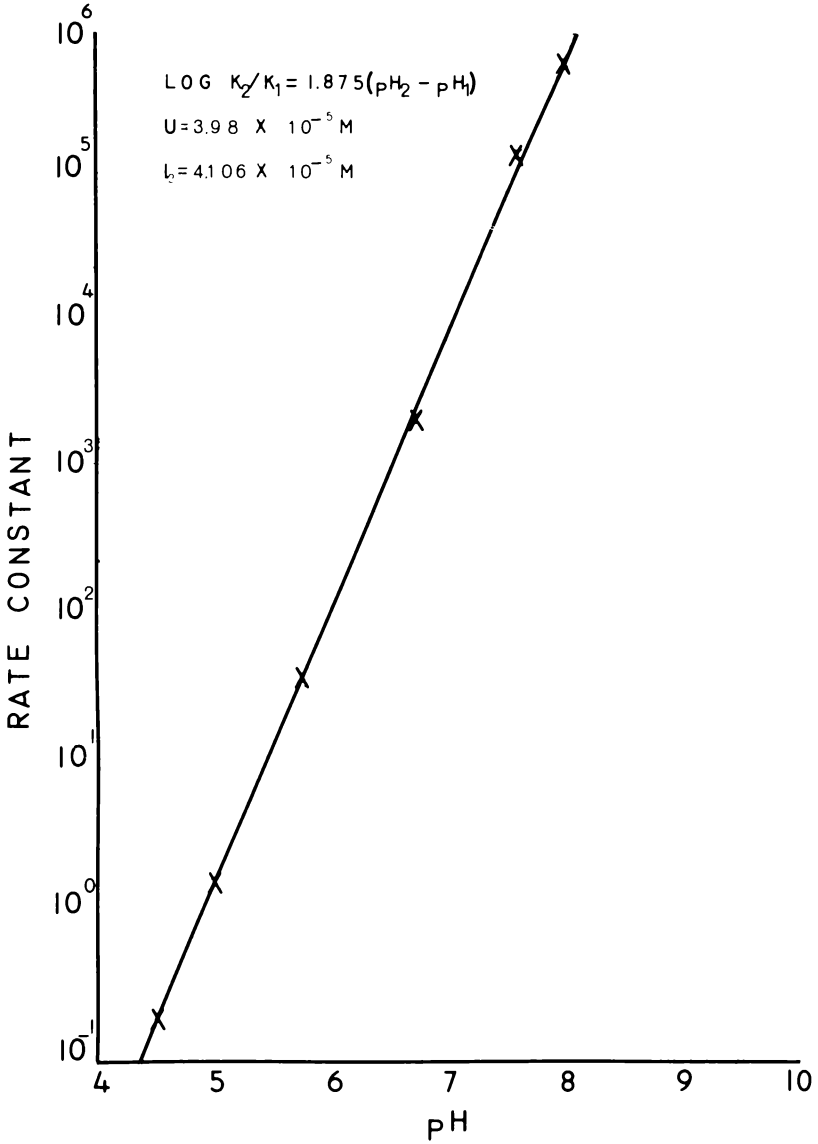

FIGURE 4—Rate constant, k, versus the pH.

REFERENCES

1. Donald Boerth and F. H. Rathmann, Paper No. 618, Abstracts of the National meeting of the American Chemical Society, Atlantic City, September, 1968.
2. C.P. Karrer, Organic Chemistry, Elsevier Publishing Company, New York, 1947, 802-805.

3a. F. A. Cotton and G. Wilkinson, Advanced Inorganic Chemistry, John Wiley and Sons, Inc., New York, 1967, 561-689.

3b. Gmelins Handbuch d. Anorgan. Chemie; Iodine; Weinheim-Berlin, 1933, pp. 111, 117, 130, 134, 173-5, 545,653.

4. W. C. Pierce, D. T. Sawyer, and E. L. Haenisch, Quantitative Analysis, John Wiley and Sons, Inc., New York, 1963, 293-298.
5. A. D. Autrey and R. E. Connick, *J. Amer. Chem. Soc.* 1951, 73(2), 1842-1843.
6. F. Daniels and R. A. Alberty, Physical Chemistry, John Wiley and Sons, Inc., New York, 1967, 325-333.

COORDINATION OF PYRIDINE 1-OXIDES WITH OXOVANADIUM (IV)

Mark Pavicic

South High School, Fargo, North Dakota 58102

Winner, Ralph E. Dunbar Award,

North Dakota High School Science Competition

INTRODUCTION

The study of the reaction of oxovanadium salts with various pyridine 1-oxide ligands may provide much valuable information concerning the bonding characteristics of the oxovanadium complexes. The investigation of those factors affecting the formation of the resulting products included effects caused by the presence of water, steric factors, and those factors due to the reaction media. The pyridine 1-oxides represent a series of ligands with many varied ligational strengths and a wide choice of substituents with which to modify steric interactions. To lend more readily to identification and possible future experimentation, pure crystalline products were desired throughout this investigation.

DISCUSSION

The electronic characteristics of the pyridine 1-oxide molecule are explained by a resonance system where the lone-pair electrons of the oxygen are in resonance with the electrons of the aromatic ring (Figure 1). There are increased contributions of structures (C) and (A) when the N-oxide oxygen is coordinated with a metal ion. The ligands used in my research were pyridine 1-oxide, 2-methylpyridine 1-oxide, 4-methylpyridine 1-oxide, and 2-ethylpyridine 1-oxide.

Through the use of various ligands and anions, past research has produced oxovanadium complexes of these general formulas: VOL_2X_2, $VOL_2X_2 \cdot H_2O$, $VOL_2X_2 \cdot H_2O$, and VOL_2X_2. I used the four ligands men-

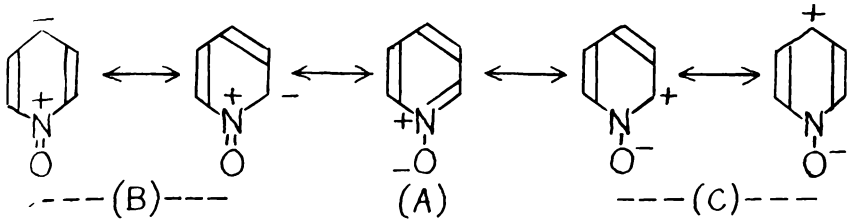

FIGURE 1—Resonance structures of pyridine 1-oxide.

tioned as well as the oxovanadium sulfate and tetrafluoroborate salts. The tetrafluoroborate anion makes use of the fact that when the anion possesses little nucleophilic tendency the N-oxide coordination is usually the maximum coordination the metal ion can express. The sulfate anion has a much greater bonding strength and would be expected to cause the formation of lower coordination groups. Therefore the proposed structure for the $VOL_4X_2H_2O$ Complex is that shown in Figure 2. Here the anions associate loosely in the secondary coordination sphere. In the case of the sulfate anion, "X" would be located in the primary coordination sphere. The water molecule may be replaced by another ligand under more anhydrous conditions. However, if steric factors are too large, it is conceivable that a complex of the general formula VOL_4X_2 would result.

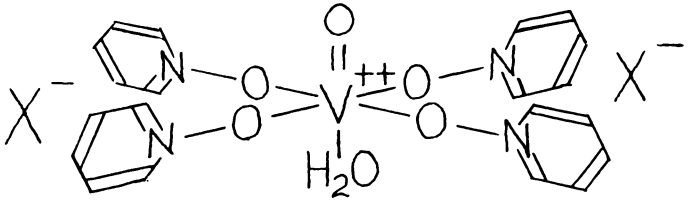

FIGURE 2—Proposed structure of the $VOL_4X_2H_2O$ complex.

Vanadium compounds are noted for their striking colors and past research has found that the complexes of the type VOL_5X_2 are generally green whereas those of the type $VOL_4X_2H_2O$ are usually blue: This fact was the only obtainable identifying factor of some of my complexes.

EXPERIMENTATION

Initial experimentation involved the reaction of oxovanadium tetrafluoroborate with the various pyridine 1-oxides. This starting material was synthesized by reacting fluoboric acid with barium hydroxide and then adding oxovanadium sulfate. After removing

the precipitate the solution was saturated by evaporation. Ethanol was present and formed a loose association with the oxovanadium, preventing it from oxidizing with the air. This solution was reacted with each member of the ligand series presented earlier.

The first ligand of the series, the pyridine 1-oxide, was reacted with the oxovanadium tetrafluoroborate solution with and without 2,2-dimethoxypropane. The 2,2-dimethoxypropane combines with excess water to form methanol and acetone which do not interfere with the coordination reactions.

The hygroscopic pyridine 1-oxide was first dissolved in 95% ethanol and then combined with the oxovanadium tetrafluoroborate solution. This resulted in the formation of large, dark blue-green, diamond-shaped crystals. The ease of formation of these crystals was expected because of the low steric interference of the parent pryidine 1-oxide. This compound had very slightly hygroscopic characteristics which caused noticeable deterioration of the crystals after being exposed to the air for about 15 days.

The same reaction was repeated with the addition of 2,2-dimethoxypropane. This resulted in the formation of large emerald-green crystals of much greater complexity. This compound was more hygroscopic and had crystallized sooner than had the reaction without 2,2-dimethoxypropane. This seems to indicate that there is definite competition between water molecules and the pyridine 1-oxides for coordination positions. Under potentiometric titration analysis the emerald-green material indicated a formula of $VO(C_5H_5NO)_2(BF_4)_2$. The former may have been $VO(C_5H_5NO)_4(BF_4)_2 \cdot H_2O$ but no definite data have been accumulated. Neither of these two compounds have been previously reported.

Another pyridine 1-oxide used was the 2-methylpyridine 1-oxide. In this ligand the increased steric hindrance increases the difficulty of pentakist formation. Little previous work had been done with single anions and, since this ligand was a liquid, a direct reaction was tried with solid oxovanadium sulfate. This resulted in an oil which was solidified by washing with acetone. A crystal product was desired, however, so various additional methods were tried and are summarized as follows:

$VOSO_4$ in 1:4 stoichiometry with 2-CH_3PyNO and 2,2-DMP	oil
$VOSO_4$ in 95% ethanol with 2-CH_3PyNO in 1:5 stoichiometry	solution
$VOSO_4$ in contact with $VOSO_4$(s)	oil
$VOSO_4$ after washing oil with acetone	solid
$VOSO_4$ in 95% ethanol and H_2O with 2-CH_3PyNO (1:5)	solution
$VOSO_4$ in 1:1 stoichiometry	solution
$VOSO_4$ in 1:5 stoichiometry and 2,2-dimethoxypropane	solution
$VOSO_4$ in 1:1 stoichiometry and 2,2-dimethoxypropane	oil
$VOSO_4$ in 1:5 stoichiometry and 2,2-DMP in contact with "excess" solid oxovanadium sulfate	oil
$VOSO_4$ in methanol with 2-CH_3PyNO in chloroform	solution
$VOSO_4$ in methanol with 2-CH_3PyNO in chloroform and 2,2-DMP	oil

From these attempts one can see that the oxovanadium sulfate was reacting with very little of the ligand and that the water molecules were successfully competing with the ligand in forming the compound. Finally, a suitable reaction medium was found by reacting $VOSO_4$ in methanol with 2-CH_3PyNO and then adding acetone. Small hemispheres of solid material formed along the container walls and may have been closely packed arrays of crystalline material. Potentiometric titrations indicated that the product was $VO(2\text{-}CH_3C_5H_4NO)_2SO_4 \cdot 2H_2O$. The sulfate anion had evidently bonded itself within the inner or primary sphere of coordination. This reaction was repeated a number of times with differing amounts of acetone and some color differences were observed among the products. This may have been due to differences in composition such as VOL_2X and $VOL_2X \cdot 2H_2O$.

The same ligand was reacted with oxovanadium tetrafluoroborate and was expected to form somewhat higher coordination complexes, for reasons discussed earlier. Initial reactions were between $VO(BF_4)_2$(aq) with the addition of 2,2-dimethoxypropane and 2-$CH_3C_5H_4NO$. Both blue and green products were observed when the stoichiometric ratio of ligand to oxovanadium exceeded about 15:1. At 40:1 and above, there was no crystallization. This shows the effects of changes in stoichiometry. A contaminant was present and potentiometric titrations of the blue material were inconclusive until the experimentation was repeated with a methanol and 2,2-dimethoxypropane solution of $VO(BF_4)_2$. (This was synthesized by evaporating the water from a $Ba(BF_4)_2$ solution and then reacting the $Ba(BF_4)_2$(s) with the $VOSO_4$(s) in methanol.) The vanadium percentage was nearly equal to that for $VO(2\text{-}CH_3C_5H_4NO)_4(BF_4)2 \cdot H_2O$. No green material was isolated satisfactorily, but this may have been $VO(2\text{-}CH_3C_5H_4NO)_5(BF_4)_2$ judging from the color and changes caused by the presence of water.

Some reactions were tried between oxovanadium in 95% ethanol with 2,2-dimethoxypropane and 4-$CH_3C_5H_4NO$ but time did not permit analysis of the light green material that resulted. The formation of this material was extremely slow and other methods should be tried.

The same ligand was reacted with oxovanadium tetrafluoroborate. Since 4- substituted ligands of this type have very little steric interaction, high coordination complexes were expected. The best results were obtained by a reaction of $VO(BF_4)_2$ in methanol and 2,2-dimethoxypropane with 4-$CH_3C_5H_4NO$ and slowly evaporating the solvent. Both blue and green rectangular crystals were formed. Recrystallization from methanol and 2,2-dimethoxypropane resulted in almost all green material but the crystals were badly formed. The colors of the products and the effects of the water factor indicated the formation of $VO(4\text{-}CH_3C_5H_4NO)_4(BF_4) \cdot H_2O$ and $VO(4\text{-}CH_3C_5H_4NO)_5(BF_4)_2$.

The most troublesome ligand was the 2-ethylpridine 1-oxide because of the large degree of steric hindrance apparently caused by its 2-substituted ethyl group. Direct reaction with solid oxovanadium sulfate resulted in an oil which was only solidified by long periods

of drying in a vacuum desiccator. The resulting material was hygroscopic and was not pure enough for further analysis.

Various reaction media were also tried in reacting the 2-ethylpyridine 1-oxide with oxovanadium tetrafluoroborate. The best results were obtained from the reaction of a methanol and 2,2-dimethoxypropane solution of $VO(BF_4)_2$ with the 2-ethylpyridine 1-oxide. Again, evaporation was necessary and some very small blue crystals were formed. The solution, however, would not evaporate completely and the crystals were imbedded in the resulting oil. Because I could not extract them, I was unable to determine the composition of the compound; however the blue color of the crystals suggests a tetrakist.

SUMMARY

Water coordination, anion nucleophilic tendencies, and steric hinderance were all factors affecting the coordination of the pyridine 1-oxides. The low steric interaction of the parent ligand, C_5H_5NO, and the 4-methylpyridine 1-oxide, combined with the low nucleophilic tendency of the tetrafluoroborate anion, resulted in the formation of the higher coordination compounds $VO(C_5H_5NO)_5(BF_4)_2$, $VO(C_5H_5NO)_4(BF_4)_2 \cdot H_2O$, $VO(4\text{-}CH_3C_5H_4NO)_5(BF_4)_2$, and $VO(4\text{-}CH_3C_5H_4NO)_4(BF_4)_2 \cdot H_2O$. On the other extreme, the high steric inter-action of 2-methylpyridine 1-oxide and especially the 2-ethylpyridine 1-oxide, combined with the high nucleophilic tendency of the sulfate anion resulted in the formation of low coordination compounds such as $VO(2\text{-}CH_3C_5H_4NO)_2SO_4 \cdot 2H_2O$. This last compound is a very curious one and is but one of the many new compounds that were encountered during this project.

FUTURE PLANS

Some of the compounds listed have very curious structures and others are in definite need of additional analysis and experimentation. I hope to continue this project at least to the point where the compounds made and attempted will have been formed by methods that will produce products of more definite identity and structure. There is also the possibility of completing an entire series of complexes with the central oxovanadium ion. The relative information from such a series could then be used to study the bonding characteristics of other metal ions.

REFERENCES

R. G. Garvey, J. N. Nelson, and R. O. Ragsdale, *Coordination Chemistry Reviews*, 3 (1968) 375-407.

E. Ochiai, *Aromatic Amine Oxides*, American Elsevier Publ. Co., (1967).

LOW-TEMPERATURE ASHING OF LIGNITE USING AN OXYGEN PLASMA

Philip G. Freeman and Walter W. Fowkes

Grand Forks Coal Research Laboratory

Bureau of Mines, U. S. Department of the Interior

Grand Forks, North Dakota 58201

ABSTRACT

Many processes utilizing lignite or other fossil fuels are concerned with the chemical and mineralogical composition of the ash. In an effort to better understand the original condition of the inorganic components in the fuel, a low-temperature oxidation unit was used to ash lignite. In this way temperature-sensitive structures are preserved. Carbonaceous material is oxidized with "active" oxygen generated in a microwave discharge under reduced pressure. The addition of a small quantity of nitrogen catalyzes the formation of active oxygen at temperatures below 60° C, as determined by a thermometer inserted in a well in the reactive chamber. The low-temperature ash was analyzed by X-ray diffraction and found to differ considerably from a corresponding high-temperature ash in that sodium occurred mainly as carbonate-sulfate in the latter and as nitrate in the former.

INTRODUCTION

Although a comparatively small percentage of lignite is inorganic ash, this ash is an important consideration in utilization of the coal. Combustion, boiler operation (including ash fouling), ash collection and disposal, solvent de-ashing, and similar processes all require an understanding of the chemical and mineralogical composition of the lignite ash. In many cases it is helpful to know the original condition of these components, particularly when they are likely to undergo alteration or phase change at elevated temperatures. For this reason we attempted to ash samples of lignites in a dilute oxygen plasma generated by microwave radiation in a partial vacuum. Under these conditions most of the carbonaceous material can be oxidized at temperatures below 60° C. Sufficient ash can be obtained to permit analysis by X-ray and spectrographic methods as well as by microchemical methods.

MATERIALS AND METHODS

The low-temperature oxidation unit is shown in Figure 1. The oxygen activation takes place in a quartz tube which is inserted through the center of the waveguide. Excess microwave energy is absorbed in a dummy load at the base of the waveguide. This unit was designed to produce sustained microwave radiation at 2,450 Mhz with an output exceeding 1 kw.

A number of parameters must be controlled to maintain efficient operation of the unit. Foremost among these is deposition along the surface of the quartz tube. It was found that if coal dust and/or ash particles were permitted to accumulate on the inner surface of

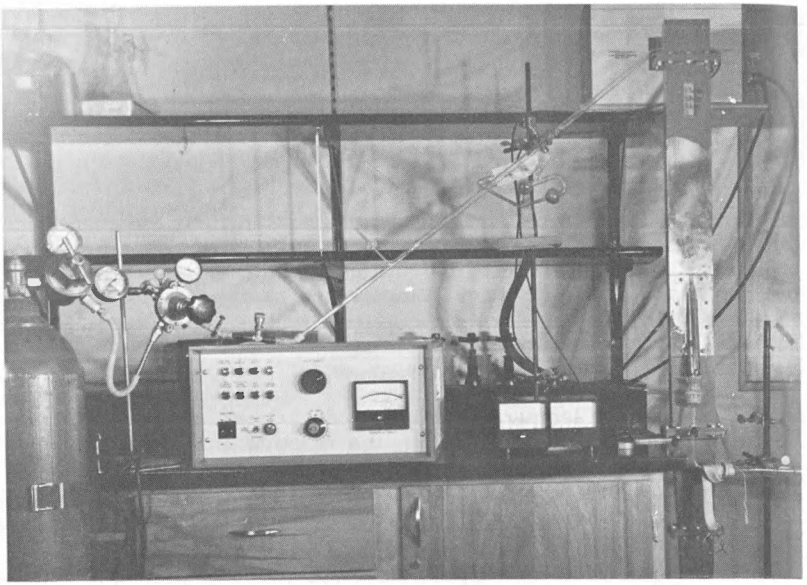

FIGURE 1—Low-temperature oxidation unit.

the tube, the transfer of microwave energy to oxygen was reduced, and an active surface was provided so that the atomic oxygen would recombine to molecular oxygen. This resulted in decreased amounts of usable oxygen plasma and a decline in the rate of oxidation. Continued use of the tube with deposits present resulted in permanent frosting of the inner surface and thereby increased active surfaces to the point where recombination was almost instantaneous and no oxidation was possible. This problem was overcome by swabbing the tube with a ramrod at intervals of 4 to 8 hours during operation.

Particle size is also important. With particles smaller than 80 mesh, accumulation of dust on the inner surface of the quartz tube is so rapid that the effectiveness of the system is severely reduced. The portion of the sample remaining in the reaction chamber packs into a semi-solid mass that reduces the effective surface. The result is a very low rate of oxidation. If particle size is between 60 and 80 mesh, accumulation of dust and ash particles is minimized, and the loose structure of the sample permits the oxygen plasma to effectively reach a greater surface area with a consequent increase in oxidation rate as shown in Figure 2.

It was reported (1) that the presence of a few parts per million of nitrogen in the feed gas supports a chain reaction that increases the concentration of active oxygen several fold. By bleeding in a very small quantity of air, it was found that it is possible to increase

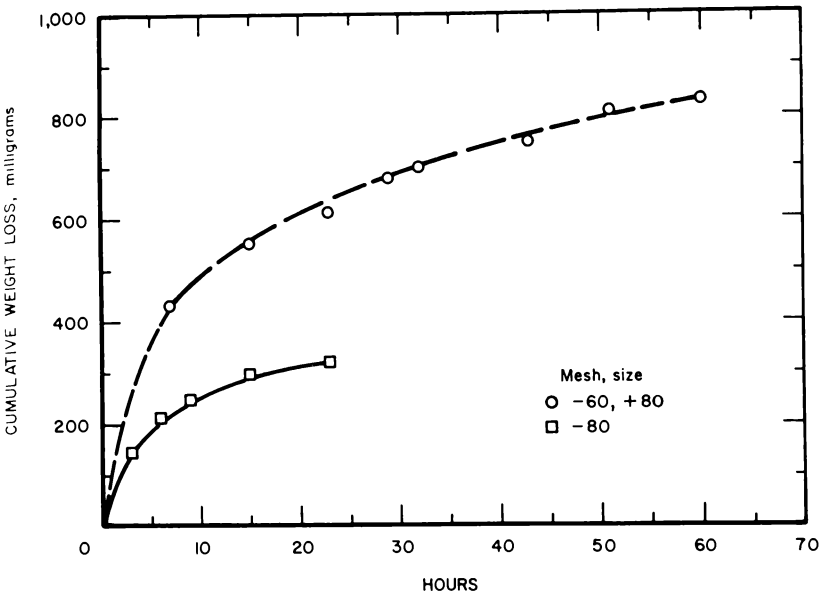

FIGURE 2—Effect of sample particle size on rate of oxidation.

the effectiveness of atomic oxygen generation. The small amount of nitrogen oxide produced also helps to oxidize the carbon and eventually appears in the ash as salts of nitrate.

RESULTS

A comparison of X-ray diffraction patterns reveals a considerable difference between ashes prepared from the same lignite by low-temperature oxidation and by standard ashing in a furnace at 800° C. However, lignite ash mixtures are complex and result in X-ray diffraction patterns difficult to interpret. If the ash is first extracted with water at room temperature, separate X-ray examination of the resulting water-soluble and water-insoluble fractions gives more easily interpreted diffraction patterns (Figure 3).

In the case of the low-temperature ash, a principal component is sodium nitrate, which results from the combination of the nitrogen oxides in the plasma with the sodium in the lignite. The water-soluble portion of this ash can be further resolved by alcohol extraction, which dissolves the sodium nitrate and permits easier identification of the residue.

As an example of the preliminary results obtained by the low-temperature ashing unit, X-ray diffraction patterns were run on fractions obtained from high-temperature (800 C) and low-temperature (60 C) ashes from a high-sodium Baukol-Noonan lignite.

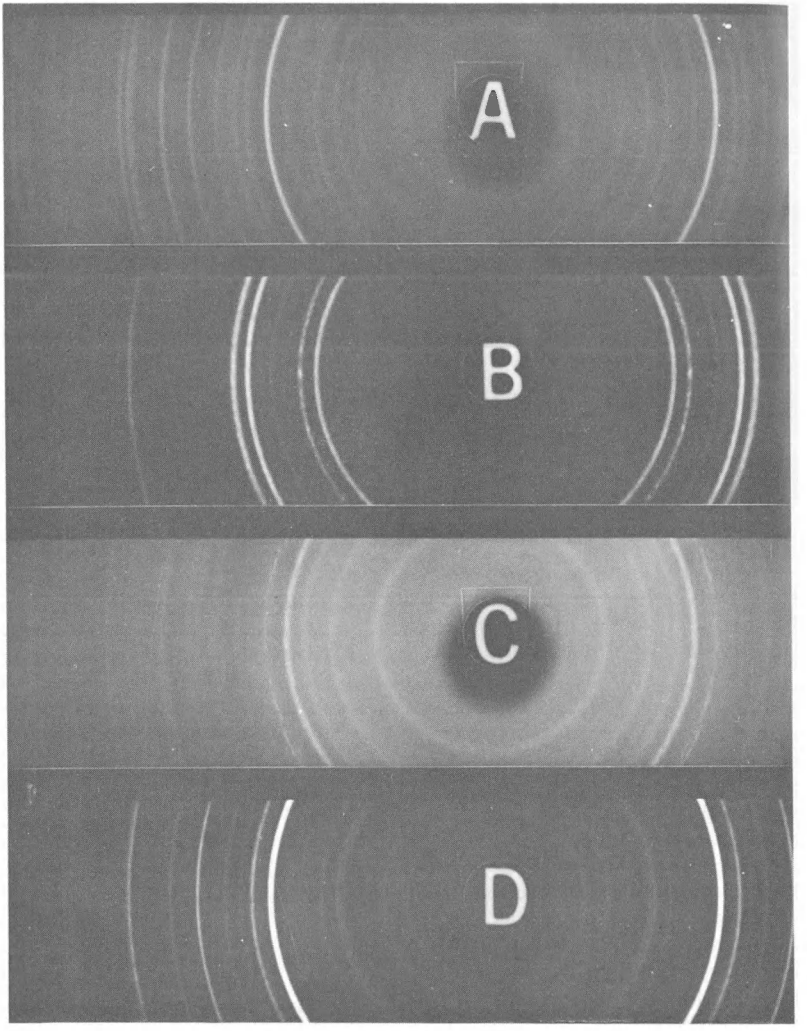

FIGURE 3—X-ray diffraction patterns: A) Water-insoluble 800° ash, B) Water-soluble 800° ash, C) Water-insoluble low-temperature ash, and D) Water-soluble low-temperature ash.

TABLE I

X-RAY DIFFRACTION ANALYSES OF FRACTIONS OF ASH FROM A HIGH-SODIUM BAUKOL-NOONAN LIGNITE

Ashing temp., °C	Ash	Components
800	Complete	Complex mixture
	Water soluble	Sodium carbonate sulfate (Burkeite), calcium sulfate
	Water insoluble	Calcium carbonate, complex silicates, + unknowns
60	Complete	Sodium nitrate + unknowns
	Water soluble	Sodium nitrate + unknowns
	Water insoluble	Basic aluminum silicates + unknowns
	Water soluble, EtOH soluble	Sodium nitrate
	Water soluble, EtOH insoluble	Calcium sulfate hydrates

Interpretations of the X-ray diffraction patterns are given in Table I.

The most notable difference between the ashes is, of course, the nitrate salts, which appear in the low-temperature ash, but which are absent in the high-temperature ash. This reflects the previously mentioned addition of nitrogen to the plasma as a catalyst. No indications of calcium nitrate or sodium sulfate were found in the ash, but the extraction process may permit exchange that would render all the calcium as sulfate and all the sodium as nitrate. Because the solubility of calcium sulfate is low, calcium nitrate would only result if excess calcium were present. Alternative separation procedures are planned to clarify this point.

Although it seems that the coal minerals in low-temperature ash are not all in their original forms, we still are obtaining some information not available by conventional methods. The number of samples has been limited. Hopefully, when additional samples are ashed and additional techniques of separation and analysis provided, we will be better able to understand the inorganic components of lignite and how they affect utilization.

REFERENCES

1. Kaufman, F., and J. R. Kelso. Catalytic Effects in the Dissociation of Oxygen in Microwave Discharges. J. Chem. Physics, v. 32, 1960, pp. 301-2.

QUICK OPENING CLOSURE FOR USE ON A LIFE SUPPORT SYSTEM

Juan R. Morales

Department of Mechanical Engineering

University of North Dakota, Grand Forks, North Dakota 58201

INTRODUCTION

A research program at the University of North Dakota is concerned with the study of animals living under pressurized environments. The task of the Mechanical Engineering Department is to provide by design, selection and fabrication, the necessary equipment in developing the program to its fullest extent. The present work underlines the design of a high-pressure, quick opening closure, which could be used on the small test chambers of the pressurized vessel complex being developed for the program.

The design requirements are as follows:

Outside diameter of pressure vessel .	18 in.
Inside diameter of pressure vessel .	17 in.
Design pressure . .	600 psi.
Design temperature	68 F.

The closure should not require inner vessel space in any phase of its operation.

The design should be such that the parts could be manufactured at the UND Mechanical Shop from commercially available stock or parts.

PROPOSED CONFIGURATION

A threaded joint was chosen as the most convenient for the present conditions (1). The threaded joint consists of a fixed part which will be attached to the pressure vessel; a movable part will act as the door, and an external coupling ring will serve as the means of closing the door. The fixed part has a set of parallel grooves machined on its exterior cylindrical surface. The movable part is furnished with an Acme centralizing thread on its external cylindrical surface. The coupling ring has half of its inner cylindrical surface machined with parallel grooves and the remaining half is machined with an Acme centralizing thread. The parallel grooves on the coupling ring mate with those on the door. Rotation of the coupling ring will cause displacement of the door due to the screw action of the threads forward or backward according to the sense of rotation of the ring. This rotation will bring therefore, the matching surfaces, which are properly machined on the fixed part as well as on the door, in contact. The matching surfaces are inclined with respect to the longitudinal axis of the pressure vessel, in order to get sealing action from the inner pressure.

In order to facilitate the opening and closing of the door a linkage, which will also act as a hinge in this operation, has been added. The linkage is in essence a four bar mechanism with one link attached to the fixed flange and the other extreme link welded to the door.

As a sealing material, an 0-ring has been chosen because of its properties and versatility in sealing effectively pressures up to 1500 psi (2).

The locking ring is split for assembly and has eight circumferentially located pegs. The two halves of the locking ring will be assembled in its original shape with two securing plates bolted to it. By the use of a lever inserted into the pegs the necessary torque for closing and opening the door will be provided (Figure 1). The operation of the locking ring and of the door linkage will be manual.

A passive safety device is provided by the pressure, because when it is acting, the necessary torque and force for opening the door is so high that the door could not be opened in this condition. A positive safety feature has been added which consists of a locking pin in shear attached to the closure in a convenient position (Figure 2).

The parts constituting the closure are selected from commercially available weld-neck flanges and caps and are modified as required. In selecting the specifications of these weld-neck flanges so that service conditions are taken into account the pressure-temperature ratings for forged flanges from A.S.A. Standard B 16.5 (3) are to be used. Therefore, for temperature from -20 to 100 F, which includes the pressure vessel operating temperature of 68 F, and for a primary service pressure rating of 300 psi, the maximum non-shocking

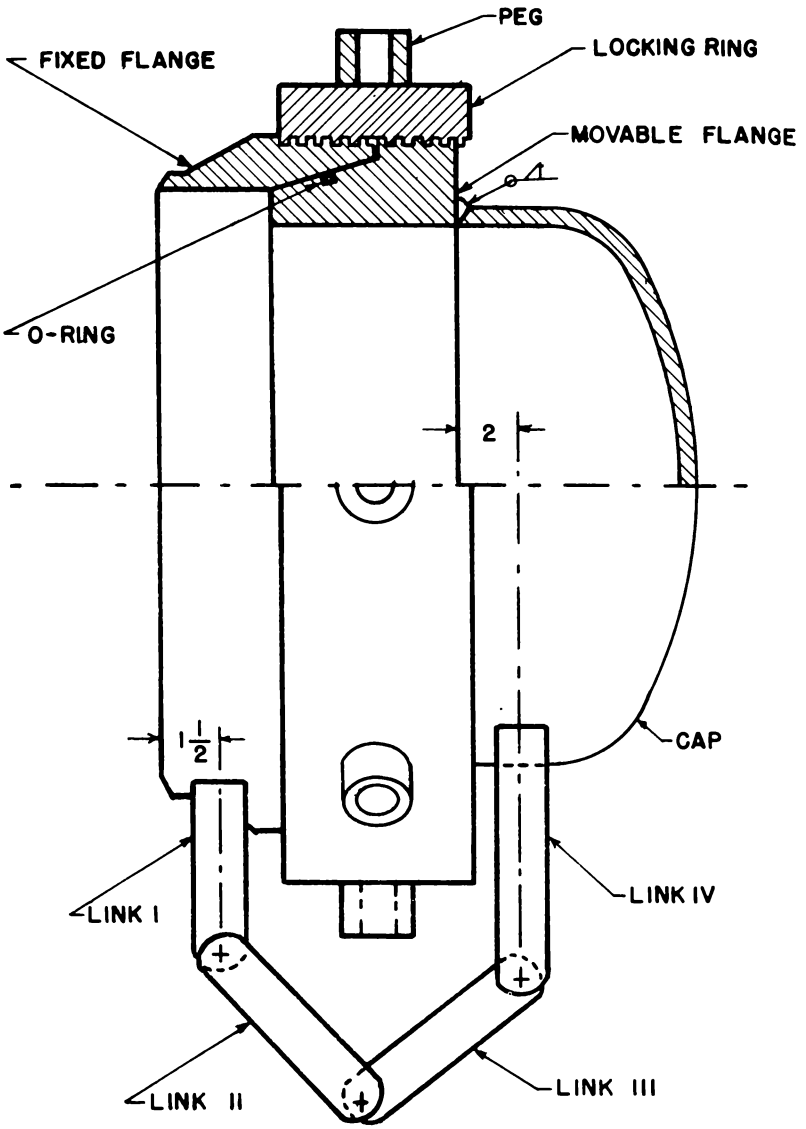

FIGURE 1—Closure Assembly.

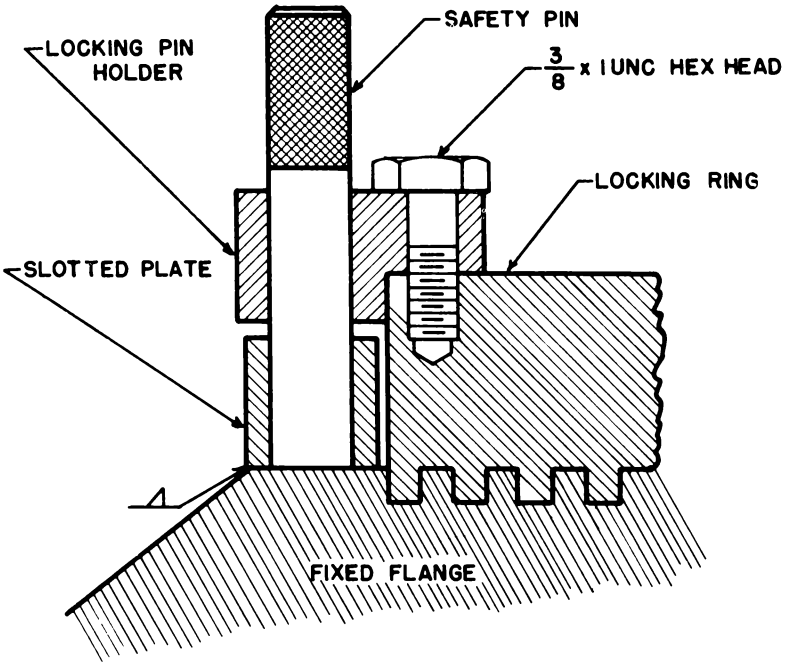

FIGURE 2—Locking Pin Assembly.

service pressure rating is 720 psi. This is well over the design of 600 psi. Thus, the specifications of the several parts are: fixed flange of 300 psi, 18 in. outside diameter, weld-neck flange; movable flange of 300 psi, 16 in. outside diameter weld-neck flange; cap 16 in. outside diameter; extra strong weld capacity. The external ring is custom made with a 23 in. outside diameter and a 20 in. inside diameter. The material for all these parts has been selected as A-105 forged steel grade II.

ANALYSIS

The components of the closure are, as it has been stated, modified commercially available parts. This presents the advantage of conforming the code specifications for pressurized containers (4) adopted by the state of North Dakota, since these parts have been fabricated according to standards accepted by the code. The main problem then is the determination of the stress concentration factor occurring on the threads as a result of the axial force produced by the inner pressure.

The problem is a three dimensional one (5), but a good approach could be reached by means of a two-dimensional analysis (6). Models of the 10° and 29° Acme thread were made in two dimensions using ¼ in. thick Homalite CR-39 as a photoelastic material. The Acme thread has been selected as the type of thread to be used in this joint due to its advantages in transmitting heavy forces (7). The two models were cut to close shape with an electric jigsaw and the final profile was developed by hand filing. Once adjustment of the thread profile was achieved, the two models were loaded using the frame load of the polariscope (Figures 3 and 4). The applied load was measured and photographs of the isochromatics, which are the loci of points of equal maximum shear, were taken (Figure 4). Fom the analysis of the photographs it is found that the maximum fringe numbers are: 4 for the 10° Acme thread, and 4.5 for the 29° Acme thread. The maximum fringe numbers occur at the inner

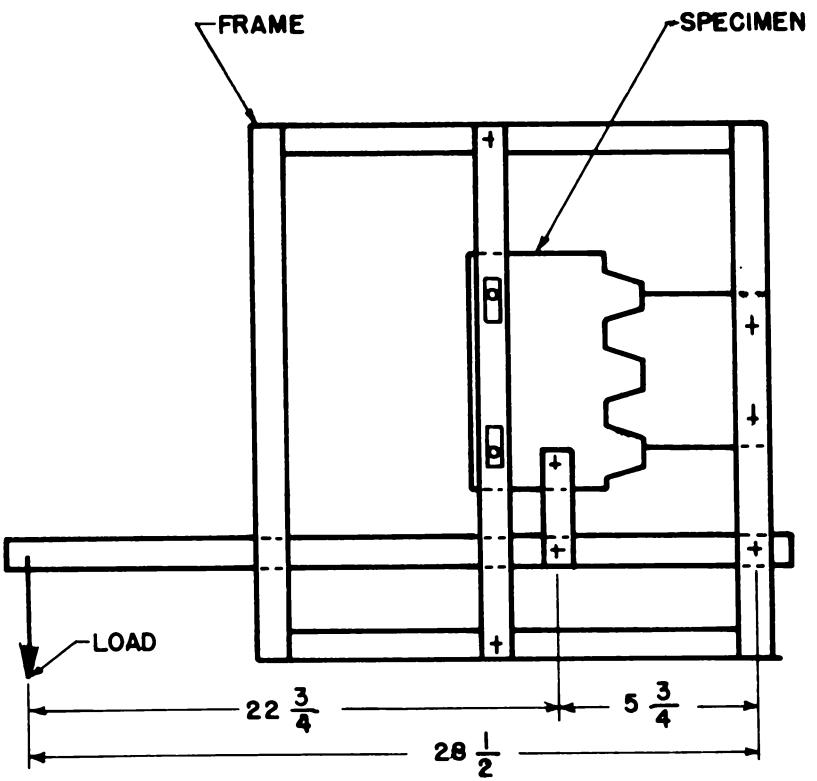

FIGURE 3—Sketch of Loading Frame.

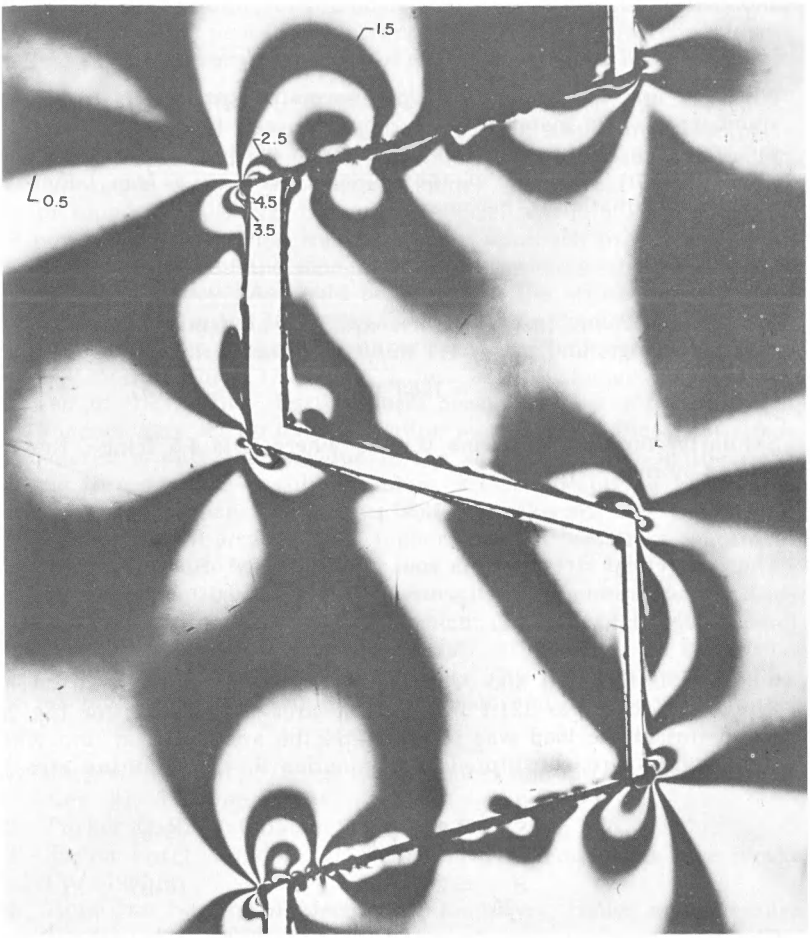

FIGURE 4—Isochromatic, 29° Acme, Light Field.

corners of the thread. Measurements of the roots of the threads were taken in order to obtain the area subjected to stresses, with the following results:

$$A_{10^\circ} = 0.52 \text{ sq. in.}$$

$$A_{29^\circ} = 0.616 \text{ sq. in.}$$

The stress-optic law is given by (8)

$$\sigma_p - \sigma_q = \frac{nf}{h} \qquad (1)$$

where σ_p and σ_q are the principle normal stresses, n is the fringe number, f is the material fringe constant, and h is the thickness of the specimen in the direction of the path of light. Since the stress concentrations occurred at the thread's root on a free boundary, $\sigma_q = 0$ and equation 1, becomes:

$$\sigma_p = \frac{nf}{h} \qquad (2)$$

For the 10° Acme thread with n equal to 4.0 fringes, f is 75.3 psi-inch per fringe, and h is 0.245 in., the normal stress is

$$\sigma_{p_{10^\circ}} = 1260 \text{ psi} \qquad (3)$$

Similarly, for the 29° Acme thread, where n is 4.5 fringe, the resulting normal stress is

$$\sigma_{p_{29^\circ}} = 1380 \text{ psi.} \qquad (4)$$

The theoretical stress at the root of the thread, S, is given by

$$S = \frac{P}{A} \qquad (5)$$

where P is the load and A is the related area. For the 10° Acme thread the load was 121.1 lbs. and the area 0.52 sq. in.; for the 29° Acme thread the load was 160 lbs. and the area 0.616 sq. in.; when these values are substituted into equation 5, the resulting stresses are

$$S_{10^\circ} = 233 \text{ psi.} \qquad (6\text{-a})$$

$$S_{29^\circ} = 260 \text{ psi.} \qquad (6\text{-b})$$

The stress concentration factor, SCF, is defined to be the quotient of the actual stress divided by the theoretical stress. Thus, the resulting stress concentration factors are:

$$SCF_{10^\circ} = 5.4 \qquad (7\text{-a})$$

$$SCF_{29^\circ} = 5.31 \qquad (7\text{-b})$$

From the results obtained it is noted that only a slight difference exists between the two stress concentration factors. Since the ma-

chinability of both threads is comparable, the 29° Acme thread was exists between the two stress concentration factors. Since the machosen. With a slight modification of the nut, an Acme centralizing thread is obtained that prevents wedging upon the flange. This will eliminate the possibility of the door being locked due to the frictional forces. Once the stress concentration factor is known, the dimensioning of the threads and parts of the closure could be done.

RESULTS AND CONCLUSIONS

The value of the stress concentration factor found in this experiment is greater than the value determined for American Whitworth threads using a three dimensional model. The stress concentration factor found in the three dimensional model was 3.75. It should also be noted that the loading conditions only approach in a limited way the actual loading of the model. This inaccuracy could lead to such a high descrepancy. As could be expected, the stress concentration factor is greater in the 10° Acme thread than in the 29° Acme thread. This is mainly due to greater inclination of the flanks of the thread in the 29° series which results in a less abrupt change in the cross section of the profile. Furthermore, because of the form in which the models were set up for the loading purposes, the theortical stress considered is only the one due to the shear occurring in the roots of the threads. The possible bending stresses, occurring because of the extended dimension of the thread teeth, are not considered. This, in turn, will also induce a higher value of the stress concentration factor, because of the way it was defined.

As for the construction of the closure itself, machining and threading the flanges poses the major problem. However, the Mechanical Engineering Shop at the University has, at present, on loan from the Navy, a 36-inch vertical turret lathe. This tool has the capability to machine the large parts to the precision and dimensions required.

REFERENCES

1. Jorgensen, S. M., "Design for Closures and Steel Joints," Mech. Eng. 91, 6 (June, 1969).
2. Parker O-Ring, Catalog OR 5700, Tech. Syn. Co. (1967).
3. Taylor Forge, Catalog 571, 3rd ed., Taylor Forge and Pipe Works Co. (1961).
4. American Society of Mechanical Engineers, Boiler and Pressure Vessel Code, (1956).
5. Hetenyi, M., "A Photoelastic Study of Bolt and Nut Fastening", Trans. ASME, 65, A-93, (1943).
6. Durelli, A. J. and Riley, W. F., "Introduction to Photomechanics", Prentice Hall Inc., Englewood Cliffs, N.J., 1965.
7. Black, P. H. and Adams, Jr., O. E., "Machine Design", 3rd ed., McGraw Hill Book Company, Inc., 1968.
8. Dally, J. W. and Riley, W. F., "Experimental Stress Analysis, McGraw Hill Book Company, Inc., 1965.

AN ANKLE EXERCISER FOLLOWING NATURAL FOOT MOTION

Don V. Mathsen

Department of Mechanical Engineering

University of North Dakota, Grand Forks, North Dakota 58201

INTRODUCTION

Proper exercising of the muscles to produce motion about a particular joint requires movement through the joint which coincides with the natural articulation. The articulations which occur in the joints of the human body, however, are often very intricate and difficult to reproduce mechanically. This paper discusses the development of an exerciser which approximates the natural articulation of the foot about the ankle joint.

There are two axes which the foot rotates to produce its range of motion. The most obvious and definable axis is found in the ankle itself. The other axis is formed within the foot and is not as easily recognized.

The ankle joint is formed by the box-like structure created by the extensions of the tibia and fibula, the major bones of the lower leg (1). Within this structure slides the curved portion of the talus, the keystone of the foot's arch. This sliding action produces a single hinge effect in the ankle (2). Dorsiflexion, the raising of the toes away from the leg, articulates through 35°. Only dorsiflexion and plantar flexion are produced in the ankle (Figure 1).

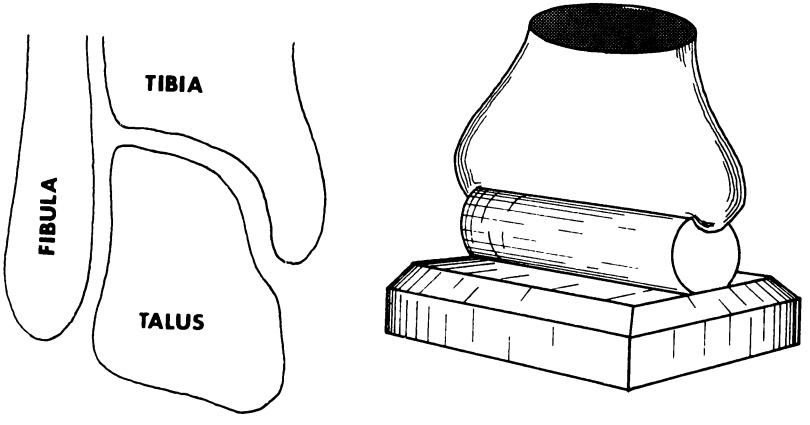

FIGURE 1—Ankle joint and mechanical model.

The axis within the foot is difficult to describe. The foot is composed of three sets of bones: phalanges, metatarsals, and tarsals. The phalanges, or toes, are not involved in this axis. The five long metatarsals form the forward half of the arch and are connected by tendons to the seven metatarsals which compose the upper and back segments of the arch. The tarsals are shaped to allow smooth, relative motion among themselves (1). It is this relative motion which permits the turning in (inversion) and the turning out (eversion) of the toes. During inversion and eversion, only the portion of the foot ahead of the ankle is displaced. As the toes are turned in and out, the axis actually changes within the tarsals. An attempt to model (Figure 2) the articulation was made. The metatarsals rotate about an axis extending along the length of the foot and pivoting at a point below the ankle.

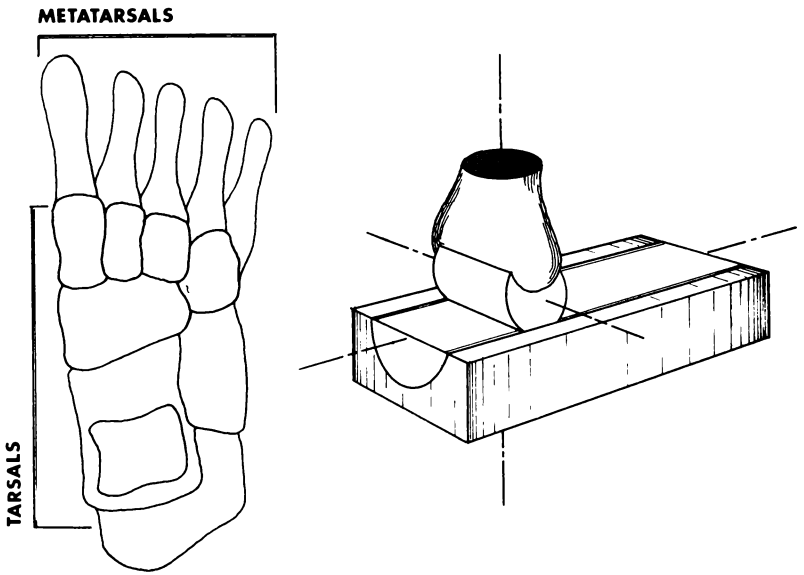

FIGURE 2—Internal foot joint and mechanical model.

EXISTING ANKLE EXERCISERS

The operation of most of the ankle exercisers in use today is the same. They consist of a foot plate onto which the patient's shoe is strapped. At each end and to each side of the foot plate, weights may be added to permit loading of the exerciser. Dorsiflexion and plantar flexion are accomplished by rotating the foot about an axis perpendicular to the length of the foot and placed under the foot plate beneath the arch of the foot. With this construction, a moment

arm exists between the long, vertical axis of the leg and the horizontal axis on which the foot plate rests. A vertical force through the lower leg may couple with the moment arm to provide the torque necessary to operate the exerciser. In this case, the muscles of the thigh and hip are employed instead of the lower leg muscles which are solely responsible for the foot's articulations. Inversion and eversion are performed by turning the entire foot about an axis beneath and parallel to the length of the foot plate. As a result, the talus is made to twist against the extensions of the tibia and fibula. Since no motion is allowed in this direction, the entire leg is forced to rotate. Again, a vertical force in the lower leg will operate the device. In addition, the patient's shoe prevents relative motion within the tarsals and metatarsals.

DESIGN

From the study of the anatomy of the foot and the existing devices, design criteria were established. The new exerciser should include two basic assemblies: a mechanism which permits natural foot motion and a method of force application capable of resisting the natural motion. The foot should be free to articulate during exercise to give proper dorsiflexion and plantar flexion and also enable natural inversion and eversion. The resisting force should be adjustable to meet the individual patient's needs and remain constant throughout the range of motion. In addition, the adjustments in resisting force should be under the control of the patient.

Achieving natural foot motion.—The foot plate on this exerciser (Figure 3) consists of two segments and the patient operates the device without wearing his shoe. One section of the foot plate supports the heel whereas the other forms a pedal to which the metatarsals and phalanges are held by a rubber strap.

To attain proper dorsiflexion and plantar flexion, the foot was made to rotate about an axis which coincided with the hinge joint of the ankle. The heel plate was therefore suspended 3 in. from the axis about which it pivots. This distance is the perpendicular distance between the ankle joint and the bottom of most adult feet. This requires all motion to be performed by the lower leg muscles, since no moment arm may be formed between the leg and the pivot.

To approximate inversion and eversion, the forefoot pedal was mounted on a shaft which is free to rotate about its own longitudinal axis. The shaft itself may pivot about a point under the heel plate. This arrangement resembles the mechanical model of inversion and eversion.

Force application. — As mentioned previously, it was desired to maintain a constant resistance through the range of motion. In addition, the patient, or operator, should be able to change the loading without removing his foot from the exerciser.

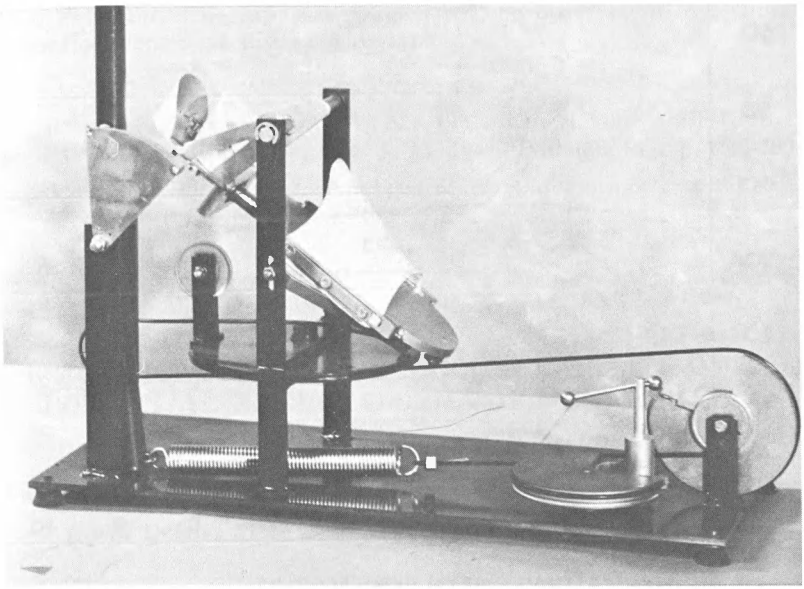

FIGURE 3—New ankle exerciser.

The selected design consisted of a tension spring attached to the foot plate with a cable. By trial and error, a point was found about which the cable could arc and produce an angle with the foot plate which decreased in a direct relationship to the displacement of the spring. As a result, the decreasing angle neutralized the extension of the spring to produce a force perpendicular to the plate which varied only slightly throughout the range of motion. A plot was made of the theoretical forces obtained from a system using three springs with constants of 2 lb/in, 5 lb/in, and 10 lb/in. As seen in Figure 4, a constant force could be approached throughout the range of motion for loads of 0 to 60 lbs. Instead of using three different springs, one spring was employed and three different con-

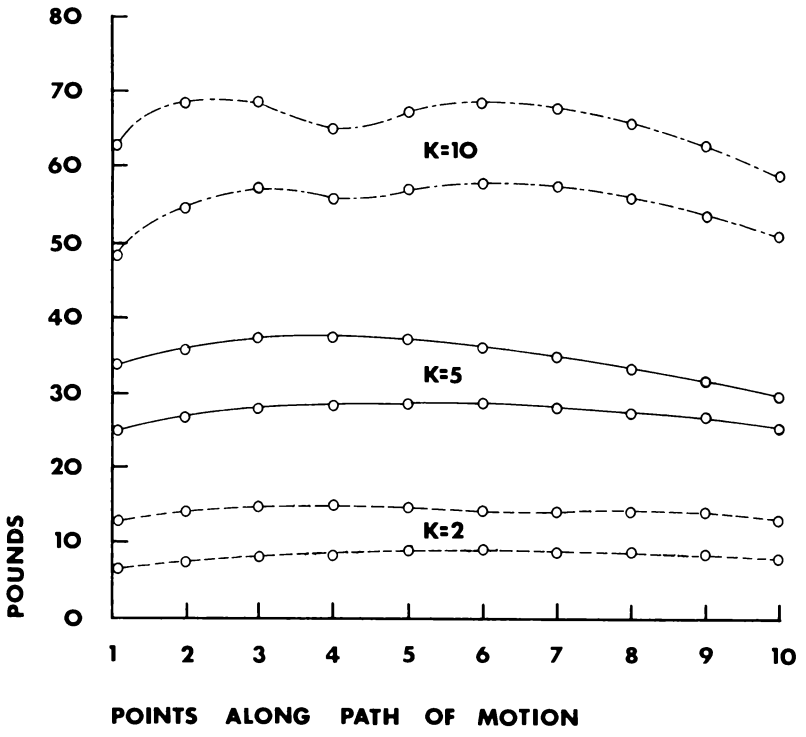

FIGURE 4—Theoretical force applied perpendicular to end of foot plate vs. positions along path of motion.

stants obtained by use of a stepped pully. A spring with the largest desired constant was attached by a cable to an arm which places the cable on the selected pulley. There are four pulleys together. The cable leading to the foot plate is fixed to run in the top pulley. The next pulley has the same diameter as the top one and utilizes the rated constant of the spring when engaged with the spring cable. The next two diameters are ½ and ⅕ that of the top two pulleys and produce spring rates of ½ and ⅕the rating of the spring. Therefore, a constant force is achieved (Figure 3).

The initial load of the spring may be changed by extending the end of the spring not attached to the cable. This is accomplished by an arm which the patient or therapist may adjust.

SUMMARY

This exerciser does not exactly duplicate natural foot motion. The principles incorporated in its design, however, do enable an approximation of the desired articulations. As of this writing, the exerciser has not been sufficiently tested in actual use. The device will be used in the University of North Dakota Medical Rehabilitation Center. Patients will be exercised on the existing device and the new exerciser. The progress of each will be observed to determine the effectiveness of this new design.

REFERENCES

1. Rasch, P. J. and Burk, R. K., 1963. Kinesiology and Applied Anatomy, 2nd Edition, Sea & Febiger, Philadelphia, p. 298-299.

2. Scott, M. Gladys, 1963. Analysis of Human Motion, 2nd Edition, Meredith Publishing Co., New York, p. 41-42.

PRECESSION OF NEARLY CIRCULAR ORBITS DUE TO POTENTIAL ENERGY TERMS OF THE FORM c/r^n

Kingsley A. Bowles and Paul Ross

Department of Physics

North Dakota State University, Fargo, North Dakota 58102

ABSTRACT

It is shown that if the interaction potential energy of two particles is given by

$$V = -\frac{k}{r} + \frac{c}{r^n}$$

the rate of precession is

$$\frac{\Delta\theta}{T} = -\frac{n(n-1)c}{2\ell a^n}$$

provided the orbits are nearly circular. The unexplained precession of Mercury recently reported by Dicke and Goldenberg of 3.4 seconds of arc per century corresponds to a ratio of perturbing to inverse square force given by $1.3 \times 10^{-}/(n-1)$.

INTRODUCTION

Only in rare cases are the orbits of bodies moving in central force fields closed. In general the situation is similar to that shown in Figure 1.

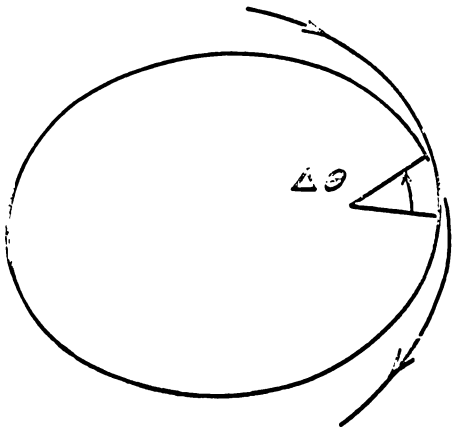

FIGURE 1—Precession of an orbit.

It is well know that a slight departure from a true inverse square force will produce orbital precession. We will write the interaction potential as

$$V = -\frac{1}{r} + \frac{c}{r^n}$$

The first term gives the usual inverse square force and the second is a small perturbation. The symbol n may represent any number, not necessarily an integer. The question of long term stability of such orbits will not be discussed. The above problem can be solved exactly for the case n = 2 (1). The objective of this paper is to produce a formula for the rate of orbital precession for general values of n. It will be necessary to assume nearly circular orbits.

Orbital precession applies to all central force motion including electronic and planetary orbits. For an illustrative example we will use the well-known case of the precession of the perihelion of Mercury but the reader should bear in mind that the argument is not restricted to the planet Mercury.

METHODS

The Lagrangian for this problem is

$$L = \tfrac{1}{2}m(\dot{r}^2 + \dot{\theta}^2 r^2 \sin^2\varphi + r^2\dot{\varphi}^2) + \frac{k}{r} - \frac{c}{r^n}$$

where m is the reduced mass of the system; r, θ, φ, are the usual spherical polar coordinates; and the dot represents differentiation with respect to time.

Conservation of angular momentum implies that the motion lies in a plane. The coordinate system can be oriented, without loss of generality, such that the polar axis is perpendicular to this plane of motion making $\phi = 90°$ and $\dot{\phi} = 0$.

The first Lagrange equation integrates readily to

$$mr^2\dot{\theta} = \ell$$

where ℓ is the orbital angular momentum.

With θ eliminated. the second Lagrange equation is:

$$m\ddot{r} = -\frac{k}{r^2} + \frac{nc}{r^{n+1}} + \frac{\ell^2}{mr^3}$$

This equation cannot be integrated in closed form except for certain specific values of n (2, 3). However, it can be intergrated for general n if the orbits are nearly circular. Let $r = a(1+\delta)$ where δ is some small variable and a is the radius of the circular orbit which has angular momentum ℓ .

The differential equation for δ becomes

$$\ddot{\delta} + \left(-\frac{2k}{ma^3} + \frac{n(n+1)}{ma^{n+2}}\, c + \frac{3\ell^2}{m^2a^4}\right)\delta = 0$$

which is the well-known equation for simple harmonic motion. A suitable solution is

$$\delta = \delta_o \cos\, \omega t$$

where

$$\omega^2 = \frac{\ell^2}{m^2a^4} + \frac{n(n-1)}{ma^{n+2}}\, c \ .$$

The period of the motion of r is

$$T = \frac{2\pi}{\omega} = 2\pi\left(\frac{\ell^2}{m^2a^4} + \frac{n(n-1)}{ma^{n+2}}\, c\right)^{-\frac{1}{2}} \ .$$

During this time r returns to its original value and θ increases by an amount θ_1 which must be nearly 2π radians.

θ_1 is calculated as follows: Putting $y = \omega t$ in the integral of the first Lagrange equation gives

$$\omega\frac{d\theta}{dy} = \frac{\ell}{ma^2(1+\delta_o\cos\, y)^2}$$

$$\theta_1 = \frac{1}{\omega}\int_0^{2\pi}\frac{\ell\, dy}{ma^2(1+\delta_o\cos\, y)^2}$$

$$\simeq \frac{2\pi\ell}{m\omega a^2} \ .$$

The precession is

$$\Delta\theta = \theta_1 - 2\pi = \frac{2\pi}{\omega}\left(\frac{\ell}{ma^2} - \omega\right) .$$

The rate of precession is

$$\frac{\Delta\theta}{T} = \frac{\ell}{ma^2} - \omega$$

$$\simeq - \frac{n(n-1)c}{2\ell a^n} .$$

This is the general formula for the rate of precession of a nearly circular orbit by a small perturbing force. Precession for many specific forces is discussed in the literature, but, to our knowledge, the above general formula is not given elsewhere.

APPLICATION

Most of the precession of the perihelion of Mercury is due to the effects of other planets (4-6). The remaining precession is 43 seconds of arc per century (0.10 seconds in each cycle). General relativity predicts 43 seconds/century (7). Dicke and Goldenberg (8) find a quadrupole moment of the sun which accounts for 3.4 seconds/century. This leaves a precession of -3.4 seconds/century to be accounted for if Dicke and Goldenberg are correct. Possible explanations include a scalar-tensor theory of gravitation (9-11) or a slight departure from a true inverse square relationship for the gravitational force.

An estimate of the required perturbing force may be made as follows:

The first Lagrange equation may be written as

$$\ell = 2m\dot{A}$$

where A is the constant rate of sweeping out of area by the radius vector. For circular orbits $A = \pi a^2/T$. Kepler's third law gives

$$a^3 = \frac{T^2}{4\pi^2}\frac{k}{m} .$$

The rate of precession can be written

$$\frac{\Delta\theta}{T} = - \frac{\pi\, n(n-1)c}{k\, a^{n-1}\, T} = - \frac{\pi\ (n-1)}{T}\ \eta$$

where

$$\eta = \frac{nc}{ka^{n-1}}$$

is the strength of the perturbing force relative to the usual inverse square force at the position of the planet.

For Mercury the unexplained precession corresponds to

$$\eta = \frac{1.3 \times 10^{-8}}{n-1} .$$

It is obvious that the Dicke-Goldenberg data can be explained by a very small perturbing force with a large value of n. Such a force could be arbitrarily small on an astronomical scale but the question of why no such force operates on the laboratory scale would then have to be answered.

As a check on the validity of the approximations made in the above treatment this result was compared to the exact result for Mercury in the case n = 2. This can be computed exactly for elliptical orbits of large eccentricity requiring only that the precession rate be small (1). For Mercury the exact formula requires a force 6% smaller than the above.

REFERENCES

1. H. Goldstein. "Classical Mechanics, (Addison-Wesley Publishing Co., Reading, Mass., 1950) p. 91.
2. H. Goldstein, op. cit, p. 71-76.
3. E. T. Whittaker, "Analytical Dynamics of Particles and Rigid Bodies". (Cambridge University Press, London, 1937) p. 80-86.
4. S. Newcomb, in the "American Ephemeris and Nautical Almanac", 1897 (U.S. Government Printing Office, Washington, D.C., 1896) Supplement.
5. G. M. Clemence, Revs. Modern Physics *19*, 361 (1947).
6. R. L. Dunscombe, Astron. J. *61*, 174 (1956).
7. G. M. Clemence, "Mercury (planet)", Astronomical papers prepared for the use of American Ephemeris and Nautical Almanac, Vol. 11, Pt. 1 (U.S. Government Printing Office, Washington, D. C., 1943).
8. R. H. Dicke and H. M. Goldenberg, Phys. Rev. Letters *18*, 313, (1967).
9. P. Jordan, Astron. Nachr. *276* 193 (1948).
10. C. Brans and R. H. Dicke, Phys. Rev. *124* (1961).
11. R. H. Dicke, Phys. Rev. *125* 2163 (1962).

THE SUBARACHNOID SPACE INTERPRETED AS A SPECIAL PORTION OF THE CONNECTIVE TISSUE SPACE[1]

Richard G. Frederickson[2] and Frederick R. Haller[3]

Department of Anatomy, School of Medicine

University of North Dakota, Grand Forks, North Dakota 58201

First Place Winner A. Roger Denison Student Research Competition

INTRODUCTION

The brain and spinal cord are bathed on their inner and outer surfaces by a fluid that is little more than an "ideal physiological saline" (1). On the exterior this fluid, the cerebrospinal fluid, permeates an area known as the "subarachnoid space". The space is customarily interpreted as a special epithelial-lined cavity similar to the coelomic cavities (2,3). However, according to recent studies in fine structure, the cells involved more closely resemble those of connective tissue (4,5). It seems proper, therefore, to present an evaluation of the subarachnoid space in respect to a fine structural classification of its lining components, the leptomeninges. It will be shown below than an interpretation of the subarachnoid space as a modified portion of the general tissue space is a natural result of such an analysis.

Previous investigations on the ultrastructure of this area involve methods of preparation that do not readily maintain proper integrity of tissues (6-9). However, perfusion with buffered aldehydes (10) produces rapid fixation prior to mechanical disturbances of dissection. Moreover, perfusion allows fixation at fluid pressures approaching normal physiological values. Therefore, the subarachnoid space does not collapse as with conventional immersion techniques.

Various divisions of the subarachnoid space emphasized in this study include the pia mater, arachnoid trabeculae, adventitia of blood vessels, nerve root sheath and arachnoid membrane. Each of these structures possesses leptomeningeal elements bordering directly on the subarachnoid space.

MATERIALS AND METHODS

Twenty-three albino rats (Sprague-Dawley strain) were perfused with buffered aldehydes (11) according to the technique of Rosen *et al.* (10). Procaine hydrochloride (0.1%) added to the washout solution (12) prevented vasoconstriction and permitted rapid flow of fixative through the circulatory system. The aldehyde solutions

[1]Supported by grant HE-09041, United States Public Health Service.
[2]National Science Foundation Trainee, No. 1-F1-GM-29, 120-01.
[3]National Defense Graduate Fellow, No. 67-08841.

were administered either by a cannula inserted through the left ventricle and into the aorta or by a large-gauge (#15, 18) hypodermic needle introduced directly into the ventricle.

The brain of each rat was exposed by careful dissection of bone and soft tissue. The dura was peeled off laterally and connections with the falx cerebri and tentorium cerebelli were severed with scissors. The brain was then lifted slowly from the basal surface of the cranial vault while simultaneously transecting nerves and blood vessels when exposed. Nervous tissue with accompanying pia and arachnoid was taken from the region of the cerebral cortex.

To obtain nerve roots and spinal meninges laminectomy was performed and a midline incision was made through the meninges, spinal cord and vertebral bodies so that the vertebral column was divided in half. With surgical needles the dorsal and ventral roots were severed at the junction with the spinal cord, which was then removed. The dura-arachnoid was cut cephalic and caudal to each set of nerve roots and was freed from its ventral connections with the vertebrae. The nerve roots were cut within the vertebral foramina and the dissected tissue, consisting of meninges and associated dorsal and ventral nerve roots, was pulled free.

Tissues for electron microscopy were post-fixed one hour in 2% OsO_4 buffered with sodium cacodylate (11). Specimens were dehydrated in a graded series of alcohols and embedded in Epon 812 (13). Thin sections were cut on the Porter-Blum MT-2 ultramicrotome and mounted on Fullam 200 mesh grids. Sections were stained with lead citrate and uranyl acetate (14) and viewed in a Philips EM-200 electron microscope.

OBSERVATIONS

Leptomeningeal cells and associated connective tissue fibrils appear as interconnecting strands of thin cytoplasmic processes and closely related bundles of unit collagen (Figure 1). These cells and fibrils together form the outer and inner boundaries of the subarachnoid space as well as the coverings of blood vessels and nerves traversing this region. The cellular elements of the leptomeninges form a discontinuous layer of cytoplasmic processes lining the immediate area, which in life is filled with cerebrospinal fluid. Connective tissue fibrils appear free in the subarachnoid space but more often are separated from it by a layer of leptomeningeal cells. Both unit collagen fibrils and elastic fibers are present. Also, certain specialized macrophages are present in association with the lining cells. These relationships will be described in more detail in the following sections..

Pia Mater. — the pia lies irregularly on a glial boundary membrane which forms the outer margin of brain and spinal cord (Figures 1-6). This portion of the leptomeninges includes a thin layer of

cellular processes separated from the boundary membrane by various amounts of connective tissue fibrils. The processes form gaps between adjacent cells, allowing communication of the subarachnoid space with the area of connective tissue fibrils (Figure 2). Typical collagen fibrils may appear in these gaps or free in the subarachnoid space (Figure 4).

The fine structure of pial cells is characteristic of all leptomeningeal cells, with a few exceptions. They possess no boundary membranes and their attenuated processes contain small, random distributions of rough endoplasmic reticulum, mitochodria, vacuoles, cytoplasmic filaments and a few lysosomes. Most of these organelles occur in the cell where there are large amounts of cytoplasm, such as near the nucleus (Figure 3). The nuclei are usually elongated and light staining except for a thin dense chromatin lamina near the nuclear envelope (Figures 1, 3, 5, 6,). Processes extend in many directions from the cell body and are commonly less than 0.2μ in width at their extremities. Occasionally certain modified pial cells are observed (Figure 1). These cells contain increased amounts of cytoplasm and have characteristically numerous cytoplasmic vacuoles, in addition to large, lobulated nuclei. Indeed, cells identified as true macrophages are often seen (Figures 4, 5), especially in the fibrillar region between glial boundary membrane and pial cells. These macrophages are described below.

Arachnoid trabeculae. — Cytoplasmic extensions of pial cells are often lifted away from the brain surface and, together with enclosed unit collagen fibrils, contribute to the formation of arachnoid trabeculae (Figures 6-9). These trabecular cells possess the cytological characteristics described for pial cells. In a single trabecula bundles of unit collagen fibrils may be incompletely enclosed by leptomeningeal cells, permitting open communication between the fibrillar area and the subarachnoid space (Figure 1). Some cellular processes appear to have no associated fibrils (Figures 1, 9). Cross-sectional diameters of trabeculae vary considerably. Figure 8 illustrates the typical fibrillar contents of a trabecula.

Macrophages are seen in trabeculae also (Figures 7, 9). In many cases they may form an integral part of the trabecular wall (Figure 7). These phagocytes tend to be ovoid in shape with extremely lobulated nuclei and only a few blunt cytoplasmic processes (Figure 9). The cytoplasm is densely populated with membrane-bound vacuoles, especially near the periphery of the cell. Small, short flaps of cytoplasm are seen projecting out from the surface and some seem to have recently fused with an adjacent area of the cell. This gives the impression of intense active phagocytosis. The cells possess a a large amount of lysosomal material and the lysosomes are seen in various stages of organization (Figures 4, 5, 13, 15, 16).

Adventita of blood vessels. — Processes from both pia and

arachnoid trabeculae are continuous with the adventitia of blood vessels (Figures 10, 11). Leptomeningeal cells here form an incomplete outer sheath for the vessels. Small gaps exist between adjacent cells and collagen fibrils may be seen occupying thse positions (Figure 10). Cytological features of adventitial cells are similar to those already described for leptomeninges in general. Interposed in the adventitial wall are macrophages similar to those also described earlier.

Occasionally a macrophage appears to be in process of migration between the adventitial wall and the free subarachnoid space (Figure 13). At the point where a vein is leaving the nervous tissue (or an artery is entering) the adventitia is directly continuous with the pia without forming a "perivascular space" (Figure 11).

Arachnoid Membrane. — The arachnoid membrane, forming the outer margin of the subarachnoid space, features a multilayered barrier of cellular processes continuous with the cells previously described (pia, trabeculae and adventitia) (Figures 14-16). The cells of the arachnoid also resemble the previously described lining cells. However, special characteristics are present. The most conspicuous feature is a relatively large number of rod-shaped mitochondria randomly dispersed throughout the cytoplasm (Figures 14, 16). Interdigitation of numerous, loosely-arranged cell processes form restricted lacunae which may or may not be filled with various connective tissue fibrils (Figure 14). In some instances the lacunae containing fibrils are directly continuous with the arachnoid trabeculae. Another feature is the presence of macrophages. Some may be found adherent to the arachnoid cells and others appear to be free in the subarachnoid space (Figures 15, 16). The macrophages are typical in appearance, containing extremely lobulated nuclei, large numbers of vacuoles of various sizes, and many lysosomes.

The arachnoid membrane is separated from the dura in most areas by specialized cells and an amorphous intercellular material. In certain experiments where dura is peeled away from the adjacent arachnoid (see Materials and Methods) the plane of cleavage occurs within the cytoplasmic compartment of this so-called "neurothelium" (15). When cleavage occurs, the plasmalemma of the "neurothelial" cell is usually left adhering to an adjacent plasmalemma (Figures 15, 16).

Root sheath. — The root sheath is composed of two to twelve flattened layers of cells (Figures 17-20). The layers adjacent to the subarachnoid space are often dark and contain many cytoplasmic organelles including mitochondria, rough endoplasmic reticulum and Golgi complex (Figure 17). Thick, rounded cell processes which may contain vacuoles and lysosomes are present between the superficial flattened layers (Figure 19). These outer layers are joined by apparent punctate junctions which allow the subarachnoid space

free communication with the root sheath intercellular spaces (Figures 18, 20). In Figure 20 a rounded cell process with vacuoles and lysosomes is associated with these outer cells. Lacunae are formed by the cells and in most cases are filled with connective tissue fibrils (Figure 18). The deepest cell layers are usually lighter than the superficial layers and contain few organelles but are highly vesicular (Figures 19, 20). Facing the endoneurium a boundary membrane is associated with the most basal layer.

DISCUSSION

The boundary membrane concept of ultrastructure (16) is useful for interpretation of the preceding observations. In this concept boundary membranes isolate the major cellular elements of the body (epithelium, nerve, muscle and fat) from the tissue space. This space is continuous throughout the vertebrate body no matter how complex the arrangement of tissues. Connective tissue elements (cells, extracellular fibrils and amorphous material) lie free within the tissue space and are not covered by boundary membranes. The cells may be "fixed," such as osteocytes, chondrocytes or fibrocytes or may be ameboid, such as wandering fibroblasts and macrophages. The extracellular materials (microfibrils, unit collagen, elastic fibers and certain amorphous material) are closely associated with the cells.

Fibrocytes are a prominent resident of the tissue space and, in the form of fibroblasts, play an important role in the production and maintenance of connective tissue. Porter (17) describes the fibrocyte as a cell with an oblong nucleus whose cytoplasm contains varying amounts of rough endoplasmic reticulum, polyribosomes and Golgi complex, randomly distributed. Extremely thin extensions of the cells are present among the extracellular components. Under inflammatory conditions it is suggested that the fibrocyte is capable of ameboid movement and can perform macrophagic activities (18).

Structural features of the subarachnoid space observed in this study illustrate an arrangement of cells and fibrils modified for special connective tissue function. Cytological characteristics of the cells lining this space resemble those seen in fibrocytes (17). They do not possess boundary membranes and have similar non-polarized distributions of rough endoplasmic reticulum, Golgi complex, cytoplasmic vacuoles, cytoplasmic filaments and lipid droplets. Also, contact between cells does not involve the junctional complexes described for various epithelia (19), but, like fibrocytes, involves small, button-like attachments between attenuated processes. On either side of these "punctate" junctions, the intercellular spaces may be quite large. Connective tissue fibrils are closely associated with all leptomeningeal cells. Bundles of fibrils are seen within lacunae, between cell layers or free in the subarachnoid space.

Macrophages appear throughout the subarachnoid space and

among the lining cells. They are closely associated with all regions described. In the pia and nerve root sheath macrophage processes are commonly found wedged in between cells. Also, macrophages are found within the adventitial walls of subarachnoid blood vessels and in some cases form parts of arachnoid trabeculae. Of particular significance is their relationship to the arachnoid membrane (described below). Characteristically, numerous vacuoles, which appear to form from small pseudopods, are located in the periphery of the cytoplasm. Lysosomes are abundant and some contain semi-digested debris. In addition, the presence of large, dark, lobulated nuclei indicates their potential mobility as phagocytes.

Studies of inflammation in the subarachnoid space suggest that one of the early reactions to noxious stimuli involves the transformation of pial and pia-arachnoid cells into active macrophages (4, 8). In the present study cells with characteristics intermediate between the fibrocyte-like cells, which constitute the leptomeninges, and the macrophages are seen, implying various stages of transformation. Recent studies indicate that such a process does not occur in the arachnoid membrane (4, 8). However, the present study shows the occurrence of numerous macrophages in this area. The apparent lack of phagocytic activity in arachnoid cells, described by other investigators, may result from their relative degree of metabolic specialization, indicated by the large number of mitochondria present. It is possible that most leptomeningeal cells are part of the reticuloendothelial system, each cell having a variable degree of phagocytic potential. Perhaps one of their prime functions is to clear the subarachnoid space of debris, thus insuring free passage of cerebrospinal fluid.

SUMMARY

It is shown in this study that the subarachnoid space is not lined by an epithelium. The cells are not associated with a boundary membrane and are not joined by "tight junctions". Rather, the subarachnoid space and its lining components meet the criteria for a tissue space and for connective tissue in general. This involves the following observations: (1) the subarachnoid space is continuous with recognized tissue space accompanying the vascular adventitia and also with intercellular spaces of the other lining cells; (2) connective tissue fibrils are conspicuous in all regions including the subarachnoid space proper; and (3) macrophages are present within all areas studied and appear to occur in all regions. Leptomeningeal cells themselves appear to transform into macrophages. The evidence presented indicates that the area under consideration is composed largely of connective tissue elements. The subarachnoid space, therefore, is best interpreted as a "cleared-out" or modified portion of the general tissue space.

ACKNOWLEDGMENTS

The authors express their appreciation to Dr. Frank N. Low, Hill Research Professor in Anatomy, for his guidance and critical evaluation of the manuscript.

REFERENCES

1. Woollam, D. H. M. and J. W. Miller, 1957 Observations on the production and circulation of the cerebrospinal fluid. In: Ciba Foundation Symposium on the cerebrospinal fluid, p. 124. Ed. by G. E. W. Wolstenholme and C. M. O'Connor, Little, Brown and Co., Boston.

2. Ham, A. W., 1969 Histology, 6th ed., pp. 517-519, J. B. Lippincott Co., Philadelphia.

3. Bloom, W. and D. W. Fawcett, 1968, A Textbook of Histology, 9th ed., pp. 347-350, W. B. Saunders Co., Philadelphia.

4. Waggener, J. D. and J. Beggs, 1967, The membranous coverings of neural tissues: an electron microscopy study. J. Neuropath. Exptl. Neurol., *26*:412-425.

5. Frederickson, R.G. and F. N. Low, 1969, Blood vessels and tissue space associated with the brain of the rat. Am. J. Anat., *125*: 123-146.

6. Pease, D. C. and R. L. Schultz, 1958, Electron microscopy of rat cranial meninges. Am. J. Anat., *102*:285-321.

7. Nelson, E., K. Blinzinger and H. Hager, 1961, Electron microscopic observations on the subarachnoid and perivascular spaces of the Syrian hamster brain. Neurology, *11*:285-295.

8. ———————————, 1962, An electron-microscope study of bacterial meningitis. Arch. Neurol., *6*:390-403.

9. Ramsey, H. J., 1965, Fine structure of the surface of the cerebral cortex of human brain. J. Cell Biol., *26*:323-333.

10. Rosen, W. C., C. R. Basom and L. L. Gunderson, 1967, A technique for the light microscopy of tissues fixed for fine structure. Anat. Rec., *158*:223-237.

11. Karnovsky, M. J., 1965, A formaldehyde fixative of high osmolality for use in electron microscopy. J. Cell Biol., *27*:137A.

12. Forssmann, W. G., G. Siegrist, L. Orci, L. Girardier, R. Pictet and C. Rouiller, 1967, Fixation par perfusion pour la microscopie électronique. Essai de généralisation. J. de Microscopie, *6*:279-304.

13. Luft, J. H., 1961, Improvements in epoxy resin embedding methods. J. Biophys. Biochem. Cytol., *9*:409-414.

14. Greenlee, T. K., R. Ross and J. L. Hartmann, 1966, The fine structure of elastic fibers. J. Cell Biol., *30*:59-71.

15. Andres, K. H., 1967, Uber die Feinstruktur der Arachnoidea und Dura mater von Mammalia. Z. Zellforsch., 79:272-295.

16. Low, F. N., 1964, A boundary membrance concept of ultrastructure applicable to the total organism. Proc. Third European Reg. Conf. on Electron Microscopy, Prague. Publishing House of the Czechoslovak Academy of Sciences, *B*:115-116.

17. Porter, K. R., 1964, Cell fine structure and bisoynthesis of intercellular macromolecules. Biophys. J., *4*:167-196.

18. Libansky, J., 1966, The source of mononculears at a site of inflammation. Blut, *13*:20-29.

19. Farquhar, M. G. and G. E. Palade, 1963, Junctional complexes in various epithelia. J. Cell Biol., *17*:375-412.

(Figures 1 through 20 on following Pages)

FIGURE 1—Subarachnoid space. The arachnoid membrance (A) is above and the pia (P) covering the brain (B) is below. A single trabecula traverses the space from upper left to lower right. Attached to the arachnoid is a large macrophage (M). Collagen fibrils (C) have free access to the subarachnoid space (large arrow) where discontinuities exist. X3,300.

FIGURE 2.—Pia mater. A glial boundary membrane (BM) closely adheres to the brain (B). Connective tissue fibrils (CF) separate it from the cellular pia (P) which is discontinuous at arrows. X18,000.

FIGURE 3—Pial cell. Various organelles are seen near the nucleus (N). These include mitochondria (M), Golgi complex (G), rough endoplasmic reticulum (ER), polyribosomes (PR), various sized vacuoles (V) and tubules (T). The nucleus is elongated with a dense outer rim. X11,000.

FIGURE 4—Pia mater. Collagen fibrils (C) appear free in subarachnoid space (S). A macrophage process (M) is interposed between the boundary membrane (BM) of the brain (B) and the cellular pia (P). Macrophage contains laminated lysosomes (L). X20,000.

FIGURE 5—Pia mater. A macrophage (M) in the fibrous layer of pia projects into the subarachnoid space (S) between two pial cells (P). The macrophage nucleus is more dense than the dark-rimmed pial nuclei. Numerous vacuoles (V) occur in the peripheral cytoplasm. X5,700.

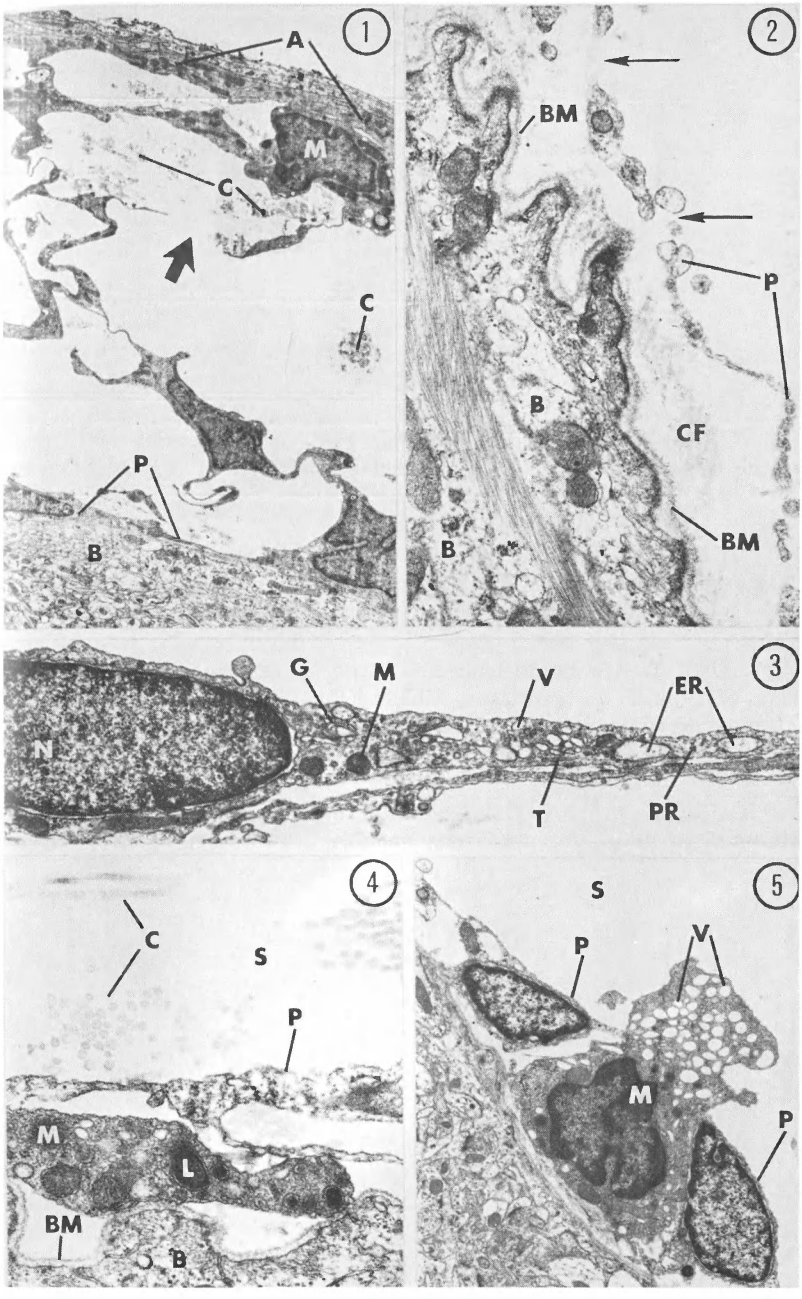
1
A
M
C
C
P
B
2
BM
P
B
CF
B
BM
3
G
M
V
ER
N
T
PR
4
C
S
P
M
L
BM
B
5
S
P
V
M
P

FIGURE 6—Arachnoid trabecula. Pial cell processes (P) contribute to trabecular wall, which encloses bundles of collagen fibrils (C). The brain (B) is present below. X5,900.

FIGURE 7—Arachnoid trabecula. The multilobulated nucleus (N) of this trabecular cell is similar to that of a macrophage. However, few vacuoles and no lysosomes are seen. X4,400.

FIGURE 8—Arachnoid trabecula. Interior of trabecula shows sections of typical unit collagen fibrils (C). Cells contain numerous cytoplasmic filaments (F). Two overlapping processes are separated by a punctate junction (arrows). X20,000.

FIGURE 9—Arachnoid trabecula. A macrophage (M) with multilobulated nucleus and numerous vacuoles (V) is represented. It is surrounded by trabecular cell processes (T). X6,100.

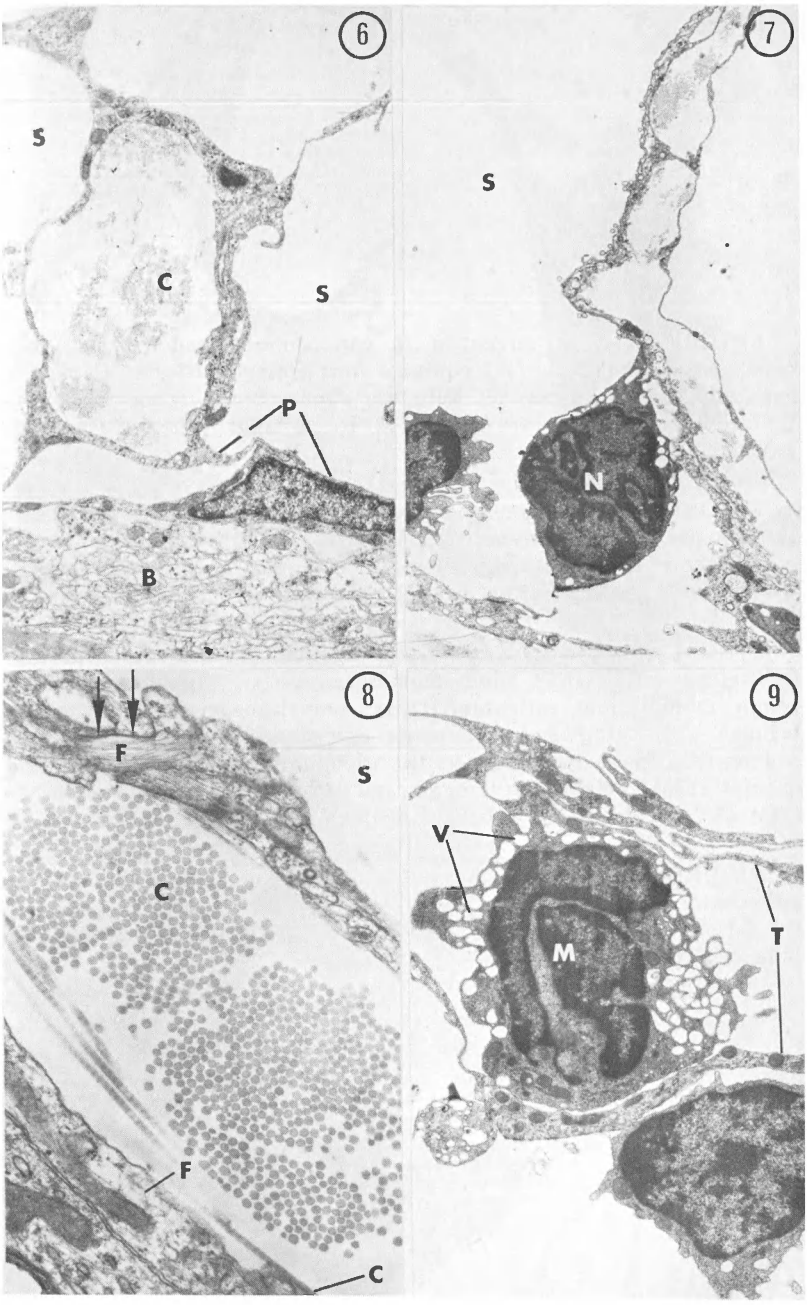
6
S
C
S
P
B
7
S
N
8
F
S
C
F
C
9
V
M
T

FIGURE 10—Vein, adventita. A gap (double-headed arrow) between adventitial cells (A) contains unit collagen fibrils (C) and a macrophage (M) in contact with the subarachnoid space (S). Two endothelial cells (E) are separated by a tight junction (arrow). X4,300.

FIGURE 11—Pia mater and adventitia of vein. Cellular processes of both pia (P) and adventitia (A) form a continuous layer at the point where a vein leaves the brain (B). Here the subarachnoid space (S) is excluded from around the blood vessel. X8,300.

FIGURE 12—Vein, adventitia. A cellular process (A) separates fibrous adventitia from subarachnoid space (S). Mitochondria (M), rough endoplasmic reticulum (ER), polyribsosomes (PR), microtubules (T), cytoplasmic filaments and a few lysosomes (L) are randomly dispersed throughout the cytoplasm. Note the large lipid droplet (LD). A boundary membrane (BM) separates the endothelium (E) from connective tissue fibrils of the adventitia. X20,000.

FIGURE 13—Vein, adventitia. A macrophage forms part of the adventitial wall and projects into the subarachnoid space (S). Notice the large extremely lobulated nucleus (N). Lysosomes (L) and vacuoles are numerous. X13,000.

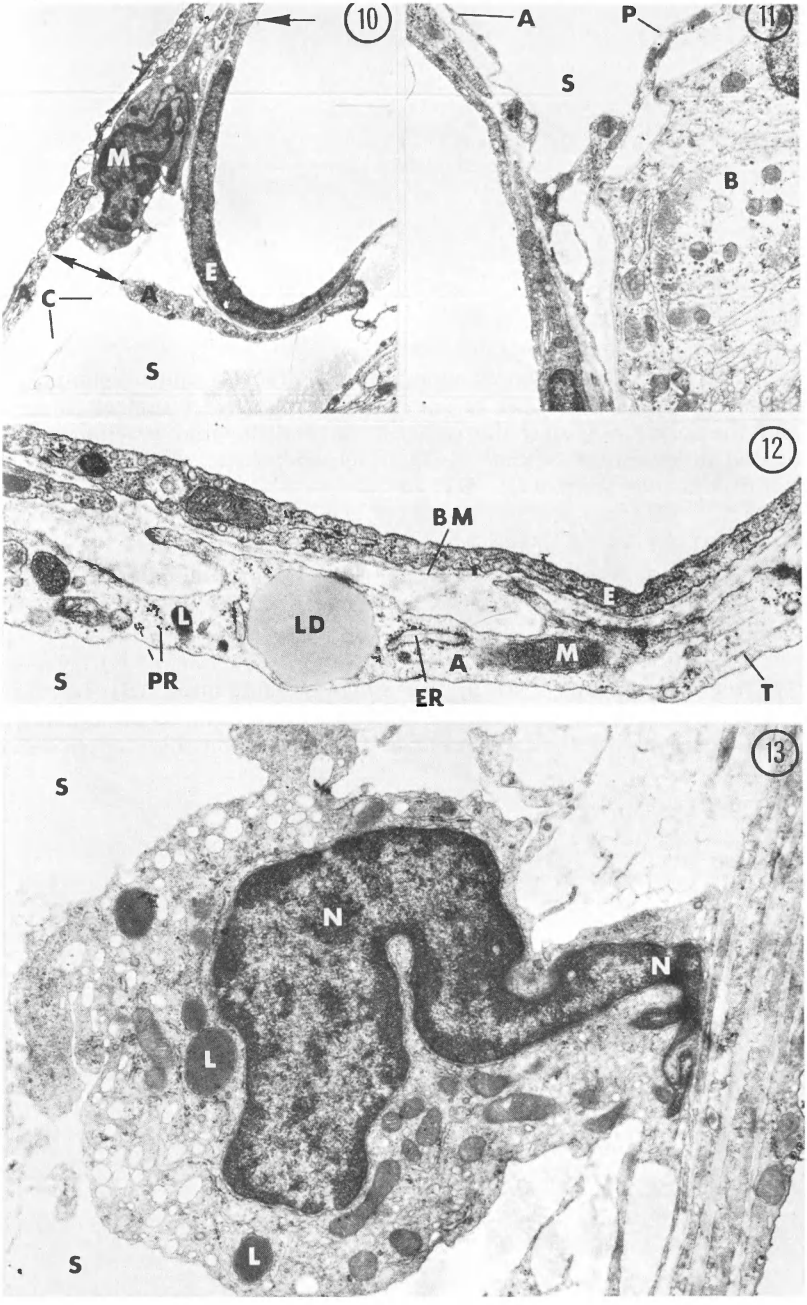
10
M
E
A
C
A
S
11
A
P
S
B
12
BM
E
LD
L
S
PR
ER
A
M
T
13
S
N
N
L
L
S

FIGURE 14—Arachnoid membrane. Dura (D) and arachnoid (A) are separated by a layer of "neurothelium" (N). A typical fibrocyte of the dura resembles the cells of the multilayered arachnoid. Isolated intercellular lacunae (LC) are characteristic. Compact collagen fibrils do not stain well. X12,000.

FIGURE 15—Arachnoid membrane. A macrophage (M) forms part of the arachnoid membrane (A). Dark intercellular material (arrows) separates the neurothelium (N) from the arachnoid. X9,000.

FIGURE 16—Arachnoid membrane. The arachnoid (A) separates a free macrophage (M) in the subarachnoid space (S) from the neurothelium (N). Numerous mitochondria are seen in the arachnoid. The macrophage shows lysosomes (L) with semi-digested material. X9,800.

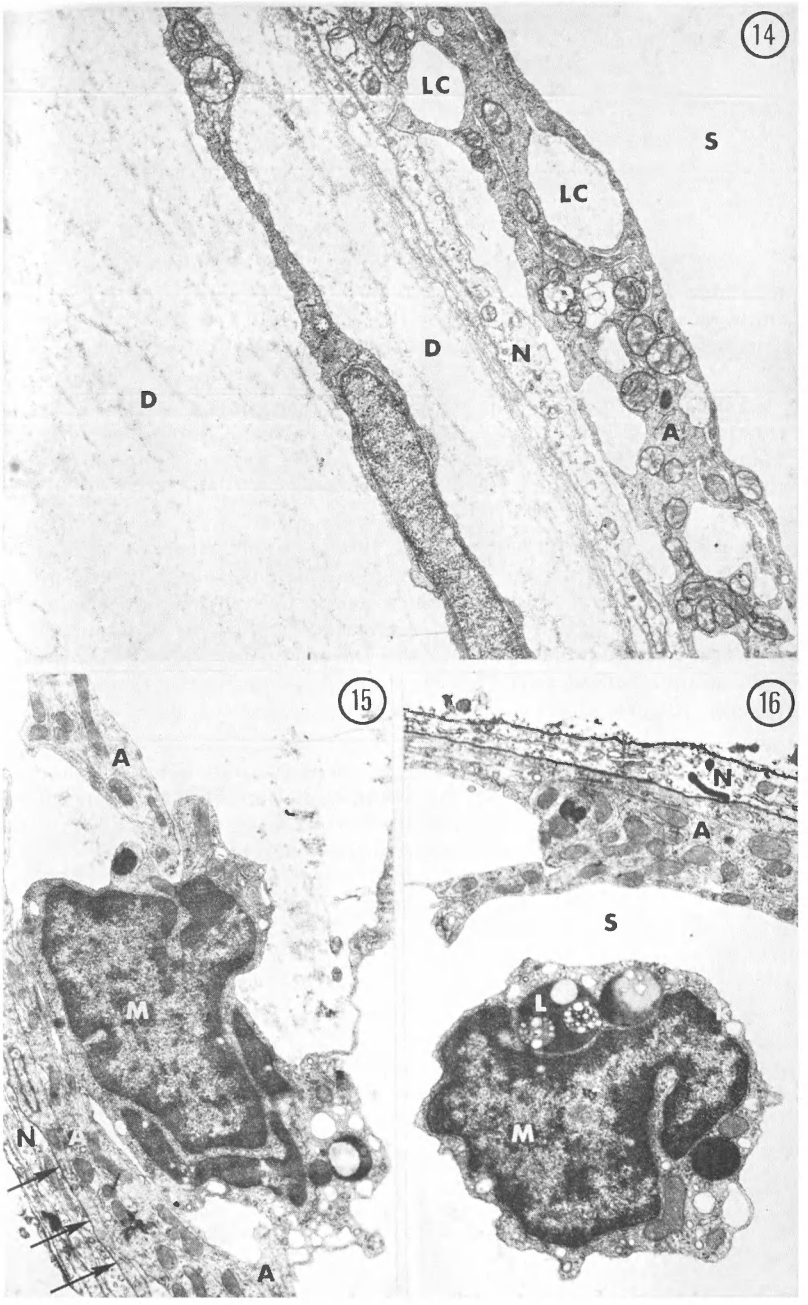
14
LC
S
LC
D
N
D
A
15
A
M
N
A
A
16
N
A
S
L
M

FIGURE 17—Root sheath. A typical root sheath (RS) includes an outer layer of dark cells with numerous organelles and a lighter inner vesicular layer. Be ween the basal cell layer and the endoneurium a boundary membrane (BM) intervenes. X36,000.

FIGURE 18—Root sheath. Uni collagen fibrils (C) are seen in the lacunae and in spaces between cell layers. Many mitochondria (M) are seen and macular junctions (J) are presen. between cellular processes in the outer root sheath layers. X21,000.

FIGURE 19—Root sheath. At times, the number of cell layers may increase but the usual arrangement of dark outer layers, lighter inner layers and a basal boundary membrane is present. Many connective tissue fibrils (C) are seen within lacunae of the root sheath and also in the endoneurium (E) of the nerve root. A cellular process (M) assumed to be part of a macrophage is present between the cell layers. X9,700.

FIGURE 20—Root sheath. Open spaces (arrow) between the outer cells of the root sheath allow communication of the subarachnoid space with the collagen filled intercellular spaces. A macrophagic process (M) is present within the open space between cells. X35,000.

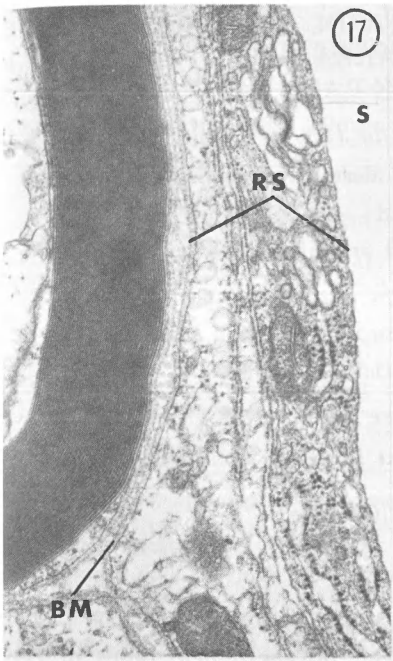
17
S
RS
BM

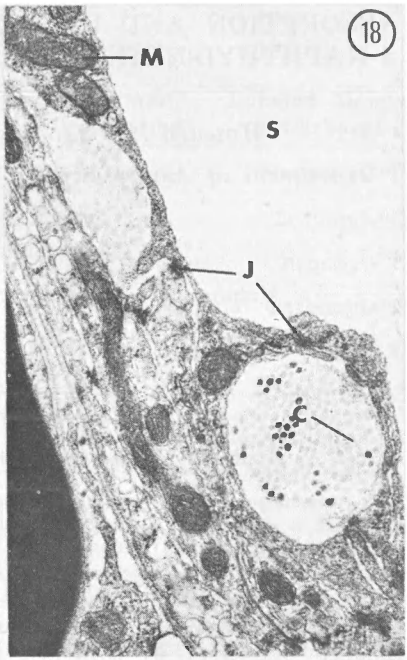
18
M
S
J

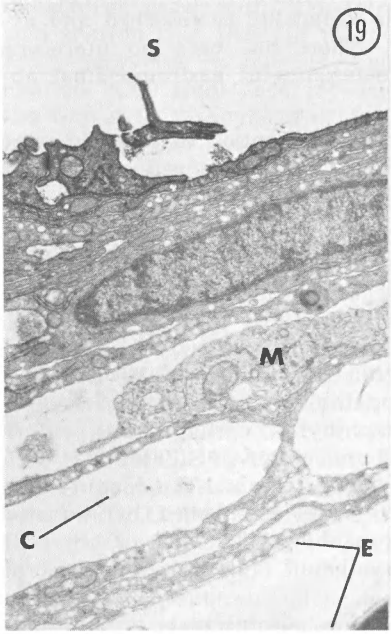
19
S
M
C
E

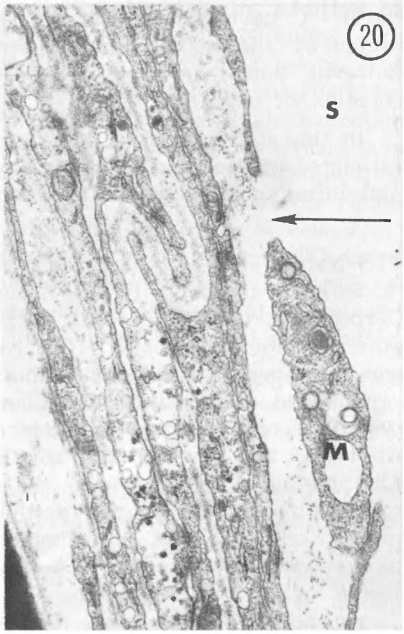
20
S
M

ABSORPTION AND EXCRETION OF RADIOLABELED 1-NAPHTHYL-N-METHYLCARBAMATE (CARBARYL) BY THE RAT

Howard H. Casper and Jerome C. Pekas

Department of Animal Science, North Dakota State University

and

U. S. Department of Agriculture

Metabolism and Radiation Research Laboratory

Animal Husbandry Research Division, ARS

Fargo, North Dakota 58102

Second Place Winner

A. Roger Denison Student Research Competition

INTRODUCTION

1-Naphthly-N-methylcarbamate (carbaryl) is a broad spectrum insecticide which is extensively used in pest control. The metabolism of carbaryl by liver homogenates, and identification of carbaryl metabolites in urine and milk have been described (4, 5, 7, 8, 10). Balance studies (7, 9) with oral and intraperitoneal doses of carbaryl -^{14}C have also shown that the radiolabel is absorbed and excreted by the mammalian system. There has been no literature. however, which describes the characteristics of gastrointestinal absorption of carbaryl.

In this study the rate and region of absorption of carbaryl were estimated by measurements of ^{14}C excretion and expiration after oral and intravenous doses of radiolabeled carbaryl.

METHODS AND MATERIALS

1-Naphthyl-N-methyl (carbamate-^{14}C), hereafter called carbonyl-^{14}C carbaryl (radiopurity 98%), purchased from the Nuclear-Chicago Corporation, was adjusted to a specific activity of 1 μc/μmole with pure nonlabeled carbaryl. The carbonyl-^{14}C carbaryl (1 μc/μmole) was dissolved in absolute ethanol (30 μmole/ml) for use in intravenous and oral dosing. The (1-naphthyl-1-^{14}C)-N-methylcarbamate (0.144 μc/μmole), hereafter called naphthyl-^{14}C carbaryl, was synthesized (12), and purified on a 2.5 x 30 cm column of Silica Gel H with 0.2% methanol in benzene as the eluting solvent. The identity and radiopurity of the eluted product were established by infrared spectral analysis and gas chomatography (11). The naphthyl-^{14}C carbaryl was dissolved in 2-methoxyethanol (10 μmole/ml) for oral dosing.

The experimental design is summarized in Table I.

TABLE I
EXPERIMENTAL DESIGN

Experiment	Procedure*	Dosing Route	Animal** Preparation*	Labeled Moiety of Carbaryl
1	I	Oral	Normal	Naphthyl-^{14}C
2	I	Oral	Normal	Carbonyl-^{14}C
3	I	Oral	Ligated pylorus	Carbonyl-^{14}C
4	I	I.V.	Portal vein cannula	Carbonyl-^{14}C
5	II	Oral	Normal	Carbonyl-^{14}C
6	II	Oral	Ligated esophagus	Carbonyl-^{14}C
7	II	I.V.	Portal vein cannula	Carbonyl-^{14}C

*See text for description of procedure and animal preparation.
**All rats were fasted (18-24 hours predosing) to ensure a stomach free of ingesta.

In procedure I the rats were individually housed in glass metabolism cages (Delmar Scientific Laboratories) to enable total ^{14}C recovery for a period of 24 hours after dosing. Calibration of the metabolism cages with $^{14}CO_2$ released from $Na_2{}^{14}CO_3$ by addition of acid showed that 100% of the $^{14}CO_2$ was trapped in 24 hours, with 86.2% recovered in the first hour and 97.1% within 2 hours. The expired $^{14}CO_2$ from each rat was collected in 1-hour intervals for the first 6 to 12 hours after dosing, followed by a single collection to complete a 24-hour collection. The rats were then sacrificed, and radioanalyses were done on the feces, carcass, urine, gastrointestinal tissue, cage rinses, and CO_2 traps. Each cage was separately rinsed with distilled water and acetone. Methods previously described (1) were used in trapping CO_2, and measuring the ^{14}C in feces, CO_2 traps, and water-soluble samples (urine and cage rinses). Samples of freeze-dried homogenates of carcass and gastrointestinal tissue were digested in NCS solubilizer (3, 6) and counted by liquid scintillation.

Interpretation of the $^{14}CO_2$ data from procedure I, however, was limited by the 1-hour intervals, and shorter intervals were not practical. Therefore, procedure II was developed to improve resolution of $^{14}CO_2$ expiration in shorter intervals of time.

In procedure II, a small restraining cage (2) enclosed in Plexiglas was used. Calibration with $^{14}CO_2$ liberated from $Na_2{}^{14}CO_3$ showed that 93.5 and 98.1% of the $^{14}CO_2$ were recovered within 5 and 10 minutes, respectively. In experiments 5, 6, and 7, the $^{14}CO_2$ was collected in 10-minute intervals for the first 4 hours after dosing, followed by eight intervals of 1 hour each, to complete a 12-hour

collection period. The rats were then sacrificed, but radioanalysis was done only on the CO_2 traps.

In both procedures, mature female rats (Sprague-Dawley) were randomly assigned to each experiment and individually dosed with 7.5 μmoles of carbaryl-^{14}C per kilogram of body weight. The required dose was dispensed with a microsyringe and the cannula rinsed before removal. In experiment 1, the rinse was 0.05 ml of 2-methoxyethanol, whereas in all other experiments the rinse was 0.20 ml of a 25% ethanol solution (v/v). Oral dosing was via a polyethylene tube passed down the esophagus (9.5 cm past the teeth). Intravenous dosing was via a portal vein cannula 3 to 12 hours after surgery. In all cases where surgery was required, the rats were under ether anesthesia.

In experiment 3 (ligated pylorus), a loose nylon ligature was placed around the pylorus, and the ends of the ligature were exteriorized. After 5 days recovery, the ligatures were pulled tight and the animal immediately dosed. Postmortem examination verified that the ligatures were secure.

In experiment 7 (ligated esophagus), a nylon ligature was loosely placed around the esophagus (1 cm from the cardia), and the ends of the ligature were exteriorized. The rats were orally dosed 12 hours after surgery and the ligatures immediately tightened. Postmortem examination verified that the ligatures were secure.

RESULTS AND DISCUSSION

The results are given in Table II and Figures 1 and 2. The absorption estimates (Table II) were made with the assumption that $^{14}CO_2$ was not eructed from the gastrointestinal lumen.

Naphthyl-^{14}C carbaryl.—The majority (84.4%) of the ^{14}C label was absorbed in 24 hours, but the naphthyl moiety apparently was not degraded to CO_2 since only an insignificant amount of $^{14}CO_2$ (0.1%) was recovered.

Carbonyl-^{14}C carbaryl.—In contrast to the naphthyl moiety, the carbamyl moeity of an oral dose (normal rats) of carbaryl was extensively degraded to CO_2 (experiments 2 and 5). However, the estimate of absorption did not differ, as at least 84.0% of the ^{14}C derived from carbonyl-^{14}C carbaryl was absorbed in a period of 24 hours (experiment 2).

Ligation of the pylorus showed that the stomach had the ability to absorb 51.2% of the ^{14}C derived from carbonyl-^{14}C carbaryl. Since this was considerably lower than was obtained with normal rats (84.0%), it appears that ^{14}C absorption also occurred in the intestine.

Ligation of the esophagus (experiment 6), to eliminate $^{14}CO_2$ eructation from the gastrointestinal lumen, markedly reduced the total $^{14}CO_2$ expired (15.2 vs 24.9%). Either $^{14}CO_2$ was produced in the lumen and eructed, or stess and the inability to swallow saliva re-

TABLE II
PERCENT RECOVERIES OF ^{14}C LABEL

Dosing Route Animal Preparation	Naphthyl-^{14}C Carbaryl				Carbonyl -^{14}C Carbaryl		
	Oral Normal	Oral Normal	Oral Ligated Pylorus	I.V. Portal Vein	Oral Normal	Oral Ligated Esophagus	I.V. Portal Vein
	PROCEDURE I				PROCEDURE II		
Experiment No.	1	2	3	4	5	6	7
CO_2 (12 hr)	—	28.8	—	19.0	24.9	15.2	23.2
CO_2 (24 hr)	0.1*	34.6*	19.0*	24.1	—	—	—
Urine	80.9*	41.1*	19.5*	56.9	—	—	—
Cage Rinse	8.2	11.0	12.6* ***	6.2	—	—	—
Feces	6.2	1.9	**	2.3	—	—	—
G.I. Tract	1.0	0.9	**	0.7	—	—	—
Carcass	3.4*	8.3*	44.0	7.9	—	—	—
Total	99.8	97.8	95.1	98.1	—	—	—
Absorption	84.4	84.0	51.2***	—	—	—	—
No. of Rats	4	4	4	3	3	5	3
Average Wt.	195 g	200 g	197 g	214 g	208 g	190 g	200 g

*Values used in forming each absorption estimate.
**Included in carcass analyses.
***Ligation of the pylorus eliminated cage rinse contamination by unabsorbed ^{14}C in the feces.

duced the ^{14}C absorption. The profiles of the $^{14}CO_2$ expiration curves of experiments 5 and 6 were quite similar (Figure 1) and indicated that the kinetics of $^{14}CO_2$ production were not affected by ligation of the esophagus.

$^{14}CO_2$ Kinetics (oral vs intravenous).—The $^{14}CO_2$ expiration kinetics resulting from oral and intravenous doses of carbonyl-^{14}C carbaryl using procedure II (experiments 5 and 7) were strikingly similar (Figure 1). The recoveries during the first 11 hours after dosing were not statistically different (F test; $P > 0.05$). This similarity (oral vs intravenous) was also observed when procedure I was used (Figure 2); the recoveries were not statistically different ($P > 0.05$)

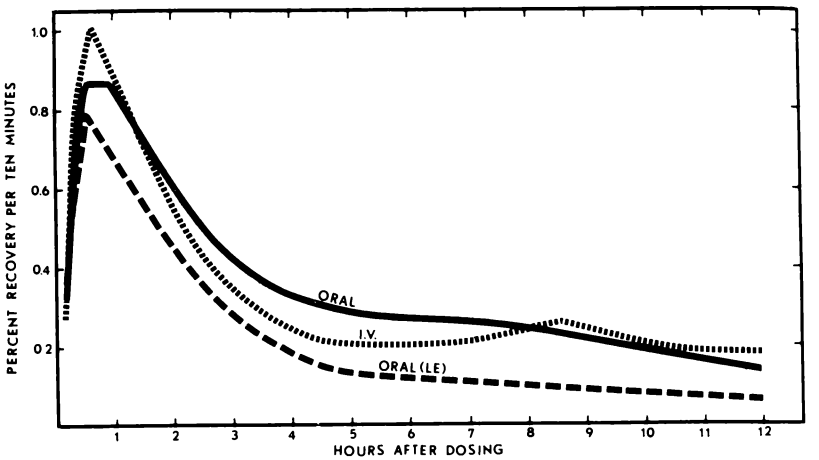

FIGURE 1—Time vs recovery of ^{14}C label in CO_2 (procedure II): experiment 5 (ORAL); experiment 6 (ORAL (LE)); experiment 7 (I.V.).

during the first 3 hours after dosing. The ^{14}C derived from an oral dose of carbonyl-^{14}C carbaryl was rapidly absorbed, metabolized to $^{14}CO_2$, and expired at rates equal to those observed with an intravenous dose. The rapid absorption of ^{14}C was demonstrated (procedure II) by detection of $^{14}CO_2$ in the first 10-minute interval, and the maximum expiration rate occurred at 30 to 40 minutes, regardless of dosing route (Figure 1). It is thus clear that the absorption of ^{14}C from an oral dose of carbonyl-^{14}C carbaryl is rapid and likely occurs in the stomach or anterior portion of the small intestine. Eructation of $^{14}CO_2$ from the gastrointestinal tract may have contributed significantly to the $^{14}CO_2$ expiration rates, and further work is required to establish this possibility.

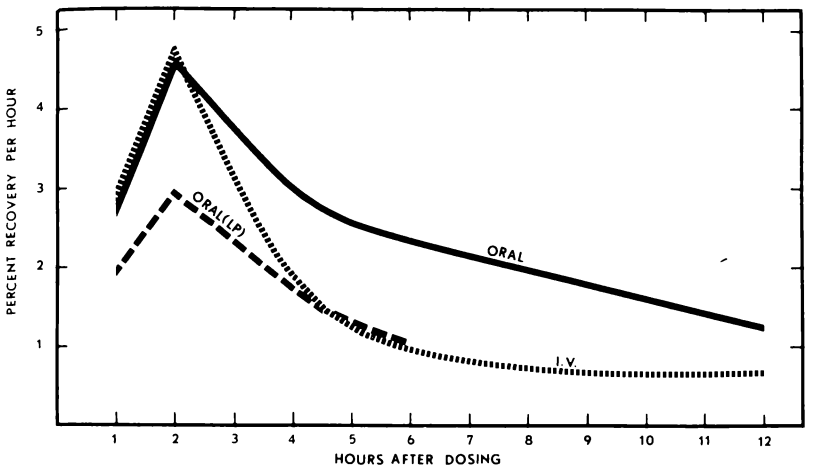

FIGURE 2—Time vs recovery of ^{14}C label in CO_2 (procedure I): experiment 2 (ORAL); experiment 3 (ORAL (LP)); experiment 4 (I.V.).

SUMMARY

Minimums of 84.0 and 84.4% of the ^{14}C in oral doses of carbonyl-^{14}C carbaryl and naphthyl-^{14}C carbaryl, respectively, were absorbed by normal female rats in 24 hours. This was reduced to 51.2% when passage into the intestine was blocked by ligation of the pylorus. Time course studies on the rates of $^{14}CO_2$ expiration after oral and intravenous doses of carbonyl-^{14}C carbaryl indicated a rapid absorption of ^{14}C in the stomach or anterior portion of the small intestine.

ACKNOWLEDGMENT

The authors are grateful to Dr. Gaylord D. Paulson for the synthesis of the naphthyl-^{14}C carbaryl.

REFERENCES

1. Bake, J. E., Robbins, J. D., Feil, V. J., Agr. Food Chem. *15*, 628 (1967).
2. Bollman, J. L., J. Laboratory and Clinical Medicine *33*, 1348 (1948).
3. Casper, H. H., Pekas, J.C., Metabolis and Radiation Research Laboratory, North Dakota State Univ., Fargo, North Dakota, unpublished data.
4. Dorough, H. W., Casida, J. E., J. Agr. Food Chem. *12*, 294 (1964).
5. Dorough, H. W. J. Agr. Food Chem. *15*, 261 (1967).
6. Hansen, D. L., Bush, E. T., Anal. Biochem. *18*, 320 (1967).

7. Knaak, J. B., Tallant, M. J. Bartley, W. J., Sullivan, L. J., J. Agr. Food Chem. *13*, 537 (1965).
8. Knaak, J. B., Tallant, M. J., Koebelt, S. J., Sullivan, L. J. J. Agr. Food Chem. *16*, 465 (1968).
9. Krishna, G. T., Casida, J. E., J. Agr. Food Chem. *14*, 98 (1966).
10. Leeling, N. C., Casida, J. E., J. Agr. Food Chem. *14*, 281 (1966).
11. Paulson, G. D., Feil, V. J., Poultry Sci. *43*, 1593 (1969).
12. Skraba, W. J., Young, F. G., J. Agr. Food Chem. *7*, 612 (1959).

PINEAL GLAND: CONTROL OF CORTICOSTERONE

Rex E. Wiederanders and Sidney M. Hirsch

Harmon Park Research Laboratory

Williston, North Dakota 58801

ABSTRACT

We have proposed a mechanism whereby the pineal gland might affect the adrenal output and have gathered some evidence for it by injecting melatonin into the median eminence and under the skin of the white rat. We found a decrease in plasma corticosterone in the injected animals that is significant to the 2% level of confidence.

INTRODUCTION

We have proposed a mechanism (1) for pineal gland function, suggesting that melatonin, the unique pineal product, lowers the feed-back set point (2) in the hypothalamus and decreases the output of such agents as FSH, LH, ACTH and production of their target hormones. The rhythm or regular fluctuations in plasma concentration of these hormones is not changed but the quantity of hormone present at each phase of the cycle is decreased when melatonin is increased (secondary to increased pineal activity or melatonin injection) and increased when melatonin is decreased (e.g. after pinealectomy). We have used the ACTH-corticostrone system of the white rat to test this hypothesis, introducing melatonin into the hypothalamus or under the skin and have found a significant decrease in plasma cortiocosterone.

MATERIALS AND METHODS

Wistar strain animals were used throughout. Male rats of the same birthdate were given approximately 1 mg of cocoa butter into the median eminence through a 20 gauge spinal needle at coordinates, anterior-posterior 5.4, horizontal $\pm$ 0, vertical -4, (3) using the Stoelting stereotactic apparatus, under pentobarbital anaesthesia, (intraperitoneal) at 25 mg/kg. The median eminence was chosen as it evidently is the site of corticosterone feed-back control (4). The site of implantations was verified by direct inspection.

Plain cocoa butter was injected in control rats and used as the vehicle to inject melatonin monohydrate, seratonin creatinine sulfate complex hydrate or cortiscosterone A grade. These chemicals were purchased from Calbiochem, Los Angeles, Calif. Matched females were given 0.5 ml daily subcutaneous injections of 1:2 absolute alcohol to deionized water by volume, either plain or containing melatonin or seotonin. The alcohol facilitates dissolving the melatonin and produces a corticosterone response (5) which amplifies the suppresent effect of melatonin. At 8:00 P.M. the males were killed five days after lesioning and the females two hours after their third injection, by guillotine decapitation. Blood was collected from each into a beaker with two drops of 1:5,000 Heparin, centrifuged, plasma removed and frozen until estimation of the total plasma fluorescence was done. We used the method of Guillemin *et al.* (6) with the following changes. Fluorescence was read on a Farrand Ratio Fluorometer. Bakelite-capped centrifuge tubes with teflon liners were used. Our standard was made by dissolving 25 mg corticosterone, A grade, homogenous on thin layer chromotography, in 100 ml absolute alcohol and further diluting aliquots of this with deionized water to a concentration of 0.25 μg/ml. This standard proved stable under refrigeration for at least six months. One-half ml of standard and ½ ml of plasma were measured; each run of 20 tubes contained 17 plasma unknowns, two standards and one blank. The two standards regularly read within 5% of each other and the day to day fluctuation was small. Calculations were done by subtracting the blank reading taking the ratio of standard to unknown reading.

RESULTS AND DISCUSSION

Both testes or both ovaries, the left kidney and both adrenals were removed, defatted and weighed immediately to the nearest milligram. No significant difference between any of these weights was found but the adrenal weights did tend to vary in the same direction as corticosterone. The bulk of the plasma fluorescence is due to corticosterone in the rat (7) and changes in fluorescence may, with reasonable confidence, be ascribed to corticosterone variations. We speak here of corticosterone but emphasize that we actually measured the total plasma fluorescence.

Table I shows how 100 μg of melatonin in the median eminence decreases the mean plasma cortiocosterone to the 2% level of confidence, the same range as animals receiving corticosterone itself. These animals are included to show the level resulting when the set point is turned off by corticosterone. Serotonin was used as a possible melatonin antagonist but produced no such effect by either route. It did lower plasma corticosterone insignificantly when placed in the hypothalmus. Melatonin in diluted alcohol solution diminished corticosterone in the female rat at the 1% level of confidence (Table II).

TABLE I

	Corticosterone (μg/ml plasma mean ± S.E.)	No. of Animals*	P Values
Cocoa-butter Controls	0.24 ± 0.015	18	
Melatonin (100μg)	0.18 ± 0.017	13	< .02
Melatonin (5 μg)	0.19 ± 0.015	7	< .05
Corticosterone (0.2 mg)	0.17 ± 0.02	7	< .02
Serotonin (100 μg)	0.19 ± 0.02	5	> .05

*Male rats, lesioned in median eminence at age six months, decapitated five days later.

TABLE II

	Cortiocosterone (μg/ml plasma; mean ± S.E.)	No. of Animals*	P Values
Control Alcohol / H_2O = ½	0.35 ± 0.022	10	
Melatonin (100 μg/day)	0.24 ± 0.021	10	< .01
Serotonin (100 μg/day)	0.36 ± 0.04	10	> .05

*Female rats, 0.5 ml solution daily subcutaneously begun age two months, decapitated on third injection day.

The plasma corticosterone concentration in the rat varies in a circadian cycle (8). By sacrificing these animals at the same hour after keeping them in the same light: dark cycle (14:10 L:D) for at least one month we probably caught the same point of their cycle and feel our results tend to bear out the theory. It seems likely that the melatonin acted locally in the median eminence as we have found staining in this area from lamp black tagged injections as long as three days post lesioning. The subcutaneously injected melatonin may have acted there as well. Wurtman *et al.* (9) have shown that

tagged melatonin is widely dispersed in the cat, concentrating in the pineal, iris-choroid, ovary, pituitary and sympathetic nerves but not in the adrenal gland, while Anton-Tay and Wurtman (10) found melatonin concentrated in the rat hypothalamus, especially when injected in the cerebrospinal fluid. In this area it may act through a serotonin mechanism as Anton-Tay *et al.* (11) noted increased hypothalamic serotonin concentration after 150 μg melatonin injection intraperitoneal. The insignificant decrease in cortiocosterone following serotonin (Table I) implantation may result from such a mechanism.

As late as 1967 Kitay (12) said the pituitary-adrenal relationship "continues to be inconsistent" and it is still that way. Barchas *et al.* (13) injected 1 mg/kg melatonin acutely and chronically in the rat and found no significant change in pituitary ACTH or plasma corticosterone. Gromova *et al.* (14) showed melatonin and serotonin increased the production of corticosterone by the adrenal glands if given one hour before decapitation provided the pituitary was intact. Our work shows the opposite effect but perhaps melatonin has a double action in time as Kinson *et al.* (15) found corticosterone elevated after pinealectomy and subsequent application of a clip to a renal artery further elevated the level in the pinealectomized animals above those of the controls. Zanoboni and Zanoboni (16) found hypertension following pinealectomy and suggested it was induced by the adrenals.

REFERENCES

1. R. E. Wiederanders, S. M. Hirsch, G. W. Evans, Proc. North Dakota Acad. Sci. 21, 171 (1967).
2. F. E. Yates, J. Urquhart, Physiol. Rev. 42, 359 (1962).
3. J. DeGroot, J. Comp. Neurol. 113, 389 (1959).
4. J. M. Davidson, S. Felman, L. E. Jones, S. Levine, Rassegna di Neurologia Vegetativa 21, 9 (1967): Davidson, J. M. S. Feldman, Endocrinol. 72, 936 (1963); K. Ruf, F. A. Steinor, Science 156, 667 (1967).
5. F. W. Ellis, J. Pharmacol. Exp. Therapeutics 153, 121 (1966).
6. R. Guillemin, G. W. Clayton, H. S. Lipscomb, J. D. Smith, J. Lab Clin. Med. 53, 830 (1959).
7. R. H. Silber, R. D. Busch, R. Oslapas, Clin. Chem. 4, 278 (1958).
8. K. Retiene, E. Zimmerman, W. J. Schindler, J. Neuenschwander and H. S. Lipscomb Acta Endocrinologica 57, 615 (1968).
9. R. J. Wurtman, J. Axelrod, L. T. Potter, J. Pharmacol. Exp. Thera. 143, 314 (1964).
10. F. Anton-Tay, R. J. Wurtman Science 162, 277 (1968).
11. F. Anton-Tay, C. Chou, S. Anton, R. J. Wurtman Science 162, 277 (1969).

12. J. I. Kitay, Neuroendocrinology 2, 641 (1967).
13. J. Barchas, R. Conner, S. Levine, J. Vernikos-Donellis, Experimentia 25, 413 (1969).
14. E. A. Gromova, M. Kraus, J. Krecek, J. Ednocr. 39, 345 (1967).
15. G. Krinson, A. K. Wahid, B. Singer, Gen. Comp. Endocrinol. 8, 445 (1967).
16. A. Zanoboni, W. Zanoboni-Muciaccia, Life Sciences 6, 2327 (1967).

IMMUNOCHEMICAL PROPERTIES OF WALKER 256 CARCINOMA HISTONES

H. W. Spencer and R. H. Wilson

Department of Physiology and Pharmacology

School of Medicine

University of North Dakota, Grand Forks, North Dakota 58201

ABSTRACT

Histones of Walker 256 Carcinoma were separated by ethanol-HCI leaching of the tumors. The resulting nucleohistones were grossly separated by Sephadex gel filtration and the resultant fractions separated by gradient elution on cellulose column. The histones were conjugated to bovine serum albumin. Both the histones and histone-BSA complexes were each dissolved in normal saline and emulsified in complete Freund's adjuvant. These antigens were injected subcutaneously into the toepads of male New Zealand rabbits. Intraperitoneal booster doses were given at 3 and 4 weeks. Sera were obtained by cardiac puncture and frozen. A microtiter complement fixation test was utilized showing that the histone preparation was weakly antigenic.

INTRODUCTION

The use of immunology as a tool to characterize proteins and nucleotide moieties of cell nuclei has become prevalent in recent years (1, 2, 3). The immunologic testing of patients with the disease systemic lupus erythematosus (SLE) has demonstrated the presence of antibodies to deoxyribonucleic acid (DNA) (4, 5). However, both histone and DNA together were required for reactivity in some of these SLE sera (3). Stollar and Sandberg (6) reported a comparison of antibodies to DNA conjugated with methylated bovine serum albumin. Other studies have shown reactivity with a reconstituted histone-DNA complex (7). The actual role of the histone in this complex in the conformation of the antigenic determinants is not well understood. There has been some question as to the degree of antigenicity of histones (1).

The fact that tumor cells are different in their growth rates and DNA activity has led us to think that the structural materials of the nuclear proteins, histones, may be different.

This paper describes an attempt to induce the production of histone antibodies in the rabbit against the Walker 256 carcinoma.

METHODS

The Walker tumor was grown in 20 male Dawley rats weighing 180-200 g and fed Purina laboratory chow *ad libitum*. The tumors were transplanted into anesthetized rats by inserting a 1 mm^3 piece of tissue subcutaneously through a small incision. After 8 days the animals were sacrificed and the tumors were excised. Blood, connective tissue and necrotic tissue areas were removed and the tumors were cooled with dry ice.

The tumors were cut into small pieces and homogenized in a Blender at full speed for 2 minutes. Five volumes of a 0.14 M NaCl and 0.01 M trisodium citrate solution were added to the tissue prior to blending. The suspension was filtered through 6 layers of wet cheese cloth and centrifuged at 1500 x g for 50 minutes. Three drops of octanol were added to prevent foaming. Diphenyl fluorophosphate was added to make the solution contain O.1 m M. The washing procedure was repeated six times.

Extraction. — Extraction of the histone fractions essentially followed the method of Hnilica and Busch (8) in which the crude deoxyribonucleoprotein was blended at high speed in 10 volumes of 80% ethanol for 30 seconds (Figure 1). The material was then centrifuged at 1500 x g for 30 minutes. The supernatant was discarded and the sediment was extracted 3 times with a solution 4:1, 95% ethanol - 1.25 N HCI for 8 hours. After reducing the volume by 1/3, the solution was dialyzed against distilled water for 24 hours at 4 C. Fractions 2a and 3 were precipitated by adding trichloroacetic acid to a concentration of 5 per cent. Fraction 1 was then precipitated by adding trichloroacetic acid to a concentration of 20 per cent.

The insoluble residue was extracted with 0.25 N HCI. The extracts were dialyzed against distilled water for 24 hours at 4 C. The combined extracts were made to contain 5% trichloroacetic acid which precipitated fraction 2b.

The fractions precipitated with trichloroacetic acid were suspended in acetone containing 1% HCI, thus converting the proteins to the hydrochloride salts. After washing with acetone and ether, the proteins were dried by evaporation at 4 C.

Chromatography — The two crude fractions F2a, 3 and F2b were separated on a column 2.5 cm x 12 cm containing Sephadex G-70 by 0.02 N HCI flowing at 7.5 ml/cm^2/hr. The two fractions were collected and dialyzed against distilled H_2O and lyophilized. The lyophilized samples were suspended in 10 ml of 0.002 N HCI and layered over a carboxymethylcellulose column 2.5 cm x 12 cm con-

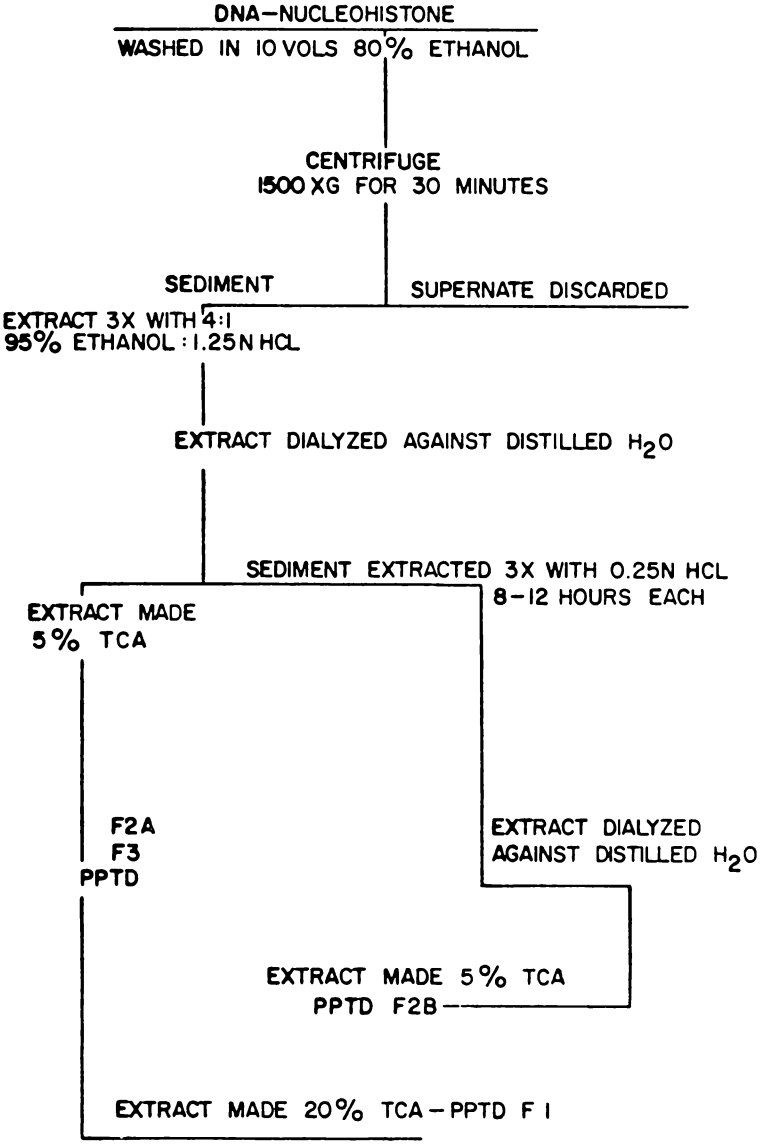

FIGURE 1—Chemical extraction of histones.

taining 20 g of 0.7 mEq/g material. Gradient elution was carried out with 1.8 x 10^{-3} M; 1 x 10^{-2} M HCl corresponding to pHs of 2.75, 2.2, 2.0, respectively, at 7.5 ml/cm^2/hr. The samples were dialyzed against distilled water and lyophilized.

The histone fractions were then recombined in the same weight proportions as recovered from the CMC column.

Amino acid analysis. — Amino acid analysis was carried out by column chromatography and the lysine to arginine ratios were compared with those of other researchers (8).

Plasma proteins. — Three Sprague Dawley rats were bled by cardiac puncture with the blood being preserved by 1 ml of 5% sodium citrate solution per 10 ml blood. To the plasma was added enough ammonium sulfate to saturate it at 4 C. The solution was stirred continuously. The precipitate was filtered and dialyzed against distilled H_2O at 4 C. The protein solution was lyophilized.

Conjugation of the histone. — The method of Goodfriend *et al.* (9) was used to conjugate the histone to the protein carrier, bovine serum albumin (BSA) purchased from the Armour Pharmaceutical Co. The method employs a water soluble carbodiimide, 1-ethyl-3 (3-dimethyl aminopropyl) carbodiimide HCl, (EDC) which was purchased from Ott Chemical Company.

One hundred mg BSA and 40 mg histone were dissolved in 3 ml H_2O. Three ml of the EDC in H_2O (75 mg/ml) were added and the solution was stirred for 30 minutes at room temperature and dialyzed against distilled H_2O at 4 C. The conjugate was then lyophilized.

Immunization. — Five groups of five animals each were used in this research. Group I served as the control and received no injections. Group II received complete Freund's adjuvant plus distilled H_2O. Group III received BSA-EDC in saline and adjuvant. Group IV received BSA-histone complex in saline and adjuvant. Group V received histone in saline and adjuvant.

The toepads on the right side of New Zealand white male rabbits received 0.2 ml of the antigen. The total dose per animal was 3 mg.

After 3 weeks each animal received 1 mg of antigen in saline and adjuvant intraperitoneally. In the 4th week, a second intraperitoneal injection was given. At 5½ weeks, the animals were bled by cardiac puncture. Following separation, the sera were stored at -20 C. Control blood samples were drawn from the ear veins by needle puncture prior to immunization.

Serologic testing. — The complement fixation test using two units of complement and the method of Kolmer (1942) (10) adapted to the use of the Takatsy (1955) (11) microtitrator was used.

RESULTS

Amino acid analysis. — amino acid analysis of the histone fractions eluted from the carboxymethylcellulose columns by the gradient HCl solutions showed a lysine to arginine ratio of the

F1 fraction of 6.26. The material extracted with acidic ethanol showed ratios of 0.7 to 0.88. The proteins extracted by 0.25 N HCl and eluted from the column with 0.002 N HCl, 0.01 N HCl and 0.02 N HCl showed lysine to arginine ratios of 2.45, 2.27, and 2.54, respectively. The lysine to arginine ratios were in close agreement with those of other researchers (8).

Serologic testing. — In the complement fixing tests a ± 4 - fold change in titer was considered significant.

As seen in Table I, animals 1 through 5 when tested with BSA-EDC showed good antibody production response in all five animals of this group.

Animals 6 through 10 having BSA-histone antisera showed a significant rise in antibody titers in the convalescent sera.

When blocked with histone prior to testing with BSA-histone, animals 6 through 10 showed a significant decrease in titer in four of the five antisera. However, when these same BSA-histone antisera were tested against histone alone, only one of the antisera showed a significant titer.

Histone antisera from animals 11-15, when tested against histone, showed significant complement fixation in two of the five tested as seen in Table I.

Table II shows the antisera of animals 12, 13, and 15 which were further tested against histone. One of the three antisera showed a significant decrease in titer.

When tested for a contaminating plasma protein, a reduction of titer was shown when the antisera were treated with mercapto-ethanol.

DISCUSSION

Histones extracted from cell nuclei have been shown to differ strikingly in composition. The lysine and arginine contents to different histones have been shown to be fairly constant and thus the lysine to arginine ratios have been used to assess the quality of the histones recovered.

The lysine to arginine ratios of histones extracted in this experiment agreed generally well with previous values in the literature.

The data obtained in the present study demonstrated that the protein complex of BSA-EDC was antigenic and elicited a good antibody response in the rabbit.

The complex of BSA-histone stimulates an antibody response in the animals. When blocked with histone, the titer decrease showed a definite portion of the antibodies present were tied up by the histone, and that the antibodies present had an affinity for the histone.

When the anti BSA-histone sera were tested, only one of the animals showed a significant increase in reactivity against histone.

Animals which were immunized against histone solely, showed 2 of 5 animals with significant titers. The histone elicited a significant antibody response. Further experiments designed to inject larger quantities of antigen are indicated, since the animals innoculated with histone and tested with histone antigen showed a low or non-significant antibody titer. The sera from the three animals innoculated with histone and treated with mercaptoethanol showed a decrease in the titer of one animal.

To test the possibility of a plasma protein contaminant, several histone antisera were treated with mercaptoethanol and tested against rat plasma proteins as antigens. The mercaptoethanol treated sera of animals 12, 13, and 15 showed that there was an increased titer of antibodies to the histone.

TABLE I

SEROLOGICAL TESTS

	Animal	Acute Titer	Convalescent Titer
BSA-EDC Antisera	1	4	32
Antigen for test—BSA-EDC	2	2	32
	3	2	32
	4	2	8
	5	2	16
BSA-Histone Antisera	6	4	128
Antigen for test—BSA-Histone	7	4	32
	8	2	32
	9	2	32
	10	4	16
BSA-Histone Antisera with	6	128	16
BSA-Histone	7	32	16
Blocked with Histone prior	8	32	8
to testing	9	32	8
	10	16	8
BSA-Histone Antisera	6	16	8
Antigen for test—Histone	7	4	8
	8	2	8
	9	2	2
	10	2	4
Histone Antisera	11	4	4
Antigen for test—Histone	12	2	16
	13	2	16
	14	4	8
	15	4	4

TABLE II
SEROLOGICAL TESTS

	Animal	Convalescent	Convalescent Buffer	Convalescent Buffer Mercaptoethanol
Histone Antisera treated with Mercaptoethanol Antigen for test—Histone	12	32	32	8
	13	16	16	8
	15	4	4	8
Histone Antisera treated with Mercaptoethanol Antigen for test—Rat Plasma Protein	12	32	32	8
	13	8	8	8
	15	8	8	8

The reaction suggests that at least one of the animals produced antibodies to a protein contaminant. The presence of a protein contaminant makes it difficult to demonstrate the antigenicity of the histone.

CONCLUSION

Antibodies against the histone protein preparation used in this research were demonstrated. However, the fact that rat plasma proteins also showed reactivity poses a question concerning the purity of the histone antigens. The decrease in the activity of the sera when tested against rat plasma protein after being treated with mercaptoethanol does not exclude the possibility that the histones are antigenic.

ACKNOWLEDGMENTS

This study was aided in part by the American Cancer Society, North Dakota Division, Inc. and Themis Contract No. N00014-68-A-0499 (NR101-753), between the Office of Naval Research, Department of the Navy, and the University of North Dakota.

REFERENCES

1. Meischer, P., N. S. Cooper, and B. Benacerraf. J. Immun. *85:* 27, 1960.
2. Holborow, E. J. and D. M. Weir. Lancet. *1:* 809, 1959.
3. Holman, H. R., H. R. G. Deicher, and H G. Kunkel. Bull. N. Y. Acad. Med. *35:* 409, 1959.
4. Deicher, H. R. G., H. R. Holman, and H. G. Kunkel. J. Exper. Med. *109:* 97, 1959.
5. Stollar, D. L., L. Levine, and H. Van Vanakis. Proc. Nat. Acad. Sci. *48:* 874, 1962.
6. Stollar, D. and A. L. Sandberg. J. of Immun. *96:* 755, 1966.
7. Friou, G. J. of Immuun. *80:* 476, 1958.
8. Hnilica, L. S. and H. Busch. J. Biol. Chem. *238:* 918, 1963.
9. Goodfriend, T.L., L. Levine, and G. Fasman. Science. *144:* 1344, 1964.
10. Kolmer, J. A. J. Bacteriology. *44:* 144, 1942.
11. Takatsy, G b.y Kwazinski, J. B. in Methods of Serological Research. John Wiley & Sons, N.Y. p. 291, 1965.

METABOLISM OF PLANT METABOLITES OF *s*-TRIAZINE HERBICIDES IN THE RAT

J. D. Larson and J. E. Bakke

Department of Biochemistry, North Dakota State University
and
U. S. Department of Agriculture
Metabolism and Radiation Research Laboratory
Animal Husbandry Research Division, ARS
Fargo, North Dakota 58102

INTRODUCTION

Plant and soil systems are able to convert triazine herbicides to the 2-hydroxy and dealkylated 2-hydroxy analogues (1, 2, 3). It is therefore probable that these 2-hydroxy triazines are present in the animal diet.

This report concerns the metabolism by the rat of 2-methoxy-4-ethylamino-6-*sec*-butylamino-*s*-triazine (I), 2-hydoxy-4-ethylamino-6-*sec*-butylamino-*s*-triazine (II), 2-hydroxy-4-*sec*-butylamino-6-amino-*s*-triazine (III), and 2-hydroxy-4-ethylamino-6-amino-*s*-triazine (IV). Compounds II, III, and IV are probably plant metabolites of compound I. The major urinary metabolites were isolated and subsequently characterized by mass spectrometry.

EXPERIMENTAL

Radiolabeled compounds. — All ring-labeled triazines (compounds I, II, III, IV; Figure 1) were obtained from Geigy Chemical Co., Ardsley, New York, and used without further purification. (Reference to a company or product name does not imply approval or recommendation of the product by the U.S. Department of Agriculture to the exclusion of others that may be suitable.) Compound I contained less than 1% radioimpurity of an unknown nature. Compounds II, III, and IV were radio-pure by paper chromatography (Whatman No. 1, isoamyl alcohol-acetic acid-water 40:10:50, v/v/v). The methoxy-^{14}C-labeled compound I was synthesized as previously reported (4).

General analytical procedures. — Quantitation of ^{14}C radioactivity in the urine, feces, tissues, and expired air, as well as the separation and quantitation of urinary metabolites on the amino acid analyzer, were performed as previously reported (5).

Animal treatment. — The labeled compounds were dissolved by adding 6N HCl to a slurry of the compounds in ethanol. The dosing solutions were prepared by diluting the ethanolic solutions with nine volumes of water. Each rat received a 1-ml dose by stomach tube. The doses are given in Table I.

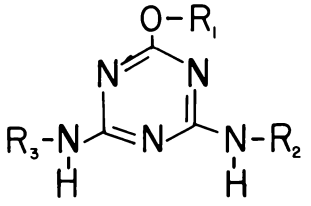

COMPOUND NUMBER	R_1	R_2	R_3
I	CH_3	CH_3CH_2-	CH_3-CH-CH_2CH_3
II	H	CH_3CH_2-	CH_3-CH-CH_2CH_3
III	H	H	CH_3-CH-CH_2CH_3
IV	H	CH_3CH_2-	H
V	H	CH_3CH_2-	CH_3-CH-CH_2CH_2OH
VI	CH_3	CH_3CH_2-	CH_3-CH-CH_2COOH
VII	CH_3	H	H
VIII	CH_3	H	CH_3-CH-CH_2CH_2OH
IX	CH_3	H	$HOCH_2$-CH-CH_2CH_3
X	H	H	H
XI	H	H	CH_3-CH-CH_2CH_2OH
X	CH_3	H	CH_3-CH-CH_2CH_3

FIGURE 1—Chemical structures of the compounds referred to in the text and tables.

After dosing, the animals were maintained in all-glass metabolism cages equipped with CO_2 traps as previously reported (5). Rats given low specific activity doses were housed in metal metabolism cages.

Isolation and characterization of urinary metabolites.—The urinary metabolites from compound I were characterized by comparing the elution volumes of the rat metabolites with those of metabolites characterized in cow and goat urine (4). This was accomplished by ion exchange chromatography on the amino acid analyzer column as previously reported (5).

The clean-up procedures for the urinary metabolites from compounds II, III, and IV prior to paper chromatography are given in

TABLE I
RAT DOSES

Compound	High Specific Activity		Low Specific Activity	
	Specific Activity μc/mg	Radio-activity μc	Specific Activity μc/mg	Radio-activity μc
I (Ring-Labeled)	91.8	0.46		
(Methoxy-Labeled)	10.0	0.45		
II (Ring-Labeled)	10.9	0.487	0.0485	0.495
III (Ring-Labeled)	10.3	0.682	0.0477	0.408
IV (Ring-Labeled)	13.3	0.614	0.108	0.598

TABLE II
METABOLITE CLEANUP PROCEDURE

Method	Solvent	% Recovery II	III	IV Organic	IV Aqueous
Organic Extraction	CH_3CN			76	24
Amberlite CG-400[Cl^-] 2.5 x 20 cm	H_2O	82	91	95	41
Bio-Rad AG-1[OH^-] 2.5 x 20 cm	1) H_2O	0	0	0	0
	2) In HCl	92	96	96	68
Bio-Rad AG-50[NH_4^+] 2.5 x 20 cm	1) H_2O	0	0	0	0
	2) In NH_4OH	79	99	100	92

Table II. All samples were freeze-dried between steps. All column operations were monitored with a flow-through scintillator system, using an anthracene packed cell for aqueous solutions and cerium activated glass scintillator beads for organic solutions.

The radioactivity eluted from the Bio-Rad AG-50 [NH_4^+] column with 1N NH_4OH (Table I) was freeze-dried, taken up in methanol, and paper chromatographed (Whatman No. 1, isoamyl alcohol-glacial acetic acid-water, 40:10:50, v/v/v). The radioactive components were eluted from the chromatograms with methanol. The methanol extracts were assayed for radioactivity and separately applied to a 0.9 X 100-cm column of LH-20 that had been poured in methanol. The radioactivity was eluted from the column with methanol.

After elution of the samples from LH-20, all samples, except the metabolite with an R_f of 0.71 (paper chromatography) from compound III, were taken to dryness and derivatized with bis-trimethylsilyltrifluoroacetamide containing 1% trimethlychlorosilane (Regisil). The metabolite from compound III was acidified to pH 3 with 6N HCI, placed on a 5-gram column of Bio·Rad Celex P[H^+] and the radioactivity eluted with 1N NH_4OH. The radioactive fraction was freeze-dried and applied to a silica gel thin-layer plate. The plate was developed with chloroform-absolute ethanol (2:1, v/v; R_1 0.32). The radioactivity was extracted from the silica gel with methanol (85% recovery) and silanized as previously mentioned.

All samples were gas chromatographed on a 6-ft column of 3% SE-30 on Chromosorb-W (60-80 mesh). The temperature was programmed at 6°/min from 100-250 C. The injector and detector temperature was 250 C. The helium carrier gas had a flow rate of 30 ml/min. The gas chromatograph (Perkin-Elmer 801) was equipped with a 10:1 splitter (10% to the hydrogen flame). The radioactive fractions were trapped in glass capillaries. Mass spectra were obtained on the silyl derivatives by placing the portion of the glass capillary containing the condensed sample into the solid sample probe of the mass spectrometer (Varian M-66).

TABLE III
RECOVERY OF RADIOACTIVITY

Compound	Hour	Urine (%)	Feces (%)	Carcass (%)	Total (%)
I	24	60.7	7.8	—	—
(Ring-Labeled)	48	65.0	10.7	—	—
	72	66.7	10.8	—	77.5
I	24	71.7	2.7	—	—
(Methoxy-Labeled)	48	77.0	6.8	—	—
	72	78.7	6.9	—	86.3*
II	24	60.1	7.8	—	—
(Ring-Labeled)	48	70.5	18.5	—	—
	72	70.5	18.9	—	89.4
III					
(Ring-Labeled	24	65.6	14.9	—	—
	48	70.7	17.8	—	—
	72	70.7	17.8	—	88.5
IV	24	51.5	8.0	—	—
(Ring-Labeled)	48	53.2	10.0	—	—
	72	53.3	10.0	—	63.3

*Total includes 0.7% of the dose exhaled in the expired air.

RESULTS AND DISCUSSION

The ^{14}C excretion and recovery data for all compounds are given in Table III. The low recoveries (63-89%) of the administered doses could arise from dosing errors or volatility of radioactivity upon freeze-drying the homogenized feces and carcasses. The dosing error is the most probable since no radioactivity was detected in the freeze-drier condensate.

The urine was the major route of excretion for all compounds. No radioactivity could be detected in the expired air from the ring-labeled compounds, with only 0.7% of the administered dose of methoxy-^{14}C-labeled compound I appearing in the expired CO_2. No detectable amounts of radioactivity were found in the homogenized, freeze-dried animal bodies 72 hours after dosing.

TABLE IV
ION EXCHANGE CHROMATOGRAPHY

			Compound				
			I		II	III	IV
Fraction Number		Elution Volume (ml)	Label Ring	Label Methoxy	Label Ring	Label Ring	Label Ring
1		40- 50		36.9			
2		170-180	1.0		0.7		21.5
3		340-350					
			1.8*				
4	VI	350-370		1.1			
5		410-420					
			2.9*	3.1	1.9		
6		420-440					
7	VII	480-490	2.2	0.6			
8	VIII, IX	500-520	20.8	16.2			
9	X	530-550	19.8	12.8			
10		560-570	3.1				
11	XI	580-600	34.2				
12		610-630	16.2				
13		640-655					
			1.4*				
14		655-670					
15		720-740			87.3	78.2	67.4
			6.6*				
16	XII	740-750					
Total Recovery			100.4	70.4	89.9	78.2	88.9

*Fractions assayed together.

The rat urinary metabolites from ring-labeled compound I separated into 15 radioactive components on the amino acid analyzer ion-exchange column (Table IV). The major fractions 8, 9, 11, and 12, accounting for approximately 90% of the urinary activity, along with fractions 4 and 16, had elution volumes identical with cow and goat urinary metabolites of compound I that have been characterized by mass spectrometry (4). The structures assigned to the characterized fractions from cow and goat urine are shown in Figure 1, and the corresponding elution volumes are shown in Table IV.

The urinary metabolites from ^{14}C-methoxy-labeled compound I separated into six fractions. The first (fraction 1, Table IV), containing 36.9% of the radioactivity, appeared near the buffer front and was not associated with a ring-labeled fraction. The remaining methoxy-labeled components had elution volumes identical with ring-labeled fractions 4, 5, 7, 8, and 9. This evidence is further confirmation that fractions 4, 7, 8, and 9 (Table IV) are 2-methoxy-triazines. Approximately 30% of the methoxy-labeled radioactivity was not recovered from the column.

The ion-exchange elution volumes of rat urinary metabolites from compounds II, III, and IV are given in Table IV. One major fraction appeared for both compounds II and III. Compound IV gave two fractions, one early in the buffer gradient where acidic compounds appear, and the other having the same elution volume as the major components from compounds II and III; the latter fraction was again the major component.

To accumulate urinary metabolites for characterization, rats were dosed with larger quantities of compounds II, III, and IV (Table I). The paper chromatography R_f values and gas chromatography elution temperatures for the metabolites separated from these three hydroxy-triazines are given in Table V. The R_f values for known compounds II, III, and IV were 0.78, 0.62, and 0.33, respectively. The elution temperatures from the gas chromatograph for the silyl derivatives of compounds II and III were 200 and 171 C, respectively. Compound IV gave two components, one at 148° and one at 185-190 C.

The mass spectra for the silanized metabolites are given in Table VI. Except for the metabolite with the R_f 0.70 from compound II, the mass spectra of all metabolites were identical with mass spectra of silanized compounds II, III, or IV.

Silanization of both known compound III and the urinary metabolites from compound III gave one component when gas chromatographed (elution temperatures 170 to 171 C.). However, the mass spectra of these derivatives gave two sets of parent ions and fragments corresponding to the mono- and disilanized derivatives (Table VI). This resulted from hydrolysis of the sample after gas chromatography and prior to ionization in the mass spectrometer since the relative intensities of the two sets change with residence time in the

TABLE V
PAPER AND GAS CHROMATOGRAPHY DATA

Compound	Gas Chromatography Fraction (Rf Value)	Gas Chromatography (%)*	Paper Chromatography Elution Temperature (°C)
II	0.20	<1	
	0.31	9	185
	0.70	79	210
	0.85	11	200
III	0.20	3.4	
	0.45	50	170
	0.71	46	170
IV (Organic Phase)	0.10	2	
	0.25	18	150
	0.33	79	150
(Aqueous phase)	0.25	100	150

*Percent of total eluted from the paper with methanol.

spectrometer, while the relative intensities of fragments within the sets remained constant.

Silanization of known compouund IV gave two components upon gas chromatography. The first at 150 C gave a mass spectrum corresponding to the disilyl derivative, and the second at 185-190 C gave a mass spectrum corresponding to the trifisilyl derivative (Table VI). Both the di- and trisilyl derivatives were found with the urinary metabolites. The trisilyl derivative gave two sets of fragments in the mass spectrometer corresponding to the di- and trisilyl derivatives, as was found for compound III.

Infrared spectra of the metabolites were of little value for characterizing their structures. The micro KBr spectra of all metabolites were very similar and supplied no useful structural details except for demonstrating the presence of the triazine ring. Absorptions at 1690 cm^{-1}, 1440 cm^{-1}, and 795 cm^{-1} indicated that the hydroxy-triazine ring was in the "iso" or "keto" form (6).

Only the parent compounds were isolated and characterized in the urine from rats given the 2-hydroxy-4-amino-6-alkylamino compounds III and IV. Each of these compounds was isolated from fractions having two different R_f values on paper chromatography (Table V). This could have resulted from hydrolysis of conjugates after paper chromatography or "silanolysis" of a conjugate during derivatization prior to gas chromatography.

Ion-exchange chromatography of the rat urinary metabolites from compound IV (Table IV) gave evidence for the presence of a conjugate. Two metabolites were separated. The first metabolite off

TABLE VI
MASS SPECTRA

Compound II			Compound III			Compound IV			Compound V		
M/e	Relative Abundance	M+1*	M/e	Relative Abundance	M+1*	M/e	Relative Abundance	M+1*	M/e	Relative Abundance	M+1*
Monosilyl			Disilyl			Trisilyl			Disilyl		
283	39	21)22.3)	327	43	29 (26.5)	371	100	32 (32.7)	371	1.2	29 (28.8)
268	64	19 (19.2)	312	84		356	98	31 (31.6)	356	7.8	27.5 (27.7)
254	100		298	100		299	23		254	100.0	20.0 (19.1)
227	50		271	52					117	2.3	
212	10		Monosilyl			Disilyl					
119.5	16		255	24		299	100	24 (24.3)			
			240	46		284	71	25 (23.3)			
			226	100		271	11				
			199	26		256	35				
			105.5	16		134.5	24				

*Expressed as percent intensity of the associated peak. Values in parentheses are calculated M+1 values for the silyl derivatives of compounds II through V in Figure 1.

the column (fraction 2) eluted in the region where acidic components would appear, and the second (fraction 15) eluted with the hydroxy triazine fraction. The first component could be an acidic conjugate, such as a glucuronide, or a sulfate ester.

The 2-hydroxy-4,6-dialkylamino-*s*-triazine (Compound II) gave four urinary metabolites by paper chromatography (Table V). Three of these were in sufficient quantity for characterization. The R_f 0.31 metabolite was characterized as compound IV. It gas chromatographed as the trisilyl derivative and had a mass spectrum identical with the trisilyl derivative of compound IV (Table IV). The R_f 0.85 metabolite gave a mass spectrum identical with the parent compound II (Table VI).

The R_f 0.7 metabolite from compound II was characterized by the mass spectrometry of its silyl derivative (Table VI). The parent ion was at m/e 371 with an m + 1 isotope peak 29.0% of the parent (calculated for $C_{12}H_{33}O_2N_5Si_2$, 28.8%). The base peak at m/e 254 corresponded to a loss of a $(CH_3)_3SiOCH_2CH_2$-(117) fragment from m/e 371, and the associated fragment appeared at m/e 117. This fragmentation mode of the *sec*-butylamino group at the C_2-C_3 bond gave rise to the base peak in the mass spectra of compounds II and III, which also contain this moiety. This evidence indicated the presence of a hydroxyl group on either C_3 or C_1 of the butyl moiety. A very small fragment at m/e 268 (less than 1% relative abundance), which would correspond to C_2-C_1 cleavage with loss of $(CH_3)_3SiOCH_2$-, indicated the presence of a silyl ether of a primary alcohol. Without a known reference spectrum, the structure of this metabolite was tentatively assigned as compound V in Figure 1.

These experiments have demonstrated that the metabolism of the 2-hydroxy triazines in the animal is different than that of the parent 2-methoxy triazine herbicide (Compound I). Approximately 90% of the urinary metabolites from compound I had the ethyl group removed, whereas the three characterized urinary metabolites from the 2-hydroxy analogue (compound II) still contained the ethyl group. None of the hydroxy compounds studied were converted to ammiline (compound X, Figure 1), which was the major rat urinary metabolite of compound I, and the 2-hydroxy-4-amino-6-alkylamino-triazines (compounds III and IV) may be conjugated, but the basic structure is excreted in the urine unchanged.

REFERENCES

1. Castelfranco, P., C. L. Foy and D. B. Deutsch. Non-enzymatic Detoxification of 2-Chloro-4, 6-*bis*(ethylamino)-*s*-triazine (Simazine) by Extracts of *Zea mays*. Weeds *9*, 580-591, 1961.

2. Plaisted, P. H. and M. L. Thornton. A Method for Separating Some Triazine Degradation Products from Plants. Contrib. Boyce Thompson Inst. *22*, 399-404, 1964.

3. Shimabukuro, R. H. Atrazine Metabolism in Resistant Corn and Sorghum. Plant Physiol. *43*, 1925-1930, 1968.

4. Bakke, J. E., J. D. Robbins and V. J. Feil. Metabolism of 2-Methoxy-4-ethlyamino-6-*sec*-butylamino-*s*-triazine by the Dairy Cow. In press.

5. Bakke, J. E., J. D. Robbins and V. J. Veil. Metabolism of 2-Chloro-4,6 - *bis*(isopropylamino) - *s* - triazine (Propazine) and 2-Methoxy-4,6-*bis*(isopropylamino)-*s*-triazine (Prometone) in the Rat. Balance Study and Urinary Metabolite Separation. J. Agr. Food Chem. *15*, 628-631, 1967.

6. Colthrup, N. B., L. N. Daly and S. E. Wiberly. Introduction to Infrared and Raman Spectroscopy. Academic Press, New York and London 234 p.